Demographic and evolutionary responses of reef-building corals to climate change

Kevin R. Bairos-Novak

College of Science and Engineering,

ARC CoE for Coral Reef Studies,

& AIMS@JCU

Acknowledgements

It takes a village, and I have so many to thank on my journey towards my doctorate. I owe so much to my wonderful supervisors who have helped me to this end. Sean – thank you for your thoroughness, completeness, and honesty towards my work, and for pushing me to be the best scientist I can be. Without you, I would have never learned to question any models, and I continue to learn from each email we exchange, even if it takes a little longer for it to sink into my thick head. Mia – thank you for believing in me and my work even when I do not, for pushing me in new directions, and for pushing me to make connections outside of my thesis. You always urged me to meet and discuss with others more knowledgeable than I – which, as a slightly closeted introvert, I still find difficult, but acknowledge that following your advice has been extremely rewarding overall. You also took me to the field with your lab despite knowing me to be a computer-based landlubber, and you always recognized when Sean and I would be stuck going around in circles on issues. Without you, I think we'd still be stuck on Chapter 2 going through the analysis in different ways, again and again! And finally Madeleine, thank you for your support and encouragement. Despite being afar from Townsville most of the year, you were the most responsive of all of us and always helped guide me in the right direction with logistics. Thank you for sharing you and your team's expertise with me, and a tremendous thank you to your lab including Carlos Alvarez Roa, Patrick Buerger, Giada Tortorelli, and Wing Yan Chan to name a few! I'd like to also greatly thank Kate Quigley for so many insightful discussions regarding heritability, symbionts, and genetics modelling.

I cannot underscore how important the Connolly lab members have been to me. CH and myself decided on the group name 'Holy Connollians', despite lacking any sense of grandeur or religiosity (save towards the drink perhaps). In order of ascending optimism, they are: Mariana Álvarez-Noriega, Alfonso Ruiz Moreno, Joanne Moneghetti, Cheng-Han Tsai, Katie Peterson, and Jessica Zamborain Mason (a.k.a. Skim). A special thank you to Mariana – our walks up Castle Hill have been all of fun, stress-relieving, and educational (i.e. regarding integral projection models) this past year of my PhD. After Sean left for Panama, I was adopted into the Hoogenboom Coral Ecophysiology lab, who have supported me ever since. I'd especially like to thank Allison Paley,

Tessa Hill, Chris Brunner, Alex Tauman, Emily Washington, Steph Di Perna, Saskia Jurriaans, Taylor Whitman, and Tory Chase for their encouragement and friendship throughout my PhD.

Thank you to Yvette Everingham and Scott Heron – two of the best supervisors one can ask for when it comes to tutoring! They always put us tutors first and allowed us some flexibility in how we ran the tutorials, allowing me to develop my teaching and communication skills that I am sure will come in handy for the rest of my career. A massive thank you to all admin staff – be it the GRS staff (thank you Jodie!), JCU's International staff, the ARC Centre for Coral Reef Excellence (CoE), the College of Science and Engineering, or the AIMS@JCU staff; they all work hard to make students' lives much easier. Thank you to members of the JCU CodeR coding club and the CoE Justice, Equity, Diversity, and Inclusion (JEDI) Committee – my involvement and connections within each of these groups has truly enriched my experience at JCU and paved the way for many more opportunities.

I'd like to personally thank my friends and family. Too many have come and gone from JCU, but thank you to my many wonderful friends: Suzanne, Lauriane, Ketki, Kevin, Amy, Alyssa, Becky, Bethan, Cristina, Emma, Gabi, Rishab, Sush, Tom, Sara, Danny, Dan-dawg, Kyana, Sunny, Emily, Jared, Lorenzo, Cesar, Wytamma, Marko, Max, Roxy, Guy, Fer, Matt; Chris, Victor, Rachel, Shannon, Sterling, Renato, Pauline, Mike, Martina, Kelly; Andy, Brit, the Katie's, Alex, Peter, Erika, Claye, Brig, Sophie, Marto, Josh, Brooke, Steph, Eric, Adam, Jodie, Laura, Alex, Stuart, Tony, Wendy, Peter, Mako, Seb, Ernie, Janine, Genevieve, Ron, Anya, so, so many more. I hope you all know you are always welcome at my door, wherever I am. A special thank you to the Townsville Drum Collective – a community led by Alex Salvador that unearthed a passion for Brazilian rhythms and drums that I never knew I had, and gave me so much joy every Wednesday night, as well as so many friendships. The rhythm never stops, and nor will I.

Finally, and most of all, thank you to my parents Lori and Manny, my younger siblings Steven and Alex, and my late grandmother, Dr. Joan McLaren, for inspiration – the first PhD in our family. Nothing pained me more than missing the past three Christmases due to COVID and my thesis wrapping up, and for that I am eternally sorry. I love you and miss you all each and every day.
I promise to be there for you all through the rest of my career. My thesis is dedicated to you.

Statement of the Contribution of Others

Nature of Assistance	Contribution	Names, Titles, and Affiliations of Co-Contributors
Intellectual support	Proposal writing and editing Data Analysis Statistical support Editorial assistance	*Prof* Sean Connolly (JCU, Smithsonian Institute), *A/Prof* Mia Hoogenboom (JCU), *Prof* Madeleine van Oppen (AIMS, UMelb)
Financial support	Fee offset/waiver Research costs Stipend support Write-up grant	AIMS@JCU Write-up Grant, AIMS@JCU Pilot Research Award, GRS-supplied scholarship extension and fee waivers, NSERC PGS-D Award
Data collection	Provided raw data for heritability calculation in Chapter 1; Provided raw data for recruit size estimates	Yingqi Zhang (USC), Hanaka Mera (JCU); Carly Kenkel (USC)
Data collection	Contributed demographic and/or recruitment data for Chapter 2	Allison Paley (JCU), Tory Chase (JCU), Saskia Jurriaans (JCU), Mariana Álvarez-Noriega (JCU), Carly Randall (AIMS), Chris Doropoulos (CSIRO)
Data collection	Pulled sea surface temperature data and informed calculation of historical DHWs	Scott Heron (JCU, NOAA)

General Abstract

Climate change has caused rising ocean temperatures that now threaten coral reefs worldwide. Mass bleaching events have resulted in widespread coral mortality, which has in turn selected for more thermally tolerant coral genotypes and altered coral population demography. The rate of coral population adaptation to climate change will depend on the proportion of phenotypic variation in thermal tolerance that is inherited by subsequent generations (i.e. narrow-sense heritability, h^2), the environment effect on phenotype, and interactions with the strongly size-dependent demography of coral populations. In this thesis, I present a meta-analysis of trait heritability in corals (**Chapter 2**), build a density-dependent, size-structured, closed-population model of corymbose corals (e.g. *Acropora millepora*) (**Chapter 3**), and combine the two to produce a size-structured eco-evolutionary model of coral population adaptation to current and future projected climate change (**Chapter 4**).

In **Chapter 2**, I synthesized 95 heritability estimates of traits across 19 species of reef-building corals. I found that traits such as gene expression exhibit low heritability ($h^2 < 0.25$), while traits such as photochemistry, growth, and bleaching are intermediately heritable ($h^2 = 0.25–0.50$), and survival and immune response traits show relatively high heritability ($h^2 \geq 0.50$). Interestingly, there was no evidence of heritability changing with temperature stress, suggesting that corals may have a greater potential to adapt to climate change than has been assumed in previous evolutionary models.

In **Chapter 3**, I constructed a size-structured, density-dependent integral projection model (IPM) of a single population of corymbose *Acropora* corals, parameterised with demographic data from the northern and central Great Barrier Reef. Survival, growth, and fecundity is strongly determined by colony size in corals, and the IPM approach allows me to more realistically model demography compared to traditional matrix models. However, in contrast to survival, growth, and fecundity processes, data on recruit intra-cohort density-dependence is rarely collected and has yet to be included in a coral IPM. To identify key data-deficiencies for modelling coral population trajectories, I evaluated the sensitivity of predicted extinction risk and equilibrium abundance to uncertainty in growth, survival, fecundity, and intra-cohort density-dependent relationships. I found that in the absence of density-dependent interactions among recently-settled individuals, realistic

levels of cover are only predicted for a small range of larval survival and settlement probabilities, whereas the inclusion of density-dependent interactions between recently-settled larval results in coral cover reaching equilibrium at more plausible levels of coral cover, and over a much larger range of proportional larval settlement. Coral dynamics depended both on the type of intra-cohort density dependence in addition to the probability of successful settlement, but are also sensitive to uncertainty related to growth and survival functions. Chapter 3 highlights the importance of better characterizing recruitment processes and juvenile interactions for understanding the demography of coral populations.

Finally, in **Chapter 4**, I develop the first evolutionarily-explicit IPM (EE-IPM) for corals using heritabilities derived from Chapter 2 to extend the IPM from Chapter 3. Current models of coral evolution fail to take into account the size-dependent demography of corals, which is likely to limit the propagation of adaptive alleles, given that: recruits take several years to reach reproductive maturity, fecundity is size-dependent – such that the oldest, largest colonies dominate the production of gametes, and background mortality is highest at early life stages. Therefore, I constructed an EE-IPM of corals that tracks the additive genetic (g) vs. environment (e) components of an individual's thermal tolerance phenotype (z). To do so, I define an individual colony phenotype z as the threshold accumulated heat stress at which corals are no longer able to survive, and decompose it into g and e based on the narrow-sense heritability (h^2) from Chapter 2. While the additive genetic component is heritable, the environmental component e is fixed at birth and represents the environmental and developmental noise that results in individuals having differing thermotolerance relative to their parents. Colonies experiencing annual DHWs greater than their phenotype die and fail to pass on their genotypes, g, to the next generation, resulting in genetic evolution across time and with accumulating heat stress. Using four different future pathways and their associated heat stress, I found that corals may be capable of adapting to low to moderate climate change when there is sufficient fecundity and recruitment, but genotype-by-size interactions may reduce the rate of population evolution due to larger, more fecund adults being less well adapted relative to more thermally tolerant juveniles.

Using novel extensions to size-structured demographic models of corals, such as intra-cohort density-dependent regulation and explicit evolution, my thesis estimates the potential contributions of

coral adaptation and demography to future population persistence. Evolutionary rescue of reefs may be possible under some specific scenarios, such as with adequate fecundity and coral recruitment during and after bleaching events. However, coral adaptation to future heat stress is contingent on significant reductions in carbon emissions, and thus coral population extinction risk remains high without coordinated geopolitical cooperation to reduce climate change on a global scale.

Table of Contents

Acknowledgements i
Statement of the Contribution of Others iii
General Abstract iv
Table of Contents vii
Chapter 1 General Introduction 1
Thesis aims 12
Chapter 2 Meta-analysis reveals high heritability across multiple traits 1
Abstract 1
Introduction 2
Methods 5
Literature search 5
Pre-processing 6
Factors of interest 7
Reported heritability estimates 10
Meta-analysis approach 12
Results and Discussion 14
High heritability of coral traits 14
Heritability across trait types in other organisms 17
Life stage and heritability type, but not growth form, mediate trait heritability 18
Low adaptive potential of juvenile growth and bleaching 20
Confounding sources of variation 21
Manipulated temperature has negligible effect on heritability 22
Trait adaptation to warming temperatures 25
Coral thermal performance and challenges to predicting future adaptation to climate change 25
Conclusion 27
Data accessibility statement 28
Chapter 3 Demographic drivers of coral population persistence and stability 29
Abstract 29
Introduction 30
Methods 35
Corymbose coral biology 35
Developing an integral projection model (IPM) 36
Vital rates: Growth 40
Vital rates: Survival 42
Vital rates: Reproduction and recruitment 43
Evaluating population outcomes 46
Results 48

Proportion of successful settlers 48
Intra-cohort post-settlement density dependence 48
Extinction risk 50
Uncertainty in equilibrium population size 51
Discussion 54
Data accessibility statement 58
Chapter 4 Size-dependent evolutionary dynamics of corals to climate change 59
Abstract 59
Introduction 60
Methods 66
Brief model description 66
Model overview 68
Characterizing a thermal tolerance phenotype 70
Initializing the IPM 73
Survival 73
DHW-limited fecundity 74
Inheritance kernel 74
Future thermal stress scenarios 75
Model outputs 76
Model hindcasts 77
Results 77
Density-dependence in intra-cohort interactions mediates initial population decline 82
Importance of sustained fecundity and larval settlement 83
Evolutionary rescue through adaptation to climate change 84
High adaptive potential with intermediate conditions 85
Eroding genetic variance impairs population adaptation 86
Discussion 86
Comparing to other modelling studies 88
Saturating effect of heritability and eroding genetic variance 89
Heat stress-limited fecundity 89
Model limitations 91
Size-dependent dynamics 92
Data limitations to modelling coral evolution 93
Summary 94
Data accessibility statement 95
Chapter 5 General Discussion 96
Variability in heritability 97
Heritability is not adaptation 98
Genotype-by-environment interaction and correlation 99

Variable larval recruitment 100
Net larval settlement rates 100
Rapid growth of juveniles 103
Other sources of genetic and environmental variation 105
Trade-offs 107
Future research 111
Implications of this thesis to future policy 112
The future of corals: adaptation or extinction? 112
Appendix A: Supplementary Text for Chapter 2 115
A1: Methods used to estimate heritability 115
A2: Pre-processing of raw heritability estimates 116
A3: Model selection results of trait type × heritability type and trait type × growth form 117
Appendix B: Supplementary Materials for Chapter 3 119
B1: Model details 119
B2: Growth model plots 122
Combining the juvenile and adult datasets 122
Radial growth models 124
Partial mortality models 126
Final growth models 128
B3: Saturating effect of bin size 130
B4: Trajectory plots 131
B4: Size distribution plots 137
B5: Extinction plots 142
B6: Equilibrium plots 148
Appendix C: Supplementary Materials for Chapter 4 154
C1: Defining a coral mortality phenotype 154
Mortality distribution from Hughes et al. (2018b) 154
Log-normal approximation to exponential distribution 157
Square root and normal numerical approximations 159
C2: Hindcast heat stress models 161
C3: Simulating future heat stress 177
C4: Model summary plots 180
References List 187

Chapter 1 General Introduction

Ecosystems have faced continual challenges due to human-induced changes throughout the Anthropocene, but anthropogenic climate change may represent the greatest threat to natural ecosystems, biodiversity, and human societies to date (Malhi et al. 2020; WHO 2021; UN Office of Human Rights 2022). In the early days of climate change science, polar ecosystems were seen as particularly vulnerable to climate change (Dansgaard et al. 1982; IPCC 2019). However, the impacts of climate change have since been observed on nearly every ecosystem worldwide (Doney et al. 2012; Hoegh et al. 2018; Olsson and et al. 2019; Malhi et al. 2020; Capon et al. 2021), and they are now recognized to have begun as early as the 1820s (Abram et al. 2016). Despite the knowledge that climate change is occurring rapidly, emissions continue to rise to unprecedented levels (IPCC 2019, 2021), escalating the chance of ecosystem collapse following unprecedented environmental changes (Jump and Peñuelas 2005; Visser 2008; Jenouvrier and Visser 2011).

Coral reef ecosystems are collectively one of the most well-known cases of anthropogenically-induced ecosystem decline, including recent mass bleaching resulting from climate change (Hughes et al. 2018c; Curnock et al. 2019; Marshall et al. 2019). Moreover, the importance of these systems to human livelihoods is irrefutable. Globally, coral reefs provide food and/or shelter to about 25% of all marine biodiversity and provide many ecosystem services, despite covering only 0.2% of the Earth's surface (Knowlton et al. 2010; Spalding and Brown 2015; GCRMN 2021), making coral reefs one of the most biodiverse ecosystems on Earth (Fisher et al. 2015; Woodhead et al. 2019; Dietzel et al. 2021a), with population diversity of corals equating or exceeding the biodiversity of Amazonian rainforest trees per unit area (Dietzel et al. 2021a). Reefs worldwide support 5,000–8,000 unique species of fish (Fisher et al. 2015; Victor 2015), many of which depend on the three-dimensional complexity of coral colonies as fish 'nursery' areas (Hamilton et al. 2017). Reefs also provide a number of crucial ecosystem services (reviewed in Woodhead et al. 2019), such as coastal protection, fisheries, tourism, and cultural services, with a total value of goods and services around $2.7 trillion dollars globally per year (GCRMN 2021). For example, reefs support about 6.1 million fishers worldwide, with ¼ of all small-scale fishers fishing on reef habitats for income or sustenance fishing (Teh et al. 2013). Coral reefs are home to many large parrotfishes of the genus

Chlorurus, which contribute a significant portion of sediment to fine white sand beaches globally, indirectly supporting ecosystem functioning, reef stabilization, and tourism (Bellwood 1996; Yarlett et al. 2021). Recreation and tourism to reefs contributes $36 billion USD/year to the global economy (Brander et al. 2007; Spalding et al. 2017). The Great Barrier Reef alone is valued at $56 billion AUD/year adding $6.4 billion AUD/year to the Australian economy and 64,000 jobs (O'Mahoney et al. 2017). Finally, coral reefs hold less readily-quantified aesthetic and cultural values for many indigenous and non-indigenous peoples worldwide; values which are often tied to the condition of the reef (Uyarra et al. 2009; Tschakert et al. 2019).

Coral reef declines throughout the world have been documented for decades due to a number of stressors (Pandolfi et al. 2003; Burke et al. 2011; De'Ath et al. 2012), and more recently, the impacts of man-made climate change on reefs have become particularly substantial through repeated mass bleaching events (Hughes et al. 2018c; Lough et al. 2018; Sully et al. 2019). Mass bleaching events occur predominantly when sea surface temperatures on the reef remain higher than average for the local area for long periods of time (Heron et al. 2016). When corals experience excessive heat stress, their symbiotic algae-like partners – dinoflagellates of the family Symbiodiniaceae – leave the coral host's tissues, creating a ghostly white or 'bleached' appearance. This symbiotic breakdown has important long-term implications for corals, as Symbiodiniaceae ordinarily provision the coral hosts with excess nutrients and products from photosynthesis in a mutualistic relationship (Muscatine and Porter 1977; Goulet and Coffroth 2003). Thus, depending on how auto-trophic (i.e. photosynthetic) vs. heterotrophic (i.e. consuming small invertebrates) the coral is (Conti-Jerpe et al. 2020), and on the intensity and duration of the bleaching event, this can result in death by starvation. Localised coral bleaching occurs sporadically on reefs each year when corals experience high summer sea surface temperatures; however, mass coral bleaching, where a large proportion of coral cover bleaches at regional to global scales, is a relatively recent phenomenon that now occurs regularly (Hughes et al. 2018c; Lough et al. 2018). For example, the Great Barrier Reef (GBR) had only experienced a single mass bleaching event from 1980–2000 (in 1998). Since then, five mass bleaching events have occurred from 2000–2022, and four of these events have occurred in the last seven years: 2002, 2016,

2017, 2020 and 2022 (BBC 2020; AIMS 2023). Globally, mass bleaching events have increased in both frequency and intensity (Lough et al. 2018; Sully et al. 2019; Dietzel et al. 2021b).

One of the most common measures and best predictors of significant bleaching and mortality on reefs are degree heating weeks (DHWs) from NOAA's Coral Reef Watch program (Heron et al. 2016; McWhorter et al. 2022b; NOAA Coral Reef Watch 2022). DHWs are calculated by integrating the number of accumulated weeks of 'severe heat stress' – i.e. the total number of weeks where average overnight sea surface temperatures (SST) surpass the historical mean monthly maximum (MMM) of overnight temperatures plus one degree, weighted by the amount by which that threshold is exceeded ($\mathrm{DHW} = \frac{1}{7}[\sum \mathrm{if}(\mathrm{SST} > \mathrm{MMM} + 1°\mathrm{C}, \mathrm{SST} - \mathrm{MMM}; \mathrm{else}\ 0)]$, over a 16 week window) (Heron et al. 2016). As a result of increased heat stress on the reef – as well as ocean acidification and a plethora of other, more local stressors such as cyclones, crown of thorn starfish (COTS) outbreaks, inshore pollution and run-off/eutrophication, coral disease outbreaks, overfishing, reef diversity and overall population – coral cover has declined significantly worldwide (GBRMPA 2017; Hughes et al. 2018c), with 75% of global reefs now considered threatened (Burke et al. 2011). Globally, coral reef cover is now estimated to have halved since the 1950s (Eddy et al. 2021). Many of the above stressors, such as frequency of coral disease outbreaks and ocean acidification, are expected to increasingly threaten the reef as climate change continues (Maynard et al. 2015; Hoegh-Guldberg et al. 2017; Burke et al. 2023).

The 'death by a thousand cuts' hypothesis posits that coral degradation is caused by multiple simultaneous and potentially synergistic stressors (Laurance 2010; Bridge et al. 2013). However, of all current stressors to date, increased temperatures due to climate change causing coral bleaching have had increasingly and disproportionately large and widespread effects on reefs worldwide (Hughes et al. 2018a; GCRMN 2021). Thus, many studies have sought to predict the future of coral reefs (e.g. (van Woesik et al. 2018; McManus et al. 2020; Logan et al. 2021; Holstein et al. 2022; Sully et al. 2022); however, this remains a challenge, as bleaching affects multiple demographic processes in corals (e.g. survival, growth, fecundity, recruitment), at many different scales (e.g. symbiont, host, holobiont) (Lasky et al. 2020; van Woesik et al. 2022). Future temperatures have previously been

predicted using representative concentration pathways (RCPs) based on varying human carbon emission scenarios that are used as forcing inputs for climatological and atmospheric models in order to predict future temperatures. Simultaneously, socio-economic studies have often attempted to imagine the world using future scenarios of social, technological, and economic collaboration across nations (Moss et al. 2008), such as the four scenarios originally developed as part of the millennial ecosystem assessment (MEA 2005). More recently, the two spheres of climatology models and socio-economic models have merged to produce the shared socio-economic pathways (SSPs), which represent climatology outcomes driven by different socio-economic trajectories that appear possible at present (O'Neill et al. 2016; Riahi et al. 2017).

The SSP1-1.9 scenario represents the most optimistic scenario with CO_2 emissions being cut to net zero by the year 2050, resulting in only a +1.5°C increase in global temperatures above pre-industrial temperatures by 2100 (Riahi et al. 2017), while the SSP1-2.6 scenario imagines a future with smaller reductions, ending the century at +2.0°C (O'Neill et al. 2016; McWhorter et al. 2022b). SSP3-7.0 represents a 'business as usual' future with increasing concerns over national security, with emissions doubling by the year 2100 resulting in a +3.6°C increase globally (O'Neill et al. 2016). Finally, SSP5-8.5 is the worst-case 'business as usual' future, with a global economy growing via burning fossil fuels readily, resulting in a doubling of emissions by 2050 and an increase of +4.4°C by 2100 (O'Neill et al. 2016). Recent temperature predictions using statistically-downscaled SSPs for coral reefs have projected the decline or disappearance of local thermal refugia for most corals within even the best-case emissions scenario (Dixon et al. 2022; McWhorter et al. 2022a), with all thermal refugia predicted to fail after +3°C (i.e. only SSP1-1.19 and SSP1-2.6 are viable) – though thermal refugia are typically based on current population thermal tolerances and recent findings of cooler, temporally-dynamic fluid substrata created by a phenomenon called 'internal gravity waves' predict the persistence of some thermal refugia even with severe climate change (Bachman et al. 2022). Mass bleaching events with severe bleaching (>8 DHWs) have been projected to occur at least 3 times per decade and potentially every year under higher emission scenarios (SSP3-7.0 and SSP5-8.5) (McWhorter et al. 2022b).

Many projections of coral reef futures assume static thermal tolerances in corals and other organisms. However, already, there have been large shifts in the distribution of thermal tolerances of corals (Maynard et al. 2008; Guest et al. 2012; Coles et al. 2018; Sully et al. 2019). Thus, to understand future population responses to climate change, it is important to consider the suite of responses corals have already exhibited in response to past bleaching. After the 1998 bleaching event, *Acropora* and *Pocillopora* coral populations bleached significantly less in response to similar heat stress (Guest et al. 2012). Similarly, GBR corals bleached 30-100% less than expected during the 2002 bleaching event relative to 1998 (Maynard et al. 2008). An empirical study of Hawaiian corals repeated a chronic heat stress exposure from 1970 using corals from the same locations and found that coral bleaching occurred 10-14 days later after 47 years (Coles et al. 2018). Finally, a global analysis of bleaching found that between 1998-2006 and 2007-2017, coral bleaching thresholds shifted +0.5°C (Sully et al. 2019).

The responses above could either be interpreted as long-term adaptation of coral populations to increasing heat stress, or as medium-term effects of selective mortality or physiological acclimation to heat stress. Indeed, there is evidence that all have occurred. Experimental selection studies have resulted in increased thermal tolerance of coral symbiont populations both *in vitro* (Chakravarti et al. 2017; Chakravarti and van Oppen 2018) and *in hospite* (Buerger et al. 2020), showcasing the adaptive potential of Symbiodiniaceae. Common garden experiments involving transplanted corals to and from warmer/more variable vs. cooler/less variable reefs have shown a significant genetic component to thermal tolerance (Oliver and Palumbi 2011; Bay and Palumbi 2017; Drury et al. 2017; Drury and Lirman 2021). A number of genotype-by-environment (GxE) interactions (where certain genotypes are more resistant to thermal stress in specific environments) have been observed in corals worldwide (e.g. Howells et al. 2013; Drury and Lirman 2021). Symbiont genetics are also important, with some genera of symbionts such as *Durusdinium* imparting increased thermal tolerance to coral hosts (Howells et al. 2016; Dilworth et al. 2021). The strongest evidence for adaptation comes from changes in underlying genetics in symbionts and the coral host related to thermal tolerance. Genome-wide studies of corals have shown a strong genetic signal related to thermal tolerance (Dixon et al. 2015; Kirk et al. 2018; Quigley et al. 2020a), while multi-locus control of thermal tolerance has been

observed in the genome of *Acropora hyacinthus* (Barshis et al. 2013; Bay and Palumbi 2014). Finally, selective sweeps across the host genome of *Platygyra daedalea* in the Persian/Arabian Gulf highlight positive and disruptive recent genetic selection to increased thermal tolerance (Smith et al. 2022). Thus, there is strong evidence of a genetic basis of thermal tolerance, both within coral hosts and their symbionts.

However, it remains to be seen if the rate of adaptation of corals to climate change is sufficiently high – and can persist for long enough – to stave off extinction. The rate of adaptation in natural populations tends to be less than 10% of the phenotypic standard deviation or 'haldane' (Burger 1995; Kinnison and Hendry 2001; Kopp and Matuszewski 2014); however, rates above 0.1 *haldanes* do exist and are plausible (Hendry and Kinnison 1999), especially for larger population sizes (Kopp and Matuszewski 2014). Higher rates of evolution have been observed in natural populations, but they may entail severe population mortality (e.g. 85% mortality in a species of Darwin's finch; Grant and Grant 2006; Kopp and Matuszewski 2014). It is therefore possible that evolution on reefs will occur over similar timescales as population dynamics, and thus models integrating both coral evolution and demography are needed to better predict coral population dynamics with future climate change (Chevin et al. 2010; Lasky et al. 2020). However, model outcomes will largely depend on parameters that determine the rate at which corals can adapt to future climate change, many of which remain unclear. Polygenic traits are very common in marine organisms, especially where high gene flow and broad dispersal ranges allow for increased genetic recombination to occur (Limborg et al. 2012; Pespeni et al. 2013; Laporte et al. 2016). Most models of adaptation typically assume polygenic traits (Lande 1981; Wright et al. 2003; West-Eberhard 2005). This includes Fisher (1919)'s infinitesimal model of quantitative genetic change – that many independent loci of infinitesimally small effects add up to produce individual phenotypes (i.e. the expressed trait). This model assumes unchanging variance due to segregation and mutational variances and weak selection on individual genes (Falconer and Mackay 1996; Barton et al. 2017; Rees and Ellner 2019). Indeed, a polygenic basis for coral thermal tolerance appears likely. For example, in one study, coral thermal tolerance was determined by 100-1000 alleles, none of which exhibited strong effects individually (Bay and Palumbi 2014; Bay et al. 2017a; Thomas et al. 2018). Assuming the infinitesimal model allows the

decomposition of phenotypic variance into its genotypic and residual/'environment' components, often symbolised *g* and *e*, respectively (Falconer and Mackay 1996; Gienapp et al. 2008), and the application of Lynch-Lande phenotype dynamics (Lynch et al. 1991; Lynch and Lande 1993). Another assumption of most models is that of predominantly additive genetic variance (V_A)– rather than non-additive sources of variance such as variance due to dominance (V_D; where alleles within the same locus interact, such as a dominant allele masking the effect of a recessive one) and variance due to epistasis (V_I; where multiple loci interact to produce an individual's phenotype) (Falconer and Mackay 1996; Varona et al. 2018). However, Hill et al. (2008) suggest that the majority of genetic variation is likely additive in nature. Fisher's fundamental and secondary theorem of natural selection states that the change in mean fitness due to natural selection is equal to the additive genetic variance in fitness, and that the rate of change in mean trait values is proportional to the additive genetic covariance between that trait and fitness, respectively (Fisher 1930). In the context of thermal tolerance evolution, Fisher's secondary theorem predicts that if thermal tolerance has a strongly genetic basis and is selected upon, corals should evolve proportional to this variation (Fisher 1930) – and this forms the intuition behind the Price equation and Robertson-Price identity for trait change in response to natural selection (Robertson 1966; Price 1970). It also relates to a fundamental tool used in artificial breeding programs for nearly a century known as the Breeder's equation (Lush 1937; Falconer and Mackay 1996), which, instead of strictly genetic covariance alone, uses the proportion of additive genetic variance to total phenotypic variance or narrow-sense heritability (h^2) to predict responses to selection.

Heritability is the proportion of a trait's relative genetic variation compared to its total phenotypic variation (V_P). Heritability is a dimensionless quantity that describes population responses to selection, and is often calculated to compare across traits, populations, or species (Visscher et al. 2008). There are generally two types of heritability that can be calculated based on the contributors to variance in the numerator: broad-sense heritability (H^2) and narrow-sense heritability (h^2).

$$\text{Broad-sense: } H^2 = \frac{V_A+V_D+V_I}{V_P} \qquad \text{Narrow-sense: } h^2 = \frac{V_A}{V_P} \qquad (1)$$

The former is 'broad' in that it includes all sources of genetic variation (V_G), including additive genetic variation (V_A), as well as non-additive sources such as dominance (V_D) and epistasis (V_I), which are

genetic effects not (necessarily) inherited by offspring produced through sexual reproduction (Falconer and Mackay 1996), and thus broad-sense heritability is calculated using comparisons of clones or genets. Narrow-sense heritability, h^2, is the proportion of phenotypic variance that is due to additive genetic variance (V_A) alone, and is the strictly 'heritable' genetic component of the trait of interest in sexually-reproducing individuals. Narrow-sense heritability is calculated using pedigree information from genetically distinct individuals. Important caveats when estimating either narrow or broad-sense heritability include controlling for common environment across individuals, as well as considering potential genotype-by-environment interactions, parental effects that may alter offspring phenotype, and the potential for epigenetic inheritance (Falconer and Mackay 1996; Visscher et al. 2008).

Narrow sense heritability can be used to predict and understand population responses to selection. Consider one population where the mean critical thermal maximum (CT_{max}) of the population is 30°C and CT_{max} is highly heritable, e.g. $h^2 = 0.5$. If a temperature anomaly occurs, resulting in the death of the more heat-susceptible individuals and shifting the mean population CT_{max} to 32°C, the univariate Breeder's equation predicts that the mean change in population response (R) in CT_{max} will be:

$$R = h^2 \cdot S = 0.5 \cdot (32°C - 30°C) = +1°C \quad (2)$$

In other words, an increase in the mean selected population CT_{max} of +2°C (S, the 'selection differential') translates to an expected increase in the next generation's average CT_{max} of +1°C (Lush 1937; Lande 1979; Falconer and Mackay 1996). Now consider a second population experiencing the same selection event, but with a relatively low heritability in CT_{max}, e.g. $h^2 = 0.1$. The predicted change in CT_{max} in the next generation would be: $R = 0.1 \cdot (32°C–30°C) = +0.2°C$, or a five-fold lower response to the same selection pressure. Thus, the relative response of a trait in a population under selection is proportional to the value of the narrow-sense heritability coefficient for said trait, h^2.

Additive genetic variance and narrow-sense heritability are typically estimated using the 'animal model' of quantitative genetics (Kruuk 2004; Hadfield 2008; Wilson et al. 2010) which uses a (generalised) linear mixed model or (G)LMM with knowledge of individual animal relatedness as the random effect in order to estimate additive genetic variance. Relatedness data can either be in the form

of random intercepts for each unique family/half-sibs/full-sibs, or more explicitly using pedigree matrices. The phenotypic variance in individual responses is then partitioned into random effect intercepts (and/or slopes) representing an estimate of additive genetic variance, while the residual variance is considered the 'environmental' component of phenotype (Hadfield 2008). The animal model is extremely powerful and versatile in that it can include non-Gaussian responses by using a GLMM and incorporate environmental covariates contributing to phenotypic variability. However, this flexibility comes at the cost of no standard and consistent method of fitting animal models, making estimates of additive genetic variance difficult to compare across studies and systems. Therefore, many authors report the narrow-sense heritability coefficient (h^2) which ranges from 0 to 1 and is more comparable across studies (Kruuk 2004; Wilson et al. 2010).

Models attempting to predict future coral evolution have varied substantially in their level of genetic explicitness, from using a constant rate of thermal tolerance change (Logan et al. 2014a), to quantitative genetic models using the heritability coefficient (Baskett et al. 2009; Logan et al. 2021) or additive genetic variance (McManus et al. 2021b; DeFilippo et al. 2022), to individual-based simulations of thermal tolerance-associated loci (Bay et al. 2017b; Matz et al. 2018, 2020). Most models assume low potential heritability (h^2 = 0–0.25) or additive genetic variance of thermal tolerance, a Gaussian-distributed fitness function of phenotypic temperature mismatch with the environment, and non-changing genetic variance in the face of strong selection (but see Matz et al. 2018). Additionally, many evolutionary models often use very simple demography out of necessity; however, interactions between demographic traits such as size and evolution may be possible and could change model outcomes (Lasky et al. 2020).

Predicting the future of corals requires knowledge of local demography (Edmunds et al. 2014; Edmunds and Riegl 2020), as the rate at which coral populations can adapt to climate change is likely to depend on their capacity to replenish populations depleted by bleaching-induced mortality, through colony growth and reproduction. In corals, demography is strongly size-dependent. For example, smaller corals grow proportionally more than larger corals (Dornelas et al. 2017; Madin et al. 2020) but have much lower whole-colony survival relative to larger colonies (Madin et al. 2014), take several years to reach reproductive maturity ((Hall and Hughes 1996; Baria et al. 2012), and have

orders of magnitude lower fecundity when they are finally gravid (Hall and Hughes 1996; Álvarez-Noriega et al. 2016). Therefore, the spread of adaptive alleles in new juveniles produced by selected adult corals may be slowed or dampened by the strong size-dependent demography of corals, as the fecundity of less well-adapted large adults will greatly exceed that of smaller individuals for years and, therefore, disproportionally contribute non-adaptive alleles to the gene pool. Larger adults are often less well adapted relative to juveniles because larger colonies can survive bleaching by virtue of being in thermally favourable microhabitats or having acclimatized over their lifetimes to bleaching stress, or both. Further complicating the matter is the fact that smaller coral juveniles (≤ 5 cm diameter) are often more resistant to bleaching, relative to larger colonies (Loya et al. 2001; Shenkar et al. 2005; Roth et al. 2010; Depczynski et al. 2013; Speare et al. 2022). Finally, there is evidence in some populations that the larval supply of adults may be critically depleted during and/or after years of impaired fecundity after bleaching events (Hughes et al. 2019; Cheung et al. 2021; Leinbach et al. 2021; Speare et al. 2022), whereas in other populations, this is either not the case (Edmunds 2017), or fecundity is overcompensatory (higher than average) and rebounds in subsequent years after bleaching (Morais et al. 2021; Nakamura et al. 2022). These factors can each interact with genetics to alter the rate at which thermal tolerance genotypes may spread through the population, and thus can alter population outcomes to climate change. Mechanistic size-structured models that track both size and genetic evolution are thus required to more accurately capture coral adaptation to climate change (Visser 2008; Lasky et al. 2020).

Structured population models track the frequency of individuals whose demographic rates depend on a specific ‘state variable’ of interest, and use the probabilistic transitions of individuals between states to analyse long-term population dynamics (Caswell 2010; Rees et al. 2014). The most common type of structured population models are matrix projection models (MPMs) (Salguero-Gómez et al. 2015, 2016), which track abundances of individuals in distinct life stages (e.g. larvae, new recruits, juveniles, adults), ages, or size classes (Doak et al. 2021). These matrix projection models require discretised or categorical state variables, but state variables such as size are inherently continuous in nature (or age, where reproduction occurs continuously throughout the year). More recently, integral projection models (IPMs) have become widely adopted as the ‘state-of-the-art’ for

studying populations whose demographic rates depend on state variables that are inherently continuous (Easterling et al. 2000; Edmunds et al. 2014) with greater accuracy, especially for data-limited populations (Ramula et al. 2009; Ellner et al. 2021, but see Doak et al. 2021). For corals in particular, demographic rates depend more strongly on size than age (and size is a readily observable state variable for corals whereas age is not) (Hughes and Connell 1987; Hall and Hughes 1996; Edmunds et al. 2014).

IPMs require longitudinal individual demographic data (e.g. individual colony survival, growth, or fecundity as a function of e.g. size), which are more rare relative to the percent coral cover typically used as input in most coral models (Matz et al. 2018; McManus et al. 2020). As a result, coral IPMs typically are built around specific populations for which these data have been collected (e.g. Montero-Serra et al. 2018; Scavo Lord et al. 2020; Cant et al. 2021). IPMs have also been expanded to include the evolutionary dynamics of diallelic traits (Coulson et al. 2011) as well as polygenic traits via the Breeder's equation to determine phenotypic change (Janeiro et al. 2017), and more recently genotypic change directly (Childs et al. 2016; Coulson et al. 2017, 2021; Simmonds et al. 2020). These 'evolutionarily-explicit' IPMs (*sensu* Coulson et al. 2021) split phenotypic variance explicitly into 'genotype' and 'environment' components of phenotype (*g* and *e*, respectively), similar to how the animal model partitions genotypic variance into (additive) genetic variance and residual variance (Childs et al. 2016; Coulson et al. 2021). Therefore, these models lend themselves well to combining animal models of genetic inheritance to determine both additive genetic variance and heritabilities of traits as well as environmental covariates that themselves can contribute to the degradation of environmental conditions (Childs et al. 2016; Coulson et al. 2021). However, for corals, no longitudinal datasets that also include genetic relatedness among corals likely exist or can be measured, given the lack of relatedness among nearby settled colonies. This is because gametes often travel hundreds of miles from their parents (Thompson et al. 2018), making the identification of parents, or even half-siblings logistically implausible in the field. Therefore, separate datasets for coral evolution and demography must be integrated in order to predict coral evolution in response to future heat stress.

Thesis aims

In this thesis, I examine a number of key questions posed above, namely: **(a) at what rate could coral populations evolve? (b) how does local demography and recruitment determine coral population persistence and stability?** And finally, **(c) how will local demography and population adaptation combine to determine coral populations in the future, given predicted heat stress due to anthropogenic climate change?** Question (a) is addressed in **Chapter 2** using a meta-analysis of coral heritability estimates across the literature to determine likely rates of adaptation across various traits. Question (b) is examined in **Chapter 3** by constructing a single-species density-dependent IPM of corymbose corals. I use corymbose corals because studies of heritability and other parameters important for evolutionary modelling have been most studied for corals with this growth form (e.g. *Acropora millepora and A. tenuis*). **Chapter 4** then combines findings from Chapters 2 and 3 to address question (c) by building the first evolutionarily-explicit IPM for corals in order to evaluate population outcomes and extinction risk under four different SSPs predicting future heat stress on the GBR over the next 80 years. Finally, I discuss the limitations to heritability and my modelling approach, as well as potential future extensions to the model that would improve its generality and accuracy in order to predict future coral population pathways in **Chapter 5**. Overall, my results show that evolutionary rescue of reefs is possible under limited scenarios and that model projections are greatly affected by density dependent regulatory mechanisms. My thesis is novel as a fundamental framework for coral evolutionary IPMs and useful to scientists and policy makers aiming to best manage reefs in the context of future climate change.

Chapter 2 Meta-analysis reveals high heritability across multiple traits

Abstract

Anthropogenic climate change is a rapidly intensifying selection pressure on biodiversity across the globe and, particularly, on the world's coral reefs. The rate of adaptation to climate change is proportional to the amount of phenotypic variation that can be inherited by subsequent generations (i.e. narrow-sense heritability, h^2). Thus, traits that have higher heritability (e.g. $h^2 > 0.5$) are likely to adapt to future conditions faster than traits with lower heritability (e.g. $h^2 < 0.1$). Here, I synthesize 95 heritability estimates across 19 species of reef-building corals. My meta-analysis reveals low heritability ($h^2 < 0.25$) of gene expression metrics, intermediate heritability ($h^2 = 0.25–0.50$) of photochemistry, growth, and bleaching, and high heritability ($h^2 > 0.50$) for metrics related to survival and immune responses. Some of these values are higher than typically observed in other taxa, such as survival and growth, while others were more comparable, such as gene expression and photochemistry. There was no detectable effect of temperature on heritability, but narrow-sense heritability estimates were generally lower than broad-sense estimates, indicative of significant non-additive genetic variation across traits. Trait heritability also varied depending on coral life stage, with bleaching and growth in juveniles generally having lower heritability compared to bleaching and growth in larvae and adults. These differences may be the result of previous stabilizing selection on juveniles or may be due to constrained evolution resulting from genetic trade-offs or genetic correlations between growth and thermotolerance. While I find no evidence that heritability decreases under temperature stress, explicit tests of the heritability of thermal tolerance itself – such as coral thermal reaction norm shape – are lacking. Nevertheless, my findings overall reveal high trait heritability for the majority of coral traits, suggesting corals may have a greater potential to adapt to climate change than has been assumed in recent evolutionary models.

346 **Introduction**

347 Anthropogenic climate change is one of the greatest selective pressures on organisms
348 worldwide (Davis et al. 2005; Hughes et al. 2018b; Nolan et al. 2018). To avoid extinction, species
349 need to either acclimatize, move to new habitats, or adapt to new conditions (Davis et al. 2005; Jump
350 and Peñuelas 2005; Gienapp et al. 2008). Acclimatization on its own may initially increase the
351 duration of time that a population can persist in an altered environment, but is bounded by
352 physiological thresholds that limit tolerance of long-term environmental change, and for populations
353 living close to their extremes already (van Heerwaarden et al. 2016; Comte and Olden 2017; Sasaki
354 and Dam 2019). Migration to new environments is similarly limited (Jump and Peñuelas 2005;
355 Schloss et al. 2012; Walters and Berger 2019), especially for predominantly sessile organisms for
356 which range extension depends upon long-distance dispersal of offspring (Hughes et al. 2003;
357 Archambault et al. 2018; c.f. Kremer et al. 2012). Consequently, understanding whether and how
358 species are likely to adapt to future conditions is crucial in predicting species persistence in the context
359 of climate change (Logan et al. 2014a).

360 Adaptive evolution to a changing environment occurs when population genotype frequencies
361 change to express traits or phenotypes that provide increased fitness (Falconer and Mackay 1996).
362 However, adaptation of a trait can only occur at a rate proportional to the narrow-sense heritability
363 coefficient, h^2, calculated as the ratio between population variance attributable to additive genetic
364 effects, V_a, and the total observed phenotypic variance, V_p. The narrow-sense heritability coefficient is
365 a key parameter in the univariate 'Breeder's equation', which predicts the mean population response in
366 trait values for a single trait undergoing selection.

367 Different traits often have different heritability coefficients, and may also covary with one
368 another (Wright et al. 2019). Counterintuitively, traits which are tied closely to biological fitness (e.g.
369 life history traits, longevity/survival, fecundity) often have relatively low heritability compared to
370 physiological and behavioural traits, and compared to morphological traits that often have higher
371 heritability (Mousseau and Roff 1987; Price and Schluter 1991; Wheelwright et al. 2014; Martins et al.
372 2019). For example, when populations have previously undergone strong stabilizing selection for a
373 trait tied closely to fitness, the narrower range and variance of trait values observed in the population

translates to a reduction in the relative contribution of additive genetic effects to total phenotypic variation, and a decrease in the heritability coefficient (Charmantier and Garant 2005; Teplitsky et al. 2009; Wheelwright et al. 2014). Understanding the potential rate and limits to adaptive evolution will therefore require an understanding of heritability across different traits (Wheelwright et al. 2014).

Selective pressures differ not only in terms of the trait being examined, but also across life stages/ages, growth forms, and environments (e.g. genotype-by-environment interactions). Thus, heritability should vary across these factors as well (Charmantier and Garant 2005; Wilson et al. 2008; Wheelwright et al. 2014). Early life stages/ages can experience strong stabilizing selection for traits associated with early life fitness, and thus exhibit reduced h^2 for these traits. Increasing importance of environmental effects and acclimation to local environments can also reduce the relative importance of additive genetic variation and thus h^2 at intermediate stages/ages (Charmantier et al. 2006a). Finally, late-acting mutations can accumulate in older individuals to cause age-dependent increases in $V_{A,}$ and thus h^2, for traits tied closely with fitness (Charmantier et al. 2006a, 2006b; Wilson et al. 2008). Similar selective pressures can result in similar h^2 values for traits of species occupying similar ecological niches. For example, in reef-building corals, colony growth form directly influences individual growth rate, fecundity, and survival (Pratchett et al. 2015; Madin et al. 2020). Tabular coral species (which form large horizontal plates supported by a central stalk) exhibit increased adult mortality relative to other coral growth forms in the same habitat due to their increased mechanical vulnerability (Madin et al. 2014). However, it remains unknown whether and how heritability of traits varies among coral species with different growth forms.

In the context of climate change, decreasing environmental suitability and increasing selective pressure on traits tied closely to fitness can reduce trait heritability, resulting in a counter-intuitive reduction in the capacity for populations to evolve to environmental change (Charmantier and Garant 2005; Wilson et al. 2006; Wheelwright et al. 2014). Conversely, other studies have found no distinguishable relationship between h^2 and environmental favourability (Rowínski and Rogell 2017), and others still identify positive correlations of h^2 with increasingly harsh environmental temperatures (Gunay et al. 2011). Clearly, further research is required to quantify how heritability may change

401 across life stages and environments of the future, especially when attempting to project population
402 outcomes in response to future conditions.

403 Reef-building scleractinian corals are particularly sensitive to climate stressors, as evidenced
404 by coral bleaching during thermal anomalies. Reef diversity and coral cover have declined throughout
405 the 21st century (Wulff 2006; Pratchett et al. 2011; Hughes et al. 2018b), with 75% of global reefs now
406 being considered threatened (Burke et al. 2011). Widespread bleaching of coral communities now
407 occurs at temperatures approximately 0.5°C higher than a decade ago, suggesting strong selection for
408 increased thermotolerance worldwide (Maynard et al. 2008; Guest et al. 2012; Sully et al. 2019).
409 However, given the rapid warming of sea surface temperatures and the increase in the frequency and
410 severity of mass bleaching events on coral reefs worldwide (Hughes et al. 2018a; Lough et al. 2018), it
411 remains unclear whether corals can adapt to the prolonged thermal stress they now experience with
412 increasing regularity (Pandolfi et al. 2011; Hoegh-Guldberg et al. 2017). Models estimating long-term
413 coral adaptation to climate change have assumed low to medium heritability of thermotolerance (e.g.
414 h^2 = 0.01–0.50; Cropp and Norbury 2020; Matz et al. 2020; Logan et al. 2021), despite some evidence
415 of model outcomes being sensitive to the rate of adaptation (Bay et al. 2017b; Cropp and Norbury
416 2020), evidence of high heritability for coral survivorship in high temperatures (e.g. h^2 = 0.75: Kirk et
417 al. 2018), and the potential for rapid symbiont evolution in response to thermal change (e.g.
418 Chakravarti et al. 2017; Buerger et al. 2020). Therefore, the ability to project the future of coral
419 populations in the context of climate change is critically dependent upon the estimates of trait
420 heritability used in eco-evolutionary models (Visser 2008; Logan et al. 2014a, 2014b).

421 Worldwide, reef-building corals are undergoing increasingly strong selection for temperature
422 tolerance due to anthropogenic climate change. Here, I undertake a quantitative meta-analysis of
423 published heritability estimates for reef-building corals to better understand which traits are likely to
424 change most rapidly given increased environmental change. I examine the relative heritability of
425 different trait types such as coral gene expression, bleaching, growth, symbiont community structure,
426 and survival, and investigate potential interactions among life stages and, for experiments that
427 manipulate temperature, to the magnitude of temperature stress to which corals are exposed. I also
428 estimate the relative heterogeneity of heritability estimates, examine differences between narrow-sense

vs. broad-sense heritability estimates, and identify how differences in coral growth forms influence estimates of h^2.

Methods

Literature search

I undertook an exhaustive literature review to find all possible heritability point estimates and associated measures of sampling variance (e.g. standard errors, confidence or credibility intervals) for scleractinian corals by canvassing two major research databases: Google Scholar and Web of Science. Keyword searches were conducted in October 2020 to identify all studies reporting heritability estimates for corals, and/or their associated symbionts. I searched for studies using the keywords and Booleans: "heritability" AND "coral" OR "familial effects" AND "coral". I found a total of 16 studies reporting heritability and one study with heritability estimates that could be extracted from the published data. I then mined the references cited within each paper from the initial search to identify two additional studies reporting heritability estimates. I contacted some study authors when text alluded to heritability estimates, but values were not reported in the final manuscript, all of whom kindly contributed those heritability estimates to this analysis. Where possible, I selected single heritability estimates calculated using a fixed effect of temperature or other treatment, rather than taking multiple heritability estimates calculated by splitting the data by each treatment. Many of the studies report multiple heritability estimates for the same or similar traits. For five studies (Lohr and Patterson 2017; Kirk et al. 2018; Manzello et al. 2019; Wright et al. 2019; Zhang et al. 2019), I selected one representative heritability estimate when there were multiple and highly related h^2 estimates (e.g. Kaplan-Meier survival and percent survival; symbiont abundance and chlorophyll A content; total linear extension and net buoyant weight). Finally, I extracted both broad-sense (H^2) and narrow-sense (h^2) heritability estimates for the same trait where both were reported together in order to examine differences between H^2 vs. h^2; however, this occurred only for a single study (Carlon et al. 2011).

The above resulted in a total of 103 unique heritability values estimated using a number of methods (see Supplementary Text A1 for a description of the different methods used). Of the 103 total

457 estimates, eight were further excluded on the basis of statistical issues for one of two reasons: (1) there
458 was insufficient variation in relatedness among individuals to properly assess heritability (one study
459 with one estimate), or (2) there was insufficient or expected null variation in the phenotype being
460 examined (two studies, with one and six estimates each). The latter was the case when studies
461 estimated heritabilities associated with coral mortality or bleaching while in ambient conditions, which
462 results in little to no phenotypic variation from which to calculate narrow-sense heritability (i.e. none
463 of the corals bleached or died). This left 95 unique and valid heritability estimates from 19 studies.
464
465 *Pre-processing*
466 Heritability is calculated as a proportion of total phenotypic variation, and thus is constrained
467 to fall between zero and one (Falconer and Mackay 1996). Because most classical meta-analytical
468 statistical models assume normally-distributed uncertainty, transformation of the estimates prior to
469 meta-analysis was necessary (Viechtbauer 2010; Lin and Xu 2020). Thus, I converted point estimates
470 of heritabilities and associated standard errors (SE) to 95% confidence intervals, then transformed
471 both the point estimates as well as the upper and lower 95% confidence (or Bayesian credible) limits
472 to the natural logarithmic scale using the transformation:

$$h_T^2 = ln[h^2 + 0.2] \quad (1)$$

473 with a horizontal displacement of + 0.2 to avoid excluding lower h^2 CIs that had slightly negative
474 values when the point estimate was close to zero (see Supplementary Text A2 and Supplementary
475 Code Documentation A for details). Other transformations were also attempted, however, the log-
476 transform of means and confidence limits was the only transformation that somewhat conserved the
477 linear relationship between original and transformed variances (Supplementary Code
478 Documentation A).
479 There were four estimates from two studies that did not report any associated SE or CI values,
480 and another three estimates whose lower CI values (when calculated from the SE) were less than -0.2,
481 which prevented their transformation to the *ln*-scale. To include these data in the meta-analysis but
482 down-weight their leverage on the overall analysis, I fit a quantile regression through the 95th quantile
483 of transformed SE vs. transformed h^2 (Koenker and Hallock 2001; Koenker 2020) using only

heritability estimates that were able to be transformed to the *ln*-scale. I then used this fitted equation ($SE_T = 0.255 – 0.452 \cdot h^2_T$) to interpolate missing SE_T values, making the conservative assumption that they would have values at the upper 95th quantile (i.e. among the most uncertain estimates).

Factors of interest

I identified five explanatory factors present in most studies: trait type, heritability type, life stage, growth form, and temperature manipulation (Table 2.1). Differences in heritability estimates among specific coral/symbiont species were also of interest; however, most studies examined only a single species and there was little overlap in species across studies, with the exception of a number of studies examining *Acropora millepora* heritability.

494 **Table 2.1.** Explanatory factors and covariates examined in the meta-analysis of coral heritability estimates

Factor/Covariate	Levels	Definition
Heritability type	Broad-sense heritability, H^2	The proportion of phenotypic variation explained by all genetic effects, which includes sources of variance associated with additive, dominance, and epistatic effects
	Narrow-sense heritability, h^2	the proportion of phenotypic variation explained by additive genetic effects
Trait type	Gene expression	Up- or down-regulation of various genes involved in intracellular stress pathways
	Photochemistry	Measures of symbiont photochemistry, chromoprotein content
	Growth	Coral or corallite growth measures including calcification rates, buoyant weight change, larval areal expansion, linear extension, and new growth branches
	Nutrient content	Total protein or carbohydrate content present in hosts or whole holobiont tissues
	Bleaching	Symbiont cell densities or change in cell densities, bleaching index scores (a proxy for symbiont cell density), and Chlorophyll A content (correlated to symbiont cell density)
	Morphology	Static intraspecific corallite measurements and larval volumes upon birth
	Symbiont community	Symbiont community indices (Leinster and Cobbald's *D*) and the proportion of symbionts that are more thermally tolerant (i.e. *Durusdinium* spp.)
	Immune response	Catalase and phenoloxidase activity within holobiont tissues
	Survival	Measures of survival/mortality/settlement success, including counts of settlement success or survival, percent survival/mortality at the end of a fixed period, larval survival through high temperatures, or differences in survival between control and temperature treatments
	Gamete compatibility	π-value, the percent larval contribution of various sires to various dams. Excluded from meta-analysis due to the presence of only a single estimate
Coral life stage	larvae	Estimates for free-swimming gamete or planula larvae stages up to successful settlement
	juvenile	Estimates from post-settlement to sexually mature adult
	adult	Estimates from colonies after sexual maturity or using coral nubbins
Coral growth forms	branching	Arborescent form; tree-like branching extensions
	corymbose	Finger-like extensions
	massive	Ball- or boulder-shaped corals
	encrusting	Low-spreading corals often occurring on hard, rocky substrates
	columnar	Upwards-growing cylindrical corals

Temperature difference	covariate	Difference (in +°C) between the study's reported control or ambient temperature and the heat treatment temperature

495

Reported heritability estimates

I collected a total of 95 valid heritability estimates from 19 independent studies of scleractinian corals (Fig. 2.1). Three studies (Császár et al. 2010; Wright et al. 2019; Quigley et al. 2020b) each involving multiple trait types, provide 59% of all heritability estimates (Fig. 2.1-left). There was an even split of studies (9:9 studies) examining narrow-sense (h^2) and broad-sense (H^2) heritability, with one study (Carlon et al. 2011) reporting both heritability types. However, the number of raw estimates produced by each study differed markedly, with more broad-sense estimates (n = 70) than narrow-sense (n = 25). The studies also differed in terms of which trait type was reported, with most studies reporting only a single estimate (12 studies), and the other seven studies reporting on two to six distinct trait types. Survival was the most frequently studied trait type (nine studies, 15 estimates), while bleaching (six studies, 10 estimates) and growth (six studies, 23 estimates) were also diversely studied. The latter often included comparisons of multiple species or symbionts within the same study, resulting in a large number of estimates. Most trait type estimates originated from at least two independent studies estimates, save for immune response (four estimates from one study) and gamete contribution (one estimate). I therefore interpret the results for immune response with caution, given that they all belong to the same study, and excluded the single estimate for gamete compatibility from the subsequent meta-analysis. Notably, there were limited studies of the heritability of coral reproduction and fecundity, and there were no heritability estimates of thermal optimum (T_{opt}), measures of performance breadth (e.g. B80, B95), or critical thermal limits ($CT_{max/min}$). Only three studies reported the total phenotypic variation and/or the level of additive genetic variation, which would be particularly useful for calculating metrics of evolvability (Visscher et al. 2008; Ma et al. 2014). I therefore recommend that future studies report these estimates of variation.

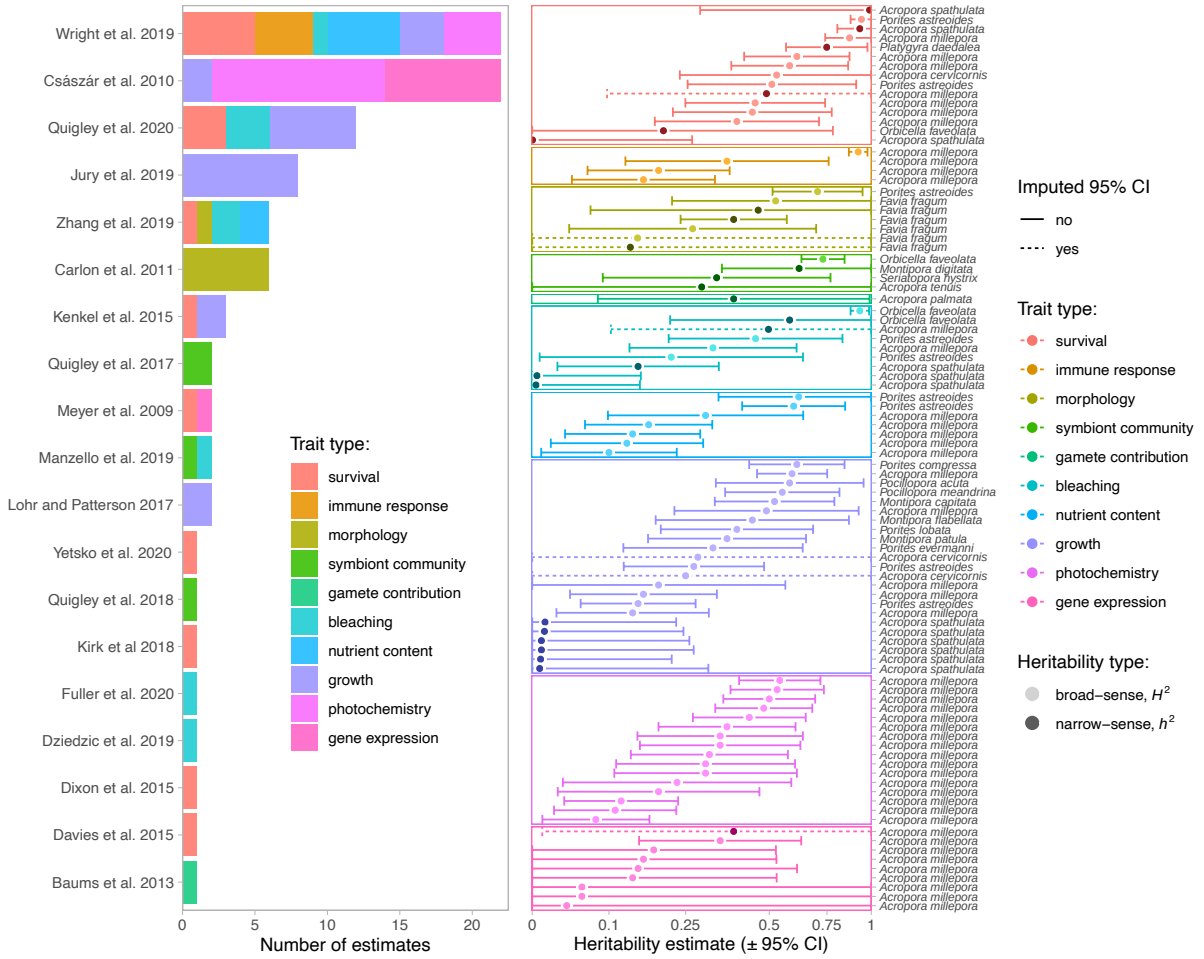

Fig. 2.1. Heritability estimates ($N = 95$) of various traits across 19 studies of reef-building corals. Colour indicates the specific trait type (hue) and heritability type (broad-sense H^2 as lighter tint circles, narrow-sense h^2 as darker shade). Left: Number of estimates reported in each study. Right: Point estimates of heritability and their associated 95% confidence/credible intervals (whiskers) on a logarithmic (*ln*) scale. Heritability estimates closer to one indicate higher heritability and thus the potential for higher rates of trait adaptation within the population. Dashed lines represent heritability estimates where standard errors/confidence intervals were imputed.

For life stage, there were 63 estimates (from eight studies) for adults, 18 estimates for juveniles (from seven studies), and 14 for larvae (from five studies), with every study reporting on only a single life stage save for two reporting on two different life stages (Carlon et al. 2011; Quigley et al. 2017). There was similar lack of overlap across heritability types (70 broad-sense vs. 25 narrow-sense heritability estimates across 10 vs. 10 studies, respectively), with only one study having both

valid broad-sense and narrow-sense heritabilities (Carlon et al. 2011). Across coral growth forms, there were 61 estimates of corymbose corals (from seven studies), 21 estimates for massive corals (from eight studies), nine estimates for branching/arborescent (from six studies), and three and one estimates for encrusting and columnar corals, respectively (each from a single study). Finally, 14/19 studies (83/95 estimates) recorded temperatures, and thus the effect of temperature manipulation on heritability could be examined for these studies. However, the difference between the manipulated vs. control/ambient temperatures varied substantially across each study, with all temperature manipulation differences being positive (i.e. control/ambient conditions were always less than the treatment temperatures) but positively skewed (a few experiments used temperatures that differed by 10°C between control and high temperature treatments, but most used smaller elevations of temperature). For example, 29 estimates of heritability originated from control/ambient conditions (from seven separate studies), while 54 estimates were obtained from above-ambient temperature treatments (from 12 studies). Additionally, there was limited overlap of control and heated temperature differences for some trait types, making it difficult to compare the effect of temperature for trait types such as symbiont community (two control estimates), morphology (one control estimate) and gene expression (nine temperature differences, but no control estimates).

Meta-analysis approach

I used the *R* package *metafor* (Viechtbauer 2010) to fit mixed-effects meta-analytic models to $ln(h^2 + 0.2)$ transformed heritability estimates (h^2_T) and associated estimate sampling variance, while accounting for both fixed and random effects. The log-transformation was determined as most appropriate in preserving a relatively linear relationship between the original variance estimate and the transformed variance. The addition of the constant 0.2 was used to minimize the studies that would need to be excluded (see Supplementary Code A for details). Due to some missing combinations of explanatory factors within the dataset (e.g. not all traits were measured for all life stages, or for all coral growth forms), the complete dataset only allowed us to consider additive effects of trait type, heritability type, life stage, and growth form in an overall analysis. Temperature was not controlled for or measured in all studies, and thus was excluded as a covariate at this stage. To further assess the

560 robustness of this model and examine interactions, I then analysed subsets of the complete dataset to
561 test for: (a) trait × life stage interactions, (b) trait × heritability interactions, and (c) main effects and
562 interactions involving growth form. Finally, I examined a subset of the complete data that reported
563 treatment temperature differences relative to ambient temperature, including trait × temperature
564 difference interactions and additive effects of life stage, heritability type, and growth form. All models
565 were fit using more conservative t-distribution approximations of confidence intervals in the case of
566 multi-level random effect models, and final models fit using the more conservative Knapp and
567 Hartung (2003) adjustment for single-level random effect meta-models when multi-level random
568 effects structures were not selected during model selection (Viechtbauer 2010; van Aert and Jackson
569 2019).

570 I considered the top model for each analysis as the model with the lowest Akaike's
571 Information Criterion, corrected for small sample sizes (AICc). I considered this model a substantial
572 improvement over other candidate models when the difference in AICc scores (ΔAICc) was greater
573 than two (Burnham and Anderson 2004). I followed the four-step model selection strategy outlined in
574 Zuur et al. (2007, 2009): (1) define the 'beyond optimal' fixed effects structure – that is, the most
575 conceivably complex yet biologically relevant fixed effects possible, (2) select (via the lowest AICc
576 value) the optimal random effects structure for models fit using restricted maximum likelihood
577 (REML), (3) select (via the lowest AICc value) the optimal fixed effects structures for models fit using
578 maximum likelihood, (4) re-fit the final model using REML. Study and species were highly
579 confounded and precluded the inclusion of both as random effects within the same model. Thus, I fit
580 models using one of the following random effects structures: estimate ID only (1|estimate ID), study
581 ID only (1|study ID), species only (1|species), estimate ID nested within its respective study ID
582 (1|study ID/estimate ID), estimate ID nested within species (1|species/estimate ID), or a random effect
583 variance fixed at zero.

584 After fitting models for each analysis, I examined the level of among-study heterogeneity (τ^2)
585 using the I^2 index (Higgins and Thompson 2002), which provides an estimate of the among-study
586 variance relative to the total variance not explained by the fixed effects. I used the Q_E statistic to test
587 for significant residual heterogeneity after accounting for fixed effects (Viechtbauer et al. 2015).

588 Higher proportions of heterogeneity indicate that variation in true effect size of heritability is a
589 distribution of study effects (i.e. due to methodological or other study differences), whereas lower
590 heterogeneity indicates that any among-study heterogeneity is likely small relative to measurement
591 error, so studies are measuring a common heritability value (Higgins and Thompson 2002; Ban et al.
592 2014). I report the pseudo-R^2 for meta-analytical models, computed by comparing the difference in $\hat{\tau}^2$
593 estimated using models including fixed effects ($\hat{\tau}^2_{ME}$) vs. a model with the same random-effects
594 structure, but with no fixed effects ($\hat{\tau}^2_{RE}$): $R^2 = (\hat{\tau}^2_{RE} - \hat{\tau}^2_{ME})/\hat{\tau}^2_{RE}$ (Raudenbush 2009). Where
595 significant interactions were found between factors with more than two levels, I employed
596 simultaneous tests for testing multiple general linear hypotheses determined by visual inspection of
597 marginal estimates, and report p-values adjusted using the single-step method.
598 Model standardized residuals were plotted against fitted values to look for strong deviations
599 from normality, and data were simulated using the fitted model and plotted with the true data to assess
600 model performance. I assessed the presence of publication bias by plotting the model residuals by their
601 precision (inverse of standard error) to produce a funnel plot (Møller and Jennions 2001). I also
602 calculated the Rosenberg fail-safe number, which indicates if model findings are robust to any
603 apparent publication bias if the number is greater than five times the number of studies plus ten
604 (Rosenthal 1991; Rosenberg 2005). Finally, I used Cook's distances to determine highly influential
605 points for each model (Cook and Weisberg 1982).
606
607 **Results and Discussion**
608 *High heritability of coral traits*
609 The results of the overall analysis reveal that the heritability of coral traits has considerable
610 heterogeneity that can be explained by trait type. The final selected model used trait type as the sole
611 explanatory factor, and had substantial residual heterogeneity ($QE_{85} = 478$, $p < 0.0001$), with the total
612 percent of variance not attributable to sampling error, $I^2_{total} = 91\%$, composed of predominantly
613 between-study variance ($I^2_{study} = 57\%$ of total), but with substantial within-study variance ($I^2_{estimate} =$
614 34% of total) as well. In all models, random effects involving estimate ID, study ID, or estimate ID
615 nested in study ID were always selected, with no support for random effects involving species.

Trait type was by far the most important predictor of heritability across all studies (see supplementary code documentation C: Supplementary Tables and Figures Table A1 – link in Appendix A), with traits such as gene expression having low heritability ($h^2 < 0.25$); photochemistry, growth, nutrient content, symbiont abundance, morphology, and symbiont community having moderate heritability ($h^2 = 0.25–0.5$); and immune response and survival/larval settlement success having the highest heritability estimates ($h^2 > 0.5$; Fig. 2.2). However, models that included additive effects of trait type + heritability type and trait type + life stage were supported by model selection (i.e. they fit almost as well as the model with trait type alone). However, the effect sizes of both were small relative to the effect of different trait types (Table A2; Fig. A2). For example, broad-sense heritabilities were 1.4–2.1 times higher than narrow-sense heritability and varied by a factor of 1.1 to 2.1 across different life stages (within the same trait type), whereas trait type differences were much larger, being up to 6.7 times larger in the case of survival vs. gene expression. Estimates for the mean heritability of different traits ranged from low to high, but most traits were moderately heritable (Fig. 2.2). Gene expression traits had the lowest estimated mean heritability (h^2=0.12), while survival had the highest (h^2=0.79), followed by immune response (h^2=0.62), with the other estimated trait mean heritabilities falling between 0.26–0.50 (Fig. 2.2). One estimate in particular, a value of 0.92 for *Acropora millepora* (Wright et al. 2019), drove the high heritability of immune response (Cook's distance = 5.2), while all other Cook's distances were relatively low (< 2). Thus, the estimated high heritability of immune response should be interpreted cautiously.

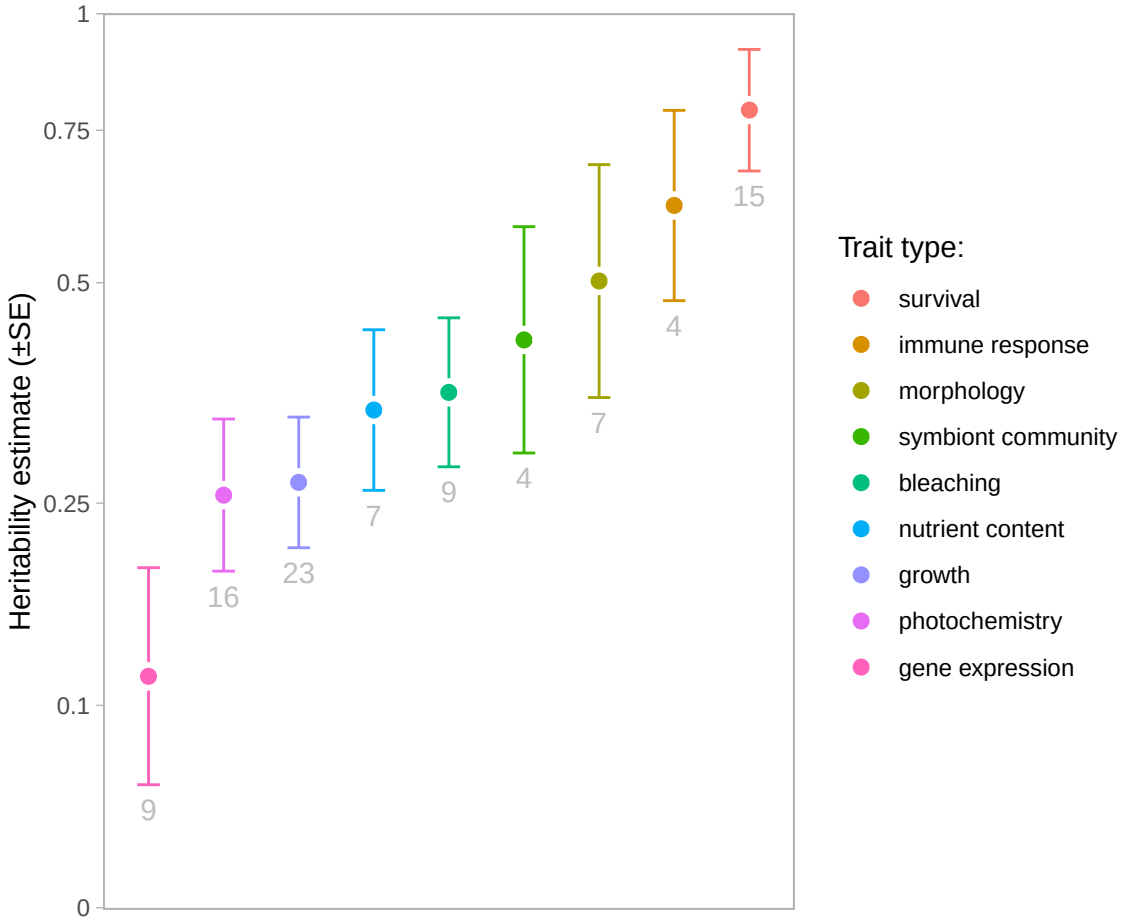

Fig. 2.2. Heritability estimates ± SE for the trait type-only model, not accounting for differences due to (i.e. pooled across) life stage and heritability type. Traits are sorted along the spectrum according to their overall relative heritability, with heritability closer to one indicating more heritable traits. The number of estimates included in the meta-analysis for each trait type are indicated below each error bar in grey. The gamete compatibility trait type is excluded due to its reliance on only a single study/estimate.

The final model's funnel plot exhibited no signs of publication bias (Fig. A1), and the fail-safe number (i.e. the number of null-result studies required to overturn a significant result) was an order of magnitude above five times the number of studies plus ten (1,285 >> 100), indicating that the model findings are robust to any underlying publication bias.

Heritability across trait types in other organisms

Heritability differences across trait types have been widely reported in other taxa (Mousseau and Roff 1987; Wheelwright et al. 2014; Polderman et al. 2015; Flood et al. 2016). Life history traits closely tied to fitness (e.g. longevity, fecundity) are often maintained due to strong stabilizing selection and thus exhibit lower heritability compared to morphological, physiological, and behavioural traits (Mousseau and Roff 1987; Price and Schluter 1991; Teplitsky et al. 2009; Wheelwright et al. 2014). However, traits may also have low heritability due to a large contribution to total variance by non-additive genetic variation, environmental variation, or through maternal effects (the latter likely to be less pronounced in broadcast spawning corals than in organisms with higher levels of parental care). Gene expression had the lowest heritability, which is consistent with many other studies noting the low heritability of mRNA (i.e. the 'missing heritability' problem, Zuk et al. 2012; Yang et al. 2014). While the exact cause of missing heritability for gene expression measures has yet to be determined, it may be due to highly variable gene expression both within (i.e. low repeatability) and among individuals, or to epistatic gene interactions, or some combination of both (Zuk et al. 2012; Yang et al. 2014). The heritability of symbiont community composition was much higher than heritabilities estimated for the diversity of human gut microbes (h^2 = 0.019), which is predominantly environmentally rather than genetically-determined (Rothschild et al. 2018). However, beneficial microbes that are related to metabolic health, such as gut bacteria of the family Christensenellaceae, and microbiomes of mice in controlled laboratory environments (Org et al. 2015), show much higher heritabilities of h^2=0.3–0.6, more consistent with my findings. Photochemical traits were estimated to have modest heritability in the analysis; however, only two studies which included only broad-sense estimates were available (H^2 = 0.26). In plants, broad-sense heritability of photosynthetic traits is variable but can be very high (e.g. H^2 = 0.87, 0.5 – 0.99, and 0.99; Geber and Dawson 1997, Flood et al. 2016, and Tuhina-Khatun et al. 2015, respectively). Moderate narrow-sense heritability estimates, similar to those reported here, have been reported for narrow-sense heritability of maximum quantum yield in plants (h^2 = 0.12–0.34) (Qu et al. 2017). Heritability associated with bleaching and symbiont abundance in corals (often using chlorophyll content as a proxy) was

676 estimated overall as h^2 = 0.36, which is similar to estimates of broad-sense heritability of chlorophyll
677 content in plants (e.g. h^2 = 0.44-0.49 in *Oryza sativa* L., Tuhina-Khatun et al. 2015).
678
679 *Life stage and heritability type, but not growth form, mediate trait heritability*
680 Using a data subset to examine trait type and life stage interactions, a model of trait type × life
681 stage + heritability type with a random effect of estimate ID only was preferred under model selection
682 (Table A3). Other analyses of trait type versus heritability type interaction and trait type and growth
683 form interaction found further support for a trait type × life stage interaction (see Supplementary Text
684 A3). The final meta-model had moderate levels of heterogeneity among estimates (QE_{55} = 96, p =
685 0.0005; I^2_{total} = 47%) and fixed effects helped explain much of the variation in heritability estimates
686 (pseudo R^2 = 78%). Parameter estimates for all trait types were similar to the previous overall model
687 estimates (Fig. 2.3; Fig. A3; Table A4), but there were significant interactions for growth and
688 bleaching in juveniles relative to other life stages as well as a for nutrient content in adults (Fig. 2.3;
689 Table A4). Cook's distances for the trait type × life stage + heritability type model were low overall (≤
690 2), but three points had moderate leverage on the analysis (Cook's distance = 2.9–3.9), but the
691 growth:juvenile interaction term remained important when any or all were excluded from the analysis.
692 Coral growth form was never an important predictor of heritability, and species was never selected as
693 an important random effect, suggesting that taxonomic differences may be too small or variable to
694 detect, given the data currently available.
695 Life stage had a strong effect for certain trait type–heritability type combinations (Fig. 2.3;
696 Table A4). For example, the estimated narrow-sense h^2 for bleaching metrics in adults was 9.1 times
697 the same h^2 for juveniles, and two times the bleaching H^2 value in adults versus larvae. Growth and
698 nutrient content broad-sense heritability also differed across life stage, with adult growth H^2 being 3.1
699 times that of juveniles and nutrient content H^2 being 3.9 times greater in larvae vs. adults. In contrast,
700 the effect of heritability type was relatively weak (1.4 to 2.5–fold higher for broad-sense heritabilities
701 vs. narrow-sense when controlling for trait type and life stage) compared to the effect of trait type on
702 heritability, which was up to 13.2 times higher heritability when comparing h^2 between juvenile
703 bleaching vs. survival (Fig. 2.3; Table A4). This indicates that either dominance and epistasis effects

are generally small relative to additive genetic effects, or that the standard errors of the heritability estimates are large enough to obscure the detection of any major differences between H^2 and h^2. While it is highly likely that there is non-negligible non-additive genetic variation in corals – as in most organisms – there also was substantial variability observed across estimates within the same trait type (Fig. 2.3).

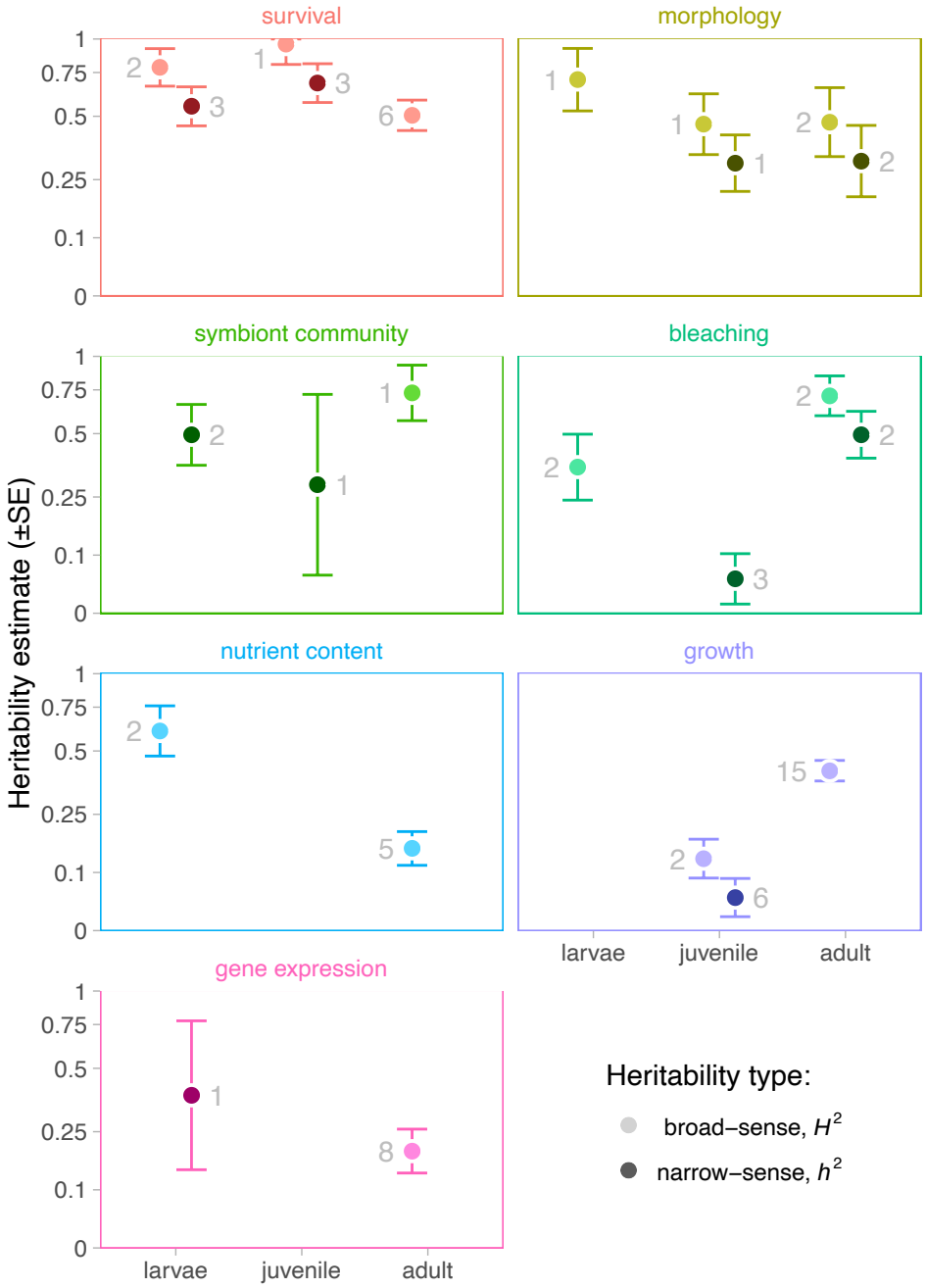

Fig. 2.3. Heritability estimates ± SE across trait types with multiple life stages (x-axis) and different heritability types (lighter points: broad-sense heritability; darker points: narrow-sense heritability).

712 Associated sample sizes (number of original estimates) are adjacent to each point in grey.

713

714 *Low adaptive potential of juvenile growth and bleaching*

715 Juvenile growth was much less heritable relative to adult growth, while bleaching was less
716 heritable in juveniles relative to both larvae and adults, highlighting the differential adaptive potential
717 of coral life stage to selection for some trait types. This reduced bleaching heritability from larvae to
718 juveniles may be the result of previous strong stabilizing selection on growth and bleaching traits in
719 juveniles, thus driving reduced additive genetic variance through the fixation of alleles and resulting in
720 lower heritabilities compared to other traits (Fisher 1930; Teplitsky et al. 2009). Indeed, bleaching
721 events likely represent a strong selective pressure for juvenile corals (Dajka et al. 2019; Hughes et al.
722 2019). Similarly, reductions in growth may result in increased mortality due to overgrowth
723 competition and size-dependent predation (Vermeij and Sandin 2008; Doropoulos et al. 2012; Madin
724 et al. 2014). There is also evidence that increases in additive genetic variance (V_A) may occur via
725 mutation accumulation across an organism's lifetime (Wilson et al. 2008b). Moreover, reduced
726 importance of local environment with age can result in reduced relative total variation, V_P (e.g. the
727 Wilson effect, Bouchard Jr. 2013). Both of these processes can therefore result in older life stages
728 having higher heritability estimates. Making the distinction between these processes requires
729 examining changes in V_A and V_P across an organism's lifetime, which no coral studies have done to
730 date.

731 Increased disturbances related to anthropogenic climate change are likely to select for
732 different species traits and communities (Herben et al. 2018; Pratchett et al. 2020), but little is known
733 regarding selection on life stages within the same trait. With increased frequency of bleaching events
734 resulting in more free space being made available to coral recruits, the adaptive potential of juvenile
735 coral growth rates may determine which corals become predominant in future communities. However,
736 negative trade-offs between bleaching and growth have been observed for coral symbionts (Little et al.
737 2004; Berkelmans and Van Oppen 2006; Cunning et al. 2015a) and juvenile coral hosts (Kenkel et al.
738 2015a; Morikawa and Palumbi 2019), such that more thermally specialised holobionts may exhibit
739 reduced growth rates in ambient conditions. If these phenotypic trade-offs are genetically based, the

genetic correlation between the two may constrain their evolution to climate change and thus would explain why the estimated heritabilities for juvenile bleaching and growth are lower compared to other life stages. More study of genetic correlations in juveniles is required to understand how juveniles are likely to respond to selection due to climate change; however, one laboratory selection experiment on adult fragments from *Acropora millepora* did find a significant positive genetic correlation ($r_g = 0.19$) between bleaching and growth (Wright et al. 2019). With increased study of narrow-sense heritabilities and especially genetic correlations among traits and at different life stages, the constraints on corals' responses to environmental change will come into sharper focus.

Confounding sources of variation

My review of the literature highlights some potential sources of bias in heritability estimates that are not well-controlled in coral studies to date. Studies that do not use shared common environments may overestimate heritability by confounding environment-driven phenotypic variation with additive genetic variation, such as when related individuals occur in the same environment and thus acclimatize similarly. Importantly, no studies examining adult corals raised corals to adulthood in a shared common environment, and thus do not control for preconditioning or canalization differences among colonies (Putnam and Gates 2015). However, coral larvae and juveniles were almost always raised in shared common environments during spawning and fertilization, thus larvae and juvenile heritability estimates are less likely to be overestimated due to this phenomenon. Despite this, there are a number of traits with higher heritability for larvae and/or juveniles relative to adults, such as survival, gene expression, nutrient content, and morphology (Fig. 2.3). This suggests that, at least for these traits, the variation associated with preconditioning and plasticity is unlikely to be particularly large relative to the additive genetic variance. Moreover, visual inspection of residuals suggested no additional unexplained variation that might be associated with whether or not a shared common environment was used (Fig. A9 in Supplementary Code C).

My results are also affected by other sources of phenotypic variation not accounted for in present studies, such as parental and epigenetic effects. Parental effects may have a larger influence on heritability than previously assumed (Noble et al. 2014; Kenkel et al. 2015b), and may be especially

768 important for brooding corals in which the offspring develops within the parent colony as well as for
769 species inheriting their symbiont communities directly from parents (i.e. vertical transmission)
770 (Kenkel et al. 2015b; Quigley et al. 2017). Vertically-transmitting brooders and broadcast spawning
771 species make up a minority of species examined (3/19 and 9/19, respectively), with the remaining
772 being horizontally-transmitting spawners. Similarly, the number of heritability estimates from vertical
773 transmitters made up only 9/95 and 16/95 heritability estimates, respectively, and thus parental effects
774 via brooding and/or vertical transmission would have impacted a minority of estimates. Epigenetic
775 effects may also inflate heritability estimates (Putnam and Gates 2015). In studies of multicellular
776 animals, there has been little support for epigenetic inheritance via CgP methylation (Torda et al.
777 2017), although at least one recent study in corals has found such evidence (Liew et al. 2020). Further
778 evidence is needed to determine if epigenetic changes confer fitness benefits similar to additive
779 genetic effects (Torda et al. 2017), thus future studies aiming to separate phenotypic variation specific
780 to parental effects, symbiont composition, epigenome, and additive genetic effects would be especially
781 valuable.
782
783 *Manipulated temperature has negligible effect on heritability*
784 When examining only studies that controlled for temperature, the magnitude of the experiment
785 temperature difference relative to ambient or control conditions had only a marginal effect on the
786 recorded heritability estimate (Fig. 2.4). The temperature difference values were all positive and
787 positively skewed, thus I square-root transformed the temperature difference data in order to reduce
788 the leverage of estimates obtained from studies using these large temperature differences. After
789 subsetting the data to exclude studies that did not report the temperature treatment used relative to
790 ambient conditions, I examined whether an interaction between trait type and temperature difference
791 was supported. Model selection favored a model of trait + heritability type, with some support for
792 alternative models of trait type only and trait type × temperature difference (Table A9; ΔAICc = 0.50
793 and 1.89, respectively) using random effects of estimate ID nested in study ID. The trait + heritability
794 type model had similar effect sizes compared to those in the analyses presented above (Fig. A6; Table
795 A10). The effect of trait type in the trait type × temperature model (3rd-optimal model) saw heritability

differences up to a factor of 3.4–4.6 when the temperature was increased +1°C to +3°C above ambient. However, within the same trait type, temperature alone had a reduced effect, with heritability differences between a factor of 0–2.1 and 0–1.6 for +1°C and +3°C, respectively. More specifically, temperatures +1°C above ambient resulted in immune response heritability increasing by a factor of 2.1, while an increase of +3°C above ambient would increase heritability by a factor of 1.6. This interaction was primarily driven by a single estimate of immune response (Cook's distance = 7.6), and when removed, resulted in no strong interactions between trait type and temperature. Within other traits, the effect of temperature was even less pronounced. Bleaching traits were decreased by 28–33% for an increase in temperature of +1–3°C (though this was not significant). Other traits such as growth, photochemistry, and survival all showed marginal declines in heritability with increasing temperature difference (~3–5% decrease in heritability with +1–3°C). Separate analyses examining temperature as a categorial variable (ambient vs elevated), as well as analyses omitting ambient treatments all resulted in similar weak to non-existent effects of temperature on heritability (Fig. A7-8; Tables A11-14), suggesting a limited effect of manipulated temperature on heritability across studies. Since a model of trait type + heritability type was preferred over the model of trait type × temperature manipulation (Table A9), and with the inclusion of heritability type precluding the ability to model a trait × temperature interaction, I fit an additive model of trait type, heritability type, and temperature difference to estimate the marginal effect of temperature and found evidence for, at most, a very weak effect of temperature (Fig. 2.4).

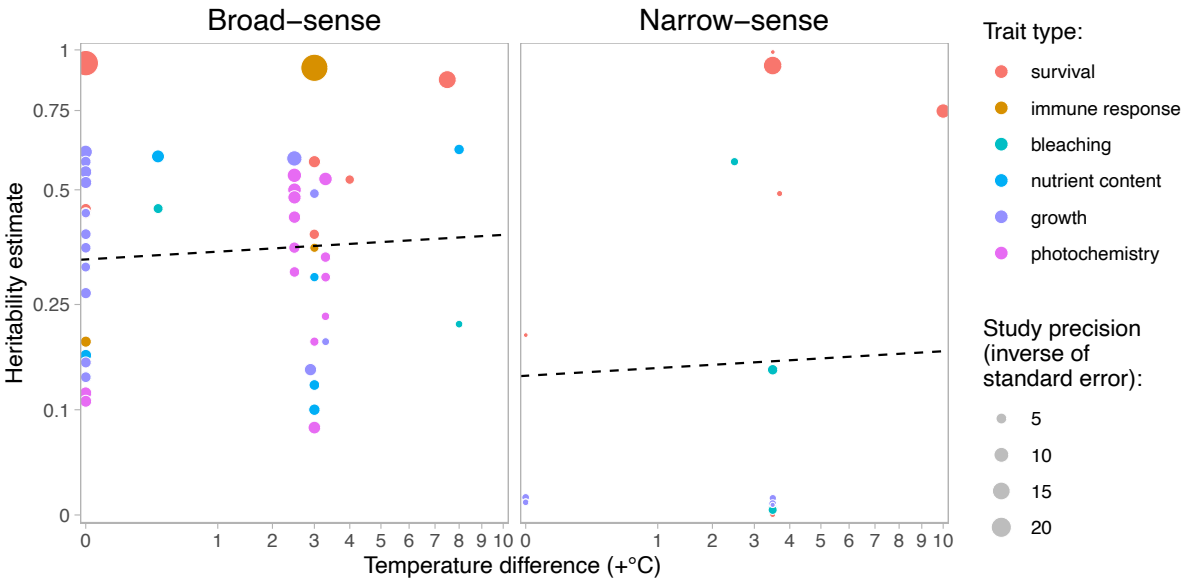

815

816 **Fig. 2.4.** Heritability vs. study temperature difference (treatment temperature relative to
817 ambient/control temperature) for each trait type and heritability type, with the size of each point
818 represents its relative precision. Dashed lines indicate the estimated marginal mean effect of
819 temperature difference, while accounting for trait type and heritability type effects. One square-root
820 degree difference (+1√°C) translates to a mean increase in $ln[h^2+0.2]$ heritability of 0.03 ± 0.05 SE.

Trait adaptation to warming temperatures

The meta-analysis suggests that the capacity for corals to adapt to warming temperatures may be relatively consistent over short periods of moderately high temperature (e.g. +1–3°C, the temperature increases used in most of the studies I analysed). However, this is contingent on the assumption that coral responses to temperature conditions in the lab are similar to their responses to temperatures in the field. Previous studies have found that many traits are expected to respond differently to climate change (Ahrens et al. 2020), that heritability measurements may change with temperature (Bubliy and Loeschcke 2002), and that the rate of temperature increase employed in each study can also affect heritability (Chown et al. 2009). Similarly, previous heritability studies in insects report trait-specific interactions with temperature (Bubliy and Loeschcke 2002; Gunay et al. 2011). Current theory suggests that more extreme environments should produce increased selective pressures that may reduce heritability (Falconer and Mackay 1996; Charmantier and Garant 2005; Wilson et al. 2006). However, despite expectations based on theory and empirical results like those described above, differences in the temperature gradients used in each study did not predict the among-treatment differences in heritability estimates for corals. Specifically, temperature had a negligible effect on the estimation of trait heritability, such that an increase of +1°C may increase high vs. low trait heritability by 4 to 9%, respectively, while an increase of +3°C results in an increase in heritability of 7 to 16% (changes that, if real, would be opposite of the predicted direction). These findings indicate that populations with sufficient genetic diversity are unlikely to experience a reduction in heritability associated with warmer temperatures, in turn suggesting substantial retention of the capacity to adapt in the face of ongoing temperature change.

Coral thermal performance and challenges to predicting future adaptation to climate change

The absence of an effect of temperature on trait heritability observed here could reflect differences among studies in the way temperature treatments were applied, and/or differences in how temperature effects were statistically modelled. Many traits of organisms are non-linearly related to temperature, and these relationships are captured by measuring thermal performance curves (TPCs). TPCs are quantified by subjecting individuals to increasing temperatures at a standardized rate while repeatedly measuring performance (Angilletta Jr. 2009; Chown et al. 2009), to identify: (1) the value of maximal performance (P_{max}), (2) the temperature at which maximum performance occurs, i.e. the thermal optimum (T_{opt}); (3) the

performance breadth (e.g. B80, B95), and, somewhat related to the latter, (4) the limits of thermal performance (e.g. CT_{max}) (Angilletta Jr. 2009; Logan et al. 2014b; Bodensteiner et al. 2020). Measuring limits to thermal tolerance involves either static assays of survival time in a constant high temperature, such as heat knockdown time (Ma et al. 2014; Castañeda et al. 2019), or dynamic assays involving gradually increasing temperature until failure, such as temperature-at-death and CT_{max} (Doyle et al. 2011; Castañeda et al. 2019).

The way in which temperature was modelled in each of the studies analysed herein – and consequently, which component of thermal performance was captured – is likely to affect the heritability estimated. For example, studies incorporating temperature treatment as a fixed effect and estimating heritability using a single model (Meyer et al. 2009; Dixon et al. 2015; Lohr and Patterson 2017; Manzello et al. 2019), or studies that calculate heritability from the difference in trait values between low vs. high temperature treatments (Császár et al. 2010; Dziedzic et al. 2019; Yetsko et al. 2020) likely estimated the heritability of thermal sensitivity (i.e. how performance changes as temperature changes). Conversely, studies that used separate models for low-temperature and high-temperature treatments (Kirk et al. 2018; Wright et al. 2019; Zhang et al. 2019; Quigley et al. 2020b) produced separate estimates of the heritability of performance under the two temperatures. One inherent problem with such an approach arises if there is little or no variation in the trait value for one of the treatment levels (e.g. no mortality of bleaching observed under control conditions or no observable growth when corals are placed in extreme heat). The absence of among-individual variation in performance in these cases means that the estimated heritability will always be near zero, regardless of any underlying additive genetic variation associated with the trait in question. For studies of thermotolerance, obtaining heritability estimates via differenced treatment values or as a fixed treatment effect (and thereby providing heritability estimates indicative of the trait's thermal sensitivity) is likely preferable, but ideally future studies would characterize responses based on many temperature points along the TPC to obtain CT_{max}, T_{opt}, and P_{max}.

In this review, I was unable to assess whether heritabilities associated with thermal sensitivity in performance were different from heritabilities of performance itself (Fig. A10). However, the evolution of both maximal performance and the thermal sensitivity are inherently linked by the shape of the TPC (e.g. a higher peak in the TPC would result in higher trait values and greater trait thermal sensitivity), and thus their relationship may be correlated (Janhunen et al. 2016). For example, with the evolution of higher upper

879 thermotolerance (e.g. increasing CT_{max}), organisms may face reduced thermal performance breadth and
880 thermal plasticity (Hoffmann et al. 2013; Comte and Olden 2017; Baker et al. 2018). Growth and the thermal
881 sensitivity of growth are negatively correlated for one-year-old rainbow trout (*Oncorhynchus mykiss*) at low
882 temperatures, but not at higher temperatures, thus while there is moderate heritability for both growth (h^2 =
883 0.46) and thermal sensitivity of growth (h^2 = 0.24), selection for higher growth is predicted to result in
884 increased thermal sensitivity in future generations held at low temperatures, but unlikely to affect thermal
885 sensitivity at higher temperatures (Janhunen et al. 2016). Similar trade-offs of growth vs. sensitivity have
886 been observed as well in adult rainbow trout (Sae-Lim et al. 2015). Further complicating the matter, some
887 genetic correlations among life history traits may be temperature-specific (reviewed in Sgrò and Hoffmann
888 2004), including cases where negative genetic correlations can become positive at higher temperatures and
889 vice-versa. Thus, coral trait evolution may further be complicated by (currently unmeasured) genetic
890 correlations across TPC metrics.
891
892 *Conclusion*
893 This meta-analysis estimates relatively high heritability for some traits, such as survival and growth.
894 This, coupled with the fact that heritability does not appreciably decline with increasing temperature
895 manipulation, suggests the potential for coral adaptation to future conditions of weak to moderate climate
896 change. Nevertheless, potential confounding factors that could bias some of the heritability estimates
897 upwards remain to be explored, including the effects of preconditioning and canalization in adults, parental
898 and symbiont effects, and transgenerational inheritance of CgP methylation. Recent evolutionary models of
899 corals consider the heritability of the thermal optimum for corals, T_{opt}, to be anywhere from negligible (e.g.
900 h^2 = 0.01) to low/medium (e.g. h^2 = 0.16–0.50) (Cropp and Norbury 2020; Matz et al. 2020; Logan et al.
901 2021). However, there are no available estimates for coral thermal performance traits such as T_{opt}, CT_{min},
902 CT_{max}, and *B80*, and knowledge of how TPC parameters co-evolve remains very limited. For example, the
903 evolution of higher thermal optima (T_{opt}) may result in reduced maximal performance (P_{max}) or performance
904 breadth (CT_{min}, CT_{max}, and *B80*). Other genetic trade-offs such as growth vs. thermotolerance for both corals
905 and symbionts may exist, further constraining coral evolution to climate change. Future studies would ideally
906 construct TPCs using multiple temperatures across a known pedigree of individuals in order to calculate
907 heritabilities and associated trade-offs for TPC parameters across one or multiple traits. Combined with the

current knowledge of trait heritabilities, this would allow better predictions regarding thermal evolution of corals in response to climate change. Nevertheless, these findings suggest that corals may be capable of adapting more rapidly to the thermal challenges imposed by climate change than previously thought.

Data accessibility statement

All extracted heritability estimates and Supplementary Code are available at https://github.com/ecolology/heritability-meta and https://ecolology.github.io/heritability-meta/.

Chapter 3 Demographic drivers of coral population persistence and stability

Abstract

Projecting the long-term trajectories of coral populations requires a comprehensive knowledge of demography. Population models for size-structured populations increasingly adopt an integral projection model (IPM) framework, which allows more realistic characterization of size-dependent demography than traditional matrix models. However, a better understanding of how model architecture and parameterisation affect population trajectories is required to improve our ability to project coral population trajectories under future environmental conditions. Here, I construct a size-structured, density-dependent IPM of a single population of corymbose *Acropora* corals, parameterised with demographic data from the northern and central Great Barrier Reef. I then analysed population extinction risk and long-term equilibrium coral cover in response to different size-dependent demographic relationships, and quantified the contribution of different demographic processes to the uncertainty in model predictions. In contrast to processes such as growth, survival, and fecundity, data on recruit intra-cohort density-dependence is rarely collected and included in coral IPMs. Yet, in the absence of density-dependent interactions among recently-settled individuals, the model predicted realistic levels of cover only within an implausibly narrow range of larval survival and settlement probabilities. In contrast, when recently-settled corals interact in a density-dependent way, more realistic levels of coral cover occur over a much broader range of larval settlement values. To identify key data-deficiencies for modelling coral population trajectories, I evaluated the sensitivity of predicted extinction risk and equilibrium abundance to estimated uncertainty in growth, survival, fecundity, and intra-cohort density-dependent relationships. I found that coral dynamics were only biologically plausible within a small window of proportional settlement of first-year recruits in the absence of any intra-cohort density dependence. However, population dynamics were much more realistic and buffered against relatively weak or strong proportional settlement when Beverton-Holt density dependent dynamics were considered. Additionally, equilibrium dynamics were determined in large part by the functional forms for growth and survival. The results of this chapter suggest an increased focus on recruitment processes and juvenile demography is warranted to improve the realism of coral population models.

Introduction

Biodiversity in natural environments has declined by as much as 68% since the 1970s (WWF 2020). It is estimated that the world's coral reef cover has declined by half since the end of World War II, due to multiple interacting drivers of population decline (Eddy et al. 2021). In response, population models have become increasingly important tools for understanding the demographic drivers of long-term changes in biological assemblages, and for informing management interventions that will aid population recovery (Walsworth et al. 2019; van Woesik et al. 2022). Structured population models aim to predict population-level responses to various environmental perturbations by synthesizing data linking individual-level organism states – such as size – to demographic rates of survival, growth and reproduction (Edmunds and Riegl 2020; Laughlin et al. 2020; Schaub and Kéry 2021). For example, smaller corals survive less, grow relatively more, and are much less fecund relative to larger individuals (Hughes and Connell 1987; Hall and Hughes 1996; Edmunds et al. 2014; Madin et al. 2014), and thus population growth is influenced by the size distribution of individuals in the population. Traditionally, matrix population models that divide individuals into discrete size categories have been used to project future population outcomes (Ruesink 1997; Caswell 2001). Such approaches are particularly well-suited to species that have life cycles consisting of a small number of distinct life stages (e.g. larvae, pupae, and adults). However, since demographic processes are often strongly size-dependent, and size typically varies continuously, ecologists have increasingly relied on integral projection models to estimate contributions to population growth, using size as a continuous variable (Easterling et al. 2000; Ramula et al. 2009; Ellner et al. 2021).

To date, a number of coral IPMs have been developed (Table 3.1), to either examine the viability of populations without disturbance, or to investigate populations' responses to external stressors, such as environmental or disease perturbation (Bruno et al. 2011; Elahi et al. 2016; Cant et al. 2023; McWilliam et al. 2023). These models are most commonly density-independent, and focus on the long-run population geometric growth factor, λ, to estimate long-term population viability, with $\lambda>1$ indicating a self-sustaining population or meta-population. Previous coral IPMs have incorporated relatively comprehensive data about size-dependent growth, fecundity, and mortality of adult corals (e.g. Scavo Lord et al. 2020; Cant et al. 2021); however, to date, the settlement, survival and growth of larval and juvenile corals has been poorly resolved due to limited data on these early life stages (e.g. Ritson-Williams et al. 2009; Cant et al. 2021;

970 Jonker 2022). Given that recruitment is a critical demographic bottleneck in the life cycle of corals
971 (Doropoulos et al. 2015, 2022), an assessment of how coral population trajectories depend on population
972 regulation mechanisms that occur at early life stages is required.

973 Recruitment in corals involves three important sub-stages: larval supply (which includes fertilization
974 success and dispersal of coral larvae), settlement, and post-settlement survival and growth (Ritson-Williams
975 et al. 2009). When larvae arrive at a reef and select a place to settle and metamorphose, space occupied by
976 adult colonies limits the substrate available to settling larvae, which do not settle on live coral. In addition to
977 adult density, larval density can also affect settlement such that the probability of a larva successfully settling
978 can be higher at high larval densities (i.e. positively density dependent, Edwards et al. 2015; Doropoulos et
979 al. 2017, 2018), or it can be unaffected by initial larval densities (i.e. density independent, (Doropoulos et al.
980 2017; Cameron and Harrison 2020). In contrast, post-settlement survival is often negatively density
981 dependent due to high densities of settlers creating increased competition and attracting predators (herein
982 referred to as 'intra-cohort effects') (Suzuki et al. 2012; Edwards et al. 2015; Doropoulos et al. 2017;
983 Cameron and Harrison 2020). Thus, any positive effects of high larval densities on settlement success may
984 be negated or even overwhelmed by post-settlement, negatively density-dependent interactions (Edwards et
985 al. 2015; Cameron and Harrison 2020).

986 Despite the complexity of recruitment processes, and their effects on local population dynamics,
987 most IPMs to date typically assign a fixed probability of recruitment from outside the reef (for open
988 populations), or a fixed rate at which larvae become first-year recruits for closed populations (e.g. Bruno et
989 al. 2011), both symbolised as q, *sensu* Edmunds et al. (2014); that is, they assume that larval supply, larval
990 settlement, and survival to age 1 are independent of the size of the cohort. These density-independent values
991 have been estimated by performing recruitment tile studies to examine the relative number of recruits to a
992 reef for a given year vs. the number of gametes produced for broadcast spawners or number of planula larvae
993 released for brooding corals (Cant et al. 2021), or simply by selecting a value of q that produces realistic
994 population dynamics (Bruno et al. 2011; Edmunds et al. 2014) Only two IPMs to date have included density-
995 dependent processes, wherein recruitment decreased with increasing adult coral cover or adult densities
996 (Kayal et al. 2018; Cant et al. 2023), and no IPMs to date have examined the effect of negative density
997 dependence due to intra-cohort interactions among recruits (Table 3.1). Additionally, the proportion of
998 successfully settling larvae (i.e. the parameter q) is likely highly stochastic in nature due to variability in

fertilization and development success, and variability in successful transport via ocean currents to suitable settlement sites (Thompson et al. 2018; Gouezo et al. 2021). By excluding post-settlement density dependence, IPMs may, for example, overestimate the feedback between decreases in the size of the reproductively mature population and decreases in recruitment arising from lower larval settlement, with potential implications for the projection of reef futures. Such mis-characterizations would also impact the robustness of projections of models with more complex extensions added (such as species interactions, or evolution).

Table 3.1. Previous coral integral projection models (IPMs) to date.

Study	Species/taxa	Aim	State variable [units]	Growth model	Survival model$^{\propto}$	Density-dependence (DD)
Bruno et al. 2011	Purple Sea Fan (*Gorgonia ventalina*)	Disease response and recovery	Colony area$^{(1/3)}$ [$cm^{2/3}$]	Size at t+1 as a Gaussian p.d.f.	First-order binomial	None
Burgess 2011 (thesis)	Patches of Boulder star coral *(Orbicella annularis)*	Hurricane response and recovery	*ln*(Patch area) [*ln* cm^2]	Size at t+1 as a Gaussian p.d.f.	First-order binomial	None†
Cant et al. 2021, 2022b	*Acropora* spp, *Turbinaria* spp., *Pocillopora aliciae* and Encrusting spp.	Response to environmental change; Transient vs. asymptotic dynamics	Colony surface area [cm^2]	Size at t+1 as a Gaussian p.d.f. with size-dependent variance	First-order binomial	None
Cant et al. 2022a	*Acropora* spp.	Transient dynamics of populations	Colony surface area [cm^2]	Size at t+1 as a Gaussian p.d.f. with size-dependent variance	First-order binomial	None
Cant et al. 2023 preprint	Various Indo-Pacific coral species	Response to environmental change	Colony surface area [cm^2]	Size at t+1 as a Gaussian p.d.f. with size-dependent variance	First-order binomial	Unimodal DD effect of adults on settlement
Edmunds et al 2014	Various coral genera	Response to environmental change	Colony area [cm^2]	Size at t+1 as a Gaussian p.d.f.	First-order binomial	None
Elahi et al 2016	Cup coral *Balanophyllia elegans*	Response to environmental change	Colony area [cm^2]	Size at t+3 as a Gaussian p.d.f.	First-order binomial	None
Kayal et al. 2018; Carlot et al. 2021	*Acropora*, *Pocillopora*, and *Porites*	Recovery from disturbance	log_{10}(Colony surface area +1) [log_{10} cm^2]	Size at t+1 as a Gaussian p.d.f.	First-order binomial	Monotonic DD effect of adults on recruitment‡
Madin et al. 2012	*Acropora hyacinthus*	Response to environmental change	Colony area [cm^2]	Size at t+1 as a Gaussian p.d.f.	Colony shape factor model of	None

					colony dislodgement	
McWilliam et al. 2022	Various coral genera	Differences in species viability	*ln*(Colony area) [*ln* m^2]	Size at t+1 as a Gaussian p.d.f.	Second-order binomial	None
Montero-Serra et al. 2017	Red octocoral *Corallium rubrum*	Population recovery vs. environmental sensitivity trade-offs	Colony height [mm]	Size at t+1 as a Gaussian p.d.f. with size-dependent variance	First-order binomial	None
Precoda et al 2018	*Plesiastrea versipora*	Viability and dynamics of populations	Colony area$^{(1/6)}$ [$cm^{1/3}$]	Size at t+1 as a Gaussian p.d.f.	First-order binomial	None
Scavo Lord et al 2020	*Porites divaricata*	Viability and dynamics of populations	*ln*(Ecological volume) [*ln* cm^3]	Size at t+1 as a Gaussian p.d.f. with size-dependent variance	Second-order binomial	None
Shlesinger and van Woesik 2021	*Dipsastraea favus* and *Platygyra lamellina*	Viability and dynamics of populations	Colony surface area [cm^2]	Size at t+3 as a Gaussian p.d.f.	First-order binomial	None
Current study	Corymbose corals	Characterize and improve upon basic coral IPMs	*ln*(Colony area) [*ln* m^2]	Constant rate of radial extension with partial colony mortality at t+1 as a logit-normal p.d.f.	Second/third-order binomial	Monotonic DD effect of adults on recruitment; Monotonic DD effect of recruits on recruit post-settlement survival

$^{\propto}$ 'First-order binomial' refers to the polynomial order for the fitted survival relationship of the form: $\text{logit}(\text{survived}) \sim \beta_0 + \beta_1 x$, where x is the state variable used in the model. Second and higher orders add additional polynomial terms (e.g. $+\beta_2 x^2$ for second-order binomial).

† Burgess 2011 examined patch fragmentation rate as the main form of patch 'reproduction', rather than sexual propagation.

‡ Kayal et al. (2018) and Carlot et al. (2021) used the ratio of successful recruits vs. total larvae in a non-linear unimodal function to predict colony density/m^2, derived in Bramanti et al. (2015).

Here, I make use of multiple sources of demographic data for corals to construct coral IPMs for corymbose corals of the genus *Acropora*. These corals are ecologically important on shallow reef habitats of the Indo-Pacific due to their relatively high abundance and provision of habitat structure for fish species (Bonin et al. 2009; Bonin 2012; Komyakova et al. 2019), and they are also vulnerable to anthropogenic impacts such as coral bleaching events and sedimentation (Mwachireya et al. 2015; Hughes et al. 2017; Fisher et al. 2019). Consequently, *Acropora* corals are of particular interest in the projection of reef futures. The IPM includes two forms of density dependence for recruits. The first involves the effect of adult colonies on recruits and the second incorporates intra-cohort effects among recruits. I evaluate these density-dependent processes across varying efficiencies with which a unit of reproductive output is converted into larvae available to settle on the reef (hereafter termed "proportional settlement") in order to examine whether and how different forms of density dependence in post-settlement survival influence projections of coral cover, depending on the value of this poorly-constrained parameter. I then explore the impact of uncertainty in growth, survival, fecundity, recruit density dependence, and recruit size on long-run population extinction risk and equilibrium coral cover. Finally, I introduce a publicly available and interactive web-based app that runs the IPM and allows users to reproduce my results, and conduct their own analyses of model variants with different parameter values. I find that free-space-limited settlement alone appears insufficient to produce realistic population dynamics, but that much more plausible dynamics are generated when density-dependent interactions among settlers are incorporated and highlight where further demographic research is needed to better understand the long-term dynamics of coral populations in an ever-changing world.

Methods

Corymbose coral biology

I develop the model using data from a number of key studies on the demography of corymbose corals (e.g. *Acropora millepora*, *A. tenuis*) for populations in the Central Indo-Pacific particularly the Great Barrier Reef (GBR). Typically, most corymbose corals are broadcast spawners, spawning annually based on the late-year lunar cycle (November-December), with less frequent biannual split-spawning occurring in the first and last half of November and December occasionally (Baird et al. 2009). Thousands of sperm and egg bundles are released per mature colony, with fertilization occurring in the pelagic environment before planula larvae settle on the reef substrate within two days to two weeks (though some larvae continue to

settle after over 100 days) (Baird et al. 2009). It is from spawning to the end of the post-settlement phase (~3–12 months after settlement) in which the majority of spawn either fail in terms of their viability, fail to encounter suitable habitat, fail to settle and establish on suitable habitat, or succumb to post-settlement mortality prior to recruiting to the juvenile population (Ritson-Williams et al. 2009; Doropoulos et al. 2017). I distinguish the efficiency with which a unit of reproductive output is converted into larvae available to settle on the reef (i.e. proportional larval settlement), while the probability of actually settling is an increasing function of the proportion of free space available (i.e. a decreasing function of the space occupied by adults; Connell et al. 1997), and post-settlement mortality is dependent on the density of newly established settlers. Once corals have survived their first year, recruit survival as juveniles is low but changes as corals increase in size and maturity (Madin et al. 2014). Similarly, radial growth of corals is assumed to be constant (Dornelas et al. 2017), implying that the relative growth in planar area (area at time t+1 / area at time t) decreases asymptotically towards unity as corals increase in size (Dornelas et al. 2017; Madin et al. 2020). Adults typically mature within three to five years of age upon attaining >12cm in diameter (Omori et al. 2008; Baria et al. 2012; dela Cruz and Harrison 2017), and are fecund proportional to their total colony size (Hall and Hughes 1996; Álvarez-Noriega et al. 2016).

Developing an integral projection model (IPM)

In this contribution, I model dynamics within a single large population across its entire geographic range; that is, at a spatial scale large enough that all recruits to the population are produced by adults in that population (e.g. Madin et al. 2012; Shlesinger and van Woesik 2021), rather than as an open population where the supply of larvae is independent of adult population size (e.g. Kayal et al. 2018). I adopt this approach because I am interested in factors affecting corals that operate on large scales (e.g. climate change), and thus would potentially impact stock-recruitment dynamics. For population projection, these adult-offspring feedbacks are removed if larval input is modelled as independent of population size (i.e. where the breeding stock is assumed to remain constant regardless of what is happening to the local population). Additionally, I model the dynamics of a single population only. This can be interpreted as corresponding either to the hypothetical case of a single population in monoculture, or conversely as an approximation of the dynamics of a single population that is conditional on an approximately static level of cover by the rest of the community (in which case, the “available space” modelled here would represent the space not occupied

by corals in the rest of the community). I adopt this idealised framework to ensure that the model produces biologically plausible dynamics prior to implementing further model extensions. That is, we need to get the single-species demography right (or at least to understand the effects of alternative plausible model structures) before we can confidently construct and interpret the results of, for example, multi-species models.

To project future population size, the number of corals at each time step n_{t+1} is a product of the previous population size multiplied by per-capita rates for survival, growth, reproduction, and recruitment processes:

$$n_{t+1} = [Survival + Reproduction \cdot Recruitment]n_t \quad (1)$$

Per-colony survival, growth, and reproduction are all strongly dependent on coral size at time *t*. Larger corymbose corals have lower mortality, slower growth, and higher fecundity, while smaller corals have higher mortality, faster growth, and low to no fecundity. I therefore use discrete-time integral projection models (IPMs) in order to explicitly account for the continuous nature of coral size, and to model per-capita rates of survival, growth, and reproduction as explicit functions of coral size (which I calibrate by fitting these functions to field data).

I begin by describing the demographic functions that will govern the IPM. Assume a single closed, panmictic population of corymbose corals with no immigration or emigration, the number of individuals at the next time step, n_t, is a product of the survival (*S*) and reproduction/recruitment of first-year recruits (*R*), multiplied by the current population size n_t.

$$n_{t+1} = [S + R]n_t \quad (2)$$

However, in a size-structured population, survival and reproduction are size-dependent processes and the model also includes a growth kernel *G* that describes how surviving individuals change from size *x* to size *x'*, giving eqn. (3):

$$n_{t+1}(x') = \int_{\mathrm{x}} [\mathrm{G}(x'|x)S(x) + \mathrm{R}(x'|x)]n_t(x)dx \quad (3)$$

Where G is the size-dependent kernel function of growth, representing a distribution characterizing the probability that a colony of size *x* at time *t* attains size *x'* at *t+1* (i.e. growth to size *x',* given current size *x*), *S* is the size-dependent whole-colony probability of survival of corals of size *x* in year *t*, R is the probability

density function of new recruits of size *x'* at time *t+1*, multiplied by the net reproductive output of adult corals of size *x* at time *t* (see 'Vital Rates' below).

Consistent with previous IPM work (Kayal et al. 2018) and demographic studies (Madin et al. 2014; Dornelas et al. 2017), I used the natural log of coral area (ln[m²]) as the state variable x. As the model must be discretised for numerical analysis (Easterling et al. 2000; Merow et al. 2014), I choose lower (l_x) and upper (u_x) limits to colony size that are 2 – 4 times smaller/larger than the observed minimum and maximum sizes ($l_x = e^{-11}$ m² or 0.17 cm²; $u_x = e^{-1}$ m² or 0.37 m²) to avoid eviction (Williams et al. 2012). To discretise the model, I then divided this size range into n_x size classes ('bins') of width $h_x = (u_x - l_x) / n_x$. I use the smallest n possible that still approximates the true continuous function in order to reduce the model's computation time ($n_x = 400$). That is, I simulated model dynamics using progressively narrower size classes until model dynamics became indistinguishable with further narrowing of size classes. I then numerically computed the integral in eq. (3) using the midpoint rule (Edmunds et al. 2014; Shlesinger and van Woesik 2021), which uses a rectangular approximation of the centre of each bin, known as the 'meshpoints' y_x, which are multiplied by the bin width h_x and summed across all sizes. I project forwards in time by calculating the value of each life history function (i.e. vital rate; Fig. 3.1) for all sizes and applying each vital rate sequentially (see Fig. B1 for a flow chart representing the model).

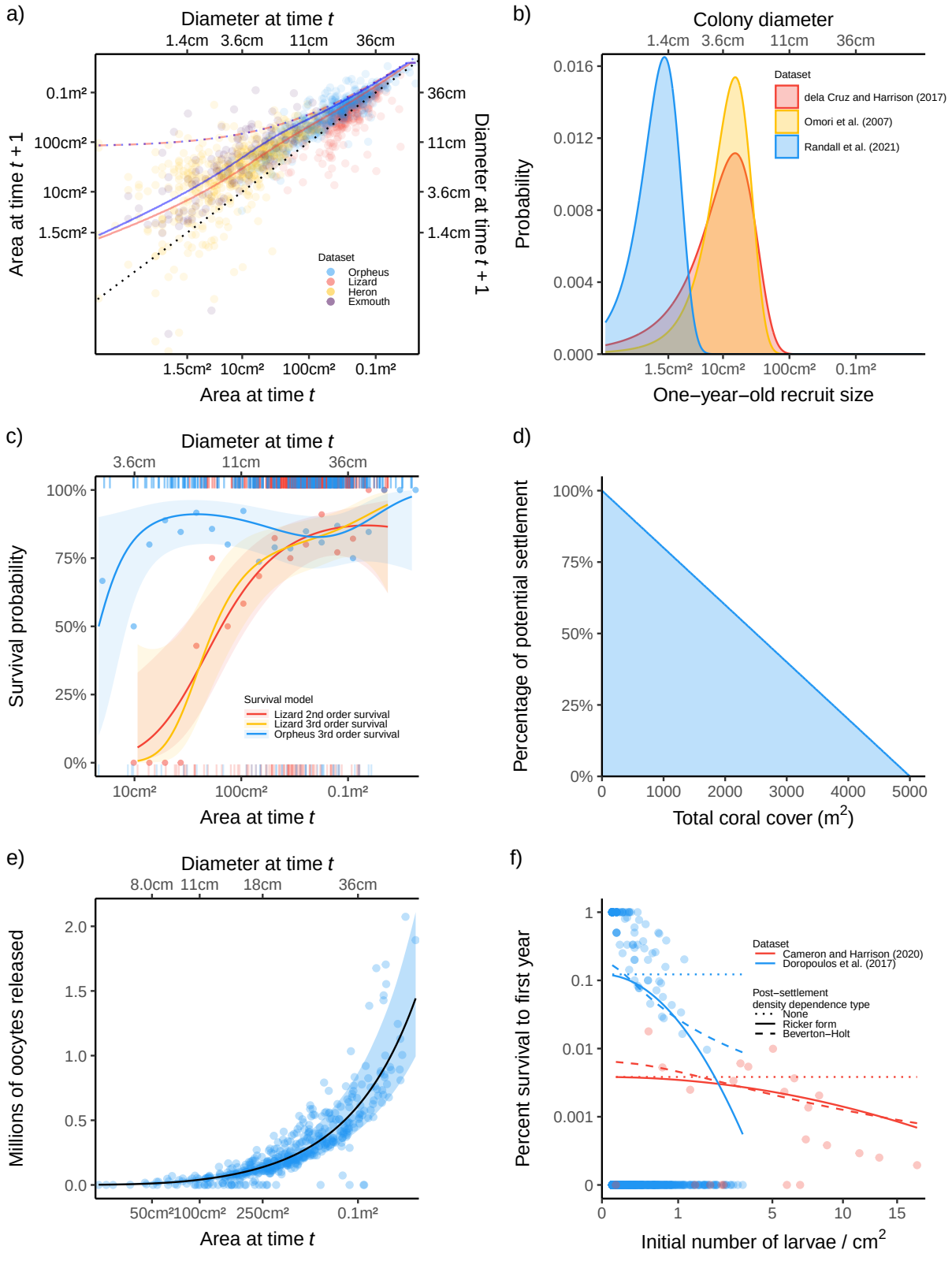

Fig. 3.1. Vital rate models and the various functional forms considered: a) size-dependent growth and partial mortality (upper dashed lines represent maximal radial growth, dotted lines represent the expectation/most likely size at time t+1, and the black dashed line is the unity line), b) whole-colony size-dependent survival (shaded areas represent 95% confidence intervals), (c) whole-colony size-dependent fecundity (shaded areas

represent 95% confidence intervals), d) first-year recruit size distributions, e) percent of settlers that successfully settle (relative to the total number of settlers in the absence of space pre-emption by adults), and f) intra-cohort post-settlement density dependence. Different coloured lines represent different parameterizations (see individual legends). Confidence intervals for whole colony fecundity in (c) are estimated using a Monte Carlo simulation to propagate uncertainty through multiple life history functions for colony maturity, fecundity, polyp density, and the proportion of the colony that is sterile.

Where possible, I estimated demographic parameters using multiple data sources to explore multiple plausible parameterizations of the model. The principal data for growth and survival come from Trimodal Reef, Lizard Island, Australia (Madin et al. 2023), as well as previously unpublished data from exposed reef sites surrounding the Northern Palm Islands, Australia (Orpheus, Pelorus, and Fantome Islands; herein referred to as 'Orpheus Island data'). However, these data sources lack observations on very small colonies. Therefore, to minimize the risk of biased model outcomes arising from systematic errors in extrapolating growth rates outside the observed range of colony sizes, I supplemented these data with observations of growth of recent settlers from Doropoulos et al. (2015, 2022), from Heron Island (QLD) and Exmouth (WA), respectively, encompassing the first two years post-settlement. Fecundity and maturity relationships are fitted using data from past (Álvarez-Noriega et al. 2016) and recent observations from the same site at Lizard Island as the growth data. Early post-settlement mortality relationships use corymbose *Acropora* spp. settlement survival data from the Philippines and Western Australia from Cameron & Harrison (2020) and Doropoulos et al. (2017), respectively, due to the lack of such data for the Great Barrier Reef. For the same reason, first-year recruit size distribution data were modelled using summary data of *Acropora* colony sizes after one year at various locations (Omori et al. 2008; dela Cruz and Harrison 2017; Randall et al. 2021). Below, I present the vital rates pertaining to each demographic process in the model.

Vital rates: Growth

The Orpheus data has uneven sampling intervals ranging from 3 months to 1.3 years, and thus must be standardized to one-year increments as in the Lizard Island dataset to be comparable. Here, I use the geometric model to do so in a simple way. According to the geometric model of growth, the size X of coral i at any subsequent time step $t + \Delta t$ is equal to: $X_{i,t+\Delta t} = X_{i,t}\lambda_i^{\Delta t}$. Note that for every 1-unit change in time,

or $\Delta t = 1$, each individual colony *i* grows by a factor of λ_i (their geometric growth rate), to attain their new size *X* at *t+1*. Solving the previous equation for λ_i yields: $\lambda_i = \sqrt[\Delta t]{X_{i,t+\Delta t}/X_{i,t}}$, which allows us to calculate the per-year geometric growth rate of each individual, regardless of the time step Δt. Taking the natural logarithm of the original geometric equation for a time step of $\Delta t = 1$ gives me: $\ln(X_{i,t+1}) = \ln(X_{i,t}\lambda_i) = \ln(X_{i,t}) + \ln(\lambda_i)$, which allows me to calculate an estimated log-size at time *t+1 as* the sum of the original log-size of each individual at time *t* and the logarithm of λ_i.

The demographic model first accounts for colony growth and survival, followed by reproduction of surviving adults (Fig. 3.1). I formulate a growth kernel, **G**(*x′,x*), which represents the probability of growing/shrinking from colony size $x \rightarrow x'$ from time $t \rightarrow t+1$ fit to growth data of corymbose corals from Trimodal reef (Lizard Island, Australia; Dornelas et al 2017) and reefs around Orpheus Island (Hoogenboom et al. unpublished). However, as noted above, juvenile corals were not well represented in either of the Lizard and Orpheus Island datasets, thus I supplemented these data with one-year-old juvenile growth data from Heron Island (Doropoulos et al. 2015) and Exmouth (Doropoulos et al. 2022). To account for general site-specific differences in growth, I subtracted the mean reef effect from the juvenile data using the estimated intercepts for Heron and Exmouth estimated from a linear regression of: Size at time *t+1* ~ Size at time *t* + Reef. This small change resulted in a better match to the Lizard and Orpheus Island data, respectively (see Appendix B2; Fig. B2.1).

Madin et al. (2020) estimated the 'maximal' constant radial extension of adult corymbose corals by fitting a 95th quantile regression with only an intercept term (the 95th quantile was used to minimize downward bias in the estimate due to partial colony mortality). This model predicts a maximal Lizard Island coral radial extension of 3.64 cm/yr (Fig. B2.2). I fit the same constant radial growth relationship to the Orpheus Island data and found a maximum radial extension of 5.07 cm/yr (Fig. B2.3). From these maximal radial extension estimates, I can approximate the maximal area that a coral of initial area a_t can attain in the next time step, $a_{max}(a_t)$. Using this maximum, the partial mortality for any pair of initial and final sizes a_t and a_{t+1}, as in Madin et al. (2020), is:

$$p_{pm} = 1 = \frac{a_{t+1}}{a_{max}(a_t)} \quad (4)$$

To obtain a model for p_{pm}, I followed Madin et al. (2020), I excluded any data points where colony area was greater than or equal to $a_{max}(a_t)$, and then fit a linear relationship predicting the logistic transform of proportion partial mortality as a linear function of log-area at initial size *x*:

$$logit(p_{pm}) = \beta_{pm0} + \beta_{pm1}x + \varepsilon(0, \sigma_{pm}^2) \quad (5)$$

where x=log(a_t), and β_{pm0} and β_{pm1} are the intercept and slope of the line of best fit for logit(p_m) proportion partial mortality for corals at time $t+1$ and $\varepsilon(0, \sigma_{pm}^2)$ represents the residual error term (Fig. B2.4 and Fig. B2.5). I used the model coefficients and residual variance (σ_{pm}^2) from this logit-scale relationship to predict the probability of growth from any size x=log(a_t) to any size x'=log(a_{t+1}) as in Madin et al. (2020):

$$G(x'|x) = \frac{1}{\sigma_{pm}^2\sqrt{2\pi}} e^{-\frac{(logit(p_{pm}) - \beta_{pm0} + \beta_{pm1}x)}{2\sigma_{pm}^2}} \quad (6)$$

where *logit*() indicates the logit transform, p_{pm} is the expression given in eq. 4, and the terms β_{pm0}, β_{pm1}, and σ_{pm}^2 are estimated from the fit of eq. (5) to empirical observations of partial mortality. This growth kernel is analogous to a transition matrix for a matrix model, translating corals of size x→ x' through the probability of future partial mortality relative to that colony's maximal areal growth based on constant radial extension. In this model, colonies can only grow to a colony size less than or equal to their maximum radial extension of 3.6 or 5.1 cm/year (Lizard vs. Orpheus Island, respectively), depending on the population.

To avoid introducing inaccuracies into the growth probabilities when calculating the probability of each size meshpoint transitioning from *ln* size x→ x' (Doak et al. 2021), I calculated probabilities as the 'CDF difference' (*sensu* Doak et al. 2021) – the difference in the cumulative distribution function at the lower and upper edges of each size bin (i.e. meshpoint ± h_x/2, in *ln* m^2). Since the total coral cover after growth occasionally surpassed the total space available in the absence of any post-settlement density dependence, I scaled the total coral cover after growth down to 100% of the reef space when corals unrealistically grew past 100% coral cover.

Vital rates: Survival

Size-dependent survival is calculated based on background rates of coral survival on Lizard Island (Madin et al. 2014) and Orpheus Island (Hoogenboom et al. unpublished). The probability of survival ($S(x)$)

dependent on size *x* was plotted on the logit-scale and observed to have a curvilinear to sigmoidal shape, with low coral survival at small sizes, higher survival at intermediate sizes, and slightly lower survival at the largest sizes. To account for this non-linearity, I fit 1st to 3rd order polynomial relationships within a binomial model and used AICc to select the model that best explained survival with the fewest polynomial parameters (Madin et al. 2014). For example, the estimated survival probability for a 3rd order polynomial is given by:

$$S(x) = logit^{-1}(\beta_{s0} + \beta_{s1}\,x + \beta_{s2}\,x^2 + \beta_{s3}\,x^3) \quad (7)$$

where β_{s0} is the logit-link intercept while β_{s1}, β_{s2}, and β_{s3} are the respective polynomial slope parameters for a first-order, second-order, and third-order relationship. A second-order to third-order polynomial relationship was supported for the Lizard Island data (ΔAICc = 0.7), while a third-order relationship was supported for the Orpheus Island data, with higher survival overall compared to the Lizard Island data.

Vital rates: Reproduction and recruitment

The number of successful settlers, $n_{settlers,t}(x)$, is determined by the sum of the number of mature polyps ($M(x)$, dependent on coral size x) and their associated size-dependent fecundity ($F(x)$) for all individuals of size x at time t ($n_t(x)$), multiplied by the proportional larval settlement parameter q, which represents the proportion of larvae that survive and find suitable substrate while competent to settle and successfully metamorphose into 'spat' (Edmunds et al. 2014). Importantly, by modelling fecundity in this way, I assume that corals produce constant larval output across varying environments, which is not realistic when thermal stress occurs (Hughes et al. 2019) but otherwise may be a reasonable assumption in the absence of pronounced thermal stress (Howells et al. 2016).

Previous studies have modelled per-capita recruitment as a density-dependent function of adult coral abundance by making q a unimodal function maximized at intermediate adult densities (Bramanti et al. 2015; Cant et al. 2023), or as a negative exponential function of adult cover (e.g. with a Ricker functional form, as in Kayal et al. 2018). Additionally, I assume that settling larvae fall as a uniform larval 'rain' across the reef, with larvae only settling if they happen to fall in the available free space on the reef. This reduces recruitment proportional to the amount of free space (i.e. space unoccupied by adult cover relative to total

space available to corymbose corals on the reef), making the total number of successful settlers at time t:

$$n_{settlers,t} = q\, p_{free\ space,t} \int_{x} M(x)F(x)n_t(x)dx \quad (8)$$

Where q is the proportional larval settlement, $p_{free\ space,t} = \left(1 - \frac{Coral\ cover,t}{Total\ area}\right)$ is the proportion of space on the reef available for settlement (i.e. the complement of the adult coral cover at time t divided by the total available reef area to corymbose corals). The composite life history functions for maturity and fecundity based on size x are provided below in Table B1 (see Table B2 for specific parameter values). I assume that corymbose coral fecundity is rate-limited by oocytes, rather than sperm (Precoda et al. 2018; Shlesinger and van Woesik 2021), and that corals less than 12 cm in diameter are non-reproductive (Baria et al. 2012; Doropoulos et al. 2015). The proportional larval settlement q dictates the proportion of larvae that successfully establish on the reef and is very poorly constrained and likely highly variable across coral populations (for instance, larvae produced on a small isolated atoll may be orders of magnitude less likely to successfully mature and return to a suitable reef habitat for settlement, compared to larvae produced within a dense and extensive reef matrix such as the Great Barrier Reef). Studies have previously estimated q via trial-and-error to attain population trajectories similar to the studied population (Bruno et al. 2011; Edmunds et al. 2014), or as a ratio of observed recruits relative to oocytes (Edmunds et al. 2014; Shlesinger and van Woesik 2021). To account for uncertainty in q, I examined model behaviour across multiple orders of magnitude of q (10^{-6} to 10^{-1}) to examine its effect on long-term model outcomes. I assume that colony size does not affect the viability of larvae or result in changes in egg provisioning. This is supported by the fact that healthy *Acropora humilis* populations produce 4x the number of larvae relative to declining populations with no change in relative egg size or provisioning (Hartmann et al. 2018; Foster and Gilmour 2020).

Here, I assume that any density-dependent effects on post-settlement success (i.e. in addition to the direct effect of space pre-emption by adults on larval settlement) are mediated through recruit-recruit interactions, either via exploitative competition for suitable space during establishment (e.g. preference for crevices; Doropoulos et al. 2017; Randall et al. 2021) or through exploitative resource competition and direct interference competition during the first year after settlement (Suzuki et al. 2012; Edwards et al. 2015; Doropoulos et al. 2017; Cameron and Harrison 2020). Multiple studies on branching and corymbose

Acropora have reported moderate to high mortality where settled larval densities exceed more than 1 larvae/cm^2 in the weeks to months after settlement (Suzuki et al. 2012; Edwards et al. 2015; Doropoulos et al. 2017; Cameron and Harrison 2020). Thus, I model intra-cohort effects (i.e. recruit-recruit) as a density-dependent function of the initial density of recruits, as observed in a number of *Acropora* species including *A. millepora* and *A. tenuis* (Suzuki et al. 2012; Edwards et al. 2015; Doropoulos et al. 2017; Cameron and Harrison 2020).

I define the probability of successful recruitment at time *t* ($p_{recruitment,t}$) as a function of the density of successful settlers, $r_{settlers,t} = \frac{n_{settlers,t}}{Free\ space,t} = \frac{n_{settlers,t}}{Total\ reef\ area - Coral\ cover,t}$. This recruitment function was fit to data from two different field-based recruitment tile experiments (Doropoulos et al. 2017; Cameron and Harrison 2020) as either the Ricker (1954) or Beverton-Holt (1957) functional form of density dependence.

$$p_{recruitment,t} = e^{(\beta_{RD0} + \beta_{RD1}\, r_{settlers,t})} \tag{9}$$

$$p_{recruitment,t} = \frac{\beta_{BD0}}{1 + \beta_{BD1}\, r_{settlers,t}} \tag{10}$$

The Ricker functional form (eq. 9) assumes strong density dependence at high population sizes, resulting in over-compensatory declines at large population sizes (meaning that the total number of settlers surviving the density-dependent process peaks at intermediate density of initial settlers, and actually decreases as initial settlement densities increase beyond that point), while the Beverton-Holt function (eq. 10) characterizes compensatory density-dependence (where the number of surviving settlers is a saturating function of the initial number of settlers). As a general rule, over-compensatory density-dependence is more likely to destabilise populations (e.g. cause population cycles), because a large enough population size can cause a subsequent decline in population size due to a decrease in net recruitment. I fit both models to two publicly-available datasets for post-settlement survival: *Acropora millepora* recruit data from Coral Bay in Western Australia (Doropolous et al. 2017) and *Acropora tenuis* data from Magsaysay Reef in the Philippines (Cameron and Harrison 2020), and examined whether these different density-dependent model parameterizations affected population outcomes within the IPM. I know of no previous coral IPM studies that include early post-settlement density dependence due to intra-cohort interactions.

To attain the final number of new recruits of size *x'* from adults of size *x*, I multiply the total number of settled recruits (which includes pre-settlement density dependence) by the post-settlement density dependence and a vector containing the probability density function of first-year recruit sizes ($\mathrm{RS}(x')$).

$$\begin{aligned} \mathrm{R}(x') &= n_{settlers,t}\, p_{recruitment,t}\, \mathrm{RS}(x') \\ &= \left[q\, p_{free\ space,t} \int_{\mathrm{x}} M(x)F(x)n_t(x)dx \right] p_{recruitment,t} \mathrm{RS}(x') \end{aligned} \tag{11}$$

I assume that the distribution of recruit diameters is Gaussian, with a mean diameter ± S.D. based on observed larval *Acropora tenuis* recruit sizes from the northwest Philippines (dela Cruz and Harrison 2017) – but model outcomes using this distribution of recruit sizes were similar to model outcomes using two alternative estimates of one-year-old recruit diameter (Fig. 3.1b; Omori et al. 2008; Randall et al. 2021). As with the growth kernel, I calculated the number of new recruits produced using the 'CDF difference' method by transforming the edges of each size bin from log-area to the diameter scale (Doak et al. 2021).

Evaluating population outcomes

I simulated each IPM for 50 years of population growth to determine the long-term equilibrium proportion coral cover and size distribution. I distinguish between the proportion of total cover for one-year-old recruits vs. adults (2+ years) in most plots to highlight the high recruit cover in models that lack any form of recruit density dependence. I examined the effects of different functional forms of vital rates by using different fitted relationships across different datasets, e.g. survival and growth models from Lizard Island vs. Orpheus Island; Ricker vs. Beverton-Holt models of density dependence fit to recruit density dependence datasets from Doropoulos et al. (2017) vs. Cameron and Harrison (2020). Apart from the proportional settlement parameter q (treated as a free parameter due to lack of available data to constrain its value; see below), I used Monte Carlo simulation to quantify overall model uncertainty by re-sampling parameter values 1,000 times from the multivariate distribution of each demographic function via the point estimates and variance-covariance matrices obtained from the original fitted models (Schaub and Kéry 2021) and ran each resulting IPM for 50 years to examine long-term population persistence. I used a wide range of plausible values of the free parameter q ($q = 10^{-6}$ to 10^{-1}), to understand the full range of likely model outcomes. In nature, q would likely be highly spatially and temporally variable and, therefore, a model that produces realistic population trajectories under only a very narrow range of values for this parameter is less

plausible. To explore the parameter space, I conducted Monte Carlo parameter re-sampling for a single process at a time (e.g. growth parameters only, survival parameters only), as well as for all processes simultaneously (e.g. growth and survival parameters both re-sampled, all processes re-sampled).

I then examined how each process affected population outcomes via two different approaches: by examining the proportion of model runs that were heading towards long-term extinction (i.e. in perpetual decline) vs. models that reached a stable equilibrium in percent coral cover, and for models fulfilling the latter, I examined the relative contribution of uncertainty in the parameter values of each major process (growth, survival, fecundity, mean recruit size, and recruit post-settlement density dependence) to overall population-level uncertainty after 50 years. I present extinction risk as the percent of simulations heading towards extinction for each combination of the settlement parameter q, growth function (Lizard versus Orpheus Island), and intra-cohort density-dependent recruitment function (Ricker, Beverton-Holt, or none; recall that all models include density-dependent effects of established corals on settlement, since settlement is proportional to unoccupied space). Note that there will be additional model uncertainty where different data sources are mixed (e.g. coral collection locations are different, or different species are measured). For example, I estimated uncertainty based on Western Australian coral post-settlement mortality (Doropoulos et al. 2017), whereas demographic rates for the model were otherwise based on populations from Lizard Island and Orpheus Island GBR corals. The uncertainty in my model's processes can thus be taken as broadly indicative of the likely magnitude of uncertainty if all demographic processes had been characterized for a single focal population.

Results

Proportion of successful settlers

Equilibrium coral cover and extinction probability were both strongly determined by larval settlement success through the settlement parameter, q. For simulations where populations reached equilibrium and did not decline to extinction, simulation outcomes exhibited a range of functional responses to the magnitude of the free parameter q, depending on the functional form of adult survival/growth (Lizard vs. Orpheus Island model fits) and the form of recruit density dependence (no density dependence, Ricker model, or Beverton-Holt model) (Fig. 3.2). If the proportion of successful settlers was too low, all simulations declined to extinction. If it was too high, populations grew to approximately 100% cover (an outcome that may be considered implausible). However, the range of values of the settlement parameter over which intermediate levels of coral cover were produced varied substantially among the models, particularly depending on the existence and functional form of density-dependent interactions among settlers (Fig. 3.2). There was also a strongly sigmoidal functional relationship between population extinction risk and q, such that extinction risk declined rapidly over particular ranges of q, depending on the functional forms of growth, survival, initial recruit size, and recruit density dependence (Fig. 3.3).

Intra-cohort post-settlement density dependence

When models included pre-settlement density dependence (associated with adult coral cover) but no post-settlement density dependence (associated with recruit densities in the model), there was often unrealistically high coral cover (approaching or reaching 100%) before size-dependent survival and near 100% coral cover after the survival process (Fig. 3.2). This occurred for nearly every model where there were sufficient larvae to prevent extinction, indicating that only a very narrow range of q values produce intermediate levels of coral cover when IPMs lack within-cohort post-settlement density dependence (Fig. 3.2). In contrast, the equilibrium coral cover associated with Beverton-Holt and Ricker model simulations resulted in more realistic intermediate coral cover well below 100% coral cover over a much broader range of larval settlement proportions (spanning several orders of magnitude). Additionally, when relative settlement success was high ($q \geq 0.01$), there is evidence of

overcompensation for models using the Ricker form of density dependence, in that the population equilibrates at the highest cover levels for intermediate values of settlement probability, and then decreases with further increases in settlement success. Notably, beyond this intermediate peak, inspection of population trajectories from individual simulations indicated that coral populations tended to overshoot equilibrium coral cover, with populations peaking then declining towards a stable equilibrium (Fig. 3.2).

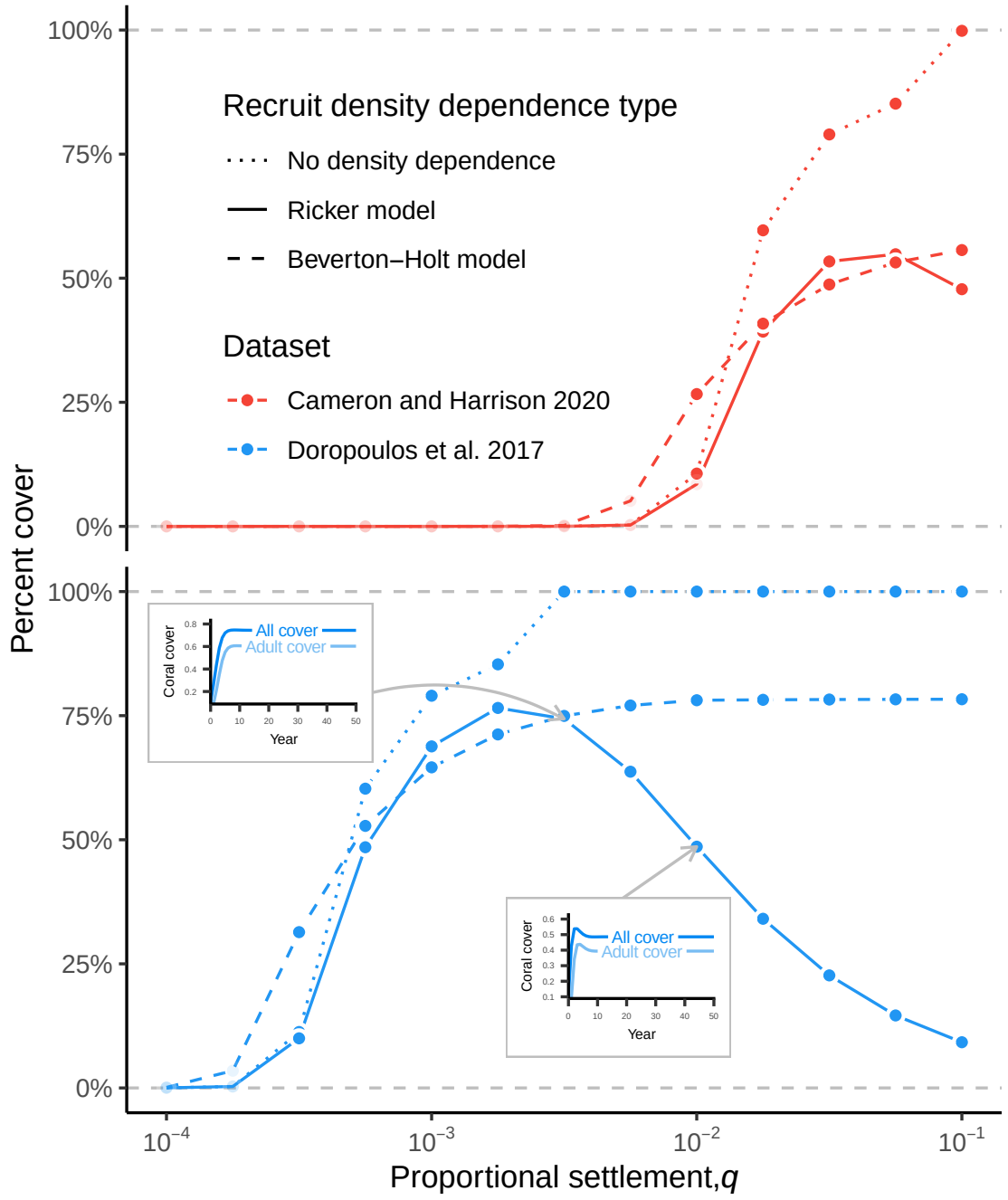

Fig. 3.2. Equilibrium percent coral cover as a function of the proportional settlement parameter, q, using various post-settlement density dependent models (Ricker, Beverton-Holt, or no density dependence; horizontal panels) calibrated using data from either Doropoulos et al. (2017) or Cameron and Harrison (2020). Insets show the temporal trajectory of coral cover for two representative parameterizations with density-dependence of Ricker form, illustrating the damped oscillations produced in the over-compensatory range of the parameter space.

Extinction risk

Lizard Island growth and survival resulted in greater extinction risk relative to Orpheus Island growth and survival (Fig. 3.3). With either Orpheus growth or survival functional forms, populations were able to sustain adult coral cover at lower levels of incoming recruits (as mediated through the probability of successful settlement of larvae) relative to Lizard Island survival and growth combined. For example, the requisite probability of settlement that allowed population persistence was an order of magnitude lower for Orpheus growth relative to Lizard growth functions ($q = 10^{-5}$ vs. 10^{-4}; Fig. 3.3a)., and similarly, the survival function for Orpheus allowed simulations to sustain themselves at settlement probabilities 10x smaller than Lizard Island survival ($q = 10^{-5}$ vs. 10^{-4}; Fig. 3.3b). These large differences are likely due to the Orpheus Island survival function allowing the persistence of a much larger adult population relative to Lizard Island, and Orpheus Island growth supporting much more rapid growth from first-year recruits to adults as well as larger equilibrium sizes relative to Lizard Island adults (Appendix B4). Recruit size had some effect on extinction risk, with the much smaller recruit size distribution of Randall et al. (2021) going extinct at much lower settlement probabilities than recruit sizes based on Omori et al (2007) and dela Cruz and Harrison (2017). Conversely, the choice of density-dependence form (Ricker vs. Beverton-Holt vs. no recruit density dependence) did not appear to affect long-term population persistence (Fig. 3.3d).

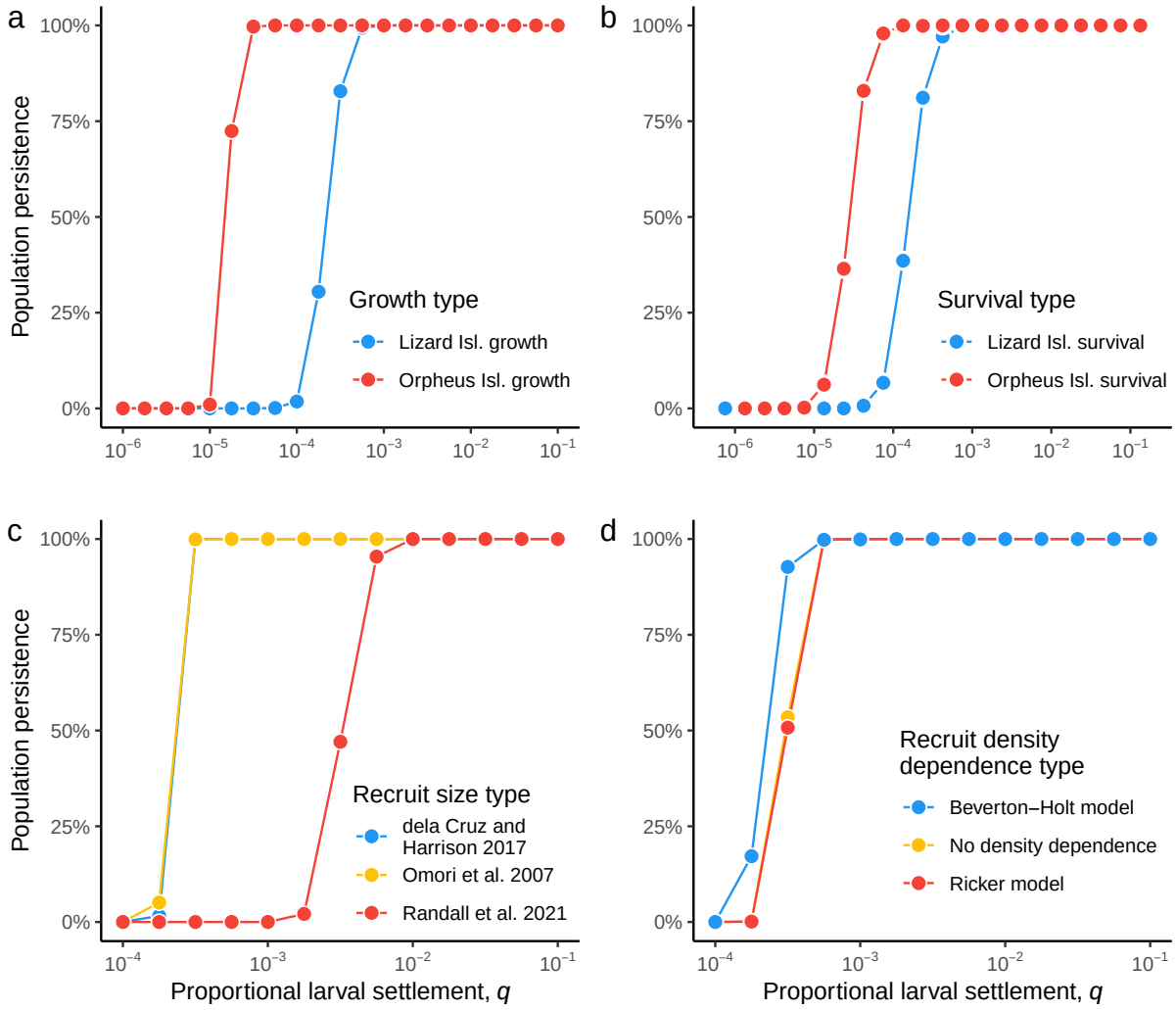

Fig. 3.3. Population persistence (i.e. the probability of population extinction for n = 1,000 Monte Carlo simulations) across different proportions of successful larval settlement (x-axis) and functional forms of: (a) growth, (b) survival, (c) recruit size, and (d) density dependence. The default model functional form when not being permuted uses Lizard Island growth and survival models, recruit sizes based on dela Cruz and Harrison (2017), and the Beverton-Holt model of recruit post-settlement density dependence fit to data from Doropoulos et al. (2017).

Uncertainty in equilibrium population size

Uncertainty in the long-run coral cover equilibria (hereafter called 'outcome uncertainty') was evaluated across four functional forms by simulating parameter uncertainty across single vs. multiple processes (Fig. 3.4). Outcome uncertainty was strongly influenced by the functional form of growth, survival, and post-settlement density dependence adopted (Fig. 3.4 – grey lines). The functional form

using Orpheus Island growth and survival as well as the Beverton-Holt model of recruit density dependence resulted in the lowest overall levels of outcome uncertainty (Fig. 3.4d), while Lizard Island growth and survival using the Beverton-Holt model showed some of the highest levels of outcome uncertainty (Fig. 3.4b).

Outcome uncertainty was also largely dependent on specific processes, and on the level of proportional larval settlement (Fig. 3.4). Uncertainty in the shape of recruit density dependence contributed the most to uncertainty in long-run coral cover equilibria (Fig. 3.4 – yellow lines) at very high levels of settlement ($q = 10^{-3.5}$–10^{-1}). The parameter q itself was also varied by many orders of magnitude, due to the lack of data to characterize uncertainty in this quantity. Therefore, we cannot quantitatively compare its impact on model outcomes relative to uncertainty in the other processes in the model (for which data are available to quantify uncertainty). Uncertainty in the shape of growth and survival functions also contributed to uncertainty in population equilibria. Uncertainty in survival and growth in combination were most important for Lizard Island corals at lower levels of larval settlement ($q \leq 10^{-4}$; Fig. 3.4a-b – green and red lines), but outcome uncertainty depended largely on uncertainty in the shape of the survival function alone (not on growth) for Orpheus Island corals (Fig. 3.4c-d – green lines), likely because the growth function for Orpheus Island corals was estimated with less parameter uncertainty. Uncertainty related to the shape of fecundity and reproduction-related life history functions was most important at lower and higher levels of settlers for the Ricker model (Fig. 3.4a,c – blue lines), but only contributed to outcome uncertainty at low larval settlement proportions for the Beverton-Holt model (Fig. 3.4b,d – blue lines). All processes contribute substantially more outcome uncertainty at low larval settlement proportions ($q \leq 10^{-3}$ for Lizard Isl.; $q \leq 10^{-4.5}$ for Orpheus Isl.). However, I cannot determine a relative contribution to overall outcome uncertainty at lower q because in a large proportion of Monte Carlo simulations at these values of q, populations are not viable and decline to extinction. Mean recruit size contributed little uncertainty overall to population outcomes (Fig. 3.4b – magenta lines).

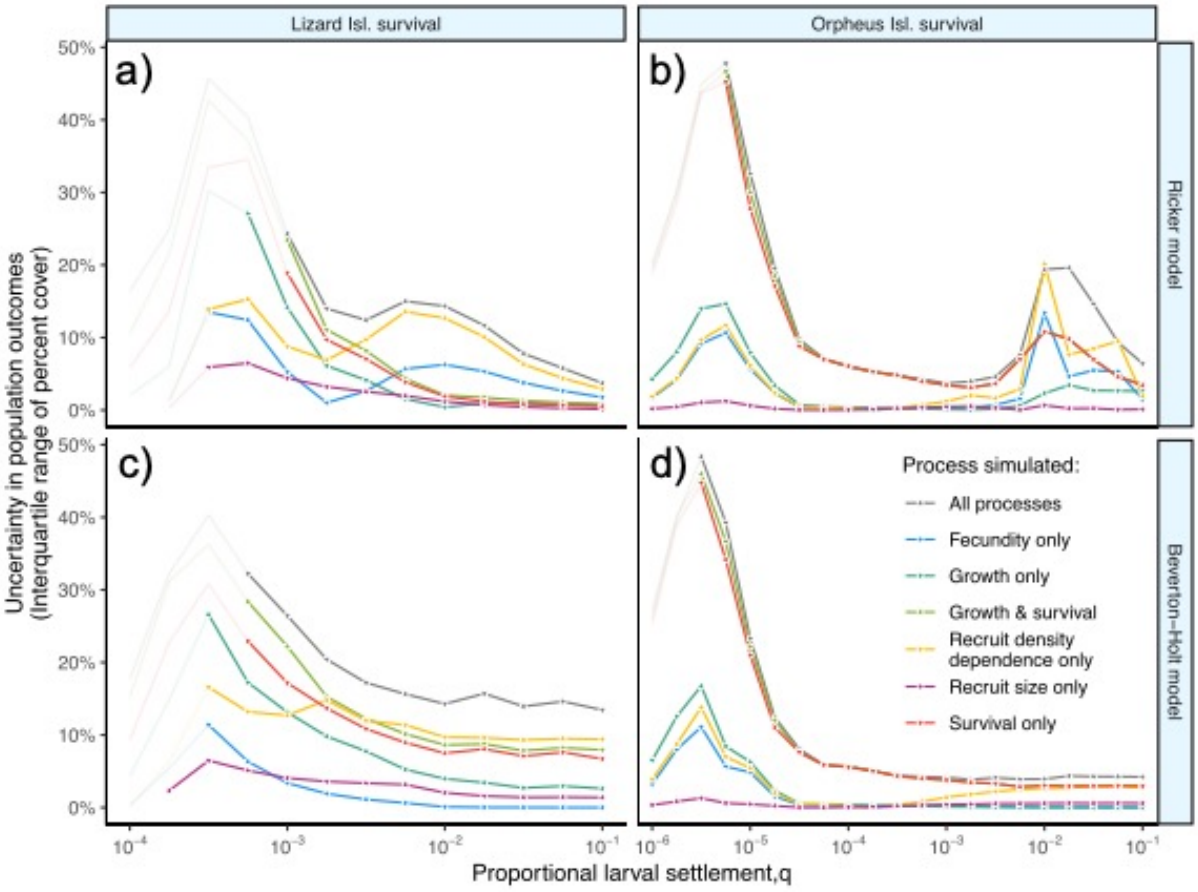

Fig. 3.4. Uncertainty in equilibrium percent coral cover vs. larval settlement (i.e. the proportion of successful settlers) for *n*=1,000 Monte Carlo simulations using 4 different model functional forms of growth/survival and recruit density dependence. Solid lines indicate where most (≥95%) of the simulations attain equilibrium, and therefore the interquartile range (IQR) is appropriate to visualize variability in equilibrium coral cover. Greyed out points and lines indicate where >5% of the simulations declined towards extinction.

Finally, to provide a broader understanding of how population dynamics are affected by various model specification and parameterizations, I include an R-Shiny web application that can be used to run the coral IPM and explore population outcomes with varying parameter values. The web app is publicly accessible at https://github.com/ecolology/Coral-IPM-Dashboard, and all code used for the app and the model can be found at https://github.com/ecolology/coral-IPM.

Discussion

Equilibrium and long-term persistence of coral populations simulated using integral projection models (IPMs) depended in some unexpected ways on the functional forms used to model population growth, survival, and post-settlement density dependence. Uncertainty related to specific processes was important, but less so relative to the functional form adopted for each life history function. One of the most important decisions in building a coral IPM is the choice of a function to mediate intra-cohort recruit density dependence (versus no post-settlement density dependence). In this study, IPMs that did not model intra-cohort recruit density dependence produced intermediate levels of coral cover (e.g. between 10–90% cover) only for a narrow range of values of the settlement probability parameter (q), which I consider unrealistic, given that the settlement parameter is likely to vary substantially in nature and there is typically unoccupied space on reefs that would be suitable for settlement. In contrast, when density dependence is included in the form of Ricker or Beverton-Holt models of density dependence, intermediate coral cover is observed over a much broader range of settlement parameter values. Models without intra-cohort density dependence attained intermediate coral cover between $q = 10^{-4.5}$–$10^{-2.75}$ proportional larval settlement for the Doropoulos et al. (2017) parameterization and between $q = 0.01\%$ to 0.056% (10^{-2}–$10^{-1.25}$) for the Cameron and Harrison (2020) parameterization. Outside of this narrow range, coral cover either declined towards 0% or approached 100% coral cover in simulated trajectories of these models. Alternatively, Beverton-Holt and Ricker forms of intra-cohort density dependence for both datasets yielded more realistic, intermediate coral covers over a broad range of proportional larval settlement (q) values, spanning several orders of magnitude.

My findings suggest that the choice of q – the proportional larval settlement – can have a large effect on model outcomes, if q is outside the 'sweet spot' of producing biologically plausible levels of coral cover. Many IPMs to date use a fixed value of proportional larval settlement, selected either as a ratio of the expected oocytes produced vs. recruitment observed (Madin et al. 2012; Edmunds et al. 2014), or as a free parameter selected by observing model dynamics until population dynamics and the size distribution roughly reflect the reality of the system (Bruno et al. 2011). The probability of successful settlement is difficult to accurately estimate (Edmunds et al. 2014) and is likely to be highly variable over space and time (Koester et al. 2021) due in large part to the inherent variability of ocean

currents and thus larval connectivity patterns (Gouezo et al. 2021), making estimation of a long-run average challenging. By including intra-cohort density dependent mechanisms, IPMs can account for high larval recruitment pulses sometimes observed using modern hydrodynamic models (Gouezo et al. 2021), and thus reduce the importance of the proportional settlement parameter q in determining long-run mean population size. In contrast, populations without intra-cohort density dependence decline or recover much more rapidly in response to stochastic larval recruitment, and thus models without density dependence may be less realistic relative to models including intra-cohort density dependence.

Comparing the two density-dependent functions, the Ricker model tended to overshoot the equilibrium percent cover initially before declining to a stable level (Fig. 3.2). This suggests that models using the Ricker form of density dependence (which assumes over-compensatory dynamics of high larval recruitment) may not be realistic (Doropoulos et al. 2017; Cameron and Harrison 2020), as there is no evidence to suggest that natural coral populations overshoot their carrying capacity during recovery and then decrease to stable levels due to intra-population density dependent effects alone. Rather, population declines are mainly driven by stochastic events such as disturbances (Done et al. 2007). Instead, Beverton-Holt density dependence seems more plausible, where recruitment levels off asymptotically after the population is saturated with larvae (Fig. 3.2).

The form of growth, survival, recruit size distributions, and intra-cohort density dependence – fit using various datasets – greatly impacted model outcomes, highlighting the site-specificity of vital rates and the importance of collecting demographic data specific to regions of interest. Lizard Island coral populations required relatively higher settlement (q) to sustain the population relative to Orpheus Island corals, and when recruits started at smaller sizes, populations could only be sustained at relatively high larval settlement proportions (Fig. 3.3c). Using combinations of growth and survival functions fit using either on Lizard or Orpheus Island measurements, extinction risk was reduced more when corals grew faster (i.e. Orpheus Island growth) compared to when they survived better (i.e. Orpheus Island survival) (Appendix B5 – extinction plots, Fig. B5.3), highlighting the increased importance of growth relative to survival for long-term population viability. However, using combinations of the two datasets amplified the uncertainty in the equilibrium coral cover, especially so for the Lizard-growth Orpheus-survival combination (Appendix B6 – equilibrium plots, Fig. B6.3).

Similarly, this combination shifted the size distribution of adults greatly towards the recruit distribution, but adults were much more common than first-year recruits, unlike the Lizard Island growth and survival model (Appendix B4 – size distribution plots, Fig. B4.3), with many more adults than recruits. I also found differences in model sensitivity to different functional forms and data sources for post-settlement recruit density dependence (Appendix B6, Fig. B6.5). Models of recruit size varied little between dela Cruz and Harrison (2017) and Omori et al. (2007); however, recruits starting at the very small sizes recorded by Randall et al. (2021) took many more years and resulted in less viable populations that required at minimum 1% larval proportional settlement for population viability (Appendix B5, Fig. B5.4), which is somewhat implausible. Models using intra-cohort density dependence fit using recruitment data of *A. millepora* settlement observations after one year in the Philippines from Cameron and Harrison (2020) required much higher proportional larval settlement (q) for viable populations compared to models fit using recruitment observations of *A. millepora* after 30 days post-settlement in Western Australia (Doropoulos et al. 2017). This is because the Doropoulos et al. (2017) data fit a greater effect of density dependence for recruits from Western Australia (Fig. 3.2; Doropoulos et al. 2017), but a lower intercept term relative to the Cameron and Harrison (2020) data, which meant that higher proportional settlement was required to sustain long-term population growth for models fit using the Cameron and Harrison (2020) data (Fig. 3.2). However, the values of q required to allow viable populations using the Cameron and Harrison (2020) fit of intra-cohort density dependence are somewhat implausible, given that most reefs likely do not experience proportions of larval settlement over 1% consistently (Price et al. 2019).

My analysis highlights several key information gaps in current coral demography that should be the focus of future studies. First year coral recruits in the model grew to reproductive size (~12 cm diameter) in as little as 1-2 years, which contrasts with field data suggesting that corymbose colonies typically take at minimum 3 years to reach sizes of that order (Baria et al. 2012). For example, *A. millepora* in the Philippines have been found to spawn when the mean colony diameter is at least 12 cm, corresponding to a circular area of roughly 110 cm^2 (Baria et al. 2012). However, gravid *A. millepora* at Lizard Island have been observed to be as small as 43 cm^2, with all colonies larger than 134 cm^2 being gravid (Hall and Hughes 1996). In my models, coral recruits grew very quickly and

easily attained the threshold for maturity within their first two years of life when using either Lizard or Orpheus Island growth models. Despite this rapid growth, my model's predicted growth at juvenile sizes are within the realm of possibility given previous growth data for early juvenile recruits (see General Discussion, Doropoulos et al. 2015, 2022). Therefore, more studies of survival and growth (including potential density-dependent effects) from settlement to reproductive maturity are needed.

Second, the uncertainty in coral cover outcomes for simulated IPMs was most related to three main processes across all model functional forms, in order of decreasing importance: (1) post-settlement density dependence, (2) survival, and (3) growth. However, I caution that additional uncertainty is likely introduced into my models by using different data sources for growth/survival vs. post-settlement density dependence (e.g. Eastern vs. Western Australia reefs). Thus, the sensitivity analysis likely underestimates the true uncertainty related to post-settlement density dependence for populations on the GBR, as this process was calibrated using data from populations on the opposite coast of Australia. Ideally, coral IPMs would be parameterized exclusively with demographic data from the population being modelled. Experiments using recruitment blocks with varying densities of settled larvae can provide a tractable method of adding recruit density dependence to future integral projection models across varying locations (Doropoulos et al. 2017; Cameron and Harrison 2020), and is especially important for reefs where larval recruitment pulses may be expected in areas with relatively high surrounding reef cover (Gouezo et al. 2021), resulting in sporadic but substantial influxes of recruits across years.

Evaluating the plausibility of single-species and single-population models such as ours is challenging, as one is assessing the plausibility of the dynamics of a hypothetical monoculture. For example, inter-species interactions such as coral-algal dynamics are important drivers of recruit post-settlement success (Ritson-Williams et al. 2009), but themselves are strongly contingent on environmental conditions such as the presence of herbivorous fish and the strength of wave action (Doropoulos et al. 2016b, 2016a; Evensen et al. 2021). While multi-species models will be needed to answer many such questions, it is critical to resolve how to model intra-population mechanisms such as density dependence prior to increasing model complexity through additional populations and

species, so as to reduce the risk of outcomes that are artefacts of poorly characterized intra-specific dynamics.

This study offers several lessons for future demographic modelling of coral populations, including the importance of incorporating post-settlement, intra-cohort density dependence, the potential for vital rates calibrated from other populations or species to differ substantially from those of a given study population, and the importance of sensitivity testing for parameters whose values are poorly constrained by empirical data (in my case the proportional larval settlement parameter, q). Density-dependent mechanisms in particular have received very little attention in demographic work on reef corals, but different density-dependent processes, and even different functional forms for a given density-dependent process, can substantially affect the dynamics of single-species models, as well as extensions that consider multi-species interactions, meta-population dynamics, environmental stochasticity, and eco-evolutionary dynamics.

Data accessibility statement

Model fits used within the IPM and the code to run the IPM itself are available at https://github.com/ecolology/Coral-IPM. The dashboard used to explore the IPM is publicly accessible at https://github.com/ecolology/Coral-IPM-Dashboard.

Chapter 4 Size-dependent evolutionary dynamics of corals to climate change

Abstract

Mass bleaching events have resulted in widespread coral mortality, and potentially drive coral populations to become more thermally tolerant via natural selection. However, while adaptive genes that promote thermal tolerance may be increasingly present in new coral recruits, the strong size-dependent demography of corals may slow population adaptation to climate change. Therefore, projecting the dynamics of coral populations under climate change will require models that account for both size-dependent demography and genetic evolution. Here, I use a size-structured, evolutionarily-explicit integral projection model (EE-IPM) of reef-building corals to estimate coral adaptation to future projected climate change. I examine future outcomes using sampled heat stress profiles from four possible shared socioeconomic pathways (SSPs) until the year 2100. The EE-IPMs show that sufficient heritability of thermal tolerance, larval settlement, and fecundity during heat stress are important to recover from and adapt to future climate change scenarios. With the loss or absence of two or more of the above, evolution to future climate change becomes unlikely in low emission pathways, and impossible with high emission pathways. However, if the surplus production of recruits is low, either because settlement probability is low or because of a demographic change such as a collapse in fecundity after bleaching, this can lead to collapses in coral cover on decadal time scales and potentially inhibit adaptation even when heritability is high. Additionally, eroding genetic variance due to repeated selection can heighten coral extinction risk. Local monitoring and management of coral populations to ensure sufficient recruitment prior to and during large-scale bleaching may aid in maintaining enough standing genetic variation for corals to adapt to warmer temperatures, but only under SSPs associated with mitigation of emissions.

Introduction

Novel environmental conditions brought about by climate change represent one of the greatest selection events experienced by natural populations to date (Davis et al. 2005; Nolan et al. 2018). Populations will have to move, acclimatise, or adapt to these new conditions if they are to persist over the long-term (Davis et al. 2005; Jump and Peñuelas 2005; Gienapp et al. 2008). Many examples of adaptation to recent climate change have already been observed, such as morphological evolution of darker winter coat colours in mammals to keep pace with reduced winter snow duration (Scott Mills et al. 2018), and phenological evolution in plants to shift mast years to better suit changing climate, with similar shifts in insect and avian herbivores (van Asch et al. 2013; Bogdziewicz et al. 2020). While there is evidence that some phenological adaptations can allow organisms to avoid long-term population declines, changes in morphological traits occur more slowly, often at rates insufficient to keep pace with climate change (Radchuk et al. 2019). Therefore the majority of studies projecting future population evolution to climate change suggest that adaptation will either narrowly keep pace with low or moderate emissions scenarios of future climate change (van Asch et al. 2013), or will be insufficient altogether (Logan et al. 2018; Radchuk et al. 2019; Bogdziewicz et al. 2020; Dixon et al. 2022). The incongruence among predicted future population outcomes in wild populations is partially due to differences in the assumed rate of population adaptation, a parameter that is fundamental to predicting long-term population persistence (Visser 2008; Logan et al. 2014a; McManus et al. 2021a).

Reef-building corals are particularly susceptible to climate change (Sweet et al. 2021), given their sensitivity to abnormally high summer sea surface temperatures resulting in mass coral bleaching (Hughes et al. 2018a; Lough et al. 2018). Recent mass bleaching events worldwide have caused large reductions in reef diversity and coral cover throughout the 21st century (Wulff 2006; Pratchett et al. 2011; Hughes et al. 2018b), with 75% of global reefs now considered threatened (Burke et al. 2011). Global warming on coral reefs to date has been roughly +0.71–0.92°C above pre-industrial levels from 1871–2017 (Lough et al. 2018; McWhorter et al. 2022b), and temperatures are expected to further increase to +1.1–1.7°C above pre-industrial levels in the next five years (2022-2026; Global Annual to Decadal Climate Update 2022, World Meterological Organization). This will further exacerbate the frequency and intensity of mass bleaching events on coral reefs (van Hooidonk et al. 2016, 2020;

McWhorter et al. 2022b), and many studies suggest near total extinction of thermal refugia for corals at higher levels of warming (Donner et al. 2005; Frieler et al. 2013; Hoegh et al. 2018).

Globally, reef-building corals are under increasing selection for greater thermal tolerance (Maynard et al. 2008; Guest et al. 2012). In the past decade alone, the threshold temperatures at which coral communities experience bleaching is estimated to have shifted 0.5°C higher than in the previous decade, on average (Guest et al. 2012; Sully et al. 2019). In Hawaiian *Montipora capitata* and *Pocillopora damicornis* corals, high bleaching temperatures in 1970 resulted in 95% and 100% mortality, while near identical bleaching temperatures in 2017 resulted in only 40% and 17% mortality (Coles et al. 2018), suggesting either adaptation or acclimation is responsible for coral responses to rising temperatures after 47 years. Coral thermal tolerance depends on both host and symbiont genetics (Bay and Palumbi 2014; Dixon et al. 2015; Strader and Quigley 2022) and varies substantially both among (Hughes et al. 2018b) and within populations (Humanes et al. 2022), such that the most thermally tolerant corals may have bleaching thresholds much higher than the most thermally sensitive corals (Humanes et al. 2022).

Previous studies of Indo-Pacific coral population adaptation have modelled evolution either implicitly via changes in bleaching thresholds across time (Logan et al. 2014a) or explicitly via forward genetic simulations such as so-called non-Wright-Fisher models – individual-based models of genetics across overlapping generations (Matz et al. 2018, 2020), polygenic models of allele frequencies (Bay et al. 2017b, 2017a), quantitative genetic meta-population connectivity models of coral population growth using the mismatch between average local population's temperature and local temperatures (McManus et al. 2021a; DeFilippo et al. 2022), and quantitative genetic models of symbiont growth rates using the mismatch between symbiont vs. their environment within the coral host (Baskett et al. 2009; Logan et al. 2021). However, the rates of adaptation used in all studies consistently assume low to moderate rates of evolution (e.g. low relative heritability or additive genetic variance), although there is growing evidence that heritability of thermal performance traits are likely higher than assumed in these models (Wright et al. 2019; Bairos-Novak et al. 2021). Additionally, initial variation in population thermal tolerance is often assumed to match variation in past reef thermal history (Baskett et al. 2009; Logan et al. 2021), which may be an inaccurate

assumption given the speed of current climate change (Hughes et al. 2018a). Finally, while these models do well in characterizing reef-level genotype changes observed across the reef to date, they may underestimate the importance of demography in dampening rates of adaptation in coral population change (Lasky et al. 2020).

1640 **Table 4.1.** Summary of various types of eco-evolutionary models of corals to date and their differences.

Type of model	Population structure	Fitness determined by	Eroding genetic variation	Size-dependent	Compensatory density dependence	Thermal tolerance vs. growth trade-off	Taxa	References
Explicit coral-symbiont dynamics models (evolution via symbionts using quantitive genetic framework)	Single population with source 'seed' population	Mismatch of mean symbiont thermal tolerance and local temperature (in °C)	Yes	No	Yes (via Lotka-Volterra competition between symbiont and coral types)	Yes – interspecific only†	Branching vs. mounding corals	Logan et al. 2021; Baskett et al. 2009
Meta-population connectivity models with evolution	Meta-population structure with reefs distributed uniformly along a temperature gradient	Mismatch of mean holobiont thermal tolerance and local temperature (in °C)	No	No	Yes (via Lotka-Volterra competition between coral types)	No/Yes – interspecific only‡	Fast' vs. 'slow' growth corals‡	McManus et al. 2021a; DeFilippo et al 2022
Individual based forward genetic simulation models (using SLiM)	Meta-population structure using the Indo-Pacific reef connectivity structure and temperature profiles	Mismatch of mean holobiont thermal tolerance and local temperature (in °C)	Yes	No	No	No	*Acropora millepora*	Matz et al. 2018, 2020
Multi-allele genomic models of thermal tolerance	Single species closed population with optional 'seed' population representing assisted migration	Mismatch of mean holobiont thermal tolerance and local temperature (in °C)	Yes	No	No	No	*Acropora hyacinthus*	Bay et al. 2017
Size-dependent evolutionarily-explicit integral projection models	Single species closed population	Maximal holobiont thermal tolerance vs. degree heating	Yes	Yes	Yes	No	Corymbose corals (e.g. *A.*	Current chapter

	weeks experienced (in °C-weeks)	*millepora, A. tenuis*)

† Baskett et al. (2009) and Logan et al. (2021) use a fast-growing heat-sensitive branching vs. slow-growing heat-tolerant mounding corals as well as a thermally-tolerant, slow-growing symbiont vs. thermally-sensitive, fast-growing symbiont

‡ McManus et al. (2021a) only includes a fast-growing, heat-sensitive, specialist corals vs. slow-growing, heat-tolerant, generalist corals

1641

The rate at which coral populations can adapt to climate change is likely to depend on the strong size-dependent demography of corals, for which growth, reproduction and mortality all change as colonies grow larger. For example, rates of change in gene frequencies may be slower in larger sizes of corals, as recruits take several years to reach reproductive maturity (Baria et al. 2012). Fecundity is also size-dependent in corals such that the oldest, largest colonies dominate the production of gametes, and mortality is highest at early life stages and for small colonies (Ritson-Williams et al. 2009; Madin et al. 2014). Moreover, larval supply can be critically depleted immediately following or in the years after a major bleaching event (Levitan et al. 2014; Hughes et al. 2019; Leinbach et al. 2021). These factors will alter the rate at which thermally tolerant genotypes spread through the population, increasing the risk of substantial population declines or local extinctions in the interim. Mechanistic models that track both colony size and genetics can help us better evaluate such potential limitations to evolution and adaptation to climate change (Lasky et al. 2020).

To investigate likely rates of population adaptation while accounting for the strongly size-dependent demographics of corals, I developed a size-dependent projection model of corymbose coral evolution, evaluated based on the number of degree heating weeks (DHWs) experienced on different reefs. DHWs are the cumulative number of weeks over the past 12 weeks where local temperatures have surpassed +1°C above the historical mean monthly maximum temperature (Donner et al. 2005; Heron et al. 2016), and are one of the best predictors of coral bleaching and mortality yet developed (Eakin et al. 2010; Hughes et al. 2018b). Coral responses to DHWs within the same population are highly variable, with the most thermally tolerant corals bleaching at accumulated heat stress nearly +5 DHWs more than the most thermally sensitive corals, equivalent to approximately 10–17 years of delayed climate warming (Humanes et al. 2022). I used spatially downscaled predictions of DHWs for GBR reefs from present day until the year 2100 under 4 future shared socio-economic pathways (SSPs) or ‘scenarios’ that expect emissions (and therefore climate change) to either slow or continue to accelerate (O’Neill et al. 2016; Riahi et al. 2017). I examined the importance of heritability in thermal tolerance, the maintenance of standing genetic variance, larval recruitment, and thermal stress-limited fecundity in determining population trajectories under predicted climate change. I predict that

with high (i.e. $h^2 > 0.4$) heritability of thermal tolerance, evolution will be sufficient to keep pace with low climate forcing pathways for a time, but unable to moderate coral loss under higher emissions (O'Neill et al. 2016; McWhorter et al. 2022b).

Methods

Brief model description

I extend the model from Chapter 3 by assuming that the probability of individual colony survival after a thermal stress event depends upon both size-dependent demographic processes and underlying genetics associated with the thermal tolerance of the coral holobiont (i.e. thermal tolerance due to corals, symbionts, their microbiome, and interactions among the three). To model the size-dependent demography of corymbose corals (e.g. growth, survival, fecundity), I build on the single-population IPM defined previously in Chapter 3, by extending it into an evolutionarily-explicit IPM or EE-IPM (Childs et al. 2016; Coulson et al. 2022; Ellner et al. 2019). To do so, I track a thermal tolerance phenotype z in addition to log-coral size (in ln m^2). The model is 'evolutionarily-explicit' because I specifically track the proportion of variation in phenotype that is attributable to additive genetic variation, symbolised by g, versus all other 'environment' components of the phenotype, symbolised as e. I make the assumption that other non-additive genetic effects are negligible (Childs et al. 2016; Hill et al. 2008; Coulson et al. 2021), and that g and e directly map to the thermal tolerance phenotype, such that $z = g + e$ (Childs et al. 2016; Coulson et al. 2021). By making the assumption of strictly additive genetics (i.e. no dominance or epistasis), g represents both the additive genetic variance and an individual's breeding value (Coulson et al. 2017, 2021) – that is, the genetic merit of the trait towards that individual's fitness. This thermotolerance phenotype is characterized based on the critical DHW values at which individual corals are expected to succumb to thermal stress (Hughes et al. 2018b). In the model, thermal stress impacts coral survival (Hughes et al. 2020) and fecundity (Hughes et al. 2019). Thermal stress also likely has sublethal effects on coral growth (Cunning et al. 2015; Bay and Palumbi 2017; Cornwell et al. 2021; c.f. Baird and Marshall 2002), and the settlement and establishment of recruits (Edmunds 2017; Hughes et al. 2019; Speare et al. 2022). While I use a number of potential recruit settlement values independent of thermal stress, I focus on survival and

fecundity due to a lack of consensus in the literature regarding the effects of thermal stress on growth and recruitment, and because the phenotypic variance in coral demographic rates is not well characterized except for survival (Hughes et al. 2018b). For example, recruitment and growth of juveniles can be very low (Hughes et al. 2019; Speare et al. 2022) to very high (Edmunds 2017) immediately following thermal stress, and new recruits from heat-stressed corals may actually do better than corals that did not face heat stress (Hazraty-Kari et al. 2022).

My model focuses on holobiont demography and evolution, and thus I sacrifice the ability to characterize detailed symbiont dynamics in exchange for characterizing the size structure and distributions of holobiont mortality thresholds across time. This aids with model parameterisation, as many reported relationships are strictly for the holobiont. Additionally, I focus on accumulated heat stress in the form of DHWs (in °C-weeks), rather than an environmental mismatch with temperature as previous studies have examined (Table 4.1). While organismal performance at the scale of individual colony physiology is likely to be influenced by environmental temperature, bleaching and bleaching-associated mortality occur on the reef scale and is believed to make corals particularly sensitive to climate change (van Woesik et al. 2022) and are better predicted by accumulated heat stress (DHWs) rather than mean environmental temperatures (Eakin et al. 2010; Hughes et al. 2018b). My novel approach to modelling coral evolution represents an important comparison of the robustness of prior conclusions from Table 4.1, given the different parameter estimates and model assumptions.

The model begins with demographic processes derived from estimates from Lizard Island (described previously in Chapter 3) immediately preceding summer bleaching, with selection first imposed on adults and recruits from the previous year via size-dependent mortality and phenotype-dependent mortality due to thermal stress (DHWs), followed by the growth, then reproduction of surviving, mature, and fecund corals. After calculating the number of larvae produced by surviving parents with phenotype z (with underlying genotype and environment components, g and e, respectively), parental genotypes are redistributed according to an inheritance kernel to determine their offspring's genotype distribution (Simmonds et al. 2020; Coulson et al. 2021). The environment component e is redistributed in offspring with a mean of 0 and variance equal to the proportion of phenotypic variance not attributable to additive genetic variance, i.e. $V_P*(1-h^2)$, to represent

environmental noise, phenotypic plasticity, and micro-environment variation that produces differing thermal tolerances among offspring (Childs et al. 2016; Coulson et al. 2021). Finally, settlement and post-settlement processes occur as in Chapter 3, translating the total number of larvae produced by fecund colonies into first-year recruits with first year recruit sizes distributed according to a fixed size distribution as in Chapter 3 (dela Cruz and Harrison 2017). Recall that, in Chapter 3, density dependence occurs via space pre-emption of larval settlement by already-established colonies as well as via post-settlement mortality due to intra-cohort competition, which increases at higher densities of settlers.

Model overview

I begin with a general IPM formula as in Chapter 3, but add an additional layer by integrating over a second dimension that captures each individual's phenotype *z* following Coulson et al. (2017) and Simmonds et al. (2020), which I treat as fixed throughout the lifetime of the organism (i.e. there is no developmental plasticity; Childs et al. 2016). Using *x* and *z* to denote coral size and thermal tolerance phenotype, respectively, the number of corals of each size and phenotype are defined as:

$$n_{t+1}(x', z') = \int_z \int_x [\mathrm{G}(x'|x)S(x', z'|x, z, DHW) + \mathrm{R}(x'|x, \mathrm{DHW})\mathrm{H}(z'|z)]\, n_t(x, z)\, dx\, dz$$

[number of corals of size x and phenotype z] = [sum of surviving and growing corals of size x and phenotype z] + [sum of new recruits of size x and phenotype z]

(eq. 1)

where corals of size *x* and phenotype *z* produce corals of size *x'* and phenotype *z*' at the next time step, based on per-capita growth (G), survival (*S*), reproduction and recruitment (R), and inheritance of thermally tolerant traits (H), which translates the phenotype of adults to the phenotype of offspring. I used the Lizard Island growth kernel $\mathrm{G}(x'|x)$ as in Chapter 3, which is phenotype-independent and thus not discussed in detail again here. I used Lizard Island growth to be conservative relative to the high growth observed in the Orpheus Island data and because the Orpheus data fits much higher growth at smaller coral sizes relative to Lizard Island growth – which was previously discussed in Chapter 3 to result in too rapid of maturation of juvenile corals. However, the survival function is now

determined by coral size (x), phenotype (z), and the experienced degree heating weeks (DHW). Similarly, the recruitment kernel $\mathrm{R}(x'|x, \mathrm{DHW})$ – which includes maturity, fecundity, larval settlement, and post-settlement survival – is determined by coral size as previously, but also includes a term to limit fecundity when thermal stress is elevated, which is discussed below (Cheung et al. 2021). The survival function uses the same size-dependent survival as previously, but includes an additional term representing the proportion of corals that survive that year's maximum DHW value experienced, thus directly selecting for corals with higher thermotolerance phenotype z and indirectly selecting on the underlying genotype g, given $z = g + e$. To examine the explicit effect on g, I now rewrite equation 1 in terms of the fixed additive genetic (herein 'genotype' or g) and environment (e) components of the phenotype z:

$$n_{t+1}(x', g', e') = \int_g \int_e \int_{\mathrm{x}} [\mathrm{G}(x'|x) S(x', g', e'|x, g, e, \mathrm{DHW}) + \mathrm{R}(x'|x, \mathrm{DHW}) \mathrm{H}(g', e'|g)]\, n_t(x, g, e)\, dx\, de\, dg \quad \text{(eq. 2)}$$

Note that all terms that included z now are separated in terms of g and e except for the inheritance function $\mathrm{H}(g', e'|g)$, which does not depend on the past values of e, only genotype. This is because e is not inherited across generations.

Due to a lack of size-dependent data, I make a number of simplifying assumptions regarding how an individual's thermal tolerance to heat stress is determined. I assume: (1) the relation between phenotype and genotype/environment components is additive only (i.e. no dominance or epistasis, which are often negligible; Hill et al. 2008); (2) both g and e are fixed throughout the lifetime of the organism (no developmental plasticity), (3) g only affects the survival function and not other demographic processes (no genetic trade-offs associated with increased thermal tolerance); (4) microhabitat variation and phenotypic plasticity are fixed (no acclimation) and not heritable (in the case of plasticity); (5) the environment component e is re-distributed in offspring independently of thermal stress or the parental values of e (no transgenerational epigenetic inheritance); and finally (6) the additive genetic and environment components of phenotype sum together to produce an individual's phenotype ($z = g + e$) – thus an individual's genotype is identical to their breeding value

(Coulson et al. 2017). The caveats associated with these assumptions are discussed briefly in this chapter's Discussion and more extensively in in the General Discussion of this thesis (Chapter 5), where ways of relaxing these assumptions in future models (and collecting the data necessary to calibrate such models) are also discussed.

Characterizing a thermal tolerance phenotype

Previous models of coral adaptation have assumed that organismal fitness declines monotonically as the environmental temperature moves away from an organism's optimal temperature (McManus et al. 2020; Logan et al. 2021). While organismal performance at the scale of individual colony physiology is likely to be influenced by environmental temperature in this way, at the reef scale, bleaching and bleaching-associated mortality are the phenomena believed to make corals particularly sensitive to climate change (van Woesik et al. 2022) and these phenomena are better predicted by accumulated heat stress (DHWs) rather than mean environmental temperatures (Eakin et al. 2010; Hughes et al. 2018b). Additionally, the temperature increases predicted by climate models do not scale linearly with accumulated heat stress (DHWs), and thus while low-to-moderate climate change of +1.5–2°C translates to ~8 DHWs (in °C-weeks), higher emission scenarios of +3.6–4.4°C may see upwards of 40 DHWs (McWhorter et al. 2022b). Therefore, I define the thermal tolerance of individual genotypes/phenotypes relative to DHW, and I define a critical DHW value (DHW_{crit}) as the key phenotype that determines when an individual will succumb to heat stress-related mortality.

The relationship between DHW and coral mortality fits an exponential distribution, with the probability density function having a long right-hand tail with a few individuals able to withstand extreme DHW values (Appendix C1). However, the EE-IPM framework works best with normally-distributed phenotypes and genotypes (Childs et al. 2016; Coulson et al. 2021), and thus I consider various normal approximations to this critical DHW distribution that differ in the scale on which critical DHW is approximately normal. Specifically, preliminary models were analysed with DHW_{crit} modelled as normally distributed either on the log-scale ($e^g = DHW_{crit}$), square root-scale ($g^2 = DHW_{crit}$), or arithmetic scale ($g = DHW_{crit}$) (Appendix C1). Results of these preliminary models tested against a hindcast from Lizard Island for 1987–2022 showed that modelling DHW_{crit} as normal on the

log-scale caused populations to evolve implausibly quickly and modelling DHW_{crit} as normal on the arithmetic scale caused populations that evolved implausibly slowly. In contrast, modelling DHW_{crit} as normal on the square-root scale generated levels of coral cover and genotype evolution that were most consistent with historical levels of coral cover and attained genotypic distributions resembling current data (Appendix C2). Consequently, for subsequent model projections, I tracked individual genotypes and phenotypes across all models as the critical square-root-DHW value at which individuals succumbed to heat stress ($\sqrt{\text{DHW}}_{\text{crit}}$).

In my EE-IPM, an individual's phenotype (z) is distributed according to a gaussian distribution of $\sqrt{\text{DHW}}_{\text{crit}}$ centred on 1.90 and with an initial total phenotypic variance of $V_P = 0.48$ (see Appendix C1). In all models, higher and more positive values indicate higher $\sqrt{\text{DHW}}_{\text{crit}}$ levels and thus greater tolerance to heat stress. I distribute the genotype with mean of 1.90 and genetic variance equal to $V_g = h^2 V_P$, where h^2 is the narrow-sense heritability of coral thermal tolerance (informed by Chapter 2), and the environment component of phenotypic variance is thus $V_e = (1\text{-}h^2)V_P = V_P - V_g$. The initial mean of the environment component is always 0, which means that a thermally tolerant individual (i.e. has a higher phenotype value and thus $\sqrt{\text{DHW}}_{\text{crit}}$) could have either a high value for genotype g (i.e. higher breeding value), a high environment component of phenotype e, or both, since the phenotype is simply the sum of these two terms (Childs et al. 2016; Coulson et al. 2021). While selection on the phenotype will indirectly select for both higher g and higher e values, only the additive genetic component is heritable and passed on to offspring (Fig. 4.1).

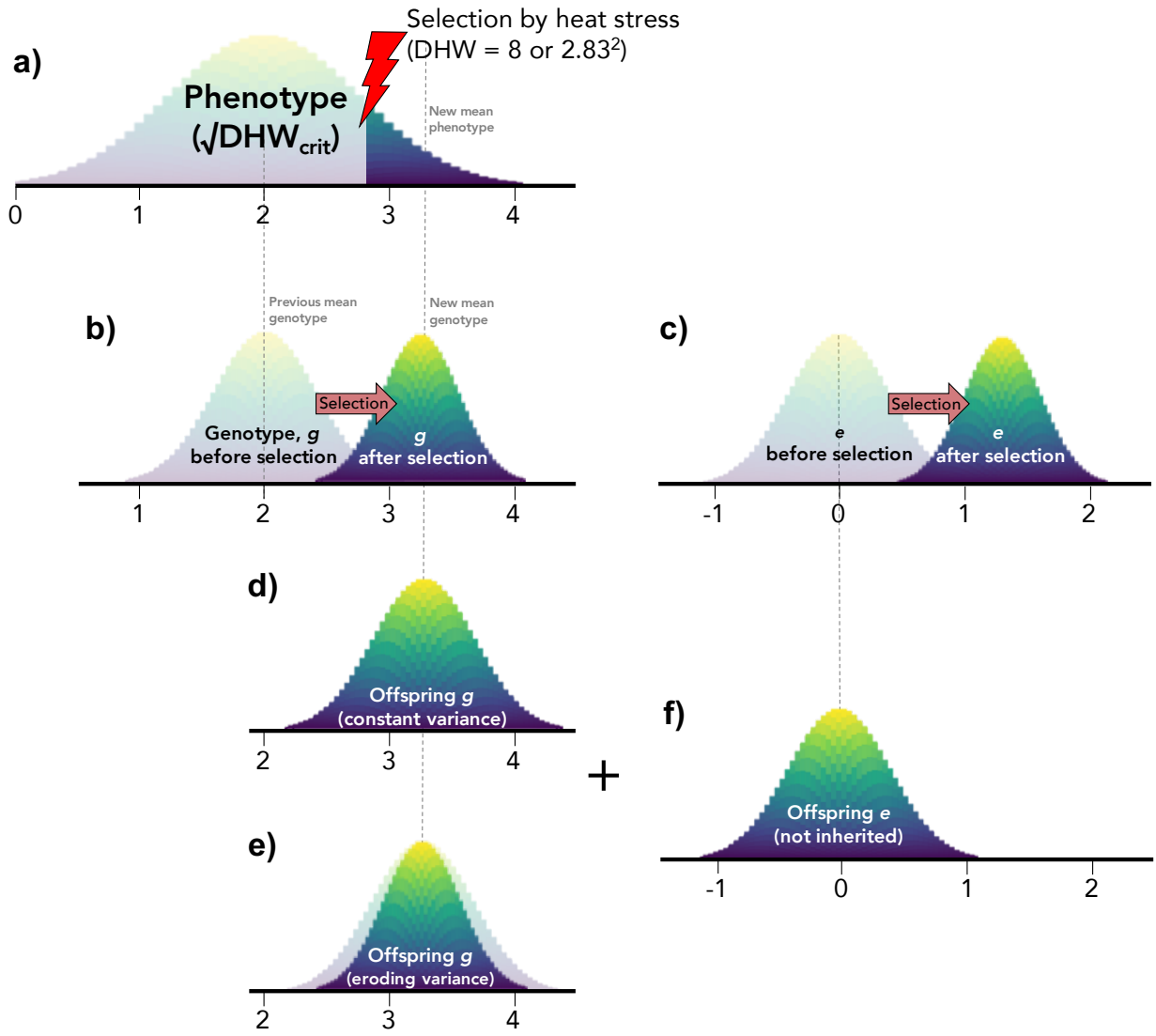

Fig. 4.1. Conceptual diagram for a single-generation adaptation in the evolutionarily-explicit integral projection model (EE-IPM) framework. Each individual's phenotype is the sum of their genotype component and 'environment' component of phenotype, i.e. phenotype = $g + e$. (a) Natural selection (e.g. experienced degree heating weeks of 8 °C-weeks) on the phenotype distribution causes truncation of the distribution, resulting in underlying changes in: (b) the genotype or g distribution, and in (c) the 'environment' component of phenotype or e distribution. When these selected adults reproduce, parental genotypes are re-distributed to offspring as a Gaussian distribution with the same mean as their parents and with either (d) constant genetic variance or (e) eroding genetic variance, according to the strength of selection. Finally, (f) the environment component is redistributed in offspring with a

mean of 0 and unchanging variance, representing non-heritable phenotypic variation that is not transmitted to offspring.

Initializing the IPM

My EE-IPM uses the same number of bins for coral size as in Chapter 3 (n_x = 400) and I use a total of n_g = 100 bins (equally spaced in dimensions of the square-root of DHW) for the genotype and environment components of phenotype. Additionally, I keep track of the 100 × 100 = 10,000 unique combinations of *g* and *e*, which produces a unique phenotype mesh of 2×100-1 = 199 unique $\sqrt{\text{DHW}_{\text{crit}}}$ values. I initialize populations close to population equilibrium at 200,000 individuals, with log-area sizes distributed according to a normal distribution with a mean and variance similar to Chapter 3 equilibrium adult size (mean = -4.93 *ln* m^2 or 72.3 cm^2, sd = 0.9 *ln* m^2).

Survival

I define the overall survival function for corymbose corals on the reef as:

$$S(x', g', e' | x, g, e, \text{DHW}) = s_{size}(x) s_{heat}(g, e, \text{DHW}) \quad \text{(eq. 3)}$$

where s_{size} is the size-dependent survival independent of thermal stress, and s_{heat} is the phenotype-specific survival (based on *g* and *e*) of corals to thermal stress:

$$s_{size}(x) = logit^{-1}(\beta_{s0} + \beta_{s1}\, x + \beta_{s2}\, x^2 + \beta_{s3}\, x^3) \quad \text{(eq. 4)}$$

$$s_{heat}(g, e, DHW) = \begin{cases} 1, & if\ g + e > \sqrt{DHW} \\ 0, & if\ g + e \leq \sqrt{DHW} \end{cases} \quad \text{(eq. 5)}$$

Eq. 4 is identical to the survival equation from Chapter 3 – defining the size-dependent whole-colony survival in the absence of DHWs, with parameters β_{s0}, β_{s1}, β_{s2}, and β_{s3} estimated in Madin et al. (2014). Heat-dependent survival s_{heat} is determined simply by the phenotype, $\sqrt{DHW_{crit}} = g + e$, which is the DHW threshold at which that individual cannot survive. This formulation of survival produces a pattern in which strongly size-dependent mortality patterns are substantially flattened during severe thermal stress, consistent with empirical observations that mortality is much less size-dependent and more equal across sizes during bleaching events (Roth et al. 2010; Speare et al. 2022).

DHW-limited fecundity

Cumulative thermal stress has been observed to critically deplete subsequent larval supply (Hughes et al. 2019), with no fecundity observed for corals following heat stress of 8 DHWs or higher. I tested the importance of DHW-limited fecundity on population evolution and outcomes by including a term to reduce fecundity according to thermal stress (Cheung et al. 2021). Using a squared convex relationship, fecundity is unaffected at low DHWs, but begins to decline and approaches zero around DHW = 8:

$$F'(x'|x) = \begin{cases} \max\left(0, \min\left(1, \beta_{f0} + \beta_{f1}\text{DHW} + \beta_{f2}(\text{DHW})^2\right)\right) F(x'|x), & if\ \text{DHW} \leq 8 \\ 0, & if\ \text{DHW} > 8) \end{cases} \quad \text{(eq. 6)}$$

The penalty on the fecundity kernel is bounded between 0 and 1 using this relationship. I ran models with and without this DHW-limited fecundity term to determine the lower and upper estimates of coral evolution if fecundity is limited. I do not model the evolution of the thermal sensitivity of fecundity with future temperatures given there are no data on the phenotypic or genotypic variance nor heritability estimates for this functional response.

Inheritance kernel

In my EE-IPM, I use an inheritance kernel to re-distribute the parental genotypes among offspring (Coulson et al. 2022). As thermal tolerance in corals is largely a polygenic trait (100–1000 loci) with few genes strongly determining thermal tolerance (Bay and Palumbi 2014; Bay et al. 2017a; Thomas et al. 2018), I assume the 'infinitesimal model' of genetic inheritance, whereby a very large number of alleles with individually very small effects contribute equally to the phenotype of individuals (Fisher 1960). The inheritance kernel is a function that takes the selected parents' distribution of genotype values and re-distributes the offspring genotype values according to a normal distribution centred at the same mean genotype as the parents (Childs et al. 2016; Coulson et al. 2021). Thus, the mean remains the same as the parents' distribution, but the variance of the offspring's Gaussian distribution of genotype values can either remain constant or can change with selection (see

Coulson et al. 2021 Table 1). While segregation and mutational variance may counteract small changes in genetic variation when populations are near equilibrium in a constant environment, it is possible that repeated large selection events reduce genetic variation to the point that it begins to impede population adaptation (Falconer and Mackay 1996). Modern-day corals of the Great Barrier Reef have experienced three mass bleaching events between 2016–2020, and thus current genetic variation may lie somewhere between constant 'best-case' genetic variation and 'worst-case' eroding genetic variation. Therefore, I use Approach 3 and 4 from Coulson et al. (2021) to redistribute offspring genotype values with either constant variance or eroding variance, respectively, as 'best-case' and 'worst-case' scenarios of genetic evolution across time. Strong selection due to high thermal stress occasionally increased genetic variance in models of eroding genetic variation when population sizes were small, thus I limited selection to either stay the same or decrease in the offspring produced from selected adults. This allows selection to erode across the population through time, representing a lower bound for genetic variation which in turn affects genotype dynamics in the model. Since the environment component of phenotype (e) is not inherited, it is re-distributed in offspring according to a Gaussian distribution with a mean of 0 and variance equal to the phenotypic variance that is not explained by additive genetic variance, i.e. $V_P(1\text{-}h^2)$.

Future thermal stress scenarios

To simulate future DHW values, I use the median DHW estimates along the GBR from five climatology models from the 6th phase of Coupled Model Intercomparison Project (CMIP6), estimated using semi-dynamic downscaling by McWhorter et al. (2022), using the interaction of predicted meteorology for the area coupled with data of local tides and bathymetry to calculate DHWs. Four different shared socioeconomic pathways (SSPs) representing future climate and socio-economic trajectories were considered, each with increasing carbon emissions/climate forcing: SSP1-1.9 (Riahi et al. 2017), SSP1-2.6, SSP3-7.0, and SSP5-8.5 (O'Neill et al. 2016). The SSP1-1.9 scenario represents the most optimistic scenario with CO_2 emissions being cut to net zero by the year 2050, resulting in only a +1.5°C increase in global temperatures above pre-industrial temperatures by 2100 (Riahi et al. 2017), while the SSP1-2.6 scenario imagines a future with less reductions, ending the

century at +2.0°C (O'Neill et al. 2016; McWhorter et al. 2022b). SSP3-7.0 represents a 'business as usual' future with increasing concerns over national security, with emissions doubling by the year 2100 resulting in a +3.6°C increase globally (O'Neill et al. 2016). Finally, SSP5-8.5 is the worst-case 'business as usual' future, with a global economy growing via burning fossil fuels readily, resulting in a doubling of emissions by 2050 and an increase of +4.4°C by 2100 (O'Neill et al. 2016). To re-simulate new DHW profiles similar to the non-linear trends observed in McWhorter et al. (2022), I fit generalised additive mixed effect models (GAMMs) to the downscaled model estimates of DHWs. GAMMs accounted for the smoothed effect of year, longitude and latitude, and random intercepts for each CMIP6 model were re-fit according to methods in McWhorter et al. (2022). I then generated random values of each year using the estimated mean and residual standard deviation from the model fits to simulate 100 unique DHW profiles between the years 2023–2100 for each of the four SSP scenarios considered (see Appendix C3).

Model outputs

I ran my EE-IPM under 1,000 unique DHW realisations using combinations of the following parameters: narrow-sense heritability (from low to high h^2: 0.1, 0.2, 0.3, 0.4, and 0.5), whether genetic variation was maintained or eroded throughout the simulation, whether or not fecundity was limited by high stress events, the proportion of larvae that successfully settle (from low to high q: 10^{-3}, $10^{-2.5}$, 10^{-2}, $10^{-1.5}$, and 10^{-1}), and using the four different SSPs for future heat stress (SSP1-1.9, SSP1-2.6, SSP3-7.0, and SSP5-8.5); i.e. 5×2×2×5×4 = 400 unique parameter combinations each with 100 DHW realisations across 97 years (40,000 model runs). Each model was run with a burn-in of 10 years without thermal stress, roughly consistent with GBR recovery times (Edmunds, 2018b; Gouezo et al., 2019), and to allow populations to attain equilibrium levels of coral cover (except where populations were declining towards extinction due to insufficient larval recruitment). Similar to Chapter 3, for each parameter combination I summarised the uncertainty in model outcomes using the median, 2.5th, and 97.5th percentiles of model outcomes for percentage coral cover, mean genotype ($\bar{g}$), genetic variance (V_g), $\bar{g}$ per each size bin, and size distribution (i.e. n per each size bin). I also calculated the proportion

of all simulation years where coral cover was less than 1% (i.e. near or at extinction levels) for each parameter combination in order to calculate a quasi-extinction risk for each parameter combination.

Model hindcasts

To assess if evolution and coral cover values produced by the model are realistic given known coral cover and genotype dynamics, I examined historical maximum DHW values of 156 reefs near Lizard Island and Orpheus Islands (from whence the demographic data originates) from 1985–2022, and then simulated historical models of evolution to compare to data from the AIMS long-term monitoring program (LTMP) and Hughes et al. (2018b) (see Appendix C2). Maximum DHWs for these years were calculated using daily sea surface temperatures and the mean monthly maximum obtained from the NOAA Coral Reef Watch Virtual Station Time Series Data with 5km-resolution (Heron et al. 2016; NOAA Coral Reef Watch 2022). Hindcasting the EE-IPM generated plausible results consistent with past historical data for GBR reefs in the same locality as Lizard Island and Orpheus Island, while attaining genotype values ranging from 1–3 $\sqrt{DHW_{crit}}$ by 2016 for the majority of initial starting values, corresponding approximately with the mean $\sqrt{DHW_{crit}} = 1.9$ from Hughes et al. (2018b) from 2016 (Appendix C2). The optimal parameter settings based on hindcast validation can be found in Table C2.1 of the supplementary to this thesis.

Results

After 10 years of population growth to equilibrium in the absence of thermal stress, all viable populations had equilibrated, populations had thermal tolerances resembling those observed to date, and populations often collapsed when exposed to the high thermal stress associated with future scenarios (Fig. 4.2). However, quick recoveries from low coral cover were often observed within 10–25 years when thermal stress did not limit coral fecundity (Fig. 4.2a,b,d; Fig. C4.1). When thermal stress limited fecundity, recovery was much more protracted, with most populations never fully recovering to their original population state, even with high heritability and larval settlement (Fig. 4.2c). The severity of the initial population crash at the onset of heat stress was largely dependent on the settlement parameter, q, which determines the number of incoming larvae at a given adult

population size. Population recovery vs. extinction after crashing depended on all factors (limited fecundity, incoming larvae, heritability of thermal tolerance, and whether genetic variance declined with selection or was maintained), as well as the emissions scenarios (Fig. 4.3). Modest to strong evolution occurred in all models in response to thermal stress. However, adaptation to higher levels of heat stress occurred for simulations based on DHW profiles from the high-emissions scenarios (SSP3-7.0 and SSP5-8.5), provided that fecundity was not impacted by heat stress, thermal tolerance was highly heritable ($h^2 = 0.5$), and genetic variance was maintained rather than being eroded by selection (Fig. 4.4).

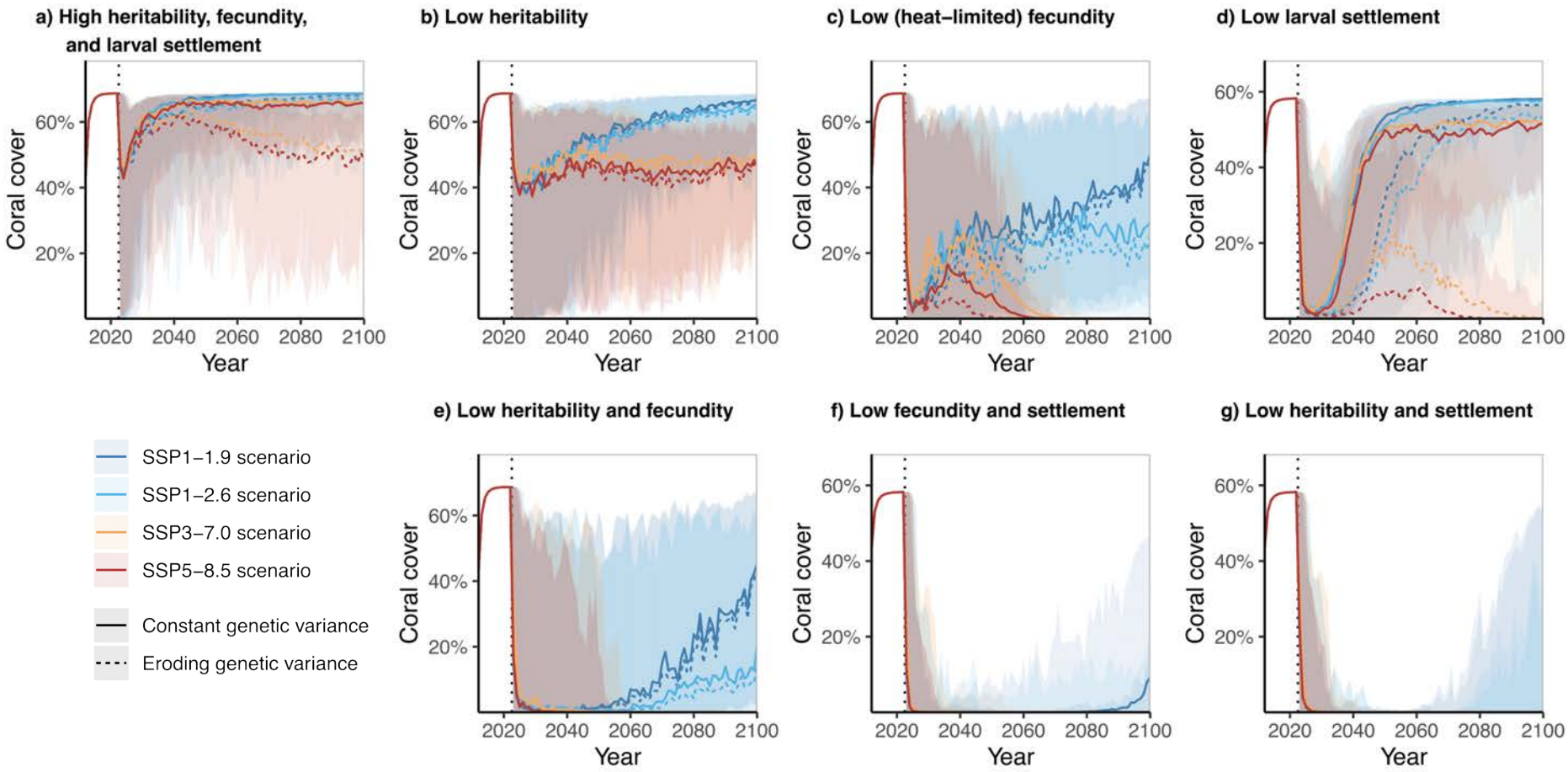

Fig. 4.2. Median coral cover of 100 simulated populations responding to future predicted heat stress based on four shared socio-economic pathways (SSP) of future emissions (colour) and whether natural selection reduces genetic variance across time (line type). In order of increasing future carbon emissions: SSP1-1.9 (+1.5°C pre-industrial temperatures) in green, SSP1-2.6 (+2.0°C) in blue, SSP3-7.0 in orange ('nationalist future'), and SSP5-8.5 in red ('business as usual'). Solid lines represent model runs where genetic variance is maintained and constant while dashed lines represent runs with genetic variance being

allowed to erode with selection. Shaded uncertainty regions represent 95% confidence intervals for each parameter combination, calculated using the percentile method. The onset of heat stress occurs in the year 2023 for all simulations (vertical black dotted line). Base parameter settings for heritability, fecundity, and settlement when not indicated are: $h^2 = 0.5$, heat-unaffected fecundity, and $q = 0.1$, whereas when 'low', these settings are: $h^2 = 0.1$, heat stress-limited fecundity, and $q = 10^{-2.5}$.

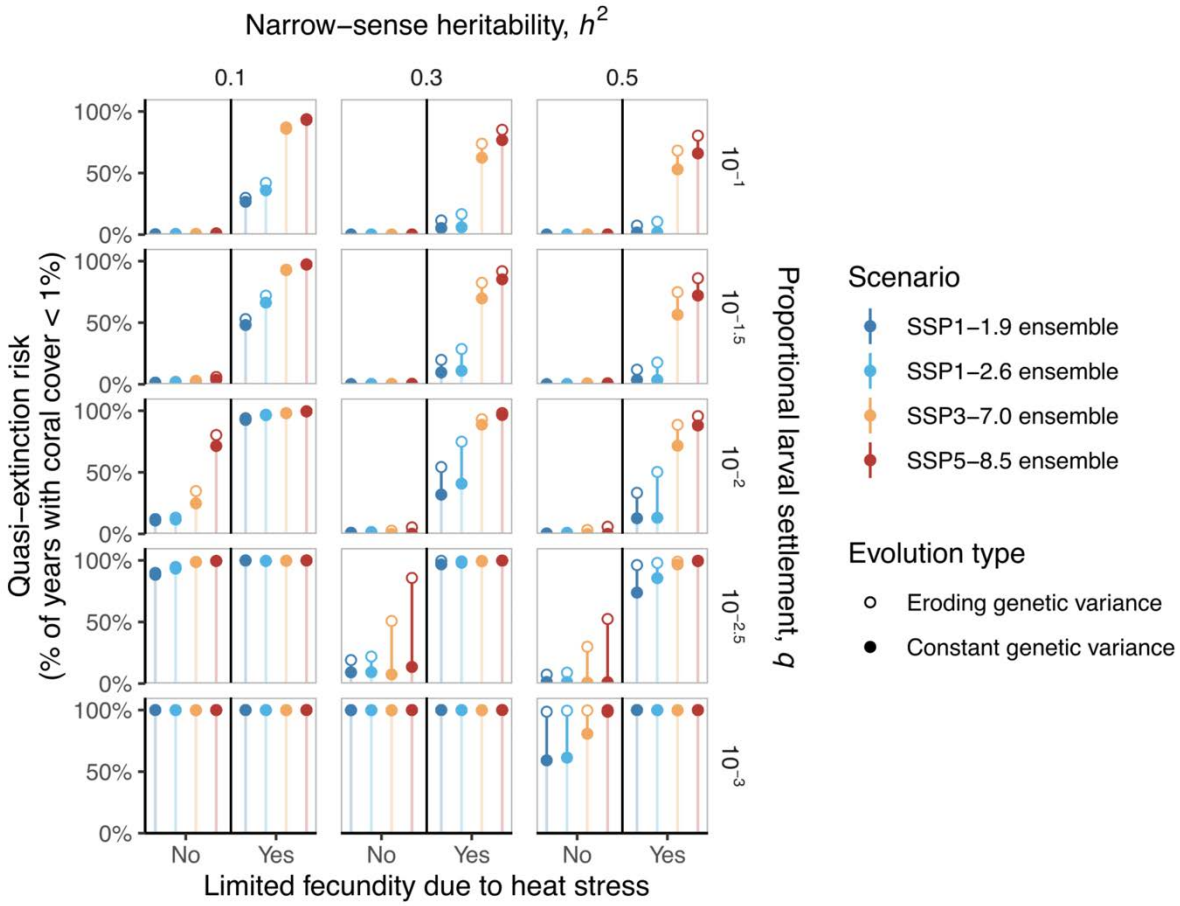

Fig. 4.3. Extinction risk (% of simulation time with coral cover below 1%) across parameter combinations (n=100 for each point). Simulations vary in terms of emissions scenario (colour), heritability of thermal tolerance (low to high h^2 from left to right panels), larval settlement (low to high proportion larval settlement from bottom to top panels), whether simulations include heat-stress limited fecundity or not (right and left of each plot), and whether genetic variance is constant (closed points) or are allowed to erode with selection (open points).

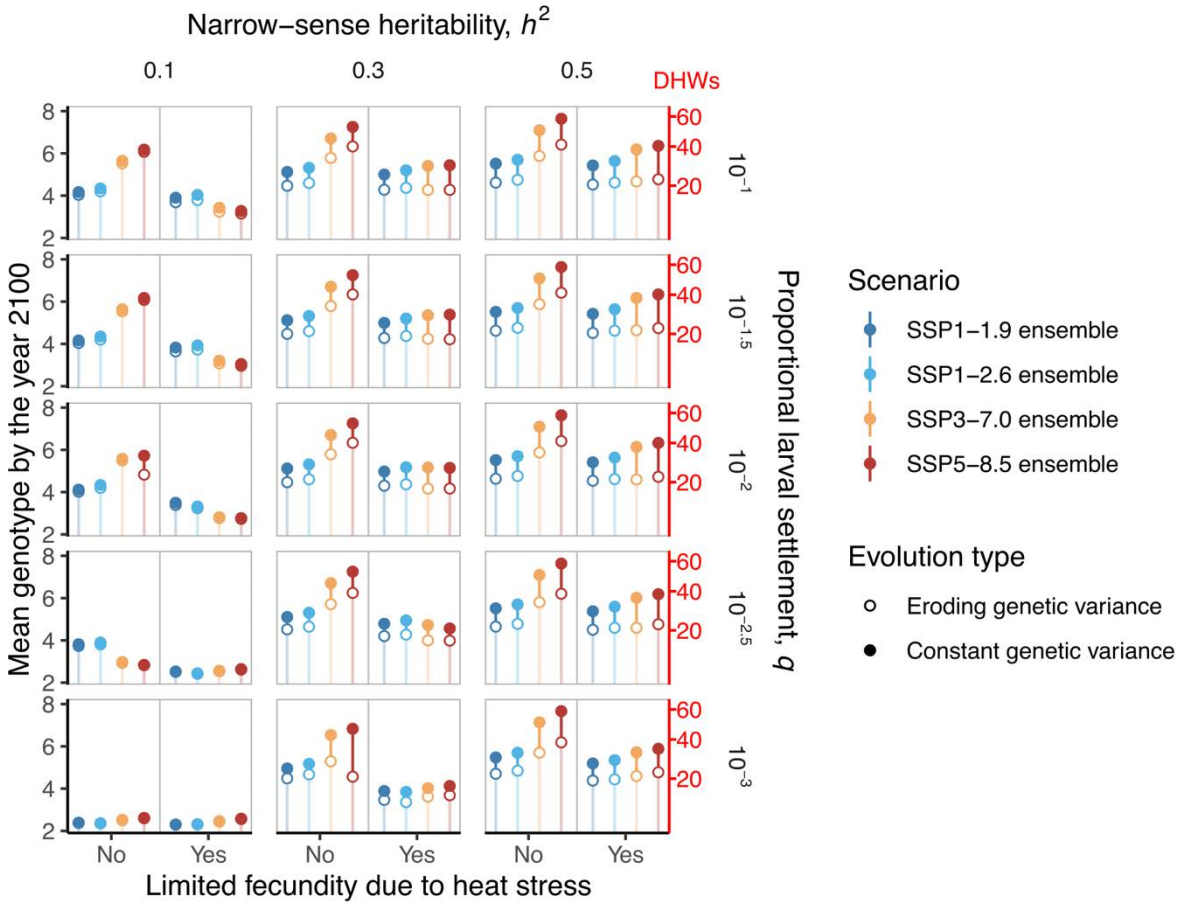

Fig. 4.4. Mean genotype evolution (in $\sqrt{DHW_{crit}}$, with equivalent critical DHW values displayed in red on the right axis) across parameter combinations (n=100 for each point). Simulations vary in terms of emissions scenario (colour), heritability of thermal tolerance (low to high h^2 from left to right panels), larval settlement (low to high proportion larval settlement from bottom to top panels), whether simulations include heat-stress limited fecundity or not (right and left of each plot), and whether genetic variance is constant (closed points) or are allowed to erode with selection (open points).

Density-dependence in intra-cohort interactions mediates initial population decline

Density-dependence in intra-cohort interactions strongly mediated the initial population decline with small adult breeding stocks attaining levels of recruitment not much lower than a much larger breeding stock (Fig. 4.2b; Fig. C4.1). However, if the number of successfully recruiting larvae relative to population reproductive output (q) is small (Fig. 4.2c), or if fecundity is diminished under future heat stress (Fig. 4.2d), the effect of intra-cohort density dependence is substantially diminished,

and recruits will decline more precipitously as the adult breeding stock declines. No previous IPMs include this form of density dependence, to my knowledge, which can greatly affect the proportion of settlers that successfully recruit at low population sizes when high larval settlement occurs (Chapter 3). Instead, most coral evolutionary models focus on proportional declines in population growth via the percent of space occupied or use a proportional larval settlement q estimated as the ratio of successful recruits to pre-existing colonies (Matz et al. 2020; McManus et al. 2021b; Sully et al. 2022).

Importance of sustained fecundity and larval settlement

Heat stress-limited fecundity greatly reduced reef resilience and recovery to future heat stress. Importantly, lower levels of larval settlement ($q = 10^{-2.5}$) were unable to stave off short-term population extinction when fecundity was limited by heat stress, and even at high levels of larval settlement, limited fecundity resulted in populations never fully recovering to equilibrium levels (Fig. 4.2g, Fig. 4.3). The lowest larval settlement parameter that sustained a coral population increased from $10^{-2.5}$ to 10^{-2}, meaning 3 times the incoming larvae were required to sustain reefs (Fig. 4.3, Fig. C4.1). With heat stress-limited fecundity, there were also striking differences among the four future scenarios. High emissions scenarios (SSP3-7.0 and SSP5-8.5) resulted in few years without high heat stress that suppressed coral fecundity (Fig. 4.2c), though populations were able to be maintained at lower coral cover in the short-term when the proportional settlement of larvae was sufficiently high, and heritability was intermediate to high (Fig. 4.2c). However, populations declined to extinction as heat stress accelerated in the high-emission scenarios by the year 2060 (Fig. 4.2c). In contrast, lower-emissions scenarios such as SSP1-1.9 (+1.5°C) and SSP1-2.6 (+2.0°C) saw limited recovery even when coral fecundity was compromised by accumulated heat stress (Fig. 4.2c). Simulations with heat stress-limited fecundity had little effect on the rate of genetic evolution relative to when fecundity was unaffected by heat stress (Fig. 4.4; Fig. C4.2), nor on genotype-size dynamics (Fig. C4.5). The size distribution of adults was also relatively unaffected when fecundity was heat-limited; however, the proportion of first year recruits was reduced or eliminated entirely in later years for SSP1-2.6, SSP3-7.0, and SSP5-8.5 (Fig. C4.4).

The intensity of the drop in coral cover following the start of simulated future heat stress in 2023 was highly dependent on the larval settlement parameter, q. At the highest settlement proportion examined ($q = 10^{-1}$ or 10% of all produced larvae), cover dropped by ~60% on average at the onset of future heat stress regimes in the absence of DHW-limited fecundity (Fig. 4.2a), and as high as ~1–5% when fecundity was limited by heat stress (Fig. 4.2c), but the depth of this drop increased even further with decreases in the larval settlement parameter (Fig. 4.2d,f,g; Fig. C4.1). Additionally, populations collapsed under a half order of magnitude lower proportional larval settlement ($q = 10^{-2}$), when fecundity was limited by heat stress (Fig. C4.1). The quasi-extinction risk (proportion of simulation time spent below 1% coral cover) was also reduced with increasing larval settlement (Fig. 4.3), and thus having more incoming larvae reduced population extinction risk. The equilibrium proportion of coral cover attained over the long run was also affected by the number of incoming larvae via the settlement parameter, so much so that at low larval settlement rates ($q = 10^{-2.5}$), the long-term viability of populations in all high emission scenarios (SSP3-7.0 and SSP5-8.5) became unlikely when genetic variance was allowed to erode (Fig. 4.2d, Fig. 4.3). However, genotype dynamics were relatively unaffected by the larval settlement parameter, with only slight reductions in the rate of adaptation when larval settlement was reduced at low levels of heritability ($h^2 = 0.1$). Additionally, no appreciable changes in the size distribution or genotype mean by size were noted across larval settlement levels (Fig. C4.4 and Fig. C4.5).

Evolutionary rescue through adaptation to climate change

The recovery of populations over the long term via adaptation to new environmental conditions, i.e. evolutionary rescue, was observed for all simulations where there was sufficiently high proportions of larval settlement and where populations maintained fecundity throughout high heat stress. At low heritabilities ($h^2 = 0.1$–0.2) but with high fecundity and proportional larval settlement, the equilibrium coral cover was reduced (Fig. 4.2b) but populations in all scenarios were able to recover and attain cover between 40 to 60% (cover was ~60% prior to heat stress due to intra-cohort density dependence). However, with either lower proportions of larval settlement or heat stress-limited fecundity, populations in all scenarios with low heritability declined to near 0% coral cover and

struggled to recover (Fig. 4.2e) or went extinct (Fig. 4.2g). Higher heritability generally reduced extinction risk (Fig. 4.3, Fig. C4.1), and often resulted in the evolutionary rescue of populations when larval settlement was low ($10^{-2.5}$ to 10^{-2}, Fig. C4.1a). Evolutionary rescue also occurred when fecundity was limited by heat stress, but only for low emission scenarios and at higher larval settlement parameter values ($10^{-1.5}$ to 10^{-1}, Fig. C4.1b). Higher heritability resulted in rapid mean genotype change occurring in the first five years during the initial onset of thermal stress (Fig. C4.2), coinciding with the strong bottleneck in coral cover during the initial onset of DHWs (Fig. 4.2), with the rate of genetic change decelerating and becoming more linear or flattening as populations recovered (Fig. C4.2). However, at the year 2100, most populations with heritabilities between 0.3 and 0.5 had relatively similar genotypes, indicating a saturating effect of heritability.

High adaptive potential with intermediate conditions

The mean of the genotype distribution was initially set to 1.90, or a critical DHW (DHW_{crit}) of $1.9^2 = 3.61$ DHWs (based on Hughes et al. 2018b). Model evolution predicts mean genotypes to evolve as high as 7.7 – translating to mean critical DHW thresholds (DHW_{crit}) of 60 °C-weeks by the year 2100 (Fig. 4.4). However, this level of evolution is only possible with unimpaired fecundity during heat stress – otherwise, evolution in the model is much slower, with final genotypes attaining values of 22–40 DHWs by the year 2100 for most viable parameter combinations (Fig. 4.4). The latter is more plausible, given that corals of the northern Red Sea have experienced accumulated heat stress greater than 15 DHWs (°C-weeks), yet have not experienced mass bleaching (Osman et al. 2018). The mean genotypes across all sizes of corals differed when populations were adapting to heat stress, with smaller corals having higher mean genotypes compared to larger individuals and the magnitude of change in mean genotype being determined by heritability (Fig. C4.5). However, the shape of the mean genotype across size remained unchanged even with higher heritability (Fig. C4.5) and the overall size distribution of corals being unaffected by heritability (Fig. C4.4).

Eroding genetic variance impairs population adaptation

When genetic variance was allowed to erode during selection, extinction risk was increased in many cases relative to simulations with constant standing genetic variance (Fig. 4.3). Similarly, evolution was also reduced for simulations with eroding genetic variance in all cases (Fig. 4.4) and the magnitude of this difference was determined by the heritability of thermal tolerance such that at low heritabilities ($h^2 = 0.1$), the mean genotype did not differ much between constant vs. eroding genetic variance simulations (Fig. 4.4; Fig. C4.2), because genetic variance was not being eroded by selection much, given the low heritability in selected phenotypes (Fig. C4.3). But at higher heritabilities, significant differences between constant vs. eroding genetic variation simulations were observed (Fig. 4.4; Fig. C4.2). Interestingly, the eroding genetic variance in all simulations where fecundity was unaffected by heat stress approached and attained similar levels of additive genetic variance to the $h^2 = 0.1$ simulations, approximately $V_a = 0.049$ by the year 2100 (Fig. C4.3). Genetic variance eroded quickly and coincided with the population bottlenecks observed early on in the onset of heat stress, then levelled off (Fig. C4.3). Where genetic variance eroded readily, coral cover was always lower (Fig. C4.1), with eroding genetic variance populations were often unable to cope with high emission scenarios relative to low-emission scenarios (e.g. Fig. 4.2d). Eroding genetic variance did not affect the shape of the mean genotype by size apart from reducing the mean genotype evolution (Fig. C4.5) and did not affect the overall size distribution of corals (Fig. C4.4).

Discussion

Population adaptation in response to climate change has the potential to rescue coral reefs from extinction, but only if sufficient adult fecundity and juvenile recruitment are maintained, and most importantly, if future emissions are curbed. As fecundity during heat stress and the proportional larval settlement increase, recruits per capita also increase, and thus population collapse becomes less likely. Additionally, with the compensatory intra-recruit density dependence incorporated in this model, there is less reduction in recruitment as the number of incoming settlers decreases due to warming. The outcomes of all models suggest that coral populations may be capable of evolving to and surviving low to moderate emissions scenarios provided populations have two or more of the

following: (1) high heritability of thermal tolerance, (2) high larval settlement success, and (3) fecundity unaffected by heat stress (Fig. 4.3). The heritability of thermal tolerance determined the extent of population adaptation (Fig. 4.4), resulting recovery in coral cover (Fig. 2), and aided to reduced population (quasi-) extinction risk (Fig. 4.3). However, the effect of heritability on population outcomes or evolution saturated around a value of $h^2 = 0.3$, with no appreciable alteration in population outcome or extinction risk beyond this moderate level of heritability of thermal tolerance. Combined with adequate fecundity and larval supply, heritable thermal tolerance of corals to heat stress allowed populations to evolve to global temperatures +1.5–2.0°C above pre-industrial levels under lower-emission SSP1-1.9 and SSP1-2.6 scenarios. Rapid genetic evolution of thermal tolerance allowed evolutionary rescue in high emission scenarios when the number of recruits produced per unit area of adult coral cover was high, due either to maintenance of fecundity in the presence of heat stress, high larval propensity to survival and settle (i.e. high q), or both. However, both larval settlement and fecundity in reality are likely to decline with higher heat stress (Hughes et al. 2019; Cheung et al. 2021), thus rapid and sustained evolution to high emission scenarios remains at best a possibility only for certain sink reefs with adequate thermal refugia and at worst spells the extinction of most reefs. Modelling the erosion of genetic variance in thermal tolerance after sequential mass mortality events resulted in increased population extinction across time, thus the extinction risk for many populations of reef-building corals remains far from absent if emissions are not curtailed in the next 50 years.

The importance of compensatory density dependence for understanding population resilience

Intra-cohort density dependence implemented in Chapter 3 resulted in models attaining plausible equilibrium coral cover levels over a broader range of proportional settlement (q). In this chapter, intra-cohort density dependence interacts with both q and the fecundity per unit area of coral cover to produce the population dynamics observed. When heat stress occurs, total fecundity is reduced; however, intra-recruit density dependence that was previously reducing the proportion of successful recruits on the reef is lessened due to population density dropping after heat stress. The result is an increased per-capita recruitment success via a reduction in post-settlement competition,

which buffers the effect of heat stress on overall population size (Jaatinen et al. 2021). This feature in turn limits population declines by reducing the downward spiral of lower adult stock producing fewer recruits, leading to even lower adult stock. Thus, the relative impact of heat stress on the incoming number of recruits is expected to be lessened in models that include density-dependent regulation relative to models without, and modelling compensatory density dependence is thus crucial to modelling populations' capacity to compensate for environmental deterioration (Bassar et al. 2016).

Comparing to other modelling studies

My results echo findings from other eco-evolutionary models, such as DeFilippo et al. (2022), which modelled a meta-population of evolving reefs across a temperature gradient resembling the GBR. They found that additive genetic variances of 0.04–0.10 allowed coral populations subject to lower relative temperatures to recover, given enough time and higher effective fecundities of 0.08–0.1 (similar to q in this study). However, at higher warming levels or at lower levels of additive genetic variance (corresponding to lower heritability in this study), population extinction was likely. In contrast, my findings suggest the increased importance of both fecundity and larval settlement relative to heritability, possibly as a result of explicit size-dependent genotype dynamics that were not included in DeFilippo et al. (2022), or because the current study is limited to only a single closed population that has no incoming or exiting coral larvae from neighbouring reefs experiencing different thermal stresses – thus variation in fecundity and larval settlement is not buffered by meta-population connectivity and therefore becomes exceedingly important. Additionally, the model in DeFilippo et al. (2022) did not include intra-cohort density dependence, which could alter the impact of fecundity and larval settlement on population outcomes. Matz et al. (2020) observed rapid evolution across meta-populations, with populations being maintained even through higher emissions scenarios except for simulations where corals could not spawn and transmit offspring when heat stress occurred. Their meta-population model highlighted the importance of immigrants from lower latitude reefs (i.e. hotter) in promoting evolution. Another meta-population connectivity model of Caribbean populations of *Orbicella annularis* to future projected temperatures (no adaptation) suggests that local efforts to increase reef resilience could maintain broader meta-population connectivity in the short-term, but

eventually, without adaptation, meta-populations are likely to collapse without significant reductions in emissions (Holstein et al. 2022). Similar to the single-population model, Bay et al. (2017c) used a genomic model of corals at Rarotonga, Cook Islands and found that genomic evolution was likely if emissions were kept low, but not when high emission scenarios were considered.

Saturating effect of heritability and eroding genetic variance

However, contrary to these prior studies, my findings suggest that the utility of higher heritability of thermal tolerance in reducing extinction risk may saturate at intermediate levels (e.g. h^2 = 0.3; Fig. 4.3), though the rate of evolutionary rescue and population growth with heat stress is still increased at higher heritabilities (Fig. C4.1). My findings also highlight the increased extinction risk from eroding genotypic variance in populations experiencing repeated and large selection events as in the case of the high emissions scenarios. This process has not been incorporated in most eco-evolutionary models to date whereas this Chapter shows that it causes, at best, lower equilibrium levels of coral cover and, at worst, population extinction relative to the assumption of constant genetic variance. Eroding genetic variance resulted in greater extinction risk specifically for simulations with higher heritability, but these differences again plateaued at higher heritability (h^2 = 0.5). While the extent of eroding genetic variance modelled here is unlikely to occur in reality due to its maintenance through segregation and mutational variances (Falconer and Mackay 1996; Coulson et al. 2021), repeated selection does have the potential to erode genetic variance over the long term, and highlights the importance of estimating genetic variance in population thermal tolerance.

Heat stress-limited fecundity

Populations that experience fecundity suppression due to heat stress may be unable to reproduce in most years under projected heat stress conditions of high emissions scenarios SSP3-7.0 and SSP5-8.5. This is concerning, as many coral populations to date have been found to have low-to-no fecundity after 8–9 DHWs (Ward et al. 2000; Donner et al. 2005; Levitan et al. 2014; Hagedorn et al. 2016; Hughes et al. 2019), and bleaching can induce sublethal impacts that reduce coral fecundity (Levitan et al. 2014; Hughes et al. 2019; Leinbach et al. 2021). However, other populations have

observed compensatory rebounds in fecundity and recruitment in later years after bleaching (Morais et al. 2021; Nakamura et al. 2022), and there is also potential for adaptation of increasingly heat stress-tolerant fecundity in adults corals. This may occur because bleaching resistant corals retain more energy and produce more offspring relative to bleached corals (Leinbach et al. 2021) and any offspring of individuals that do spawn during heat stress will experience much higher fitness relative to corals that wait for optimal temperatures to spawn. Additionally, natural selection is equally likely to act upon fecundity under heat stress just as it does survival under heat stress, thus further capacity for corals to spawn to heat stress may evolve if this trait exhibits intra-population variability and is heritable. Some mussid corals already are capable of spawning while entirely bleached (Godoy et al. 2021). Additionally, trade-offs in terms of fecundity (e.g. number of eggs) vs. egg size in thermally tolerant corals have been observed (Hazraty-Kari et al. 2022), and could be examined in future models. While this was not modelled, as more evidence of improved fecundity under heat stress becomes available – either through adaptation or acclimatization – future models may be able to narrow down potential population outcomes related to coral fecundity declines after heat stress.

Given the above, predictions from my model when fecundity is limited by heat stress (i.e. unable to spawn at ≥8 DHWs) appear pessimistic. Corals are likely to be limited in terms of fecundity initially, but may experience population recovery and evolution in the subsequent years following heat stress-limited fecundity – as have been observed previously (Morais et al. 2021; Nakamura et al. 2022) – if not impacted by other previously mentioned stressors in the meantime such as COTS, cyclones, ocean acidification, disease, and more. The synergistic negative impacts of all these stressors combined are already likely underestimated when modelled independently (Setter et al. 2022). On the other hand, additional sources of larval and juvenile mortality due to heat stress were not examined, such as reductions in sperm motility or recruitment failure due to bleaching before, during, or after spawning (Levitan et al. 2014; Hagedorn et al. 2016; Hughes et al. 2019),. These and other sources of mortality may cause population responses to be more similar to the DHW-limited fecundity results presented here. Similar to variability in thermal tolerance (Yetsko et al. 2020; Humanes et al. 2022), the functional response of fecundity to heat stress is likely to vary within populations, between populations, and across species. To be able to better model this in future work, more longitudinal data

of intra- and inter-population variability in fecundity during bleaching events are required. Many studies have focused on variability in intra- and inter-population coral recruitment rates (e.g. Fisk and Harriott 1990; Dunstan and Johnson 1998; Jouval et al. 2019), but few have linked heat stress with patterns of fecundity or successful recruitment to date.

Model limitations

In the absence of fecundity limitation due to heat stress (which itself is unlikely to be true), corals were able to adapt to climate change given moderate-to-high larval settlement (proportional settlement of all larvae exceeding 0.1%) even when the heritability of thermal tolerance was low (h^2 = 0.1). While the model predicts population resilience even with low heritability, in reality, reductions in population size are expected for other demographic processes and concerning life stages apart from adults. Future climate change can alter adult demographic rates apart from survival and fecundity (as implemented in this study), such as reducing coral growth as a result of reduced skeletal growth with increased ocean acidification due to climate change (Hoegh-Guldberg et al. 2017) or due to demographic trade-offs with increased thermal tolerance (Cunning et al. 2015b; Bay and Palumbi 2017; Cornwell et al. 2021). Additionally, future heat stress is likely to reduce fecundity and energetic reserves in adults and juveniles (Hagedorn et al. 2016; Leinbach et al. 2021; Hazraty-Kari et al. 2022) and larval settlement and establishment of recruits (Edmunds 2017; Hughes et al. 2019; Speare et al. 2022). The repeated bleaching effects on coral adults and juveniles remain unknown, but one recent study suggests that the limits of juvenile acclimation are surpassed after three years of constant heat stress, resulting in coral mortality after this time frame (Hazraty-Kari et al. 2023), thus my estimate of coral cover may be optimistic without significant adaptation in traits related to successful coral reproduction and recruitment. Additionally, my model suggests that adaptation to high heat stress can continue to progress even under high emission scenarios, given adequate recruits produced per unit area of adult coral cover. However, no population can evolve to gradual environmental change indefinitely, as eventually population evolution will reach functional and developmental limitations that cause the population to succumb to extinction (Burger 1995; Klausmeier et al. 2020). When these critical thresholds are surpassed, mean fitness becomes negative and populations decline rapidly

(Klausmeier et al. 2020). Thus, while critical limits to heat stress adaptation are unknown, they are likely present, and represent an important upper bound to evolutionary rescue that require further investigation.

Size-dependent dynamics

Interestingly, the size distribution of corals was relatively similar across all simulations and parameter combinations (Fig. C4.4), save for the collapse of recruit populations in high-emission scenarios when fecundity was suppressed at high levels of heat stress. The size distribution of corymbose corals has previously been examined by Dietzel et al. (2020). Corymbose ('Other Acropora') have experienced a decline in the abundances of small, medium, and large-sized corymbose colonies in recent years relative to historic records of size distribution; however, no noticeable shift towards larger or smaller sizes of acroporids has been observed in response to recent bleaching events (Dietzel et al. 2020), which is consistent with the models analysed here. The size-dependent demography of corals not only impacts the outcomes of non-bleaching years (e.g. Chapter 3 of this thesis) but also affects coral mortality and genotypic evolution. Heat stress can disproportionately affect specific life stages of corals and sizes. For example, during the 2019 bleaching event in Moorea, French Polynesia, heat stress disproportionately reduced adult acroporid survival such that juveniles and adults survived similarly and total fecundity was reduced by 60% as a result of the loss of adult corals, with recruit survival in the following year being as low as 2% (compared to 33% in the preceding year without bleaching) (Speare et al. 2022). Some authors have noted that with the extinction of entire cohorts of adults due to bleaching, a uniform size distribution of juveniles can emerge and enter bleaching-sensitive stages at the same time, resulting in so-called 'boom-and-bust' dynamics that are especially sensitive to bleaching (Morais et al. 2021; Speare et al. 2022). However, no such cycling was observed in the models of this chapter, despite the explicit incorporation of episodicity in thermally-induced mortality events.

Notably, larger corals in the present study often had mean genotypes up to 1 unit of genotype lower, translating to a difference in critical heat stress tolerance of ~9 DHWs for the largest vs. smallest corals. This is slightly higher than the difference in DHW sensitivities between lower and

upper deciles observed in Humanes et al. (2022) of 4.8 (95% CI: 3.1 – 6.8), and is thus high but not implausible. While not implemented in this model explicitly, the size-dependent effects of bleaching disproportionately affect adults relative to smaller juveniles (Bena and van Woesik 2004; Shenkar et al. 2005; Depczynski et al. 2013; but see Baird and Marshall 2002 showing equal mortality across sizes). Additionally, considerable recruitment and juvenile growth rebounds have been observed after large-scale recruit mortality (Morais et al. 2021; Nakamura et al. 2022). In the present study, large-scale mortality due to heat stress strongly selected for heat tolerant genotypes, but corals took years to attain adulthood and higher levels of fecundity. The result was a slightly narrower log-normal shaped size distribution for adults, with a large peak of juvenile corals, similar to the narrowing of size distributions observed in (Roth et al. 2010).

Data limitations to modelling coral evolution

Important gaps in available empirical data required me to keep the evolution characterized in my models relatively simple, in terms of the underlying genetics, traits under selection, and the environment component of phenotype. Thus, caution is warranted in extending my current model to predict future reef evolution. For example, there is some evidence for genotype-by-environment interactions in coral bleaching patterns, and thus thermal tolerance (Drury and Lirman 2021). However, these data appear highly population-specific due to local adaptation, and thus would require extensive empirical data from transplant studies of different coral genotypes in a number of environments to be able to be incorporated in a model such as the one analysed here. Apart from the simplifying genetics mentioned previously (e.g. strictly additive genetic variance, no genotype x environment interactions, no non-genetic inheritance), there is some evidence that trait adaptation may be limited by physiological, demographic, and evolutionary trade-offs such as reduced thermal performance breadth with higher temperatures (Rezende et al. 2014; D'Angelo et al. 2015; Comte and Olden 2017; Baker et al. 2018), upper vs. lower critical limit trade-offs (Schou et al. 2022), and growth–thermal tolerance trade-offs (Cunning et al. 2015b; Bay and Palumbi 2017; Cornwell et al. 2021). However, to fit models involving multiple trait trade-offs and to parse out additive genetic trade-offs within these data will require extensive multivariate, longitudinal data combined with

animal pedigrees to calculate genetic trade-offs, which do not exist to date (but see Wright et al. 2019). One area of focus that may greatly aid evolutionary modelling of corals would be the quantification of the effect of deteriorating environments on the environment (*e*) component of phenotype (McCleery et al. 2004; Coulson et al. 2021). For example, if human-induced environmental degradation has a negative effect on the mean of the environmental component, then the amount of selection acting on additive genetic variance will increase, in turn leading to accelerated change in mean breeding value while reducing total phenotypic responses to environmental change (Coulson et al. 2021).

Summary

Projecting the long-term outcome of ocean warming due to climate change on coral populations will therefore depend on population projection models that include realistic evolutionary dynamics of thermal tolerance. The EE-IPM framework for corals developed here simulates size-dependent and genotype-dependent population dynamics, allowing size-by-genotype interactions to occur, and can be extended to more complicated assumptions about genetics and meta-population structure as the data needed to calibrate such relationships become available. This study represents a proof-of-concept for how genetic evolution shaped by size-dependent demography can manifest in eco-evolutionary models of corals. My model finds that with sufficient heritability of thermal tolerance combined with adequate per-capita recruitment success (through higher proportional larval settlement and maintained fecundity during heat stress), population declines can be reduced and time for adaptation to occur in response to low emission heat stress scenarios. However, with the loss or absence of sufficient heritability or per-capita recruitment, evolution to future climate change becomes increasingly unlikely if not impossible, depending on if emissions are curtailed by the end of the first half of the century. Eroding genetic variance due to repeated selection increased coral extinction risk – representing an important aspect of evolution that is rarely examined by current eco-evolutionary models to date. Local monitoring and management of coral populations to ensure sufficient and healthy population numbers prior to large-scale bleaching is the only path that can buy time and fuel for coral adaptation to short-term climate change, while emissions are curbed globally. Without lower emissions, coral adaptation is unlikely to suffice for many populations.

Data accessibility statement

All R code will be made available at https://github.com/ecolology/evolIPM.

Chapter 5 General Discussion

This thesis examined three main questions related to understanding coral population responses to climate change, namely: (a) at what rate can coral populations evolve? (b) how does local demography and recruitment determine coral population persistence and stability? And (c) how will local demography and population adaptation combine to shape coral population trajectories in the future, given predicted heat stress due to anthropogenic climate change? These questions are answered in Chapters 2, 3, and 4 of my thesis, respectively. In Chapter 2, I assessed the likely rate of adaptation of coral traits using a meta-analysis of the narrow-sense heritability coefficient, h^2, and found that heritability was higher than assumed in some recent models of coral evolution and there was no change in heritability across increasing temperatures, suggesting that heritability may be well maintained across future heat stresses. In Chapter 3, I constructed a density-dependent integral projection model (IPM) of coral demography to assess population sensitivity to varying parameter values and functional forms characterizing demographic rates, and found that how early recruitment and density dependence is characterized substantially influences the plausibility of population trajectories. Finally, in Chapter 4, I built the first evolutionarily-explicit IPM for coral responses to climate change using plausible heritability estimates from Chapter 2 combined with size-dependent demography in Chapter 3. My findings were consistent with outcomes of previous modelling studies in highlighting the importance of reducing emissions to provide more time for natural population evolution to occur with sufficient population maintenance and recruitment, but also reveal significant size-dependent lags in the abundance of thermally-tolerant genotypes that can reduce natural evolution, but that have not been included in prior models.

In this final Chapter, I begin with a thorough consideration of the limitations to each of my chapters. I then discuss future research that would fill gaps in our understanding of coral adaptation and demography that currently constrain the robustness of projections from all models of such processes, as well as model extensions that would be worthwhile to improve our knowledge of reef adaptation and responses to climate change. I note the implications of my models to inform marine policy and management pertaining to reefs. Finally, I discuss my thoughts on the future of coral reefs, based on the findings presented in this thesis.

Variability in heritability

Narrow-sense heritability is often inferred via a variety of methods, via parent-offspring regressions, as 'realised heritability' in artificial selection studies using the Breeder's equation, and most commonly for corals with the animal model – which lends itself well to the (G)LMM structure used to analyse most biological experiments. Within each of these approaches, the heritability retrieved is likely to be different (e.g. Kirk et al. 2018). and within even the animal model, results can differ depending on how temperature and other covariates are parameterized (Wilson 2008; see Chapter 1 discussion), e.g. as a covariate (preferred), a treatment, or as separate traits/analyses of heritability.

Additionally, narrow-sense heritability and the 'additive genetic variance' estimated using even the animal model for pedigrees that include non-clonal individuals are still likely to carry other sources of variation including permanent environmental variance, maternal/paternal environment, maternal/paternal genetics, and some variation associated with genetic dominance (Wilson et al. 2010). It is often assumed that these sources of variance are weak or negligible relative to additive genetic variance, and this may be true in some cases (Hill et al. 2008), but is not guaranteed, and can result in problems such as 'phantom' or 'missing heritability' due to variance unexplained by gene epistasis (Zuk et al. 2012; Yang et al. 2014). Most of the additional sources of variance can only be identified with a high level of data on individuals and their associated pedigrees, such as through repeated measures of individuals within and across different environments (Wilson et al. 2010) or possibly via explicit genomic analysis (Quigley et al. 2020a). Heritability can also increase across the age of the organism (Wilson et al. 2008), while additive genetic variance can either increase or decrease with selection (Wheelwright et al. 2014; Rowínski and Rogell 2017). Taken together, heritability estimates throughout the literature are likely to be inflated and highly variable, depending on the way the animal model is constructed and conditioned (Wilson 2008). While estimates produced by different methods are expected to converge to similar values when true heritability is high (e.g. Meher et al. 2022), the heritabilities presented by my meta-analysis may be biased somewhat high for both broad-sense and narrow-sense estimates. While there are advantages to specific, targeted studies examining sources of variance, which could reduce the effects of these biases on a case-by-case basis, the end objective of my meta-analysis was to summarise across all h^2 estimates, rather than extract more exact additive genetic variances from a single coral species, life stage, or across a temperature regime.

Heritability is not adaptation

Single-trait heritability is not good at predicting adaptive evolution relative to multi-trait heritability models (Hansen et al. 2011; Morrissey et al. 2012; Hajduk et al. 2020). Simplifying evolution to a single trait often a necessary simplification due to the data available, but the multivariate Breeder's equation shows that if there is negative genetic covariance between two traits under selection, evolution will be constrained (Falconer and Mackay 1996; Walsh and Blows 2009). There have also been critiques of the heritability coefficient itself. For example, the additive genetic variation (from which heritability is calculated) is correlated with other sources of phenotypic variation, such as additive-by-additive epistasis associated with a diallelic locus. Instead, Hansen et al. (2011) advocate for the use of 'evolvability' or e, calculated as the mean-scaled (rather than variance-scaled) additive genetic variance (i.e. $e = V_A/m^2$, where m is the trait mean), similar to the square of the coefficient of variation. While no studies of corals to date have reported this metric, and only a couple of studies examined in Chapter 2 provide estimates of V_A and m for calculating this quantity, it is worthwhile reporting in future studies alongside heritability – though it is unclear to what extent epistasis and additive genetic variances are correlated when considering a polygenic model of trait inheritance involving many hundreds of loci.

A larger issue with heritability both in terms of univariate and multivariate forms of the Breeder's equation is the underlying assumption that all other factors affecting the relationship between phenotypic trait(s) and their contribution(s) to fitness are experimentally controlled for (Morrissey et al. 2010, 2012). This is never the case in ecological studies, and may be especially problematic for observational studies that use the Breeder's equation to estimate trait heritability while not controlling for variation in (micro)environmental covariates (Morrissey et al. 2010). One alternative to the Breeder's equation is the Robertson-Price identity, which predicts phenotypic change in a trait (Δz) as the additive genetic covariance between the trait (z) and absolute fitness (ω): $\Delta z = \sigma_A(z, \omega)$. Estimating the covariance between a trait and fitness requires fitting a bivariate or multivariate 'animal model' (just as the univariate animal model often used for trait heritability), with one of the response variable acting as a proxy for fitness (e.g. binary survival), and the other variable(s) acting as traits of interest. From this, one can estimate the proportion of genetic and phenotypic covariance between the two traits, which, using the Price-Robertson identity, can be

used to predict adaptation given a trait value (Morrissey et al. 2010; Hajduk et al. 2020). However, the Robertson-Price identity does not differentiate between direct and indirect selection, it simply models the proportion of trait variation that is associated with fitness (and thus, either the direct result of or indirectly related to the trait in question). Therefore, Stinchicombe et al. (2014) advocates the use and comparison of both the multivariate Breeder's equation and the Robertson-Price identity when estimating heritability to make the most of both equations. Again, however, the meta-analytical approach adopted in Chapter 2 limits me to the most prevalent estimates reported – of which narrow-sense heritability for a single trait (i.e. univariate Breeder's equation) is the most common.

While most studies measuring heritability and adaptive change in corals occur over the short-term via thermal stress experiments on parents and/or offspring, not all studies measured symbiont-specific variation shared among related corals, and no studies quantified the importance of a shared microbiome on holobiont thermal tolerance (Bairos-Novak et al. 2021). Therefore, heritability of coral responses again could be biased, and the long-term adaptation of coral populations will likely be rate-limited by the least evolvable aspects of the coral holobiont, presumably the coral host itself. Despite this, many studies have highlighted the enormous adaptive potential of symbiont shuffling in thermal tolerance (Barfield et al. 2018), and strongly heritable symbioses (Quigley et al. 2018a; Quigley et al. 2019) and microbiomes (Webster and Reusch 2017; Marangon et al. 2021), which may in turn lead to an underestimation of holobiont evolvability (Drury 2020).

Genotype-by-environment interaction and correlation

The presence of genotype-by-environment (GxE) interactions have the potential to influence results. GxE interactions occur when specific genotypes do better in specific environments, as is the case for local adaptation (Kawecki and Ebert 2004). Additionally, genotypes and environment may be correlated. Substantial GxE interactions have been noted in corals (Mieog et al. 2009a; Howells et al. 2013; Lundgren et al. 2013; Drury et al. 2017), such as for Central and Southern GBR *A. millepora*, transplanted between two sites separated by more than 600km (Howells et al. 2013), as well as in Floridean *A. cervicornis* transplanted only 60km away (Drury and Lirman 2021). The latter noted a strong genetic basis for thermal tolerance but no single genotype that did predominantly better than average at all sites relative to others. This is also reflected in the strong evidence of local adaptation of symbionts, microbiome, and host genetics that has

2459 been previously noted (Howells et al. 2012; Kelly et al. 2014; Kenkel et al. 2015a). Thermally-adapted
2460 genotypes from other locations can be maladapted to local conditions in habitats where they might otherwise
2461 spread, and thus thermally-adapted genotypes may perform poorly despite their thermal suitability. Thus, the
2462 spread of thermally-adapted loci across the GBR is unlikely to occur through a universal sweep of loci with
2463 the current amount of local adaptation currently present on the reef, and thermal tolerance in one location
2464 may not necessarily translate to thermal tolerance in another location. GxE interactions in bleaching may
2465 also suggest the presence of coral genotypes that are more thermal generalist vs. thermal specialist, which
2466 requires investigation to properly model meta-population evolution with larval migrants.
2467
2468 *Variable larval recruitment*
2469 Larval recruitment on coral reefs is known to be highly variable – both spatially and temporally
2470 (Fisk and Harriott 1990; Dunstan and Johnson 1998; Edmunds 2018; Jouval et al. 2019; Evensen et al. 2021;
2471 Koester et al. 2021; Thomson et al. 2021), likely due in large part to local currents and hydrology that is
2472 seasonal but often semi-stochastic in nature and difficult to forecast accurately (Gouezo et al. 2020, 2021).
2473 Therefore, stochastic simulations may be more reasonable to model larval recruitment, where parameter
2474 values are re-drawn from their uncertainty distributions each year, resulting in stochastic recruitment. This
2475 was not examined in the scope of my thesis, in part because I did not find data for reasonable distributions of
2476 recruitment rates across years for Lizard or Orpheus Islands – though one may exist. However, stochasticity
2477 in larval recruitment is not expected to affect model outcomes apart from adding noise if stochasticity is
2478 somewhat normally distributed, but this may depend on the shape of the distribution of larval recruitment
2479 densities observed across time. For example, if the distribution of larval settlement is left- or right-skewed,
2480 modelled larval settlement will be greater than or less than true larval settlement of the system.
2481
2482 *Net larval settlement rates*
2483 Overall, however, the levels of larval recruitment produced in my models was within the range of
2484 what is observed in the field. For example, the maximum settler density observed for any parameter
2485 combination from Chapter 3 before accounting for density dependence was 18.5 settlers/cm^2, which is higher
2486 than most studies (Table 5.1), but within the realm of plausibility. For example, Gouezo et al. (2021)
2487 observed recruit settlements on one particular reef as high as 11 recruits/cm^2 (Gouezo et al. 2021). Even

higher larval settlement densities have been observed, though the longer the tile is immersed, the lower the observed larval settlement density (Price et al. 2019), making comparisons difficult without accounting for differences in time. Across a meta-analysis of recruitment tiles (Price et al. 2019), studies after 1 year of immersion time reported mean recruit densities as high as 0.2 juveniles/cm^2. After post-settlement density dependence, the maximum number of recruits in my models was 0.03 juveniles/cm^2 (Fig. 5.1), suggesting that rates of recruitment in my model are realistic. This also happens to be the threshold density described by Thomson et al. (2021), above which sites are considered to have 'high recruitment' (but this level is likely prior to any post-settlement density dependence). As mentioned in Chapter 4, intra-cohort density dependence aids to mitigate losses of recruitment when adult coral cover is depleted. This is because even with smaller numbers of fecund adults, the population is able to attain the same coral cover as with larger numbers of adults – something that is missing from many models of corals (Matz et al. 2020; Holstein et al. 2022).

Table 5.1. Examples of maximum larval densities on settlement tiles from the literature.

Study	Maximum observed density	Taxon
Thomson et al. (2021)	0.273 recruits/cm^2	Various; *Acropora* predominantly
Jouval et al. (2019)	1.7 recruits/cm^2	Various; *Pocillopora* predominantly
Roth et al. (2010)	0.0009 recruits/cm^2	*Acropora spp.*
Gouezo et al. (2021)	11 recruits/cm^2	*Acropora* spp.
Koester et al. (2021)	0.0366 recruits/cm^2	*Acropora* spp.
Koester et al. (2021)	0.1545 recruits/cm^2	*Pocillopora* spp.

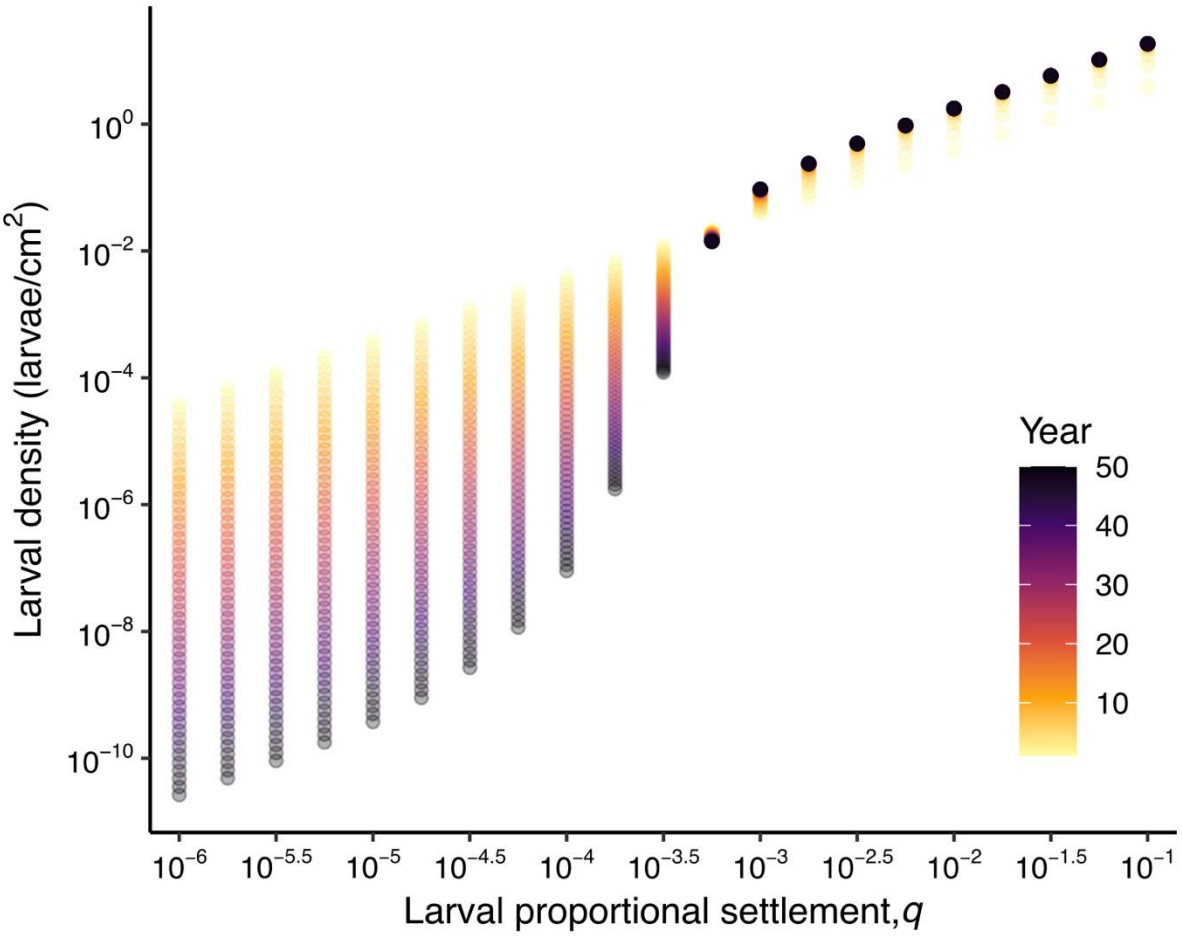

Fig. 5.1. Realised larval densities across time (colour) and differing proportions of larval settlement, q (x-axis) after intra-cohort post-settlement density dependence (Beverton-Holt model) using Lizard Island growth and survival settings from Chapter 3's model of coral demography in the absence of heat stress. When the level of per-capita recruitment no longer supports population regulation at equilibrium (i.e. $q < 10^{-3}$), realised larval densities decline towards extinction through time during the simulation.

Allee effects at low population densities

Allee effects may occur in natural populations that limit the potential for reef recovery (Allee 1931). At low coral cover, larvae may not recruit to the reef due to a lack of chemical cues (Gouezo et al. 2021; Sims et al. 2021), or due to reduced particle settlement in the absence of coral thickets to slow down settling larvae. My model used a simple proportional relationship to determine coral recruitment, with the proportion recruiting declining as the proportion coral cover increased. Thus, my models might be overestimating the likelihood of successful population recovery when populations decline to very low densities, especially in high emission scenario models, where high thermal stress results in a large proportion of the population

bleaching and dying, which emits chemicals that may further impair or interact with larval settlement cues (McCormick et al. 2014).

Rapid growth of juveniles

My model consistently finds high levels of first-year recruits (~25% of available reef area at equilibrium, vs. ~50% adult coral cover for Lizard Island parameter settings) and these recruits grow rapidly to meld with the adult size distribution within a single generation – meaning many are able to reproduce within a single year. This suggests that my model overestimates the contribution of the recruit population to population viability, and thus could yield somewhat optimistic estimates of extinction risk and equilibrium cover. However, similar to recruitment rates, the proportion coral cover of juveniles and adults is also highly variable, such as for North Reef (Fig. 5.2), suggesting that the maximal proportion coral cover observed in my models remains plausible. Additionally, the mean abundance of juvenile corals was highly dependent on the choice of growth and survival functions, with Orpheus Island having much less juvenile cover relative to Lizard.

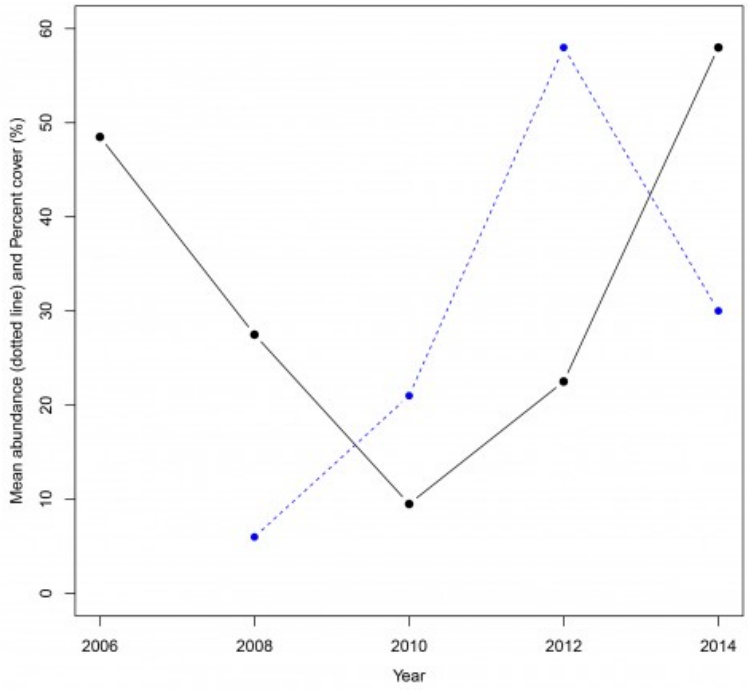

Fig. 5.2. Mean abundance of hard coral juveniles (less than 5 cm in diameter; dotted blue lines and points) and hard coral percent cover (solid black lines and points) at North Reef. (Plot adapted from EAtlas.org.au, 2022).

2536 However, the rapid growth of juveniles in my model relative to the literature is also an issue. Most
2537 studies suggest that corymbose corals mature in about 3–5 years, with individuals becoming gravid after
2538 about 12–15 cm in diameter (Baria et al. 2012). However, using the growth curves fit in Madin et al. (2020)
2539 for Lizard Island, most corals attain adult fecundity within 1-2 years in my model for Chapters 3 and 4, and
2540 even faster (1 year) for growth curves from the Orpheus Island population. This inconsistency in my model
2541 may be explained by a lack of data on juvenile coral growth in the Lizard Island and Orpheus Island
2542 longitudinal datasets. However, the growth trends observed in Madin et al. (2022) remain consistent across
2543 smaller juvenile coral colony sizes reported in Doropoulos et al. (2015, 2022) (Fig. 5.3), suggesting that
2544 growth rates based on Lizard Island at least are plausible. Thus, I am unsure of why my model's growth is so
2545 rapid relative to the literature, but until more data becomes available on recruit sizes, the growth function
2546 used in my model for at least Lizard Island appears reasonable for recruits (Fig. 5.3).
2547

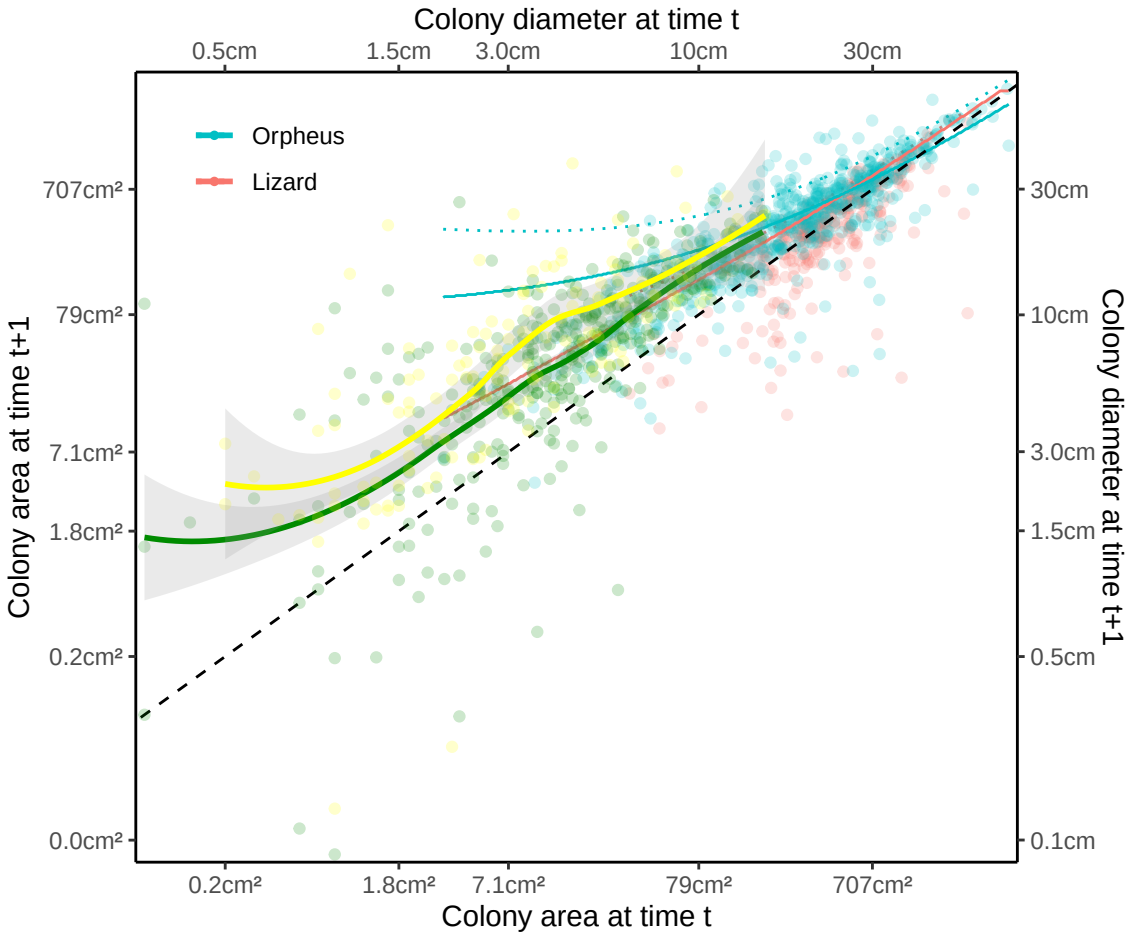

2548

2549 **Fig. 5.3.** Time-corrected colony growth data from Orpheus (blue) and Lizard Island (red) vs. *Acropora*
2550 recruit growth observed in Doropoulos et al. (2015, in green) and Doropoulos et al. (2022, in yellow). Most

likely colony growth curves for Orpheus and Lizard are displayed using a solid line, while maximum growth curves (i.e. 95% quantiles representing no partial mortality) are represented by the dotted line. Green and yellow lines represent loess smooth fits for Doropoulos et al. (2015, 2022), respectively. Note the similarity of green and yellow lines to the red line indicating most likely growth for Lizard Island corals.

Other sources of genetic and environmental variation

The evolutionary component of the model presented in Chapter 4 makes some simplifying assumptions about the underlying genetics, traits, and environment (Fig. 5.4). However, as more data become available, these processes may be added to the model, given its structure. For example, regarding assumption #1 (Fig. 5.4), non-additive genetic variance and other environment-based forms of thermal tolerance have already been discussed previously to contribute to phenotype (and see Richards et al. 2023); however, if the mathematical relationship between additive genetics and dominance/epistatic genetics is determined with high precision population genetics methods in the future, the effect of additive genetics interacting with dominance/epistasis could be quantified similar to: $z = g*x + e$, where z represents the thermal tolerance phenotype and x the multiplicative effect of dominance and/or epistasis. Similarly, there is evidence for genotype-by-environment interactions in coral bleaching patterns (assumption #2) (Drury and Lirman 2021), and thus, this is likely also true for coral survival in response to heat stress. This could be added in a straight-forward way to my EE-IPM using equations derived for specific study sites (e.g. $z = g + e + C*g*e$, where C is a constant representing the genotype-by-environment interaction).

There is also ample evidence of developmental or phenotypic plasticity changing throughout coral lifetimes, e.g. studies noting 'preconditioning' in corals (Bellantuono 2013; Bay and Palumbi 2015; Kenkel et al. 2015b; Putnam and Gates 2015). Plasticity in an EE-IPM can be implemented by allowing the e term to change based on previous heat stress. For example, e might be a modelled as part fixed (e.g. e_{fixed}) and part variable based on previous heat stress. If e depends on the previous five years of experienced heat stress, this would look like: $e = e_{fixed} + C\frac{\sum \mathrm{DHW}_i}{5}$, where C represents a constant describing how the mean of the past 5 years of DHWs alters the environmental component of phenotype, and thus causes changing phenotypic plasticity across an organism's lifetime.

Another component of the environmental component may be the effect of deteriorating environments on the capacity for organisms to respond (Coulson et al. 2021). This is typically modelled using the 'animal model' for a specific trait, with covariates describing how an organism's trait changes relative to environmental change, input as a covariate (Simmonds et al. 2020; Coulson et al. 2021). Studies that aim to assess the effects of environmental degradation on the environmental component of thermal tolerance could track individual coral adults and their experimental responses to heat stress, harvest and artificially cross gametes in the lab, then outplant and monitor these corals unto adulthood to again measure their thermal responses to naturally-occurring bleaching events and fit them using the animal model to determine important environmental covariates. This also could potentially be done entirely in a laboratory given a long-running coral breeding research program, but the sample sizes and time required to attain enough statistical power to detect these sorts of inter-generational environmental effects would make the endeavor unfeasible. Instead, with advances in seascape genetics and assessing relatedness via single nucleotide polymorphisms (SNPs) (Quigley et al. 2020a), in combination with long-term demographic studies tracking wild individuals, the effect of environmental deterioration on the environmental component of phenotype may be discerned in the future; however, to date they remain unquantified.

Assumption #4 assumes that the environment component of phenotype is not transmitted to offspring (Fig. 5.4); however, new evidence from studies of DNA methylation suggest that corals may be capable of transgenerational inheritance of thermal tolerance (Putnam and Gates 2015; Liew et al. 2020; Smith et al. 2022). As more evidence and data come to light, this important process would expedite apparent 'adaptation' in corals, which would delay extinction in the short term. However, depending on the rate at which the inherited environment component of phenotype (e) is genetically assimilated (i.e. changed to permanent genetic variation or Vg), high transgenerational inheritance could slow or reduce coral adaptation in the long run, similar to phenotypic plasticity that is not able to be genetically assimilated (Price et al. 2003; Ghalambor et al. 2007).

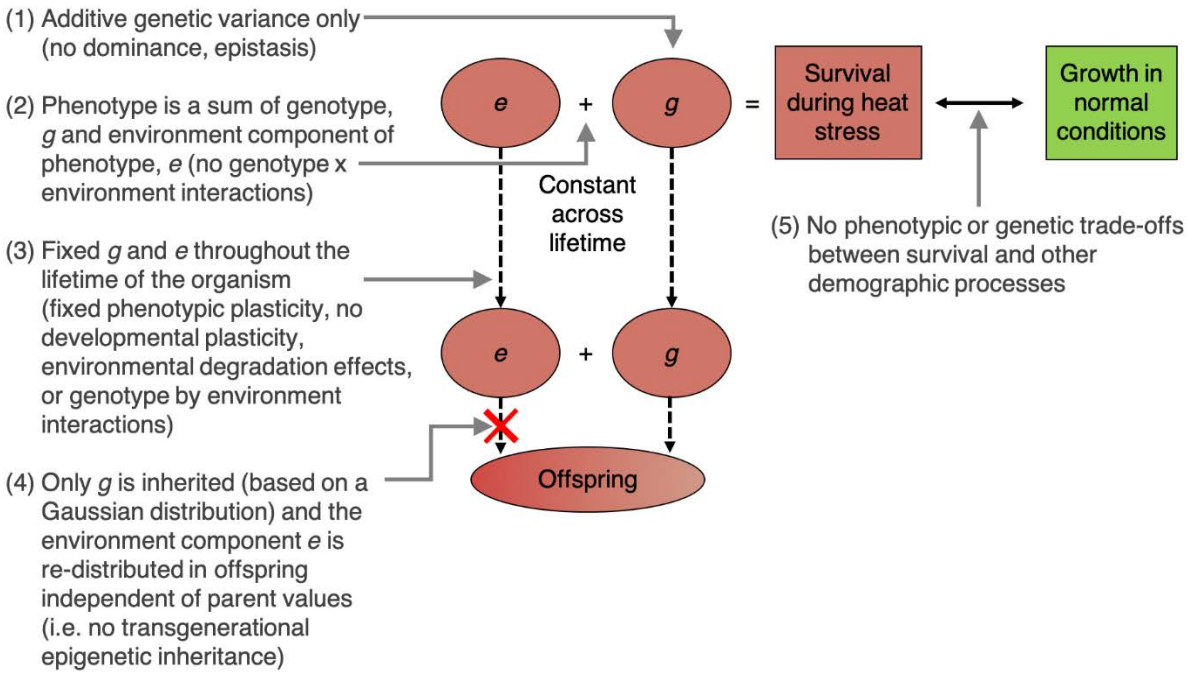

Fig. 5.4. Conceptual diagram of the different genetic assumptions that are assumed by the EE-IPM framework (with model extensions easily added given available data).

Trade-offs

Finally, exploring the assumption of demographic and genetic trade-offs will be crucial in predicting coral population responses to climate change. There are many such trade-offs that may occur, such as physiologically, where individuals adapted to higher temperatures experience reduced thermal performance breadth (Rezende et al. 2014; D'Angelo et al. 2015; Comte and Olden 2017; Diamond 2017; Baker et al. 2018; Schou et al. 2022). However, it is unclear how this sort of trade-off would manifest in terms of DHWs and accumulated heat stress. Another type of trade-off is evident in corals – between thermal tolerance and growth in normal temperatures (Fig. 5.4) (Cunning et al. 2015b; Bay and Palumbi 2017; Cornwell et al. 2021). With a growth-thermal tolerance trade-off, adult corals would experience reduced growth, and therefore reduced fecundity for newborn recruits, which would likely further exacerbate the size-dependent trend in genotypes observed in Chapter 4 (i.e. larger, fecund corals having reduced thermal tolerance genotype relative to smaller corals). Additionally, adapted recruits may similarly fail to recruit to the adult population if growth is reduced. Growth-thermal tolerance trade-offs have been observed previously in juveniles/recruits (Little et al. 2004; Cantin et al. 2009; Yuyama and Higuchi 2014; McIlroy et al. 2016; Quigley et al. 2020b; Williamson et al. 2021), adults/fragments of adults (Jones and Berkelmans 2010;

Cunning et al. 2015b; Morikawa and Palumbi 2019; Walker et al. 2022), and in free-living coral symbionts (Yuyama et al. 2016; Schaum et al. 2018; Bayliss et al. 2019). However, these studies often use interspecific comparisons, rather than observing intra-specific trade-offs within the same species.

However, the exact nature of the trade-off between growth and thermal tolerance is not clear, either energetic/physiological (i.e. corals that invest more into survival during heat stress/heat shock protein synthesis pathways cannot invest in permanent growth and calcification) or genetic (i.e. negative genetic covariance exists between increased thermal tolerance and increased growth). Wright et al. (2019) found positive genetic correlations between coral nubbin growth and survival under high temperatures; however, the use of clonal individuals precludes the effect of non-additive and shared environment sources of genetic variation (Wilson et al. 2010). Additionally, little to no data exist on intra-population growth vs. thermal tolerance tradeoffs to inform a growth-thermal tolerance trade-off in eco-evolutionary models, and thus most eco-evolutionary models include only an inter-specific trade-off of growth and thermal tolerance. Examining the coarse relationship between relative thermal tolerance and growth across species suggests that such a relationship could exist (Fig. 5.5). The topic is in dire need of synthesis in the future, as the shape of the relationship may determine the extent to which adaptation is limited or accelerated in corals.

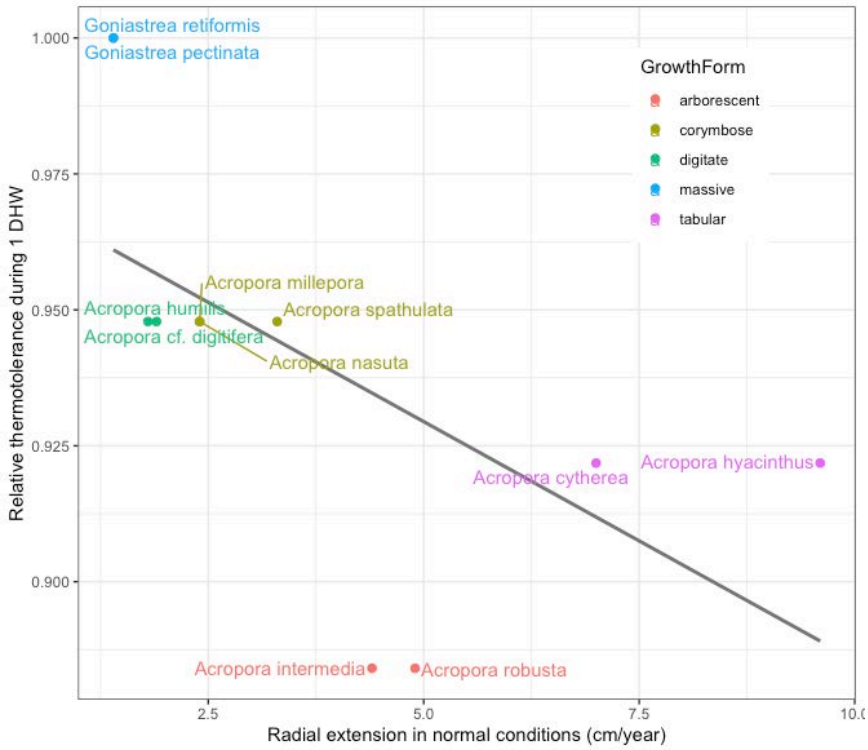

Fig. 5.5. Relative thermotolerance to 1 degree heating week (DHW, in °C-weeks) vs. maximum radial extension for 11 species of coral, with colour indicating growth form. Adapted from data in Hughes et al. 2018b and Madin et al. 2020. A grey line of best fit is added for visualisation of a hypothetical negative relationship between growth and thermal tolerance in corals.

Symbiont and microbiome effects

One aspect of coral biology that is omitted from my models are the complex interactions and symbiosis of corals and their dinoflagellate symbionts of family Symbiodiniaceae. Symbionts represent enormous adaptive potential for host thermal tolerance (Barfield et al. 2018). Symbiodiniaceae are highly evolvable relative to the coral host, given their short generation time, as has been demonstrated by *in vitro* populations who mainly reproduce via asexual reproduction (Chakravarti et al. 2017; Chakravarti and van Oppen 2018; Buerger et al. 2020). Only a few studies to date explicitly have modelled symbiont evolution (Baskett et al. 2009, 2014; Baskett and Salomon 2010; Logan et al. 2021), and this represents a crucial step towards understanding the full extent of adaptive potential in corals. These modelling studies use the inverse relationship between symbiont densities and coral mortality (e.g. Mieog et al. 2009b) to predict resulting

coral-symbiont dynamics across two types of symbionts reflecting more and less thermally tolerant symbiont populations. These models also include potential trade-offs associated with increased thermal tolerance and growth for both symbionts and coral hosts through inter-specific differences in thermal performance curves of the symbiont (Baskett et al. 2009) or coral host (McManus et al. 2021a).

A complex interplay of symbiont density and community composition, is increasingly recognized to govern host thermal tolerance, while also mediating trade-offs in terms of host growth. There is extremely high variability (Scheufen et al. 2017; Suggett et al. 2017) and host specificity (Díaz-Almeyda et al. 2017; van Dang et al. 2019; Hoadley et al. 2021) in symbiont contributions to host thermal tolerance, and more diverse symbiont communities are often indicative of lower thermal tolerance (Howe-Kerr et al. 2020). More thermally-tolerant symbiont types such as *Durusdinium trenchii* confer increased thermal tolerance when they are the dominant type, but corals associated with them have reduced polyp sizes and lower overall symbiont densities – which in turn may reduce growth (Williamson et al. 2021). High symbiont loads may be indicative of better growth but result in lower final symbiont densities after heat stress events (Cornwell et al. 2021). Finally, many symbionts – even within the same symbiont type – are highly host specific (Díaz-Almeyda et al. 2017; van Dang et al. 2019; Hoadley et al. 2021) and symbioses are often heritable across parents and offspring (Quigley et al. 2018a; Quigley et al. 2019), meaning while symbiont shuffling may be advantageous to host fitness, corals may not immediately uptake more thermally tolerant symbionts even if they are available from their local environment (Coffroth et al. 2001; Weis et al. 2001; Abrego et al. 2009). With most demographic parameters reported for corals at the holobiont level, symbiont parameters often require estimation using parameters associated with phytoplankton or other model organisms (e.g. growth rate, mutational variance, heritability), or thermal breath parameters via simulation using past historical temperature data (Baskett et al. 2009; McManus et al. 2020). Considering the intricacies in symbiont community composition change observed to date, I decided to model symbionts implicitly as part of the coral holobiont. However, with more studies of broad-scale symbiont patterns, symbiont vs. host genetics could easily be modelled as separate components of phenotype (e.g. $g_{symbiont}$ vs. g_{host}) given the EE-IPM framework implemented in Chapter 4. Microbiomes may also play a role in thermal tolerance (Webster and Reusch 2017; Marangon et al. 2021); however, to date the predictability of microbiome communities across colonies found in different environments and their direct contributions to host fitness in terms of thermal tolerance or growth remain unclear.

Future research

My thesis presents many new questions. Chapter 2 identified the range of trait heritability estimates in corals, but found significant differences between broad-sense and narrow-sense heritability estimates, suggesting substantial non-additive genetic variance or shared-environment sources of variation. Additionally, it highlighted a lack of study of the heritability of thermal performance curve metrics, such as CT_{max}, and tolerance breadth, which provide a direct link between tolerance thresholds and environmental temperatures. Moreover, no heritability estimates to date pertain directly to the thermal tolerance of corals to accumulated heat stress (i.e. DHWs). Future studies could measure the lethal dose at which 50% of corals die after exposure (i.e. LD_{50}) and use repeated field observations of coral survival across heat stress combined with measurements of the genetic relatedness of colonies such as via SNPs (short-nucleotide polymorphisms; e.g. Quigley et al. 2020a) in order to determine the heritability of colony LD_{50} thresholds for accumulated heat stress. Chapter 3 found the need for more attention to how density-dependent processes are characterized in coral population models. Estimating intra-cohort recruit density dependence and other forms of post-settlement density dependence will be important for modelling coral populations and ultimately determine maximal rates of population growth possible when thermal stress is low. Finally, Chapter 4 sought to determine how coral population adaptation to future heat stress may manifest. Yet, as previously discussed, there are several assumptions that can be relaxed and incorporated into the model, should the data linking traits to genotypes and/or size be available (Fig. 5.4). Additionally, understanding the scale at which evolution of thermal tolerance takes place relative to degree heating weeks and other accumulated heat stress metrics will be crucial in forecasting evolution. In this thesis, I used model predictions based on hindcast DHWs to determine that the square-root scale produces realistic model outcomes under the assumption that regular scale produced too little evolution and logarithmic scale produced too rapid of evolution. However, the accuracy of this assumption remains to be seen through empirical data, and given the non-linear relationship between temperature and accumulated heat stress metrics such as DHWs, more study as to exactly the relationship between DHWs and evolution, or even temperature and evolution, in corals is warranted. Such a study could again be conducted similar to the LD_{50} method described above for the heritability of thermal tolerance of corals to heat stress.

Implications of this thesis to future policy

My thesis findings have many implications for marine policy. From Chapter 3 alone, density-dependent processes can limit reef recovery, and therefore restoration activities on coral reefs may experience diminishing returns as larval densities reach intermediate levels. The sensitivity analysis in Chapter 3 identified uncertainty in survival, growth, and intra-cohort density dependence as having the greatest effect on population outcomes, and therefore marine policy needs to also reflect these uncertainties in demographic parameters. A number of local management policies follow from Chapter 4 in order to improve the natural rate of coral adaptation to climate change, such as: (1) reducing local stressors that decrease or limit larval fecundity or recruitment, such as by reducing sediment loads coming from terrestrial runoff, maintaining healthy populations of macroalgal herbivores that may provide space for recruits, and controlling crown of thorns starfish that may predate upon new recruits or highly fecund coral colonies, and (2) reduce the erosion of genetic variance during extreme heating events through maintained reef meta-population connectivity or ensuring functional thermal refugia habitats nearby to reefs exist in order to mitigate extreme selection on reefs that may cause bottlenecks in genetic variance that cannot be replenished. Additionally, technologies such as assisted gene flow may somewhat benefit reefs if no strong local adaptation or strong genotype-by-environment interactions exist that limit coral recovery. One option that both maximizes genetic connectivity and is cost-effective would be the assisted gene flow and settlement of larval slicks to reefs after major bleaching events in order to provide recruit cover that would otherwise have been missed in bleaching years. Other technologies such as assisted evolution, if possible and practical, would aid the reef to adapt, but are less likely to improve upon the natural adaptation on reefs while at the same time balancing multi-trait selection in a wild reef environment.

The future of corals: adaptation or extinction?

My thesis has shed light on the importance of coral adaptation in responding to climate change. However, the broader question remains: what does the future of coral reefs worldwide look like? Climate sceptics for a long time have decried that coral bleaching observed to date is ‘natural’ and if not, corals can adapt to any future stresses. (Mackenzie and Ridd 2019)On the other side, many news articles have pushed very harsh tones of all reefs perishing by 2100 or even 2050 due to climate change. However, the truth is likely somewhere in the middle. No, reefs cannot evolve indefinitely to climate change, nor will they perish

entirely. Some species of corals are likely to be able to withstand extremely high temperatures, while others that are much less thermal tolerant and incapable of adapting fast enough to climate change will likely perish from reefs in the future. The community composition of reefs is likely to get simpler and simpler, depending on the level of heat stress experienced on the reef, which in turn depends on the future emissions of human society. Rates of decline due to bleaching are unlikely to cause the extinction of most Indo-Pacific coral species, in part because many global population sizes range from 10 million to as high as 10 billion individuals worldwide (Dietzel et al. 2021a). However, while coral vary both vastly in quantity and across space, local species extinctions may very well accelerate with climate change (Dietzel et al. 2021a), changing the face of reefs as we know them (Hughes et al. 2018b). With the extreme warming predicted by high emission scenarios (Dixon et al. 2022; Kalmus et al. 2022; McWhorter et al. 2022b, 2022a), many coral reefs are predicted to fail or bleach regularly every year in the future. Many reefs could survive and thrive in deep water refugia (Laverick et al. 2018), thermal refugia (but see Dixon et al. 2022; Kalmus et al. 2022) or newfound transient refugia resulting from internal gravity waves (Bachman et al. 2022). Yet, shallow-water reefs are unlikely to find suitable habitat in the majority of locations in which they currently occupy (Dixon et al. 2022; Kalmus et al. 2022; McWhorter et al. 2022b, 2022a), unless they can adapt to future heat stress. Additionally, ocean acidification under most high emission scenarios will see the erosion of most coral calcium carbonate (Cornwall et al. 2021), and thus reef growth will not be possible under higher emission scenarios.

One key finding from my Chapter 4 model is that evolution to thermal tolerance must be fuelled by high recruitment, but when recruitment or fecundity fails during or after major heat stress, this ability of populations to adapt may in turn be impaired, and with too rapid warming will inevitably lead to population extinction. A quote by Klausmeier et al. (2020) summarises this simply: “If environmental change is sufficiently slow or there is abundant additive genetic variance, then population persistence is guaranteed”. Currently, corals of the Indo-Pacific are recovering after three consecutive bleaching events in the past five years, with a 36-year high for coral cover (AIMS 2022) – however, the community has since shifted towards pioneering species rather than later successional species. Corals gain worldwide attention for their natural beauty and striking bleached appearance as they die *en mass* due to climate warming, and are likely to act as the canaries in the coal mine for worldwide attention to ecosystems in decline due to climate change. Therefore, they are a priority to conserve as we do everything in our power to reduce climate emissions and

curtail anthropogenic climate change. Conserving the world's coral reefs in their pristine conditions can either be a success story passed on for generations for how the world came together to solve the climate crisis, or a tombstone marking a failure of humanity to reduce emissions in order to save reefs.

Appendix A: Supplementary Text for Chapter 2

The Supplementary Code Documentation A-C (including all supplementary figures and tables) are published as HTML files and accessible at: https://ecolology.github.io/heritability-meta/.

A1: Methods used to estimate heritability

Methods to estimate the heritability coefficient have themselves evolved in recent years. Many different methods exist, each with different drawbacks (see Visscher et al. 2008). Realised (narrow-sense) heritability is calculated using the Breeder's equation as $h^2_R = R/S$ (Falconer and Mackay 1996; Visscher et al. 2008), but becomes unreliable when selection acts on multiple co-evolving traits and when viability selection is operating (Falconer and Mackay 1996; Hadfield 2008).

The (mid)parent-offspring regression and ANOVA models for partitioning intra-familial variance are also common, but are strongly sensitive to rearing environments (Falconer and Mackay 1996). Genetic marker-based methods such as the Ritland multiple regression method (Ritland 1996) have also been used, but rely on large numbers of markers for accuracy (Visscher et al. 2008). More recently, a quantitative genetic mixed-effects model called the 'animal model' has become the standard for estimating heritability in wild populations due to their flexibility and power to estimate heritability (Kruuk 2004; Wilson et al. 2010). The animal model uses relatedness information from a known pedigree (or other methods, such as inferred pedigrees from genetic markers or genet ID) as a random effect in order to estimate the additive genetic variance, V_A, associated with the breeding values of individuals (Kruuk 2004; Wilson et al. 2010). While this method is more flexible, heritabilities estimated while conditioning on unneeded fixed effects may result in estimates not being especially comparable among studies (Wilson 2008); thus, careful model construction is a crucial step in estimating heritability (see Wilson et al. 2010 for a step-by-step guide).

The majority of these studies in my meta-analysis (14/19 studies accounting for 53/95 estimates) used the 'animal model' to estimate heritability, while the remaining estimated heritability using an ANOVA-method of variance partitioning (4/19 studies and 33 estimates), while one study used the Ritland genetic marker method (accounting for six estimates). Visual inspection of residuals from the model fits suggested no additional unexplained variation that was related to heritability measurement method (Fig S11 in Supplementary Code C).

A2: Pre-processing of raw heritability estimates

Heritability is calculated as a proportion of total phenotypic variation, and thus is constrained to fall between zero and one (Falconer and Mackay 1996). Because most classical meta-analytical statistical models assume normally-distributed uncertainty, transformation of the estimates prior to meta-analysis was necessary (Viechtbauer 2010; Lin and Xu 2020). The variance of heritability is often reported either as standard error of the mean (herein 'SE') and associated 95% confidence intervals or 95% Bayesian credible intervals (herein 'CI'). Some Bayesian credible intervals are relatively asymmetric when the heritability estimate is close to zero or one, and thus are not easily converted to SEs without some information being lost. Additionally, transformations of proportional SE generally only work well for non-extreme point estimates (e.g. 0.2–0.8 for logit and arcsine-square root transformations) (Warton and Hui 2011; Wang 2018), while others have difficulty in back-calculating and interpretation (e.g. double arcsine transformation) (Schwarzer et al. 2019). Symmetric standard errors can have associated 95% confidence limits with non-sensical meanings, such as including negative values of heritability or values above one, meaning additive genetics contributing more than 100% of total phenotypic variance. On the other hand, posterior distributions and associated CIs can often be asymmetric near the boundary, violating the assumption of Gaussian-distributed SEs required in standard meta-analysis (Jackson and White 2018). To avoid and correct for these problems, I modelled h^2 and its associated CI limits on the logarithmic scale using the transformation:

$$h_T^2 = ln[h^2 + 0.2] \quad (1)$$

Since heritability values tended more towards the lower bound of 0 rather than the upper bound of 1, logarithmic transformation provides better estimates upon back-transformation for these low values while preserving the relative difference in standard errors compared to other transformations (see Supplementary Code Documentation A: Pre-processing). I selected a value of +0.2 to add, as this value allowed the inclusion of nearly all estimates save for three outliers with extremely large CIs (see Supplementary Code Documentation A: Pre-processing). Additionally, the logarithmic transformation somewhat normalizes the asymmetric Bayesian posterior distributions that tended to characterize heritability estimates near the lower boundary. I tested seven other transformations of proportions, such as the logit transformation on SE as well as CI and the double arc-sine square root transformation of SE, all resulted in similar model selection

outcomes, suggesting that the results are robust to the choice of transformation. For estimates reporting SE (n = 32), I calculated the equivalent 95% CI limits on the original scale as:

$$95\%\ \mathrm{CI}_{\mathrm{lwr/upr}} = h^2 \pm \mathrm{SE} \cdot z^* \quad (2)$$

where z^* = 1.96 in the case of large sample sizes (N > 30). For estimates reporting CIs (n = 56), I make the assumption for simplicity's sake that frequentist 95% confidence intervals are comparable to Bayesian credible intervals (Gray et al. 2015). Next, I convert all intervals to the logarithmic scale by calculating the point estimate and the confidence/credibility interval limits, then directly convert them using the same 95% $\mathrm{CI}_{\mathrm{lwr/upr,T}} = ln(95\%\ \mathrm{CI}_{\mathrm{lwr/upr}} + 0.2)$ transformation as above. Finally, I obtain the transformed standard errors (SE_T) based on a rearrangement of the previous formula:

$$SE_T = \frac{95\%\ \mathrm{CI\ range}_T}{2z^*} \quad (3)$$

For example, a heritability estimate and 95% CI of h^2 = 0.25 [0.1,0.4] would be transformed using the $ln[h^2+0.2]$ transform to h^2_T = –0.80 [–1.2,–0.51], then $\mathrm{SE_T}$ computed as: [–0.51 – (–1.2)]/(2*1.96) = 0.176.

A3: Model selection results of trait type × heritability type and trait type × growth form

Model selection to examine possible trait type × heritability type interactions used a subset of data that also allowed the inclusion of a trait type × life stage interaction. I did not fit a three-way interaction of the above factors, given that there were no studies for some combinations of levels of the three factors. Model selection supported the model of trait type × life stage (Table A5). This model again had significant residual heterogeneity (QE_{51} = 98, p < 0.0001; I^2 = 59%; R^2 = 71%), and had coefficient values similar to the previous model of trait type × life stage + heritability type (Fig. A4; Table A6). There was one highly influential point for adult bleaching (Cook's distance = 3.7). However, when this point was removed, both juvenile bleaching and growth remained significantly low. The fail-safe number was again large, indicating robustness to any publication bias (127 > 100). Additionally, the outcome of model selection was unchanged when data were re-analysed without this estimate.

Finally, I tested for possible trait type × growth form interactions. Again, no three-way interactions were possible given the combinations of levels of factors with adequate representation in the data. There were limited estimates for some growth forms, such as for columnar (n=3 estimates) and encrusting (n=1)

corals, thus these levels (and thus the corresponding estimates) were excluded in order to examine a complete trait type × growth form interaction. Thus, I examined interactions across branching (n=8), corymbose (n=32), and massive (n=14) coral growth forms for five traits: bleaching, growth, nutrient content, survival, and symbiont community, and this also allowed interactions of trait × life stage and trait × heritability type. Similar to results of the previously reported analysis, a model of trait type × life stage was the most strongly supported by the data (Table A7-A8; Fig. A5).

Appendix B: Supplementary Materials for Chapter 3

B1: Model details

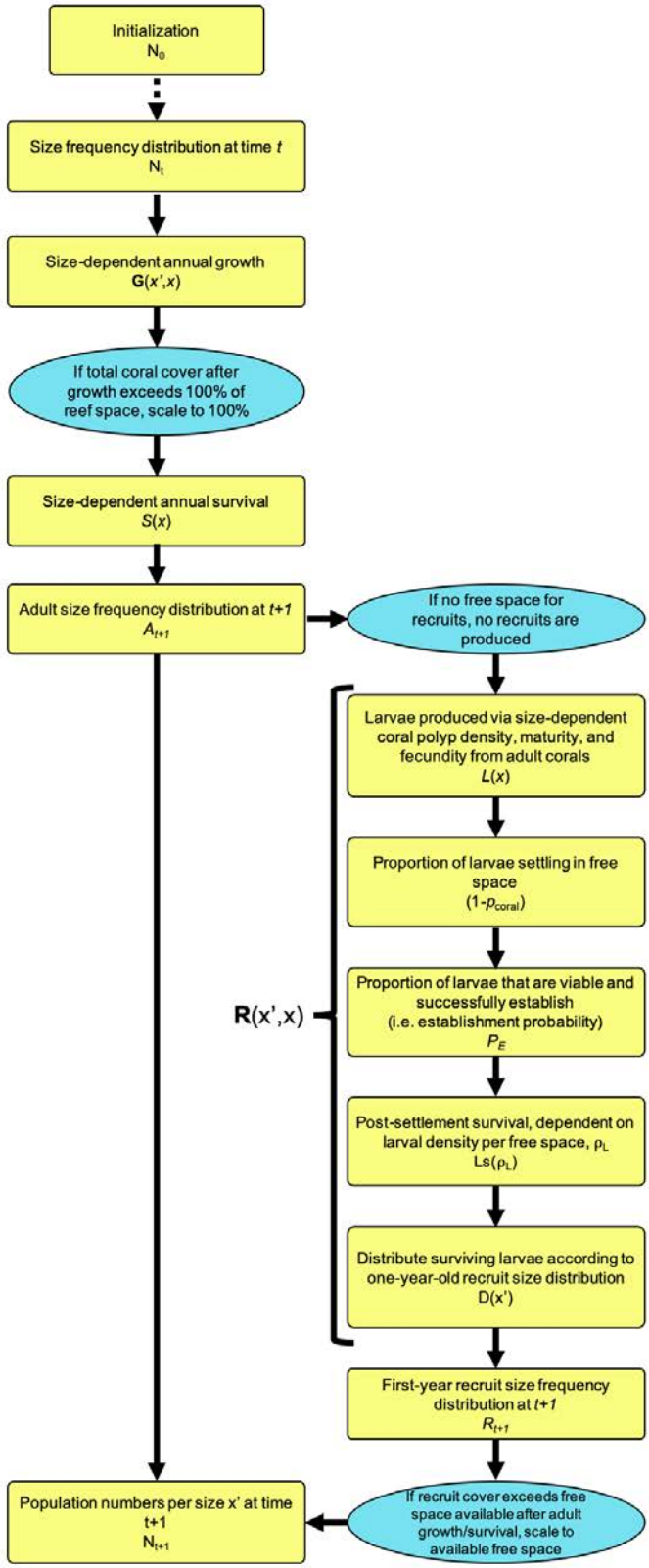

Fig. B1. Diagram of model vital rates and order applied. Blue bubbles represent if-else statements within the model structure.

Table B1. Recruitment sub-processes used in the integral projection model (IPM). Specific parameter values can be found in Table B2.

Vital rate (family, link)	Function Definition	Reference
Recruitment	$\mathrm{R}(x') = n_{settlers,t}\, p_{recruitment,t}\, \mathrm{RS}(x')$	
Number of settlers	$n_{settlers,t} = q\, p_{free\ space,t} \int_x M(x)F(x)n_t(x)dx$	
Proportion free space	$p_{free\ space,t} = \left(1 - \frac{Coral\ cover,t}{Total\ area}\right)$	
Polyp maturation probability, given colony size x (binomial, logit-link)	$M(x) = \mathrm{logit}^{-1}(\beta_{m0} + \beta_{m1}\, x)$	(Álvarez-Noriega et al. 2016)
Number of oocytes produced per polyp, given colony size x (negative binomial, log-link)	$F(x) = e^{\beta_{o0} + \beta_{o1}\, x}$	(Álvarez-Noriega et al. 2016)
Ricker recruit density dependence (binomial, log-link)	$p_{recruitment,t} = e^{(\beta_{RD0} + \beta_{RD1}\, r_{settlers,t})}$	(Ricker 1954)
Beverton-Holt recruit density dependence	$p_{recruitment,t} = \frac{\beta_{BD0}}{1 + \beta_{BD1}\, r_{settlers,t}}$	(Beverton and Holt 1957)
Density of settlers	$r_{settlers,t} = \frac{n_{settlers,t}}{Free\ space,t}$	
First-year recruit kernel from size x colonies to size z recruits	$\mathrm{RS}(x') = \frac{1}{\sigma_{RS}\sqrt{2\pi}} e^{-\frac{1}{2}\left(\frac{x' - \mu_{RS}}{\sigma_{RS}}\right)^2}$	(dela Cruz and Harrison 2017)

Table B2. Vital rate parameter values from the literature for corymbose corals across Lizard Island (LI) and Orpheus Island (OI), Australia.

Parameter and value	Description	Reference
β_{s0} = 1.198 (LI); β_{s0} = 6.76 (OI)	Intercept of whole colony survival polynomial logistic regression (binomial model with logit-link)	Madin et al. 2014 Table 1 corymbose; Hoogenboom et al. unpublished
β_{s1} = -0.738 (LI); β_{s1}=4.26 (OI)	First-order term of whole colony survival polynomial logistic regression (binomial model with logit-link)	Madin et al. 2014 Table 1 corymbose; Hoogenboom et al. unpublished
β_{s2}=-0.194 (LI); β_{s2}=1.102 (OI)	Second-order term of whole colony survival polynomial logistic regression (binomial model with logit-link)	Madin et al. 2014 Table 1 corymbose; Hoogenboom et al. unpublished
β_{s3} = 0 (LI); β_{s3} = 0.086 (OI)	Third-order term of whole colony survival polynomial logistic regression (binomial model with logit-link)	Hoogenboom et al. unpublished
r_s= 0.0364 (LI); r_s = 0.0507 (OI)	Species-specific natural growth mean radial extension (independent of colony size)	Dornelas et al. 2017; Madin et al. 2020 Table 1; Hoogenboom et al. unpublished
c_s = –1.86 (LI); c_s = –2.72 (OI)	Intercept of logit partial mortality distribution as a function of colony size	Dornelas et al. 2017; Madin et al. 2020 Table 2; Hoogenboom et al. unpublished
m_s = –0.468 (LI); m_s = –0.582 (OI)	Slope of logit partial mortality distribution as a function of colony size (linear kernel density)	Dornelas et al. 2017; Madin et al. 2020 Table 2; Hoogenboom et al. unpublished
σ_s^2 = 1.388 (LI); σ_s^2 = 1.331 (OI)	Standard deviation of logit partial mortality distribution as a function of colony size (linear kernel density)	Dornelas et al. 2017; Madin et al. 2020 Table 2; Hoogenboom et al. unpublished
β_{m0} = 8.89	Intercept of probability of polyp maturity (logit-link)	Álvarez-Noriega et al. 2016
β_{m1} = 1.76	Slope of probability of polyp maturity (logit-link)	Álvarez-Noriega et al. 2016
β_{o0}= 1.86	Intercept of the number of oocytes produced per mature polyp (log-link)	Álvarez-Noriega et al. 2016
β_{o1} = 0.017	Slope of the number of oocytes produced per mature polyp (log-link)	Álvarez-Noriega et al. 2016
ρ_{polyp} = 9.98E+05	Density of polyps per colony size	Álvarez-Noriega et al. 2016
$p_{fertile}$ = 0.999	Proportion of total colony that is fecund (i.e. not in sterile zone)	Álvarez-Noriega et al. 2016
q = 10^{-6} to 10^{-1}	Probability of larvae establishing after settlement	Free parameter
μ_{RS} = 3.4	Mean of recruit size distribution	dela Cruz and Harrison 2017
σ_{RS} = 2.1	Standard deviation of recruit size distribution	dela Cruz and Harrison 2017

B2: Growth model plots

Combining the juvenile and adult datasets

Within a linear model of log colony area at time t+1 ~ log colony area at time t + data source, there were significant differences in the reef-specific intercepts of Lizard Isl. (adult data) vs. Heron Isl. and Exmouth (juvenile datasets), suggesting a lack of model fit (Fig. B2.1a). Therefore, I subtracted the difference in reef-specific intercepts from the juvenile datasets to better align the adult to juvenile data sources for Lizard Isl. (Fig. B2.1b). For Orpheus, the juvenile and adult data sources were not significantly different (Fig. B2.1c), therefore no correction was necessary.

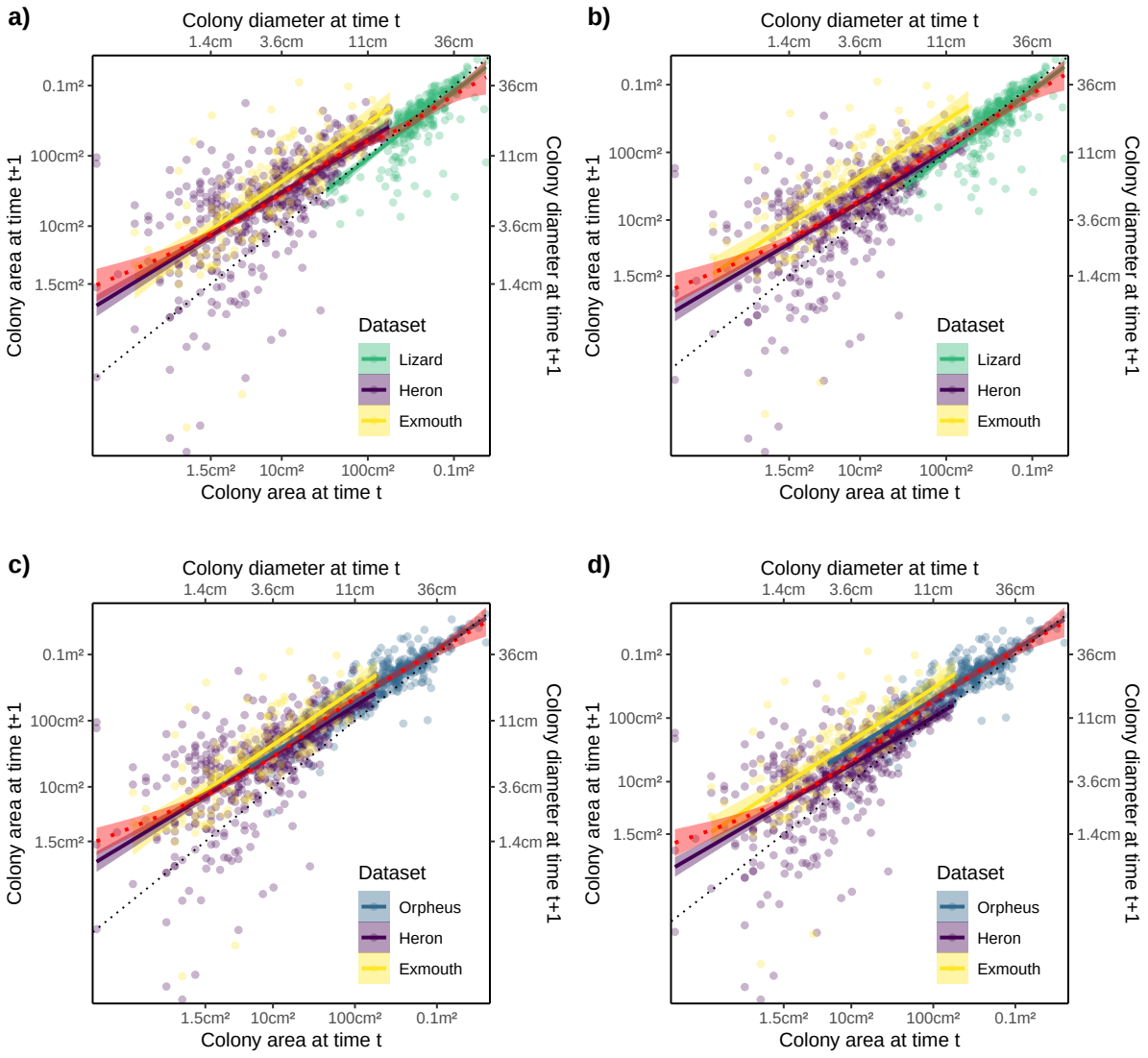

Fig. B2.1. Comparing Lizard (a, b) and Orpheus (c, d) annual growth vs. juvenile coral growth at Heron Island and Exmouth reefs using either uncorrected/raw data (a, c) or juvenile corrected (b, d)

colony sizes at the next year ($t+1$) vs. the preceeding year's colony size (t). Corrections subtract the reef-specific intercepts for Heron and Exmouth data to obtain corrected juvenile data. The red dotted line and ribbon represent a GAM smoother term used to highlight inconsistencies across the datasets.

Radial growth models

For the Lizard Island data, there was a slight discrepancy even after correction between the juvenile and adult datasets (Fig. B2.2) – highlighting the relatively low growth measured at Lizard Island. A model of constant radial growth was better supported relative to size-dependent radial growth, with radial growth being ~3.6 cm/year. For Orpheus Island, the model of size-dependent radial growth was supported (Fig. B2.3); however, with the removal of the juvenile dataset, the size-dependent relationship changed from significantly positive to significantly negative, suggesting that this relationship was instead driven by a mismatch between the adult and juvenile datasets. Therefore, I opted to again use a size-independent radial growth model for Orpheus Island, with radial growth being ~5.1 cm/year (Fig. B2.3). However, plotted below for comparison with the Orpheus constant radial growth model are the remainder of the growth model results assuming a positive size-dependent radial growth model for Orpheus.

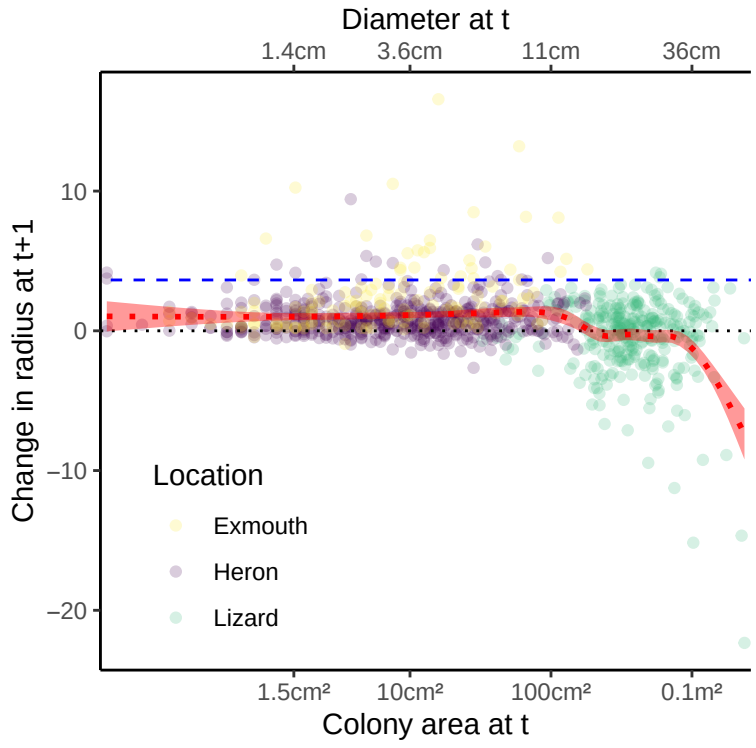

Fig. B2.2. Lizard Isl. and juvenile data (Exmouth and Heron Isl.) radial growth across size. The blue dashed line represents the maximum estimated constant radial growth using a 95th quantile regression model (best supported model). The dotted line represents stasis (no growth) and a GAM cubic regression spline model is represented with a dotted red line.

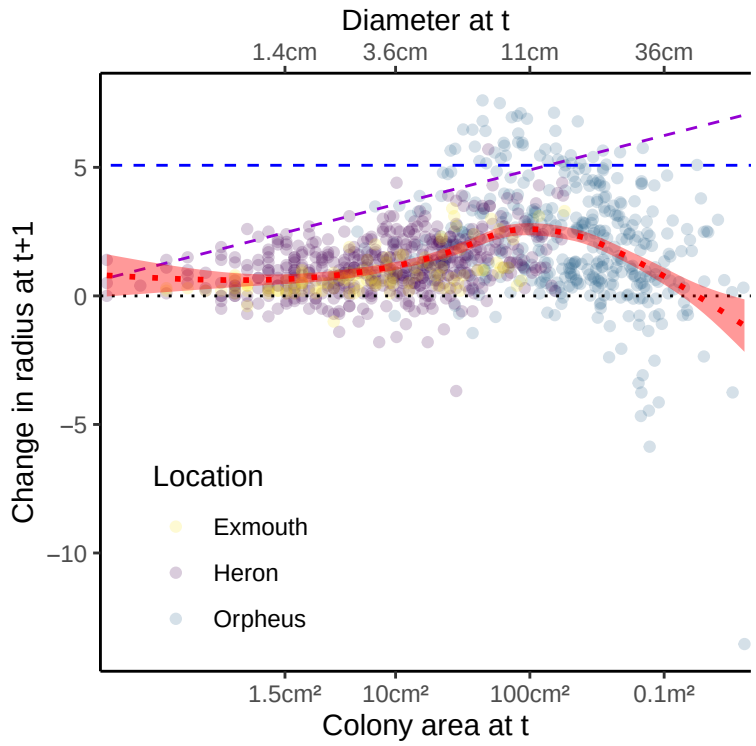

Fig. B2.3. Comparing maximum radial growth models for the Orpheus and juvenile datasets (Exmouth and Heron Isl.). The dashed lines represent the maximum estimated constant radial growth (blue) and size-dependent radial growth (purple) radial growth using a 95th quantile regression model. The dotted line represents stasis (no growth) and a GAM smooth model is represented with the red dotted line.

Partial mortality models

Partial mortality for both Lizard and Orpheus was approximated well by a GAM cubic regression spline, indicating a good model fit using the assumed linear relationships (Fig. B2.4 and B2.5, respectively). However, for Orpheus Island, the size at which expected net growth (growth minus partial mortality) was zero was relatively higher and beyond the sampled data. Nonetheless, this relationship still results in biologically realistic growth for juveniles, especially when considering the constant radial growth model (Fig. B2.5a,c), and whole-colony mortality likely reduces the proportion of individuals actually attaining this size.

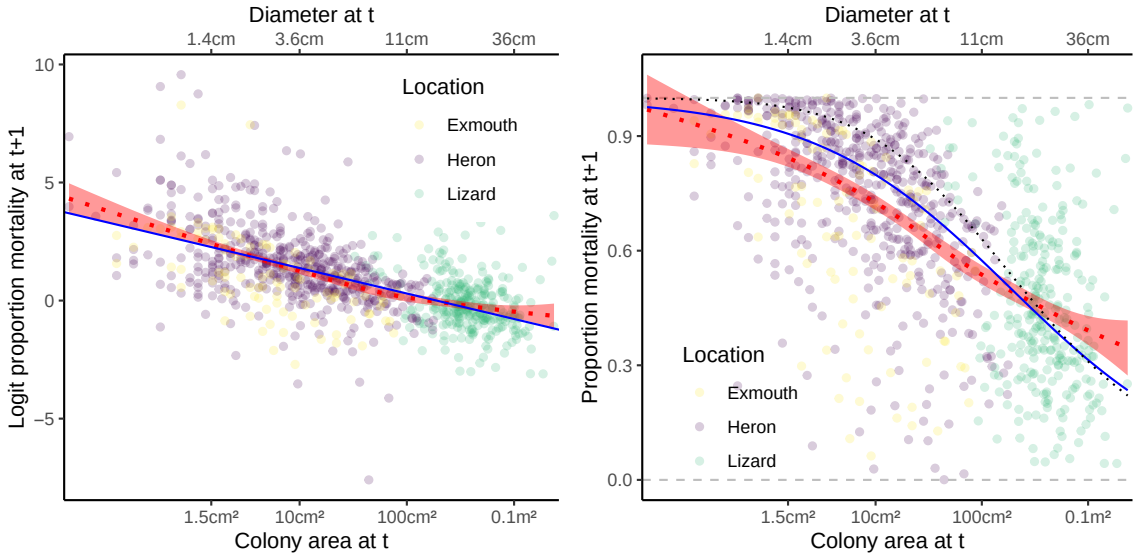

Fig. B2.4. Estimated logit proportion partial mortality (left) and back-transformed proportional mortality (right) estimated by the growth model for Lizard Island assuming constant radial growth (solid blue line) vs. a smoothed GAM curve (red dotted line). The black dotted line on the right plot represents colony stasis – where colonies tend to neither grow nor shrink. Where model estimates fall below the stasis line, colonies tend to increase in size each year on average, and where the two lines intercept demarcates the average maximum colony size.

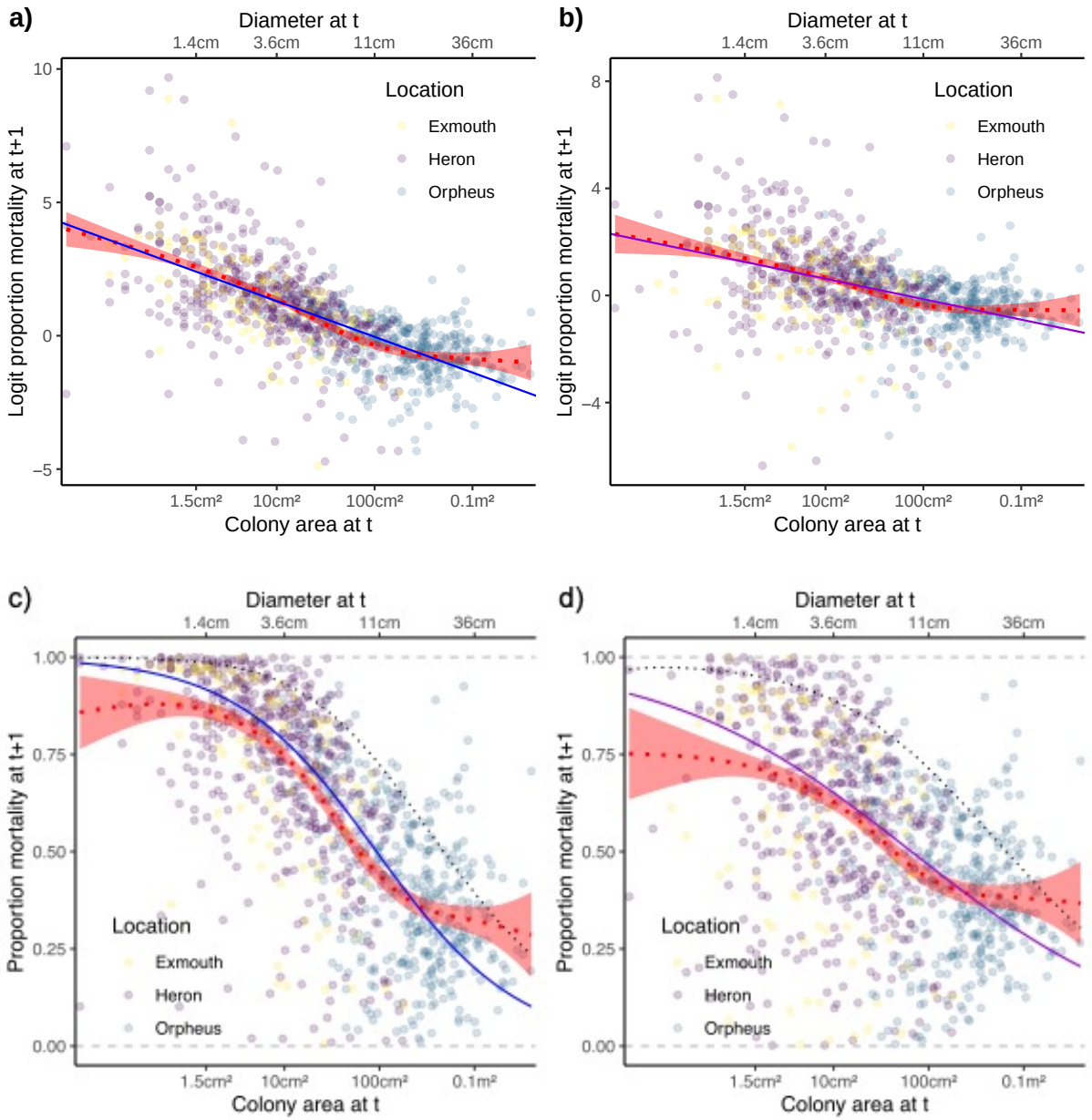

Fig. B2.5. Estimated logit proportion partial mortality (a,b) and back-transformed proportional mortality (c,d) estimated by the growth model for Orpheus Island assuming either a) constant radial growth (a,c – blue solid lines), or b) size-dependent radial growth (b,d – purple solid lines). The black dotted line on c) and d) represents the colony stasis line – where colonies tend to neither grow nor shrink. Where model estimates fall below the stasis line, colonies tend to increase in size each year on average, and where the two lines intercept demarcates the average maximum colony size.

Final growth models

Overall models of Lizard Island and Orpheus Island with the supplemental juvenile datasets had more conservative but biologically realistic growth at smaller colony sizes (Fig. B2.6 and B2.7). The Lizard Island model may underestimate the maximal growth of corals of intermediate size (Fig. 2.6), but both models are more accurate in terms of small coral growth – which reduces the rate at which individuals attain maturity (currently ≥3 years, but without juvenile datasets, maturity could be attained in as little as 2 years).

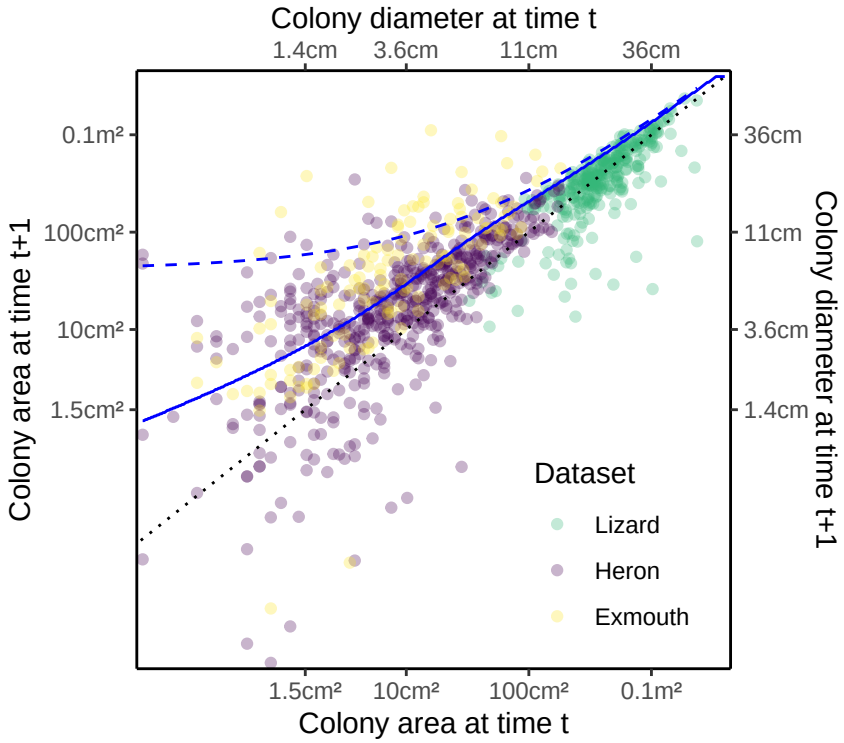

Fig. B2.6. Lizard and juvenile annual growth models assuming constant radial growth (blue lines). The dashed blue line represents the maximal radial growth predicted by the model across different colony sizes, while the blue solid line represents the highest probability of growth. The dotted line is a 1:1 line representing no change in colony size.

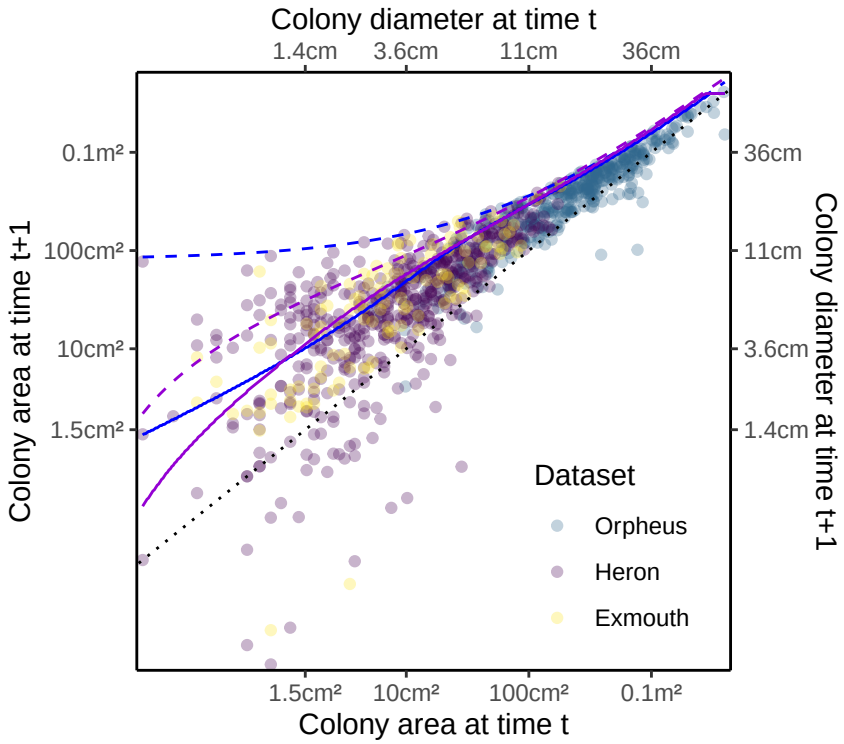

Fig. B2.7. Orpheus and juvenile annual growth models assuming constant radial growth (blue lines) or size-dependent radial growth (purple lines). Dashed lines represent the maximal radial growth predicted by each model across different colony sizes, while solid lines represent the highest probability of growth for each of the two models. The dotted line is a 1:1 line representing no change in colony size.

B3: Saturating effect of bin size

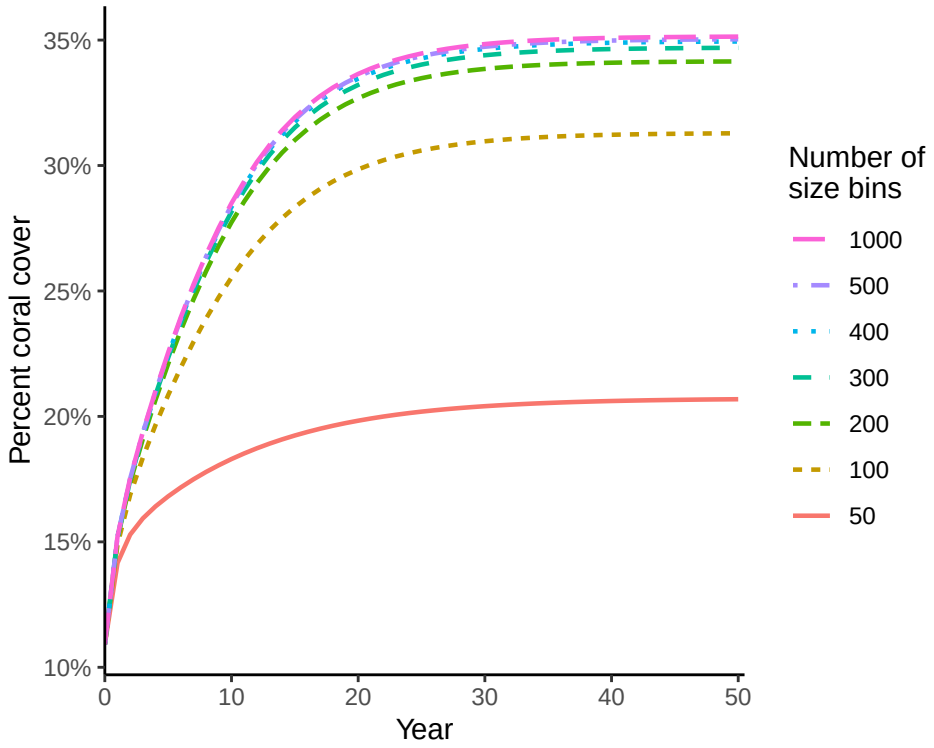

Fig. B3. Predicted coral cover across time based on a single parameterization set (using the Ricker model of intra-cohort density dependence and Lizard Island survival and growth), with the difference in population outcomes being negligible after $n = 300$ bins.

Appendix B

B4: Trajectory plots

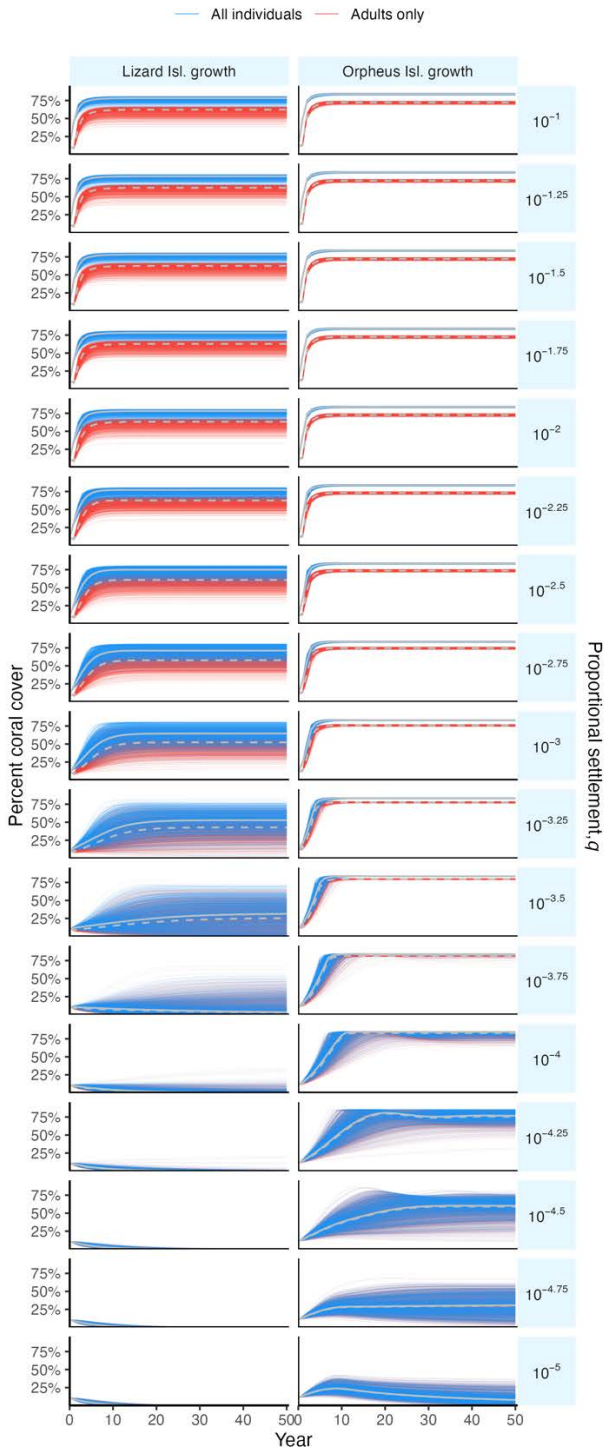

Fig. B4.1. Percent coral cover trajectories for adults (red lines) and total cover (blue lines) across 1,000 Monte Carlo simulations of either **Lizard Island (left) vs. Orpheus Island (right) growth** functional forms, across varying proportions of larval settlement, q (vertical panels). The median value for adults and total cover is demarcated for each panel by a solid and dashed grey line, respectively.

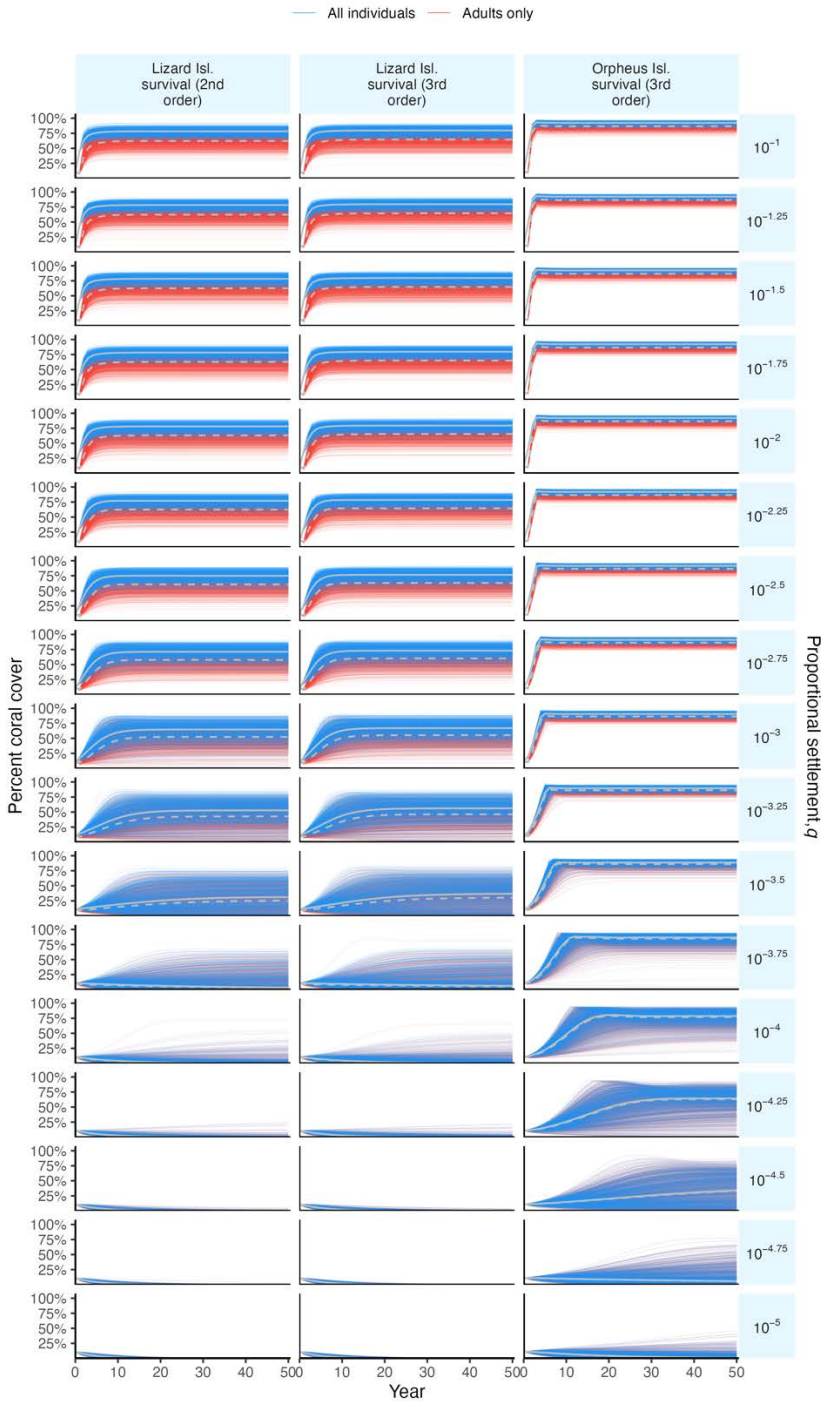

Fig. B4.2. Percent coral cover trajectories for adults (red lines) and total cover (blue lines) across 1,000 Monte Carlo simulations of either **Lizard Island (left panels), vs. Orpheus Island (right) survival** functional forms fit with either a 2nd or 3rd order polynomial of size, across varying proportions of larval settlement, *q* (vertical panels). The median value for adults and total cover is demarcated for each panel by a solid and dashed grey line, respectively.

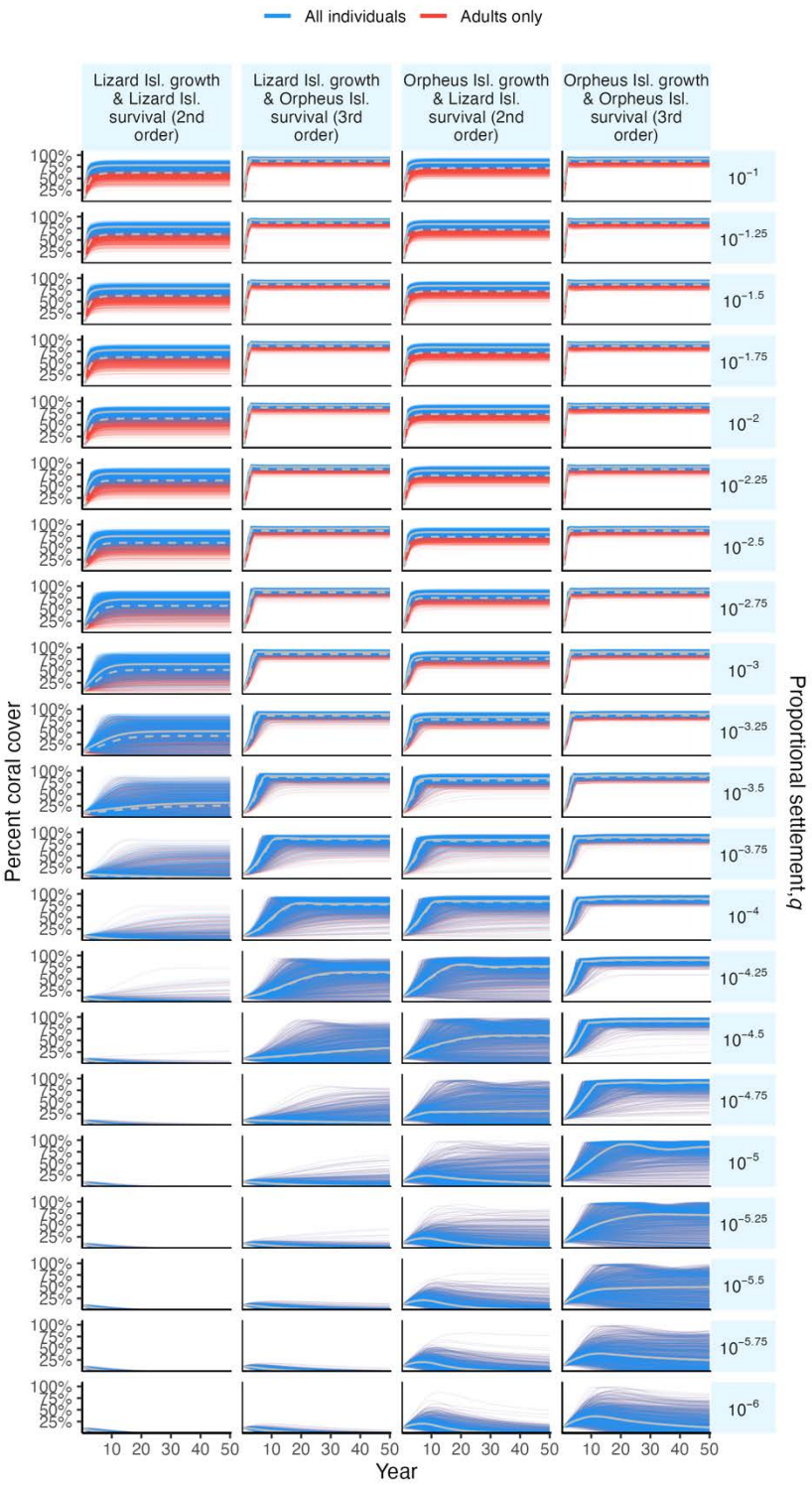

Fig. B4.3. Percent coral cover trajectories for adults (red lines) and total cover (blue lines) across 1,000 Monte Carlo simulations of various functional forms for various functional forms of **growth and survival**, across varying proportions of larval settlement, *q* (vertical panels). The median value for adults and total cover is demarcated for each panel by a solid and dashed grey line, respectively.

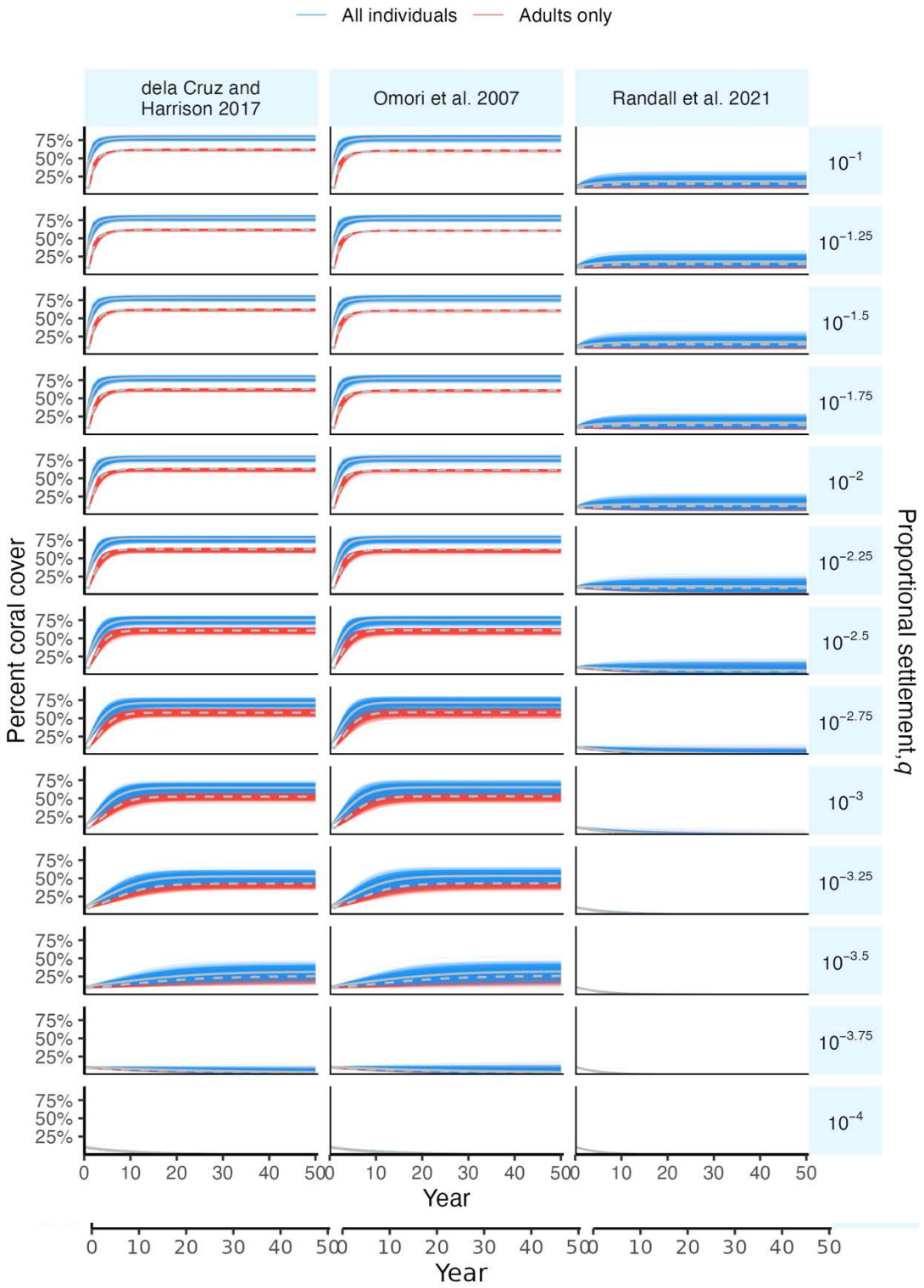

Fig. B4.4. Percent coral cover trajectories for adults (red lines) and total cover (blue lines) across 1,000 Monte Carlo simulations of various **recruit size distribution** parameterisations, across varying proportions of larval settlement, q (vertical panels). The median value for adults and total cover is demarcated for each panel by a solid and dashed grey line, respectively.

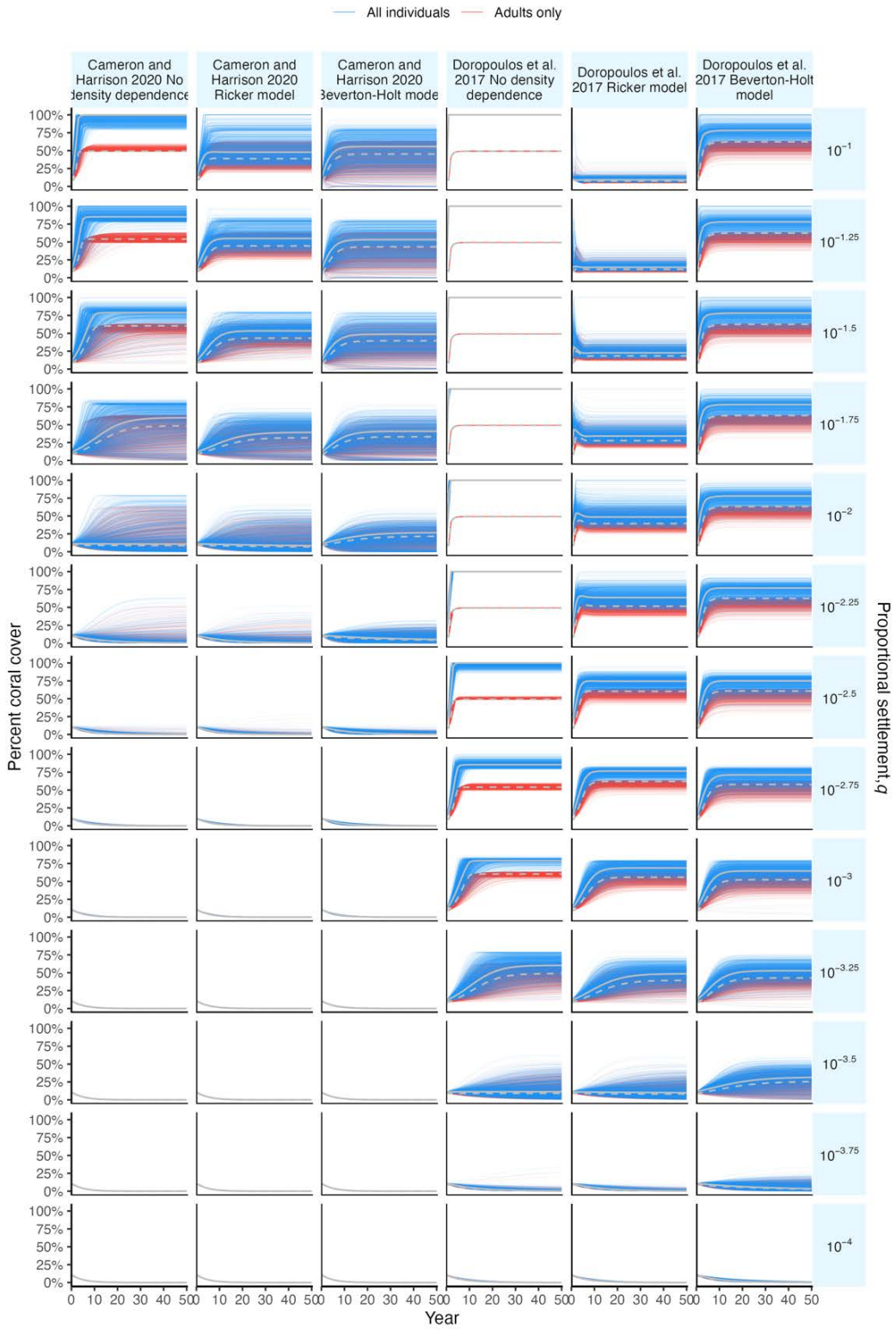

Fig. B4.5. Percent coral cover trajectories for adults (red lines) and total cover (blue lines) across 1,000 Monte Carlo simulations of various functional forms of **recruit intra-cohort density dependence**, across varying proportions of larval settlement, *q* (vertical panels). The median value for adults and total cover is demarcated for each panel by a solid and dashed grey line, respectively.

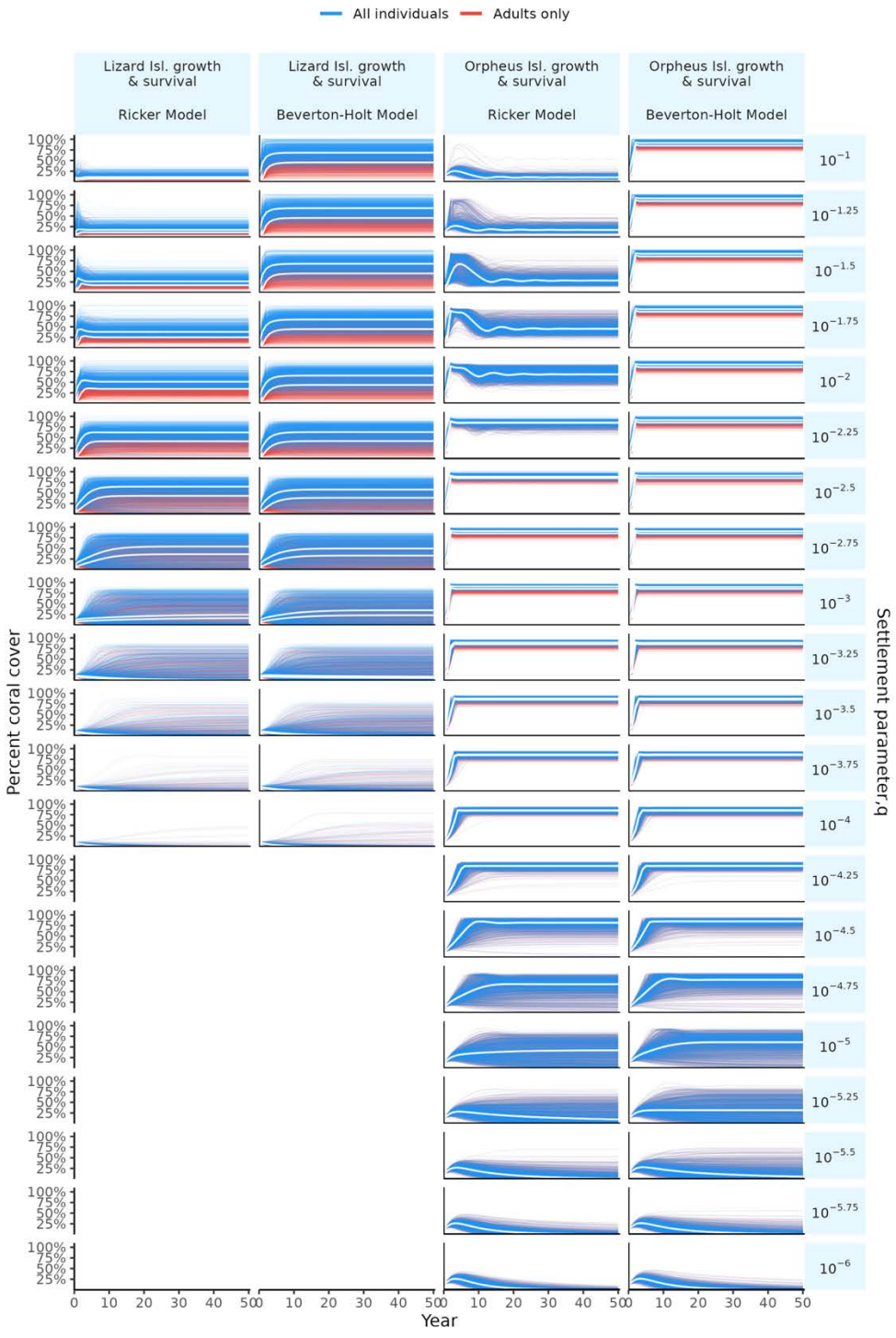

Fig. B4.6. Percent coral cover trajectories for adults (red lines) and total cover (blue lines) across 1,000 Monte Carlo simulations of **all parameters (complete uncertainty propagation)** for select functional forms of **growth, survival, and recruit intra-cohort density dependence**, across varying proportions of larval settlement, q (vertical panels). The median value for adults and total cover is demarcated for each panel by solid white lines.

B4: Size distribution plots

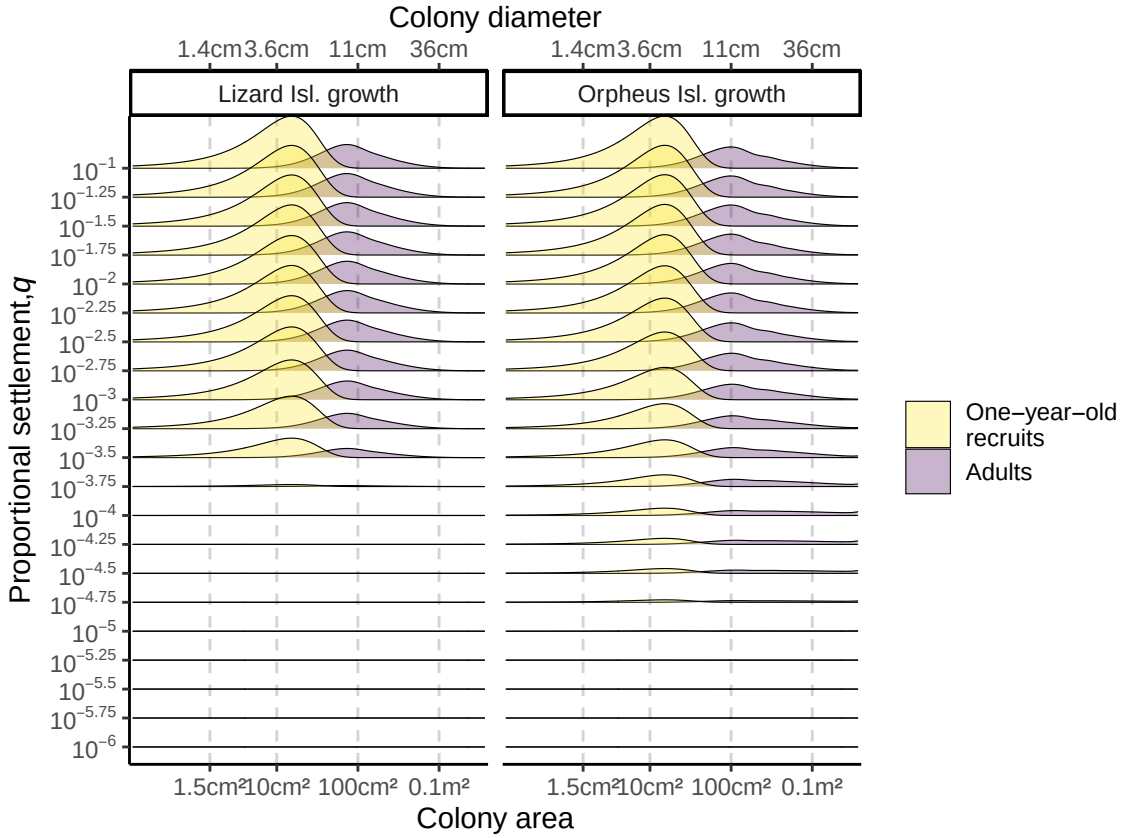

Fig. B4.1. Median size distributions of adults (purple) and one-year-old recruits (yellow) after 50 years of simulation for 1,000 Monte Carlo simulations of either **Lizard Island (left) vs. Orpheus Island (right) growth** functional forms, across varying proportions of larval settlement, q (y-axis).

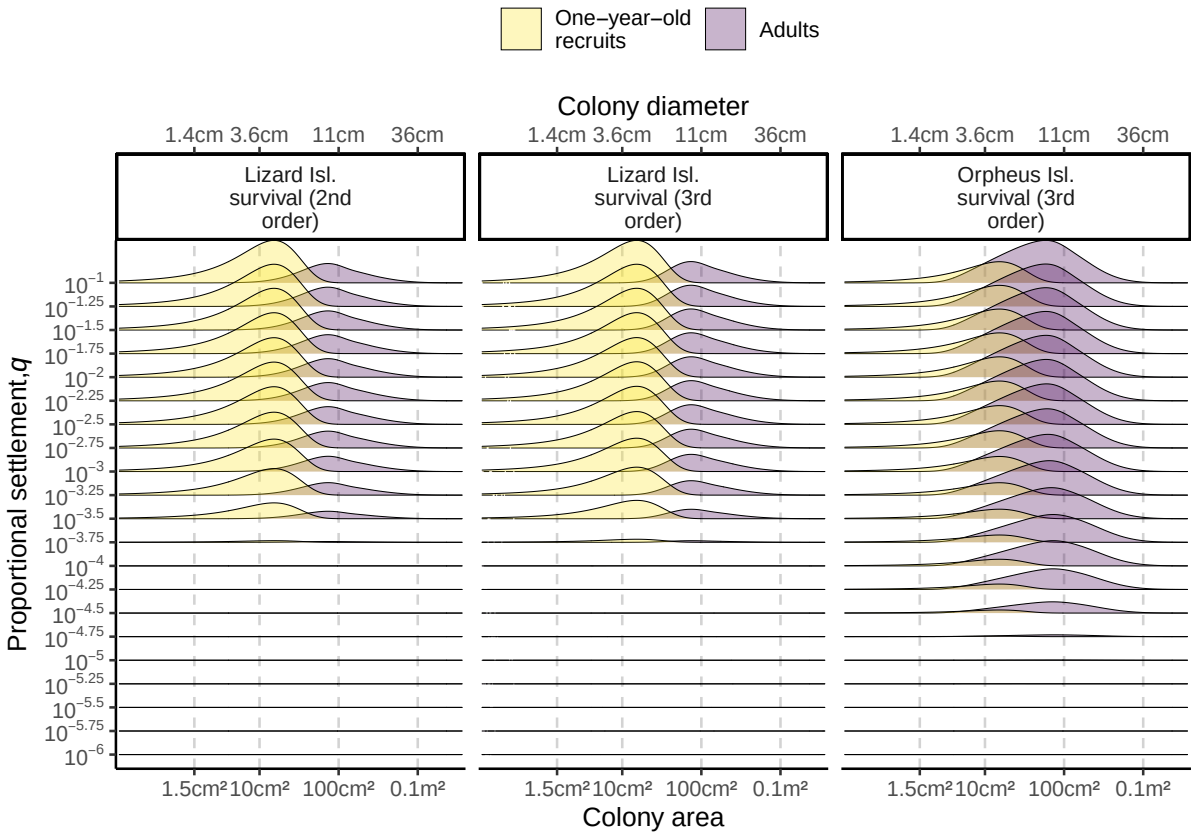

Fig. B4.2. Median size distribution of adults (purple) and one-year-old recruits (yellow) after 50 years of simulation for 1,000 Monte Carlo simulations of either **Lizard Island (left two columns) vs. Orpheus Island (right) survival** functional forms fit with either a 2nd or 3rd order polynomial of size, across varying proportions of larval settlement, q (y-axis).

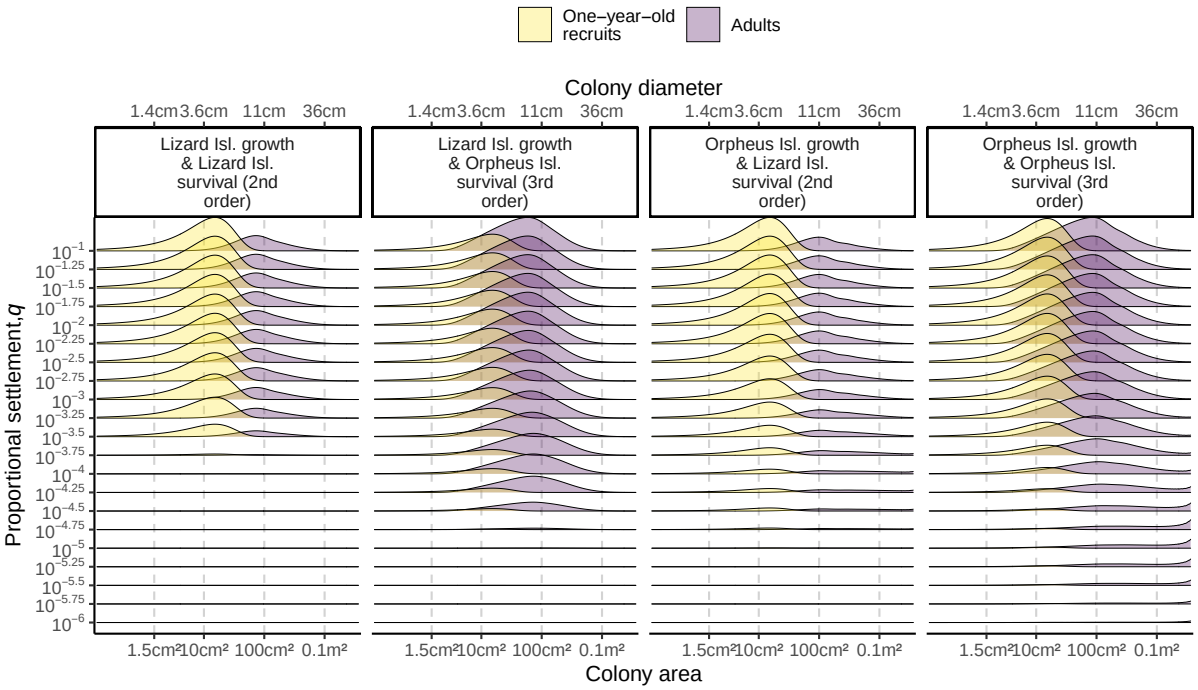

Fig. B4.3. Median size distribution of adults (purple) and one-year-old recruits (yellow) after 50 years of simulation for 1,000 Monte Carlo simulations of simulations of various functional forms for **growth and survival**, across varying proportions of larval settlement, q (vertical panels).

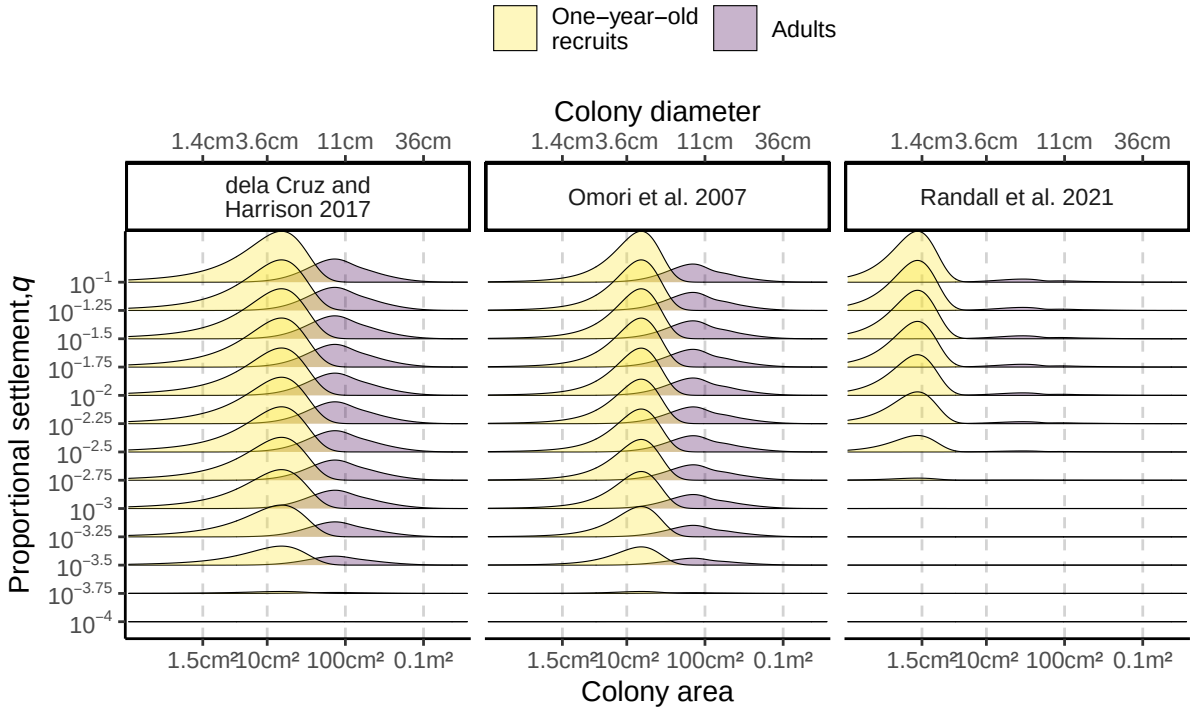

Fig. B4.4. Median size distribution of adults (purple) and one-year-old recruits (yellow) after 50 years of simulation for 1,000 Monte Carlo simulations of various **recruit size distribution** parameterisations, across varying proportions of larval settlement, q (vertical panels).

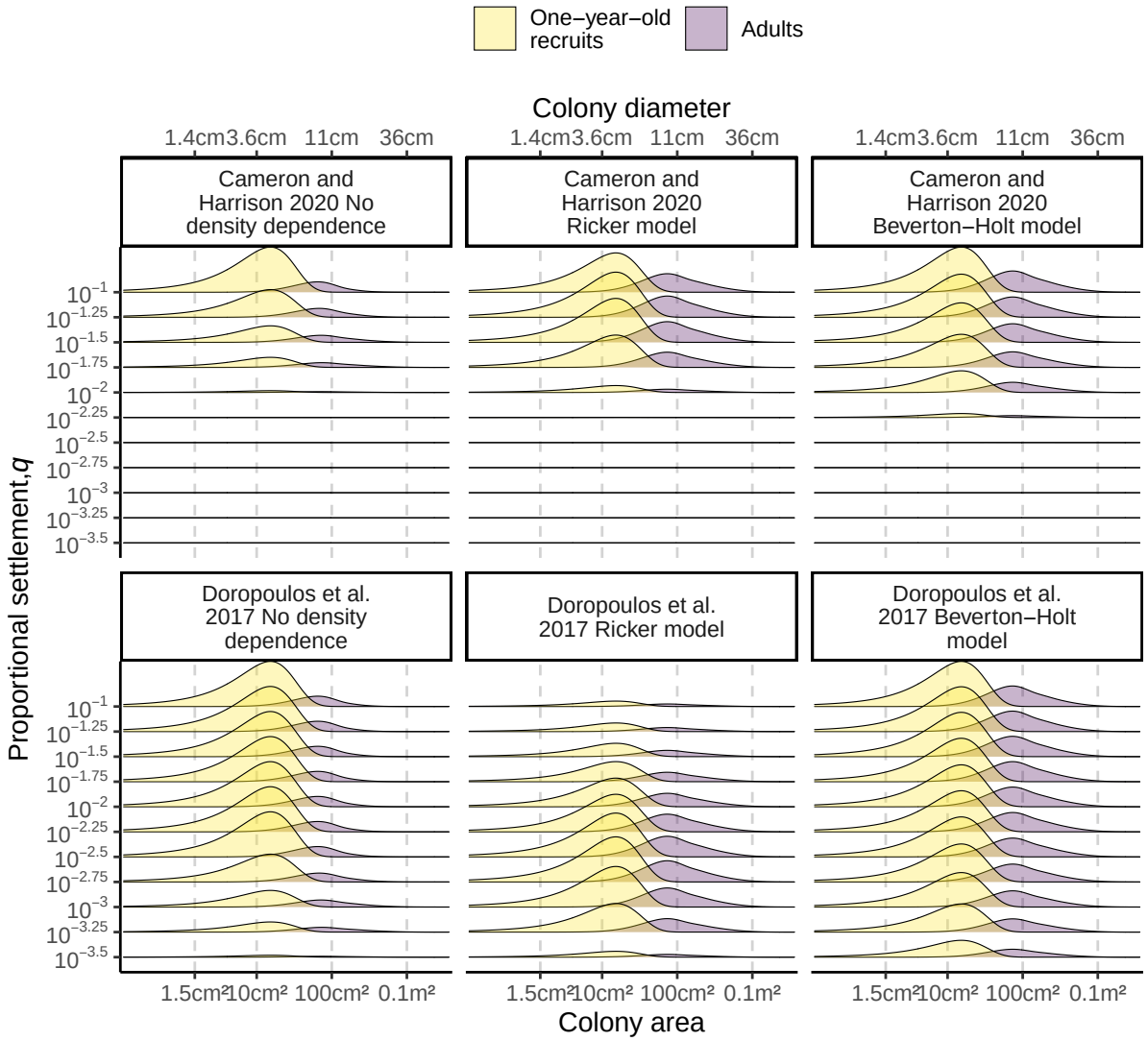

Fig. B4.5. Median size distribution of adults (purple) and one-year-old recruits (yellow) after 50 years of simulation for 1,000 Monte Carlo simulations of various functional forms of **recruit intra-cohort density dependence**, across varying proportions of larval settlement, *q* (vertical panels).

B5: Extinction plots

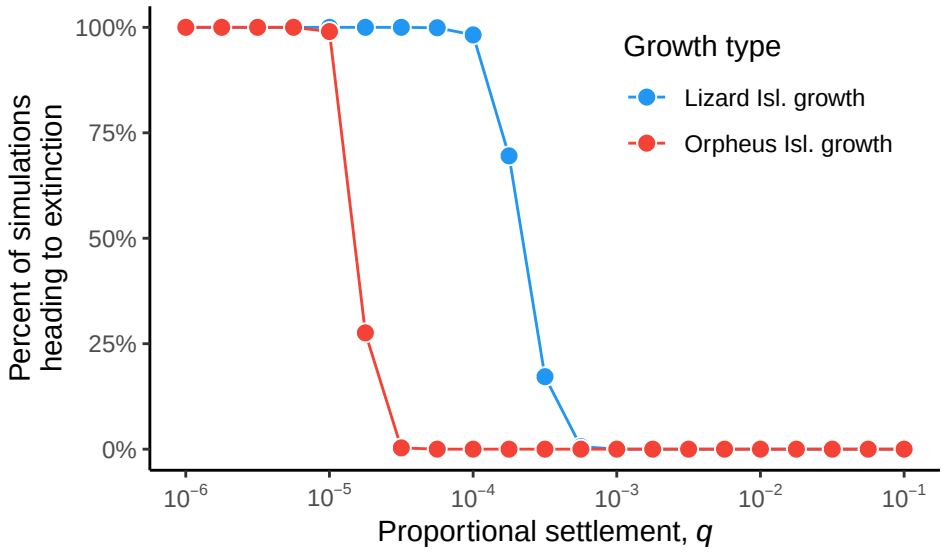

Fig. B5.1. Probability of population extinction across varying proportions of larval settlement, q (x-axis) for 1,000 Monte Carlo simulations of either **Lizard Island (left) vs. Orpheus Island (right) growth** functional forms.

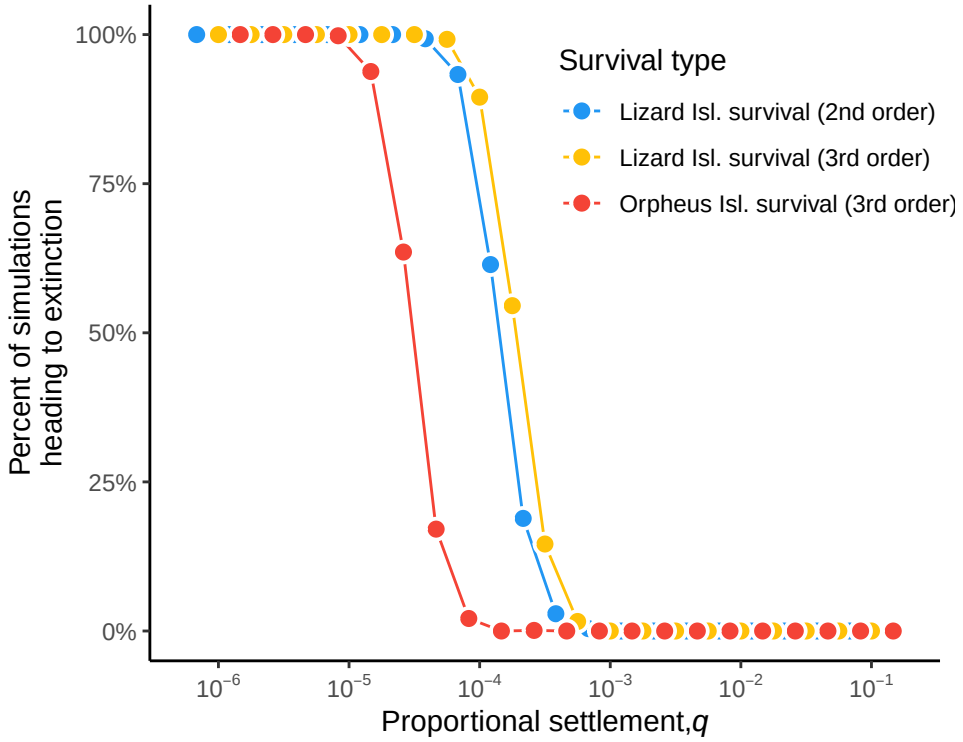

Fig. B5.2. Probability of population extinction across varying proportions of larval settlement, *q* (x-axis) for 1,000 Monte Carlo simulations of either **Lizard Island (left panels) vs. Orpheus Island (right) survival** functional forms fit with either a 2nd or 3rd order polynomial of size.

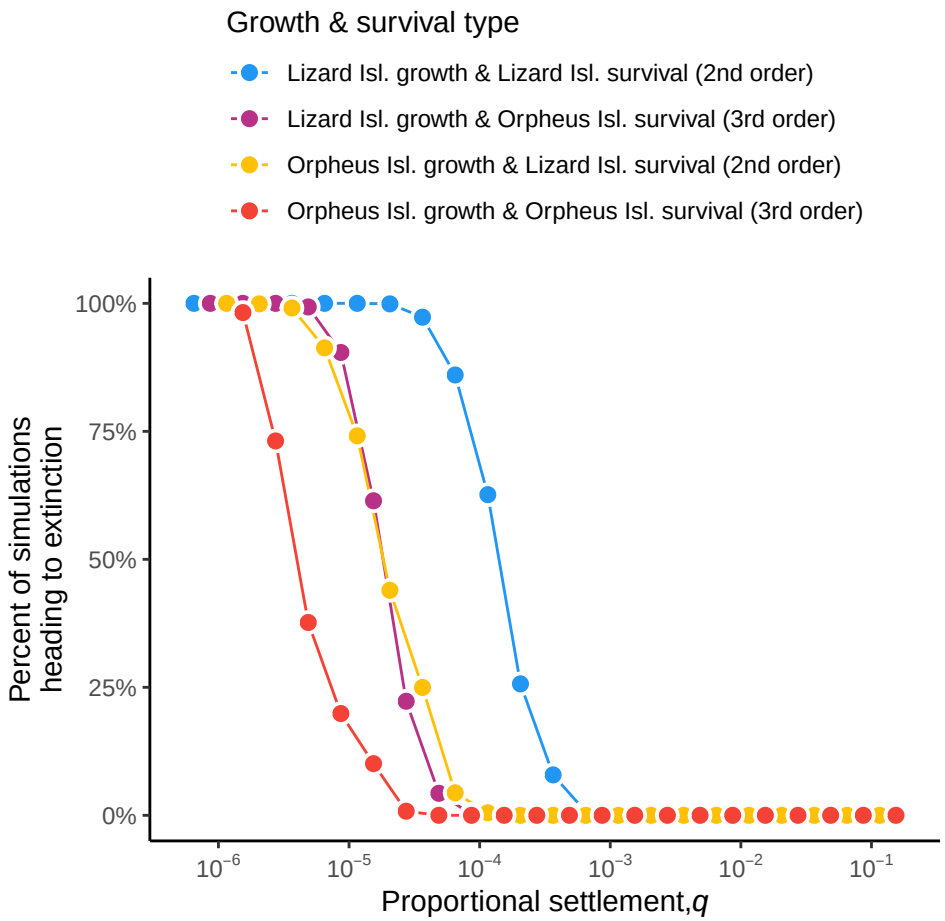

Fig. B5.3. Probability of population extinction across varying proportions of larval settlement, q (x-axis) for 1,000 Monte Carlo simulations of various functional forms of **growth and survival**.

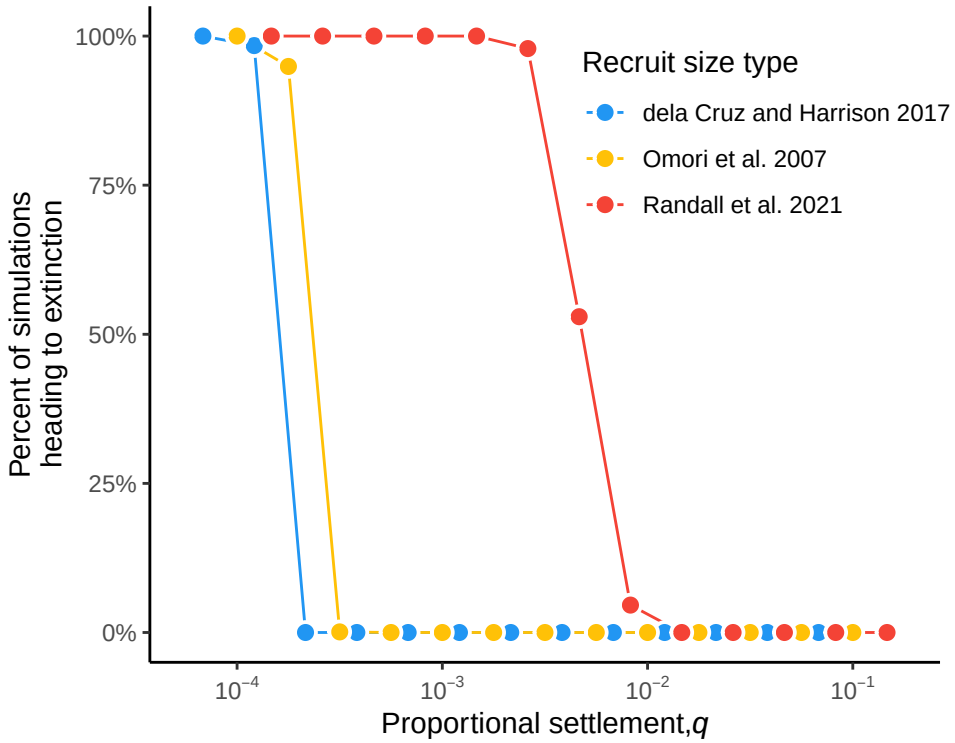

Fig. B5.4. Median size distribution of adults (pink) and one-year-old recruits (blue) after 50 years of simulation for 1,000 Monte Carlo simulations of various **recruit size distribution** parameterisations, across varying proportions of larval settlement, *q* (vertical panels).

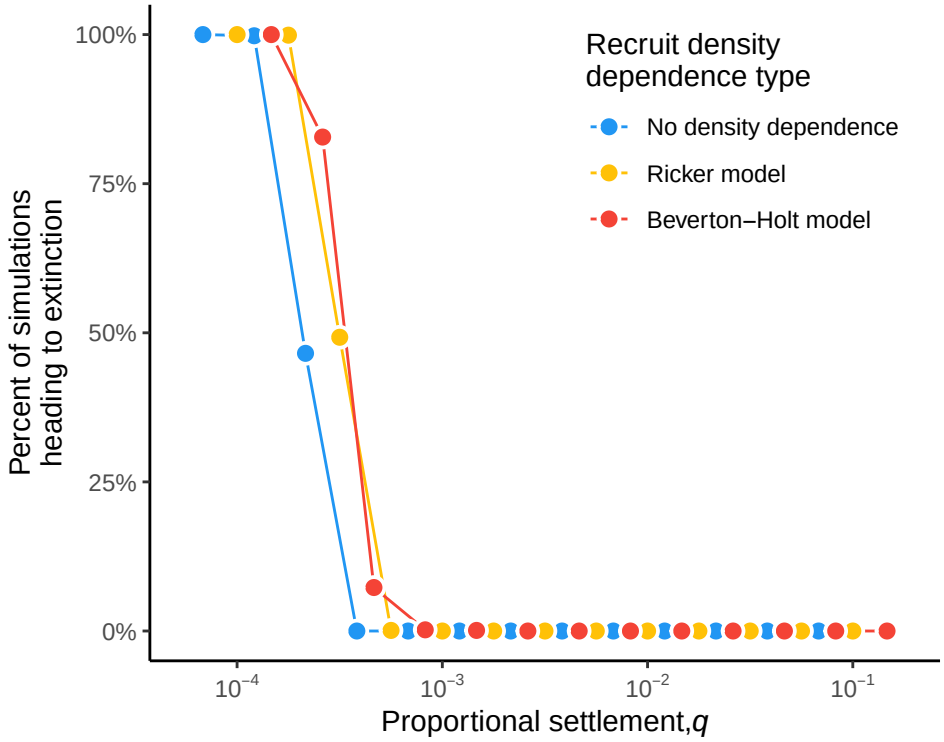

3035

3036 **Fig. B5.5.** Median size distribution of adults (pink) and one-year-old recruits (blue) after 50 years of

3037 simulation for 1,000 Monte Carlo simulations of various functional forms of **recruit intra-cohort**

3038 **density dependence**, across varying proportions of larval settlement, *q* (vertical panels).

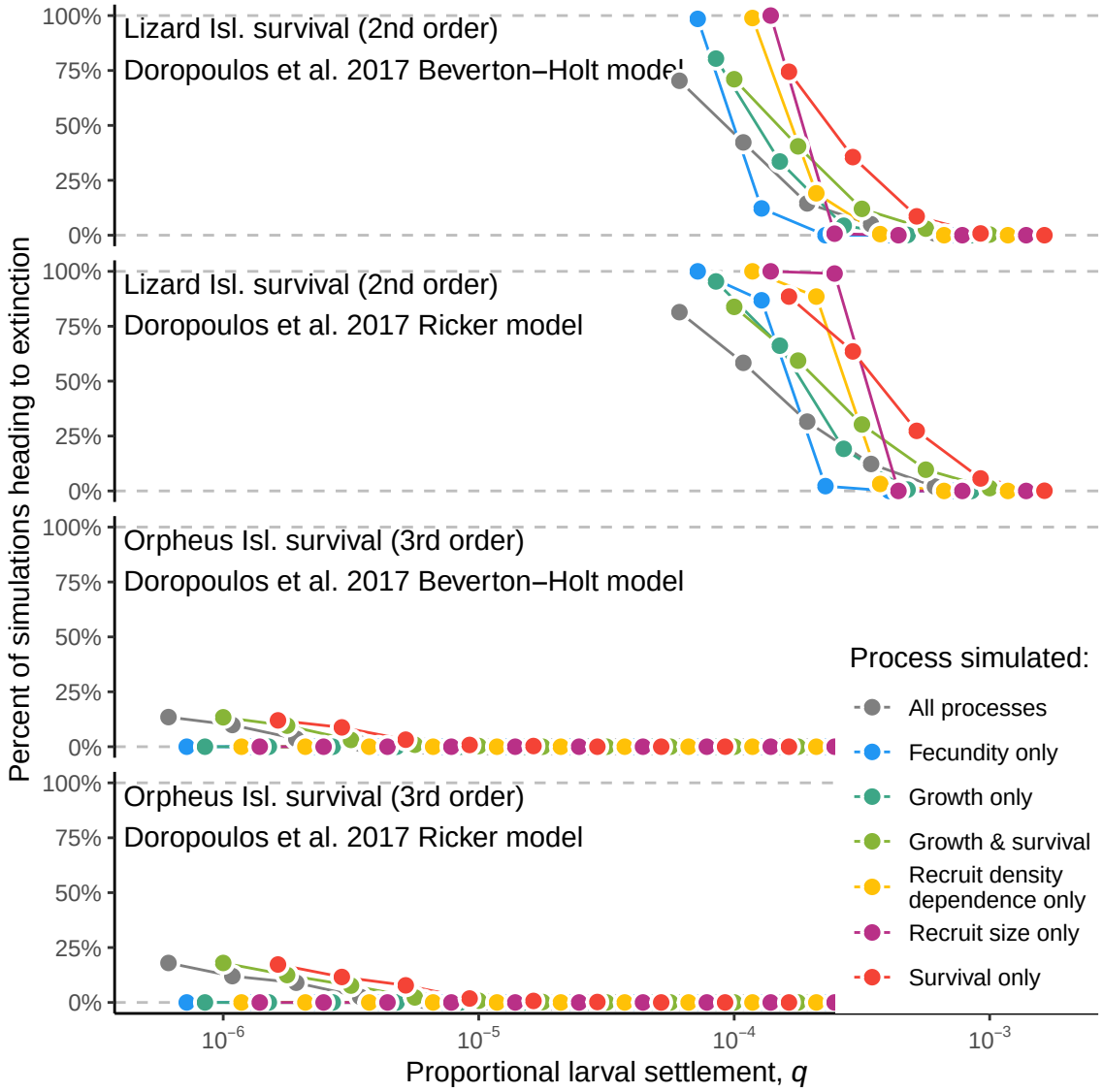

Fig. B5.6. Median size distribution of adults (pink) and one-year-old recruits (blue) after 50 years of simulation for 1,000 Monte Carlo simulations of various functional forms of **recruit intra-cohort density dependence**, across varying proportions of larval settlement, q (vertical panels).

B6: Equilibrium plots

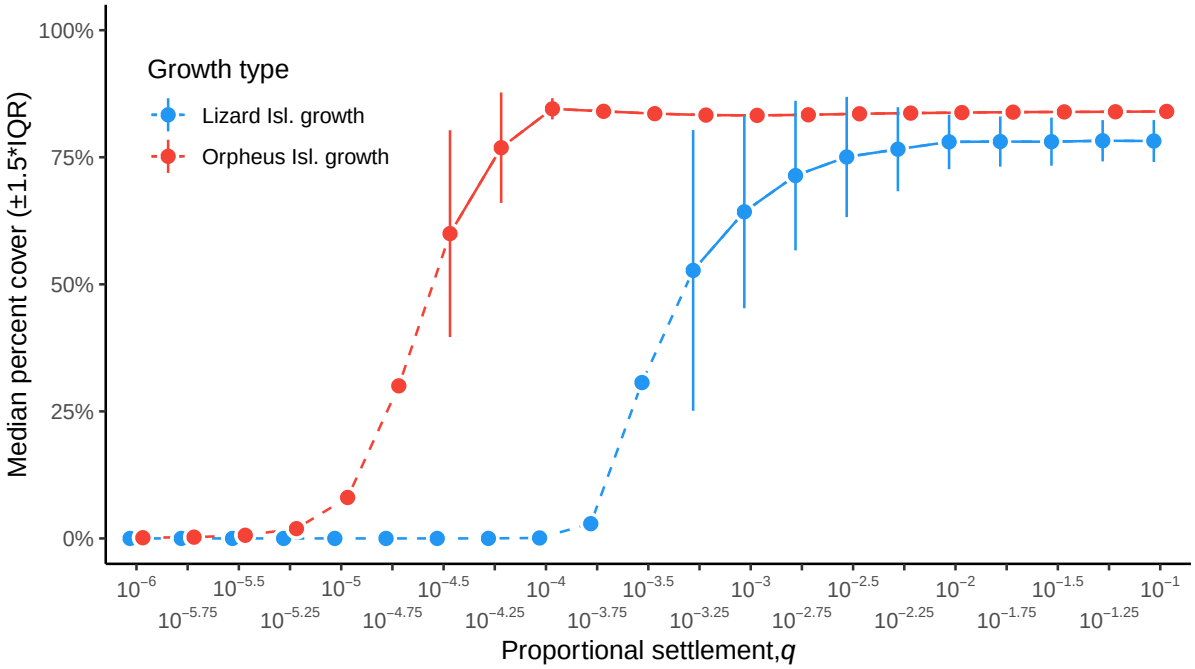

Fig. B6.1. Median of equilibrium coral cover after 50 years across varying proportions of larval settlement, *q* (x-axis) for 1,000 Monte Carlo simulations of either **Lizard Island (blue) vs. Orpheus Island (red) growth** functional forms. Dashed lines connect populations that were in transient states, declining towards extinction.

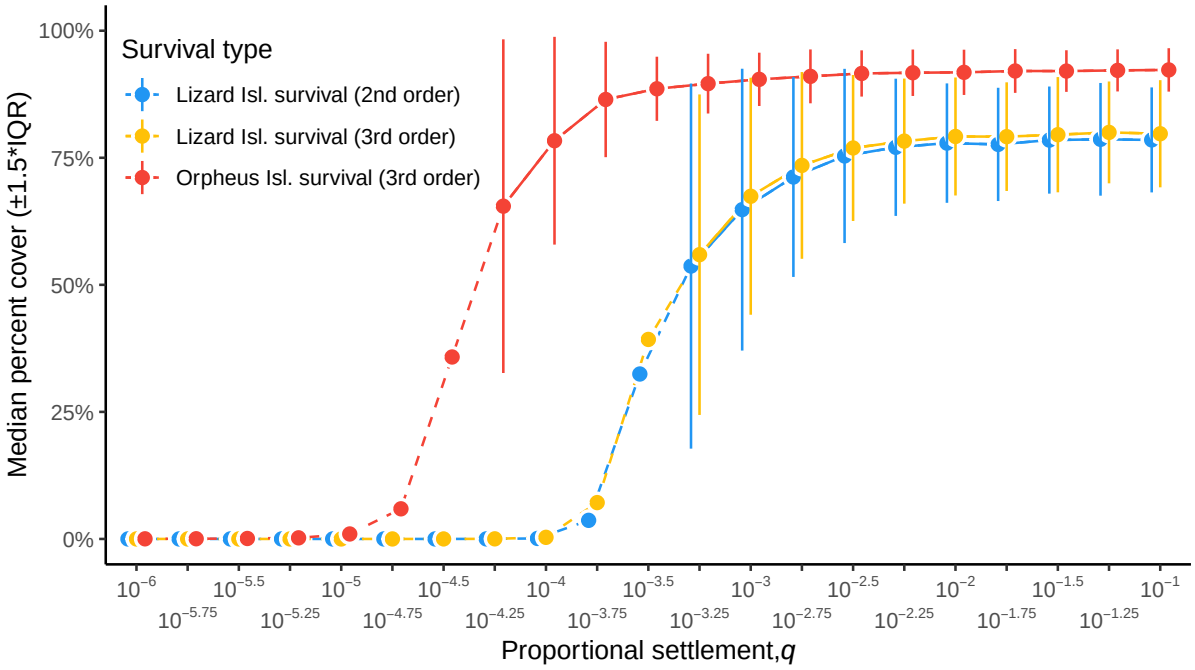

Fig. B6.2. Median of equilibrium coral cover after 50 years across varying proportions of larval settlement, q (x-axis) for 1,000 Monte Carlo simulations of either **Lizard Island (blue) vs. Orpheus Island (red) survival** functional forms with either a 2nd or 3rd order polynomial of size. Dashed lines connect populations that were in transient states, declining towards extinction.

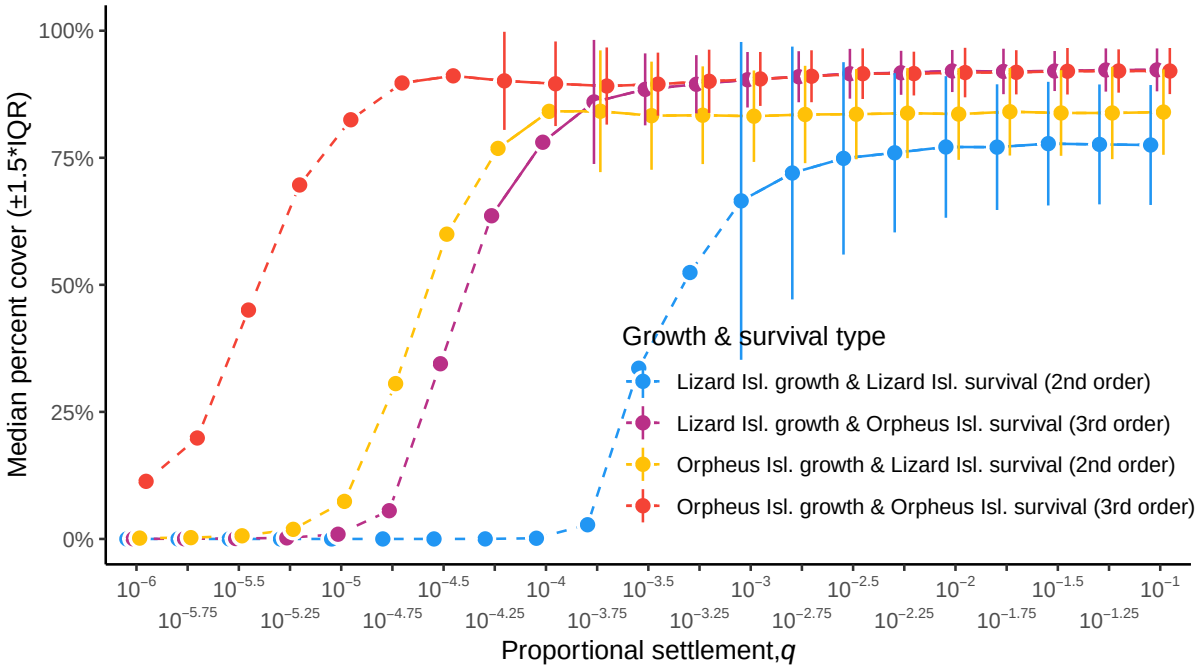

Fig. B6.3. Median of equilibrium coral cover after 50 years across varying proportions of larval settlement, q (x-axis) for 1,000 Monte Carlo simulations of various functional forms of **growth and survival** (see colour). Dashed lines connect populations that were in transient states, declining towards extinction.

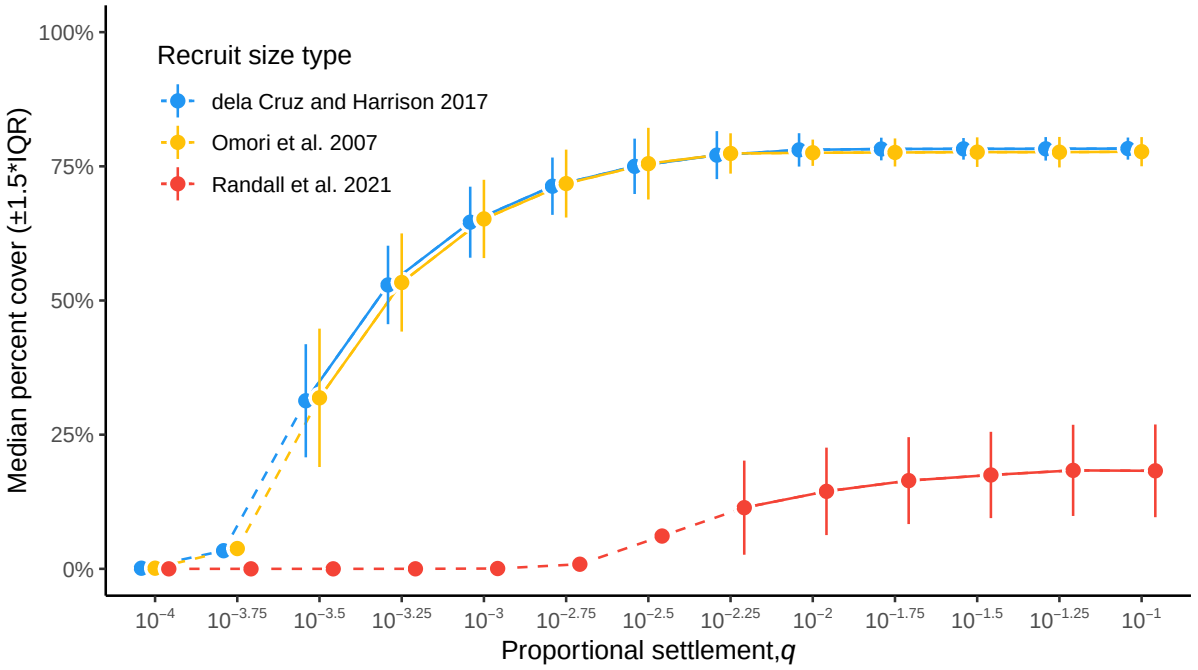

Fig. B6.4. Median of equilibrium coral cover after 50 years across varying proportions of larval settlement, q (x-axis) for 1,000 Monte Carlo simulations of various **recruit size distribution**

parameterisations (see colour). Dashed lines connect populations that were in transient states, declining towards extinction.

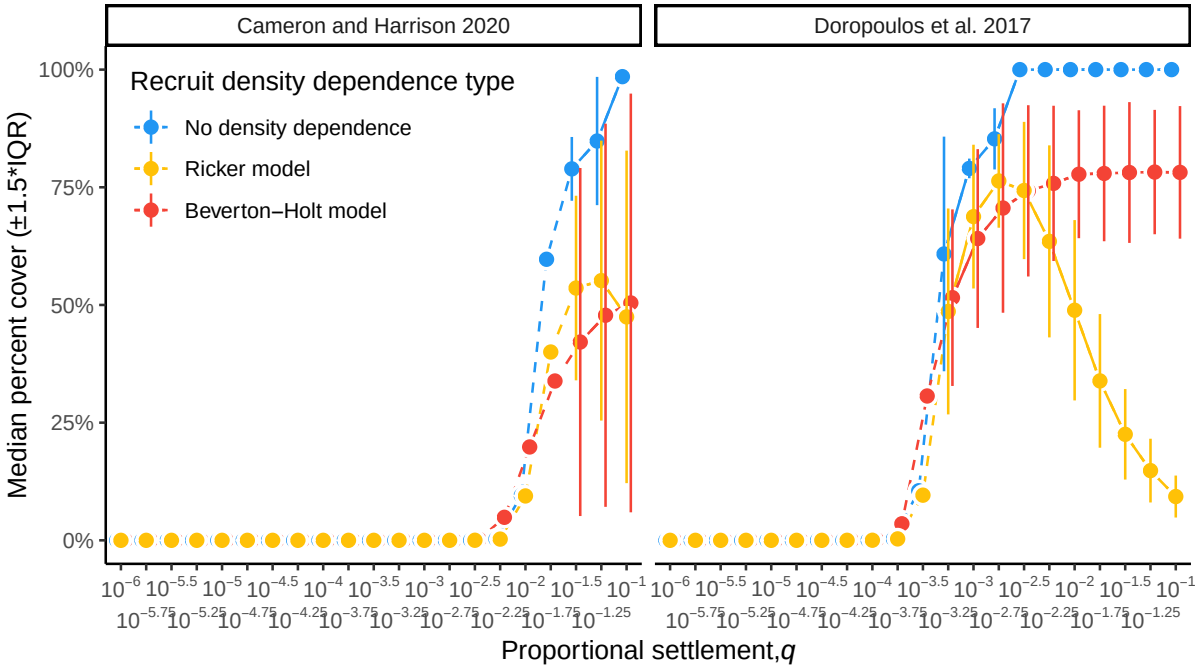

Fig. B6.5. Median of equilibrium coral cover after 50 years across varying proportions of larval settlement, *q* (x-axis) for 1,000 Monte Carlo simulations using **Cameron and Harrison (2020; left)** or **Doropoulos et al. (2017; right)** recruit data for select functional forms of **recruit intra-cohort density dependence**. Dashed lines connect populations that were in transient states, declining towards extinction.

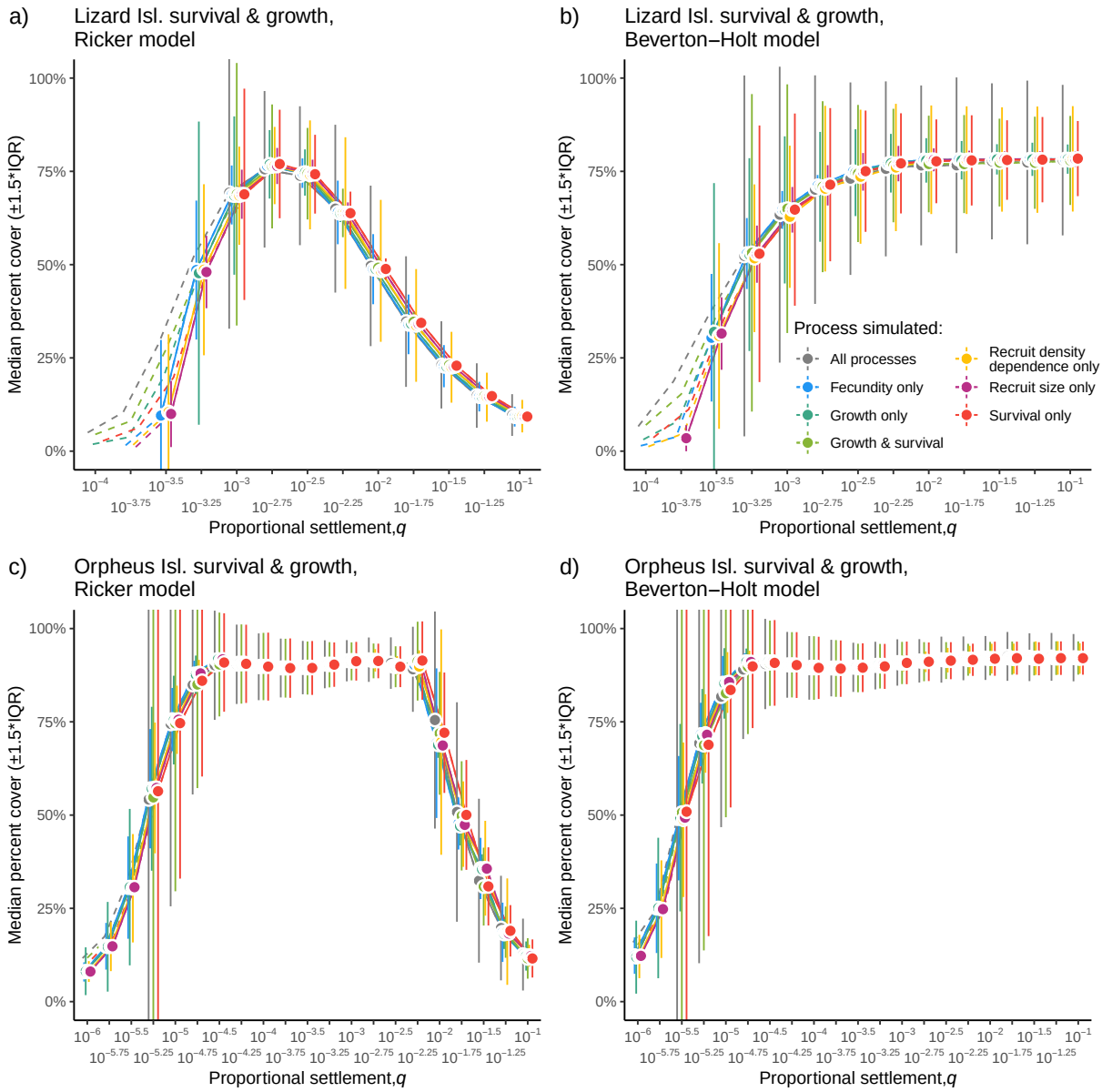

Fig. B6.6. Median of equilibrium coral cover after 50 years across varying proportions of larval settlement, *q* (x-axis) for 1,000 Monte Carlo simulations of **all parameters (complete uncertainty propagation)** for select functional forms of **growth, survival, and recruit intra-cohort density dependence**. Dashed lines connect populations that were in transient states, declining towards extinction.

Appendix C: Supplementary Materials for Chapter 4

C1: Defining a coral mortality phenotype

Mortality distribution from Hughes et al. (2018b)

I consider coral mortality after experiencing thermal stress as an exponential relationship with the degree heating weeks (DHW or θ, in °C-weeks) experienced on each reef. This relationship was estimated using linear mixed slopes model of log-proportion coral cover loss along the Great Barrier Reef in Hughes et al. (2018), where β_0 and β_1 represent the model's fitted intercept and slope, respectively, for various coral taxa. The cumulative distribution function (CDF) of coral mortality with thermal stress as DHW (θ) on a reef is thus:

$$F(\theta) = \begin{cases} 1 - e^{(\beta_0 - \beta_1 \theta)} & if\ \theta > \beta_0/\beta_1 \\ 1 & if\ \theta \leq \beta_0/\beta_1 \end{cases} \quad (1)$$

where $F(\theta)$ represents the CDF dependent on the reef's maximum experienced DHWs (θ), and β_0 and β_1 represent the exponential model's fitted intercept and slope, respectively. Note that at some positive values of θ, thermally-dependent survival is 100%, until the degree heating weeks pass a critical thermal threshold, β_0/β_1, at which point mortality begins to accrue rapidly.

The associated probability density function (PDF) of this non-central exponential distribution is:

$$f(\theta) = \begin{cases} \beta_1 e^{(\beta_0 - \beta_1 \theta)} & if\ \theta > \beta_0/\beta_1 \\ 0 & if\ \theta \leq \beta_0/\beta_1 \end{cases} \quad (2)$$

Which closely resembles the PDF of the standard exponential distribution:

$$f(x) = \begin{cases} \lambda e^{-\lambda x} & if\ x > 0 \\ 0 & if\ x \leq 0 \end{cases} \quad (3)$$

The standard exponential distribution uses a rate parameter λ, has a mean of $\mathbb{E}(x) = 1/\lambda$, and variance of $Var(x) = 1/\lambda^2$. The expectation of θ (i.e. the mean) for the non-central exponential distribution (Eq. 2) is defined as:

Appendix C

$$E\left[\theta|\theta > \frac{\beta_0}{\beta_1}\right] = \int_{\frac{\beta_0}{\beta_1}}^{\infty} \theta f(\theta) dx = \beta_1 e^{\beta_0} \int_{\frac{\beta_0}{\beta_1}}^{\infty} \theta e^{-\beta_1 \theta} d\theta \quad (4)$$

To solve the integral, I use integration by parts. Let $u = \theta$ and $dv = e^{-\beta_1\theta}d\theta$, then $du = d\theta$ and $v = -\frac{1}{\beta_1}e^{-\beta_1\theta}$:

$$\int \theta e^{-\beta_1\theta} d\theta = \int u dv = uv - \int v du$$

$$= -\frac{1}{\beta_1}\theta e^{-\beta_1\theta} - \int -\frac{1}{\beta_1} e^{-\beta_1\theta} d\theta$$

$$= -\frac{1}{\beta_1}\left(\theta e^{-\beta_1\theta} - \int e^{-\beta_1\theta} d\theta\right)$$

$$= -\frac{1}{\beta_1}\left(\theta e^{-\beta_1\theta} + \frac{e^{-\beta_1\theta}}{\beta_1}\right)$$

Substituting the integral's solution back into Eq. 4, I can begin to solve the definite integral:

$$\beta_1 e^{\beta_0}\left[-\frac{1}{\beta_1}\left(\theta e^{-\beta_1\theta} + \frac{e^{-\beta_1\theta}}{\beta_1}\right)\right]\Big|_{\beta_0/\beta_1}^{\infty}$$

$$= -e^{\beta_0}\left[\theta e^{-\beta_1\theta} + \frac{e^{-\beta_1\theta}}{\beta_1}\right]\Big|_{\beta_0/\beta_1}^{\infty}$$

$$= \frac{-e^{\beta_0}}{\beta_1}\left[e^{-\beta_1\theta}(\beta_1\theta + 1)\right]\Big|_{\beta_0/\beta_1}^{\infty}$$

$$= -\frac{e^{\beta_0}}{\beta_1}\left[\left(\left(\lim_{\theta\to\infty}(\beta_1\theta e^{-\beta_1\theta}) + \lim_{\theta\to\infty}(e^{-\beta_1\theta})\right)\right) - \left(\beta_1\left[\frac{\beta_0}{\beta_1}\right] + 1\right)e^{-\beta_1\left[\frac{\beta_0}{\beta_1}\right]}\right]$$

Since $\lim_{\theta\to\infty}(e^{-\beta_1\theta})$ approaches 0 faster than $\lim_{\theta\to\infty}(\theta)$ approaches ∞, both limits will shrink to 0, simplifying to:

$$= \frac{e^{\beta_0}}{\beta_1}\left[(\beta_0 + 1)e^{-\beta_0}\right]$$

Therefore, the mean of Eq. 2 is:

$$E\left[\theta|\theta > \frac{\beta_0}{\beta_1}\right] = \frac{1 + \beta_0}{\beta_1} \quad (5)$$

Note that an identical solution can be obtained by letting $\theta = x + \frac{\beta_0}{\beta_1}$, where x is the standard exponential distribution (Eq. 3), and letting $\lambda = \beta_1$:

$$\mathbb{E}(\theta) = \mathbb{E}\left(x + \frac{\beta_0}{\beta_1}\right) = E(x) + \frac{\beta_0}{\beta_1} = \left[\frac{1}{\beta_1}\right] + \frac{\beta_0}{\beta_1} = \frac{1 + \beta_0}{\beta_1}$$

Similarly, the variance of the distribution given in Eq. 2 is unchanged from the standard exponential distribution (Eq. 3), since shifting all values by a constant does not affect the variance:

$$Var(\theta) = Var\left(x + \frac{\beta_0}{\beta_1}\right) = Var(x) = \frac{1}{\beta_1^2} \quad (6)$$

Using the estimates of $\beta_0 = 0.2917$ and $\beta_1 = 0.3165$ for corymbose coral ('Other Acropora') from Hughes et al. (2018), the mean degree heating weeks with the highest probability of mortality is expected to be at ~4°C-weeks, with a variance of ~10°C-weeks.

Appendix C

Log-normal approximation to exponential distribution

I now approximate this non-central exponential distribution using a log-normal distribution with identical mean and variance. The mean ($\mathbb{E}_L(\theta)$) and variance ($Var_L(\theta)$) of the log-normal distribution are:

$$\mathbb{E}_L(\theta) = e^{\left(\mu+\frac{\sigma^2}{2}\right)} \tag{7}$$

$$Var_L(\theta) = \left(e^{(\sigma^2)} - 1\right)e^{(2\mu+\sigma^2)} \tag{8}$$

Using the method of moments, the solutions for μ and σ are:

$$\mu = \log\left(\frac{\mathbb{E}_L(\theta)}{\sqrt{\frac{Var_L(\theta)}{\mathbb{E}_L(\theta)^2} + 1}}\right) \tag{9}$$

and

$$\sigma = \sqrt{\left(\log\left(\frac{Var_L(\theta)}{\mathbb{E}_L(\theta)^2} + 1\right)\right)} \tag{10}$$

Thus, for corymbose corals, $\mu = 1.172$ and $\sigma = 0.685$ for the log-normal approximation of the PDF of coral mortality.

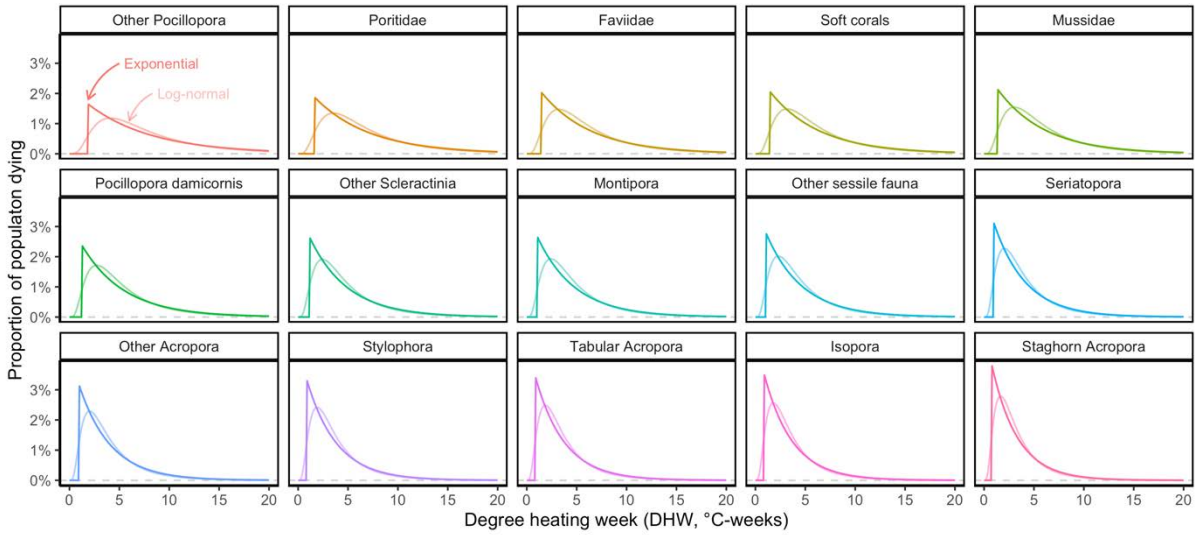

Fig. C1.1. Coral mortality modelled as a non-central exponential probability density function (PDF) for all major taxonomic groups in Hughes et al. (2018) vs. the log-normal PDF approximation described above. The group 'Other Acropora' in the bottom left-hand corner includes corymbose *Acropora* spp. corals that are the subject of this study.

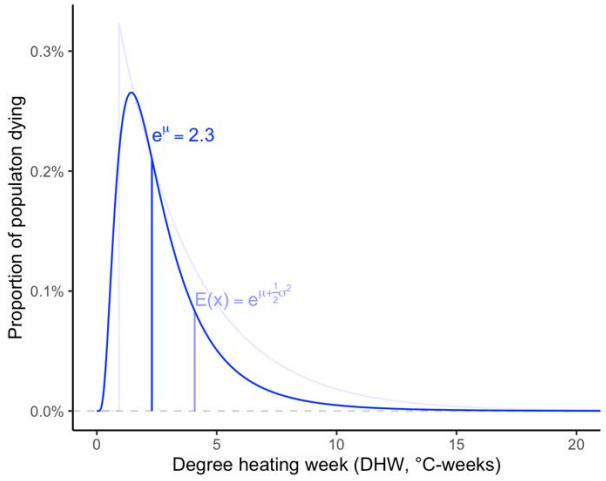

Fig. C1.2. Example log-normal approximation to the exponential distribution. A log-normal distribution is normally distributed on the log(x) scale, which is required for the EE-IPM framework when re-distributing offspring genotypes.

Square root and normal numerical approximations

I employed a numerical simulation method to approximate the exponential model as the square-root of a normal distribution. To do so, I sampled 10,000 different DHW values from the exponential model using the CDF inversion method. This involves solving the non-zero CDF equation for proportion mortality, $F(\theta) = e^{(\beta_0 - \beta_1 \theta)}$, in terms of DHWs or θ, which thus becomes:

$$\theta = \frac{\beta_0 - \log\big(F(\theta)\big)}{\beta_1}$$

Next, I simulate values of $F(\theta)$ as a uniform random variable U(0,1) to attain a distribution of simulated DHW values based on the original exponential function of Hughes et al. (2018), depicted below in Fig. A1.3 (Fig. A1.3a). Then, I can square-root transform these values and take the mean and variance of this distribution to obtain a square-root approximation of the exponential distribution (Fig. A1.3b). Similarly, I can obtain a numerical approximation of the logged values that produces a similar mean and variance to the log-normal analytical approximation above (Fig. A1.3c). After sampling 1 million DHWs from the exponential distribution, I obtained the approximations in Table C1.1.

Table C1.1. Normal distribution approximations on different scales of the critical heat stress (*DHWcrit*) of coral mortality from Hughes et al. (2018) using 1 million samples from the original exponential distribution.

***DHWcrit* scale**	**Mean**	**Variance**	**Standard deviation**
Regular	4.084	10.029	3.167
Square-root	1.899	0.478	0.692
Natural logarithmic	1.159	0.484	0.696

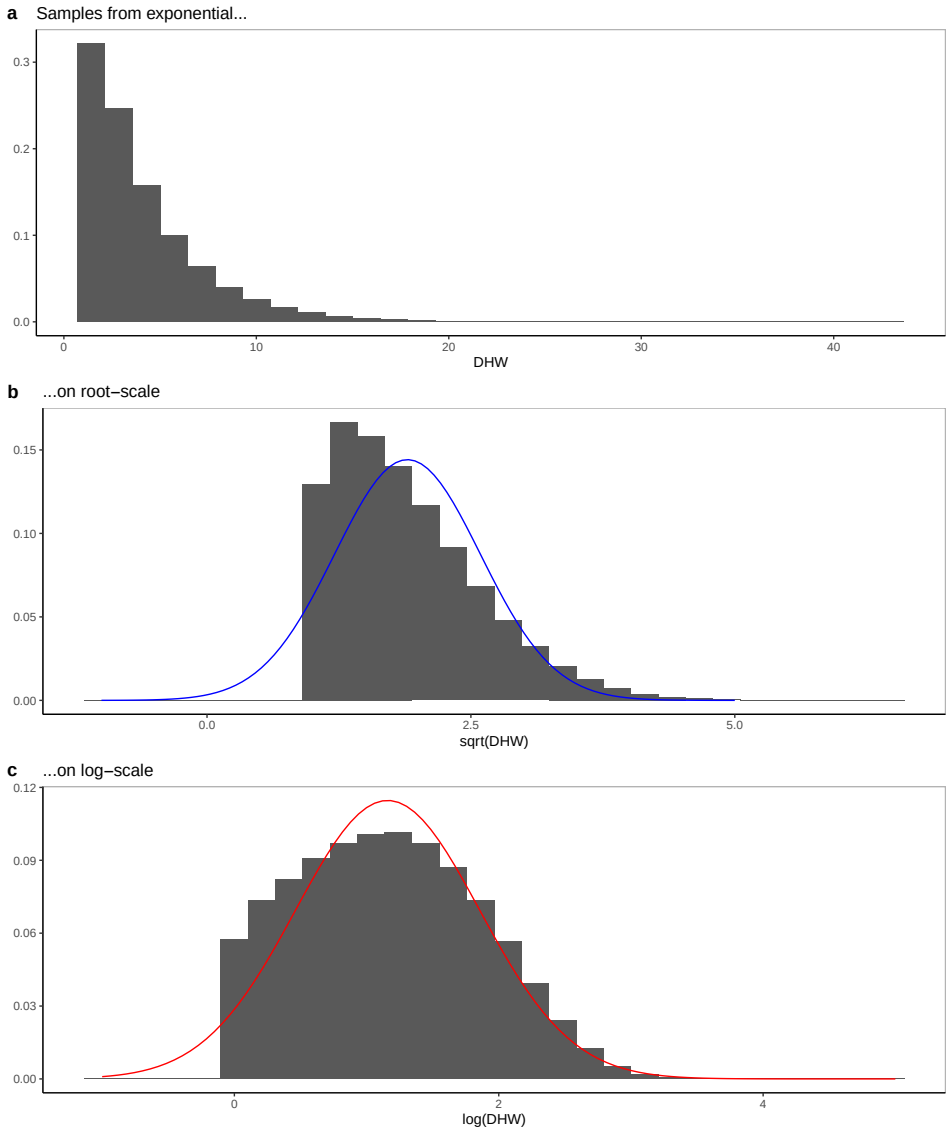

Fig. C1.3. a) Simulated DHW values (n = 1,000,000) from the exponential distribution. b) Square-root transformed DHW values from the sampled exponential distribution, overlaid by a normal distribution approximation on the root-scale. c) Log-transformed DHW values from the sampled exponential distribution, overlaid by a normal distribution approximation on the log-scale.

C2: Hindcast heat stress models

Methods

Historical sea surface temperature profiles from 1987–2022 for 156 Great Barrier Reef sites nearby Orpheus Island and Lizard Island (the locations providing the demographic data) were downloaded from the NOAA Coral Reef Watch FTP server (NOAA Coral Reef Watch 2022). From these data, DHWs were calculated according to (Donner et al. 2005; Heron et al. 2016) using the threshold of the mean monthly maximum (MMM) + 1°C for the accumulation of heat stress over a 16-week window. After determining the weekly accumulated DHW values, I summarised the maximum DHW for each calendar year and used these values from the 156 reefs in the historical model simulations. I also downloaded and merged the Manta Tow and Marine Monitoring Program (MMP) datasets from the AIMS Long-term Monitoring Program (LTMP) database (AIMS Data) to use as validation data for my model. I use only reefs with >10 years of observation of percent coral cover to ensure that there is a long-enough time series to compare to my model's outputs. These observations make up my 'observed coral cover' data, denoted by the red lines/points in the plots following.

Since the equilibrium % coral cover in the absence of DHWs in my models is determined entirely by growth/survival demography relationships (generally ~80% coral cover) and because my model considers only the 'area available to corymbose Acroporid corals' instead of total reef area surveyed – as in the AIMS LTMP, I rescaled my model's estimates of coral cover to directly compare trends to reef % coral cover in the AIMS LTMP. To do so, I divided percent coral cover in my models by the maximum value observed, then multiplied them by the maximum value of the LTMP time series for each reef to obtain 'predicted coral cover'.

Determining the most plausible scale of DHWcrit genotype evolution

I used model hindcasts to compare the biological plausibility of different DHWcrit scales on which the genotype could evolve. These were compared to the AIMS LTMP dataset after rescaling for each reef (Fig. C2.1). Overall, all scales overestimated coral cover from 2000-2014, but during the first major mass bleaching event in a decade in 2016, the coral cover of the square-root scale and log-scale DHWcrit models matches somewhat closely, whereas the arithmetic/normal scale models move

towards extinction overall (Fig. C2.2). Regressing the observed vs. predicted coral cover to one another and calculating the coefficient of determination, r^2, allows me to plot the model accuracy for each reef and model combination as points (Fig. C2.3), to assess the accuracy of model parameter combinations and different DHWcrit scales. Doing so reveals that models using the arithmetic scale perform variably well, ranging from very accurate predictions up to r^2=0.8 or 80% of the variation in observed coral cover being predicted by models, to very poor, with near 0% of the variation predicted (Fig. C2.3). Conversely, both square-root and log-scale models were more predictable, around r^2 = 30% and highest for models with DHW-limited fecundity and greater initial starting values of mean genotype (Fig. C2.3). However, square-root scale performed marginally better overall compared to log-scale models, and is more conservative in terms of future evolution to DHWs in that it results in more plausible, slower evolution, relative to log-scale models. For instance, log-scale models allow corals to evolve to biologically implausibly high DHW values after 100 years. Therefore, I used root-scale models for the remainder of my models, which best balance hindcast accuracy with plausible future evolution.

Appendix C

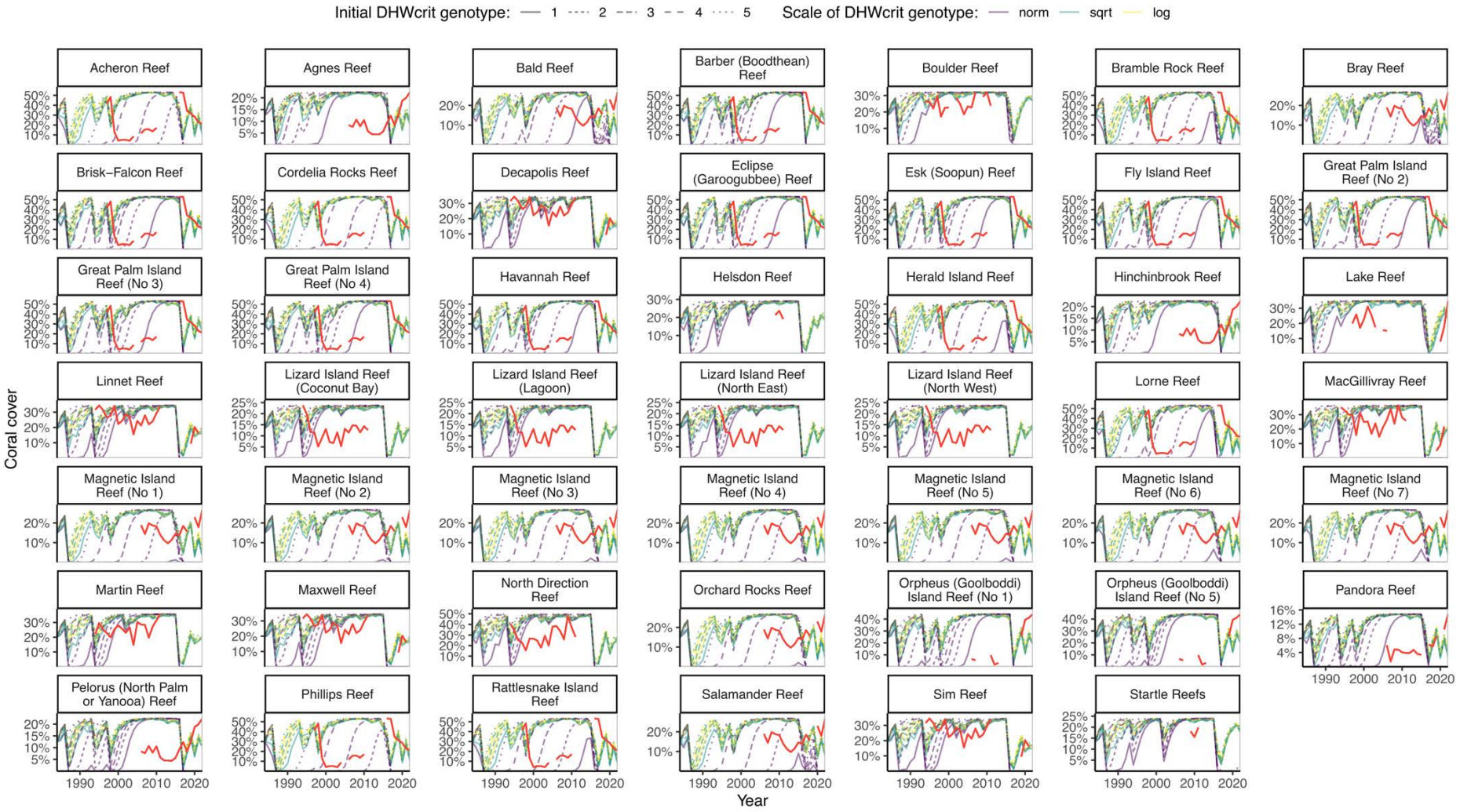
Initial DHWcrit genotype: 1 2 3 4 5
Scale of DHWcrit genotype: norm sqrt log
Acheron Reef
Agnes Reef
Bald Reef
Barber (Boodthean) Reef
Boulder Reef
Bramble Rock Reef
Bray Reef
Brisk–Falcon Reef
Cordelia Rocks Reef
Decapolis Reef
Eclipse (Garoogubbee) Reef
Esk (Soopun) Reef
Fly Island Reef
Great Palm Island Reef (No 2)
Great Palm Island Reef (No 3)
Great Palm Island Reef (No 4)
Havannah Reef
Helsdon Reef
Herald Island Reef
Hinchinbrook Reef
Lake Reef
Linnet Reef
Lizard Island Reef (Coconut Bay)
Lizard Island Reef (Lagoon)
Lizard Island Reef (North East)
Lizard Island Reef (North West)
Lorne Reef
MacGillivray Reef
Magnetic Island Reef (No 1)
Magnetic Island Reef (No 2)
Magnetic Island Reef (No 3)
Magnetic Island Reef (No 4)
Magnetic Island Reef (No 5)
Magnetic Island Reef (No 6)
Magnetic Island Reef (No 7)
Martin Reef
Maxwell Reef
North Direction Reef
Orchard Rocks Reef
Orpheus (Goolboddi) Island Reef (No 1)
Orpheus (Goolboddi) Island Reef (No 5)
Pandora Reef
Pelorus (North Palm or Yanooa) Reef
Phillips Reef
Rattlesnake Island Reef
Salamander Reef
Sim Reef
Startle Reefs
Coral cover
Year
1990 2000 2010 2020

Fig. C2.1. Predicted (purple, green, and yellow lines) vs. observed (red lines) percent coral cover across 48 reefs from the AIMS LTMP dataset. Predicted coral cover has been rescaled to more closely match the max coral cover observed at each reef. Different-coloured predicted lines represent different DHWcrit scales assumed for the genotype to evolve upon; either arithmetic or normal scale ("norm", in purple), square-root scale ("sqrt", in green), or the natural logarithm ("log", in yellow). Different patterned lines represent different magnitudes of initial starting mean genotype values (scale-dependent), from lower (1) to higher (5). All predicted data here use a proportional larval settlement of $q = 0.01$, heritability of $h^2 = 0.3$, and have DHW-limited fecundity turned on (optimal parameter settings, as per below).

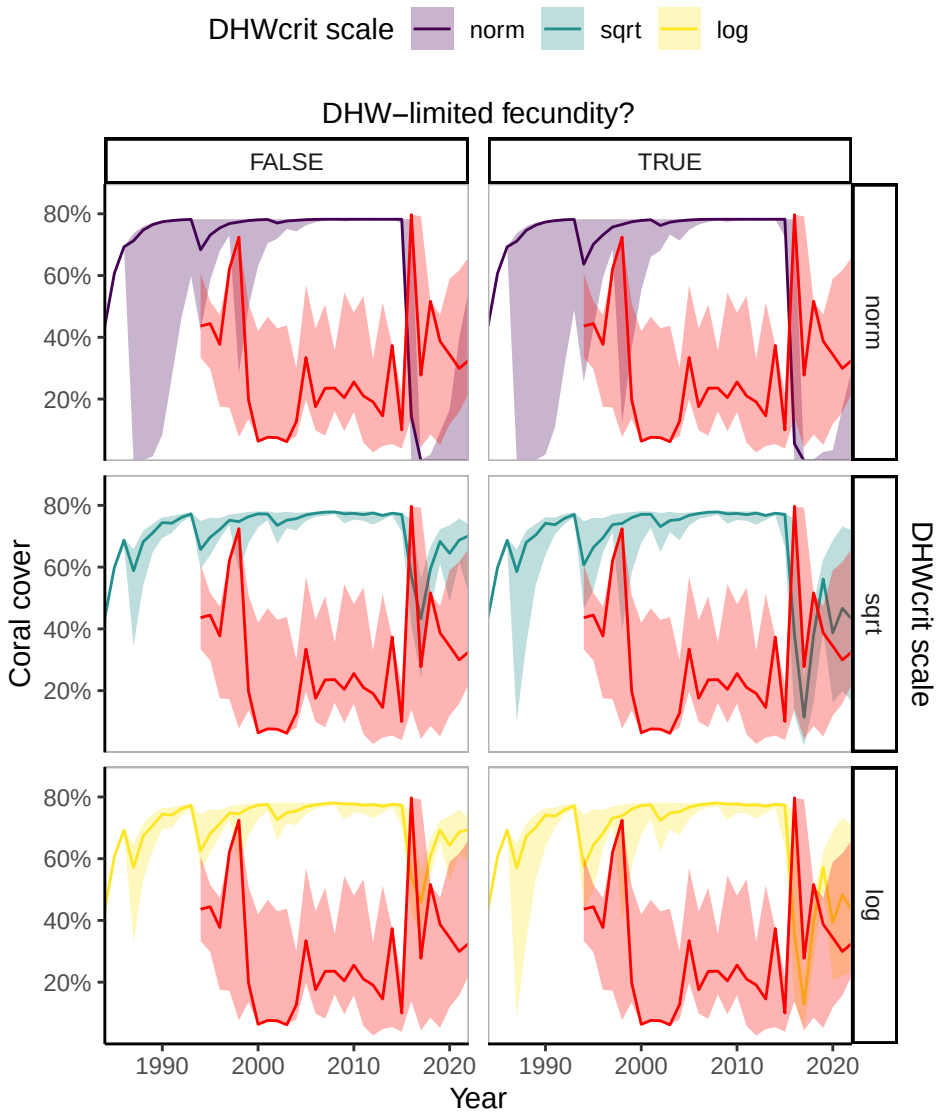

Fig. C2.2. Summarised percent coral cover (median and 95% CIs) from Fig. C2.1 for normal scale ("norm", in purple), square-root scale ("sqrt", in green), natural logarithm scale ("log", in yellow), or the observed coral cover (in red, rescaled). All predicted data here use a proportional larval settlement of $q = 0.01$, heritability of $h^2 = 0.3$, an initial mean genotype identical to that observed in Hughes et al. (2016), and have DHW-limited fecundity turned on (optimal parameter settings, as per below).

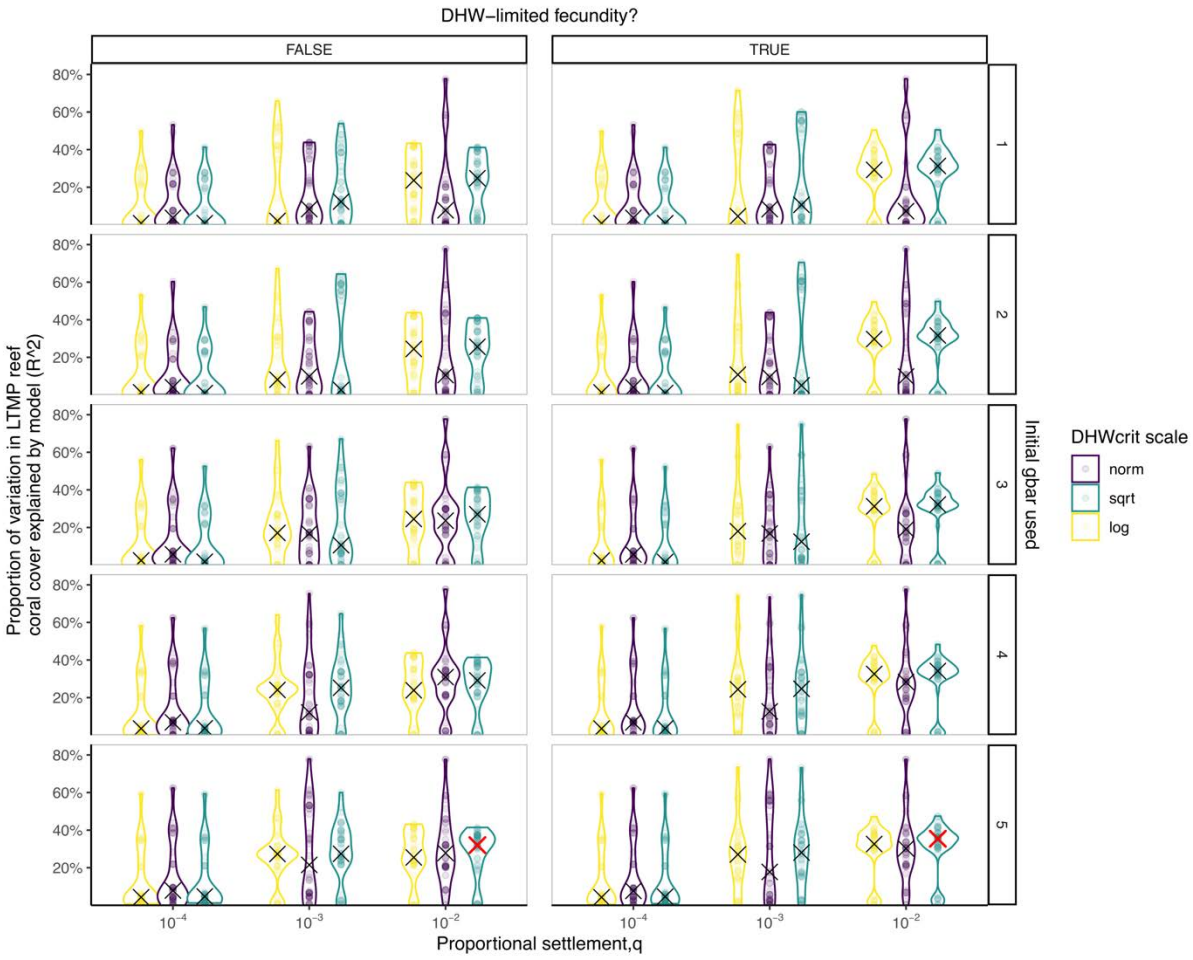

Fig. C2.3. Model accuracy across all 48 LTMP reefs and various parameter combinations, as assessed through model r^2 using the regression of observed ~ predicted coral cover. Points represent a single reef, with violin plots denoting the distribution of r^2 values and 'X's representing the median value of r^2. Red 'X's denote the highest r^2 for both cases of DHW-limited fecundity – each being the square-root scale DHWcrit transformation with the highest magnitude of initial starting mean genotype (initial gbar = 5).

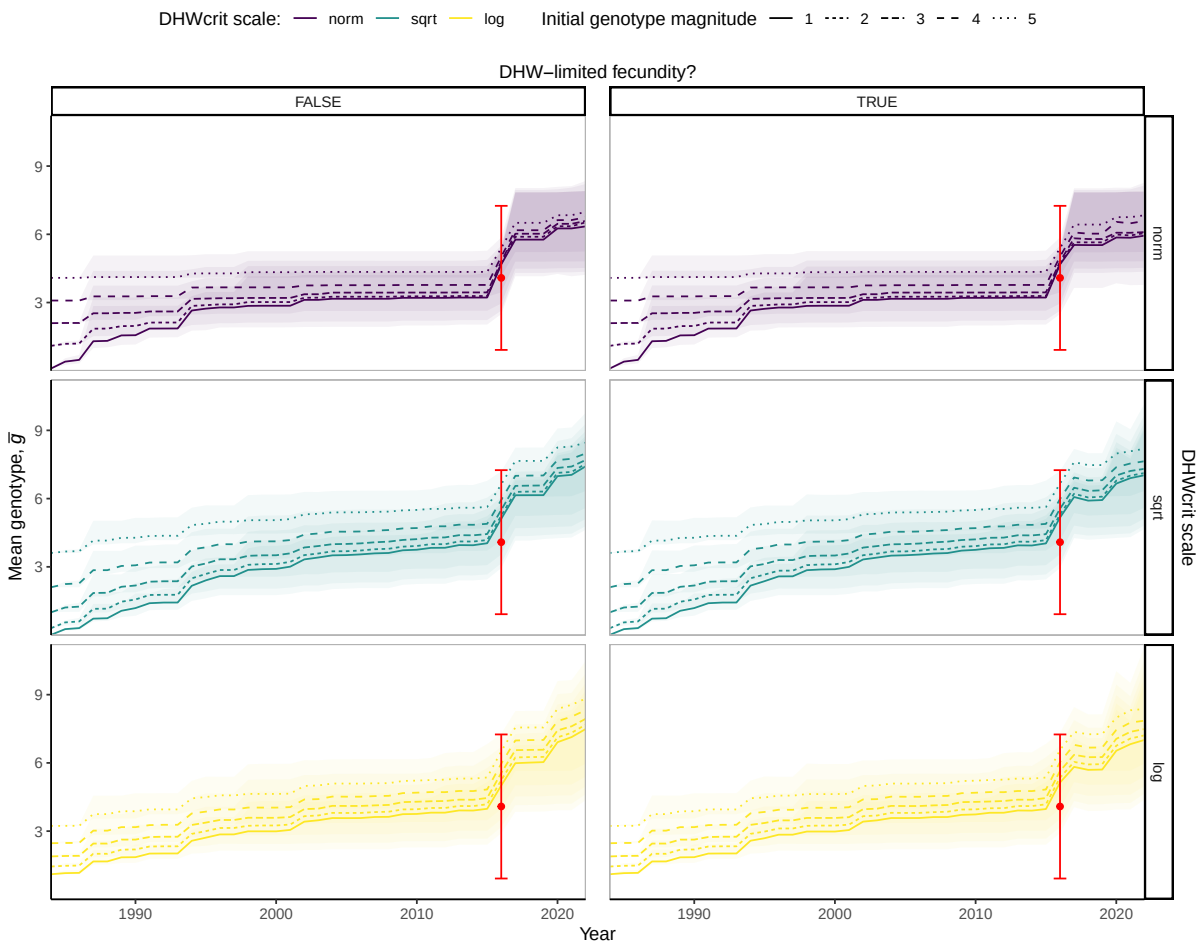

Fig. C2.4. Predicted evolution of genotypes using three different scale transformations for the distribution of *DHWcrit* values and five different magnitudes of starting mean genotypes (1 = mean genotype of 0.1, 5 = mean genotype equal to the red dot in each plot [scale-dependent], with even spacing on the given scale). Red points and error bars represent the 2.5th, 50th, and 97.5th quantiles from the exponential distribution of Hughes et al. (2018). All models were run using a settlement parameter, q = 0.01 and h^2 = 0.3.

Determining an optimal root-scale

To determine the 'optimal' parameter settings including the root-scale value, I calculated the coefficient of determination, r^2, obtained from the simple linear regression of observed vs. model predicted coral cover for every reef in the AIMS LTMP with at least 10 observations (n=48) vs. my models' predicted coral cover (rescaled to match the maximum coral cover observed for that reef). Then, summarising the distribution of r^2-values for each parameter combination in terms of the median, 2.5th, and 97.5th percentiles, I determined the 'optimal' parameter settings based on the parameter combinations producing the highest median r^2, as in the previous section.

I determined the 'optimal' value of the root-scale parameter – i.e. the optimal value of a within the equation: $z_i = [DHWcrit_i]^{1/a}$, where *DHWcrit* is the threshold at which individual i succumbs to heat stress and z_i is the phenotype of individual i that is determined by their genotype and environment component of genotype – as 2.5 (Table C2.1). Similar to the previous section, models tended to over-predict coral cover between 2000-2014 (Fig. C2.5 and C2.6) but overall performed relatively well in predicting actual coral cover, with the median r^2 value being near 40% for the best supported parameter set (Fig. C2.7). This parameter set used an intermediate $\bar{g}$ starting value and scored a higher median r^2 at a root-scale of 2.5, and was also near-optimal using a root-scale value of 2 (i.e. square root) for DHW-limited fecundity vs. 3 (i.e. cubic root) if there was no DHW-limited fecundity (Fig. C2.7, C2.8, Table C2.1). The optimal heritability in the model was between 0.2 and 0.3 (Fig. C2.8, Table C2.1), with slightly more support for the latter. Interestingly, heritability had little to no effect on hindcast outcomes except when starting at relatively low initial genotype values (Fig. 2.10).

In all future simulations, I used the optimal parameter settings from Table C2.1. Thus, phenotype is determined by the 2.5th root of an individual's critical DHW threshold:

$$z_i = [DHWcrit_i]^{1/2.5}$$

However, for future simulations, I also investigated the effect of varying heritability (h^2), proportional settlement (q), DHW-limited fecundity either on or off, and with either constant or degrading genetic variance.

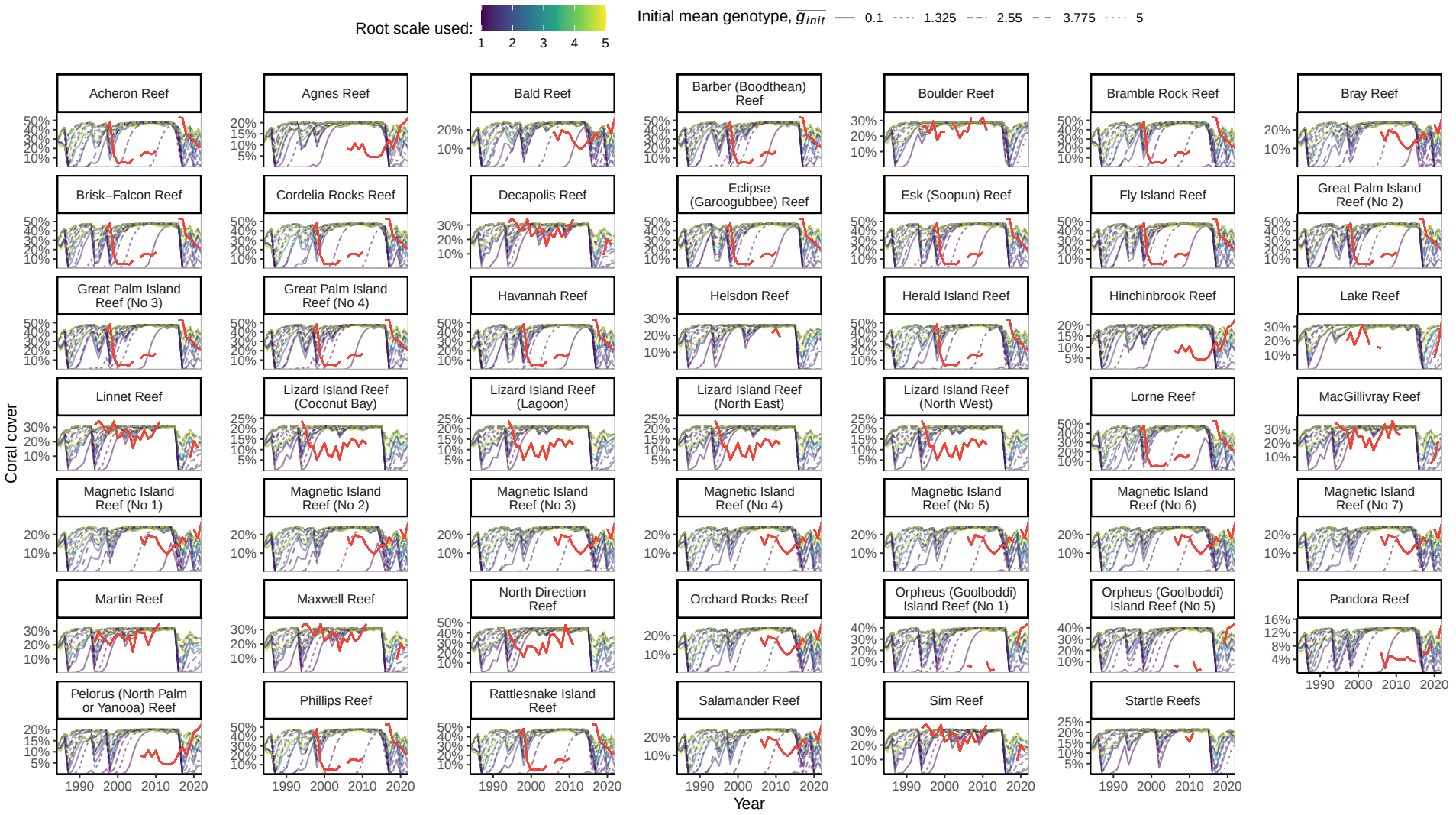
Root scale used:
1 2 3 4 5
Initial mean genotype, $\overline{g_{init}}$ 0.1 1.325 2.55 3.775 5
Acheron Reef
Agnes Reef
Bald Reef
Barber (Boodthean) Reef
Boulder Reef
Bramble Rock Reef
Bray Reef
Brisk–Falcon Reef
Cordelia Rocks Reef
Decapolis Reef
Eclipse (Garoogubbee) Reef
Esk (Soopun) Reef
Fly Island Reef
Great Palm Island Reef (No 2)
Great Palm Island Reef (No 3)
Great Palm Island Reef (No 4)
Havannah Reef
Helsdon Reef
Herald Island Reef
Hinchinbrook Reef
Lake Reef
Linnet Reef
Lizard Island Reef (Coconut Bay)
Lizard Island Reef (Lagoon)
Lizard Island Reef (North East)
Lizard Island Reef (North West)
Lorne Reef
MacGillivray Reef
Magnetic Island Reef (No 1)
Magnetic Island Reef (No 2)
Magnetic Island Reef (No 3)
Magnetic Island Reef (No 4)
Magnetic Island Reef (No 5)
Magnetic Island Reef (No 6)
Magnetic Island Reef (No 7)
Martin Reef
Maxwell Reef
North Direction Reef
Orchard Rocks Reef
Orpheus (Goolboddi) Island Reef (No 1)
Orpheus (Goolboddi) Island Reef (No 5)
Pandora Reef
Pelorus (North Palm or Yanooa) Reef
Phillips Reef
Rattlesnake Island Reef
Salamander Reef
Sim Reef
Startle Reefs
Coral cover
Year
1990 2000 2010 2020

3269

Fig. C2.5. Predicted (purple, green, and yellow lines) vs. observed (red lines) percent coral cover across 48 reefs from the AIMS LTMP dataset. Predicted coral cover has been rescaled to more closely match the max coral cover observed at each reef. Different-coloured predicted lines represent different DHWcrit scales assumed for the genotype to evolve upon; either arithmetic or normal scale ("norm", in purple), square-root scale ("sqrt", in green), or the natural logarithm ("log", in yellow). Different patterned lines represent different magnitudes of initial starting mean genotype values (scale-dependent), from lower (1) to higher (5). All predicted data here use a proportional larval settlement of $q = 0.01$, heritability of $h^2 = 0.3$, and have DHW-limited fecundity turned on (optimal parameter settings, as per below).

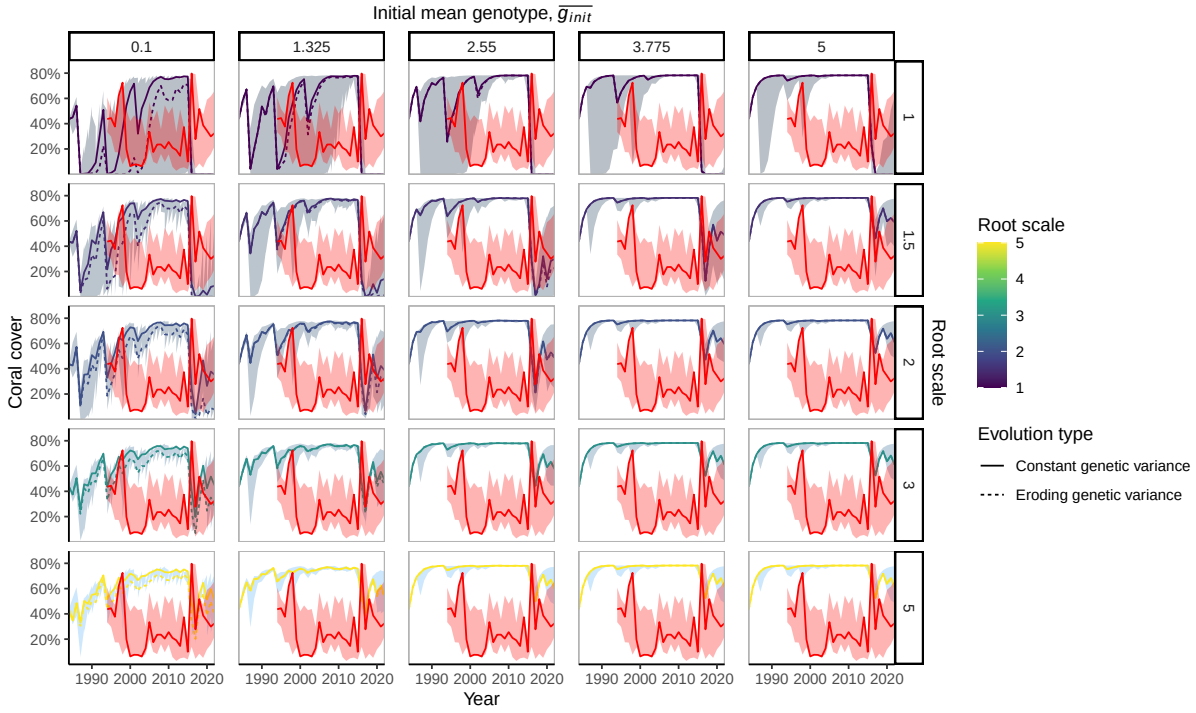

Fig. C2.6. Summarised percent coral cover (median and 95% CIs) from Fig. C2.1 predicted for various root-scales of DHWcrit evolution vs. observed coral cover (in red, rescaled). All predicted data here use a proportional larval settlement of $q = 0.01$, heritability of $h^2 = 0.3$, an initial mean genotype identical to that observed in Hughes et al. (2016), and have DHW-limited fecundity turned on (optimal parameter settings, as per below).

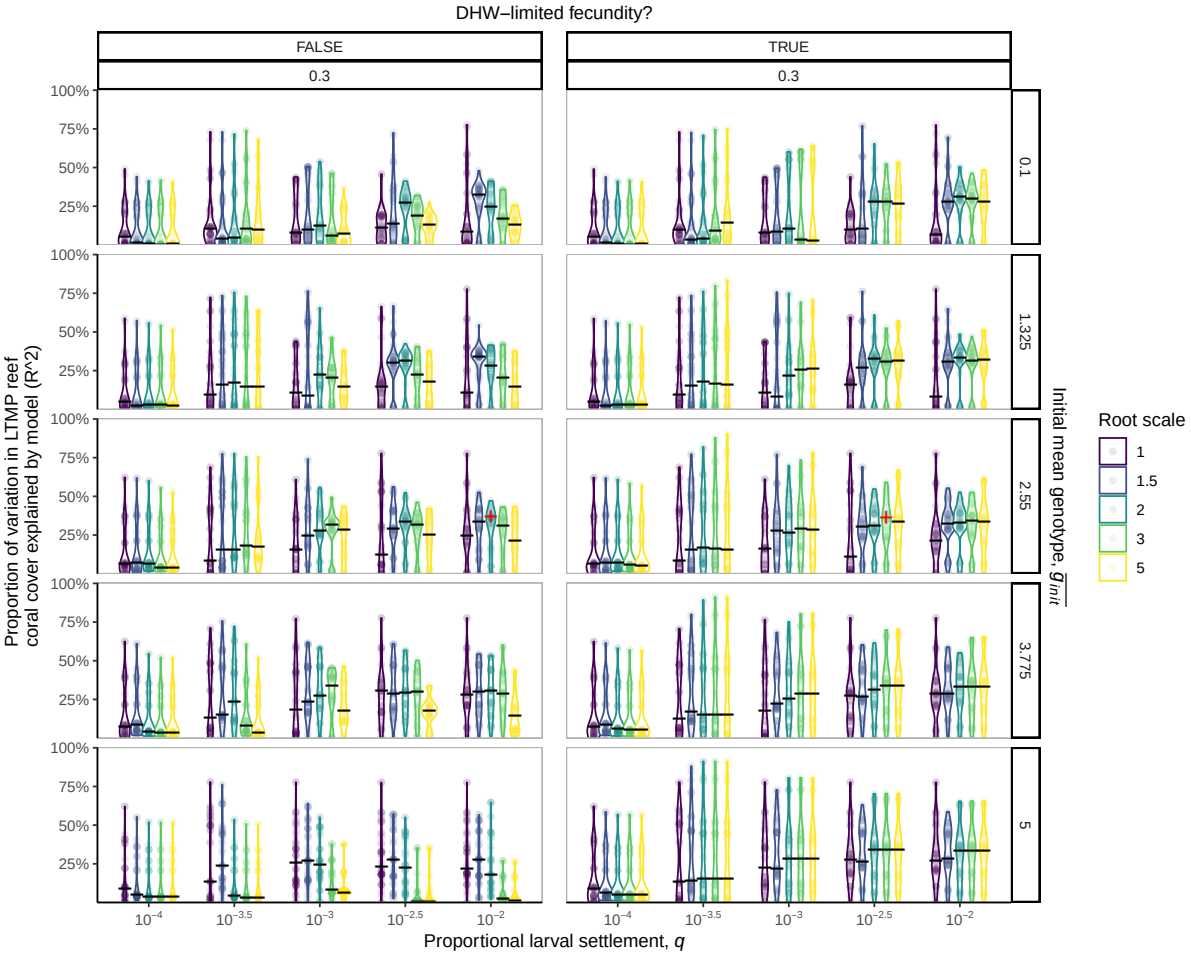

Fig. C2.7. Model accuracy across all 48 LTMP reefs and various parameter combinations, as assessed through model r^2 using the regression of observed ~ predicted coral cover. Points represent a single reef, with violin plots denoting the distribution of r^2 values and 'X's representing the median value of r^2. Red '+'s denote the highest median r^2 for simulations either with or without DHW-limited fecundity. All simulations use the root-scale DHWcrit transformation and heritability of $h^2 = 0.3$.

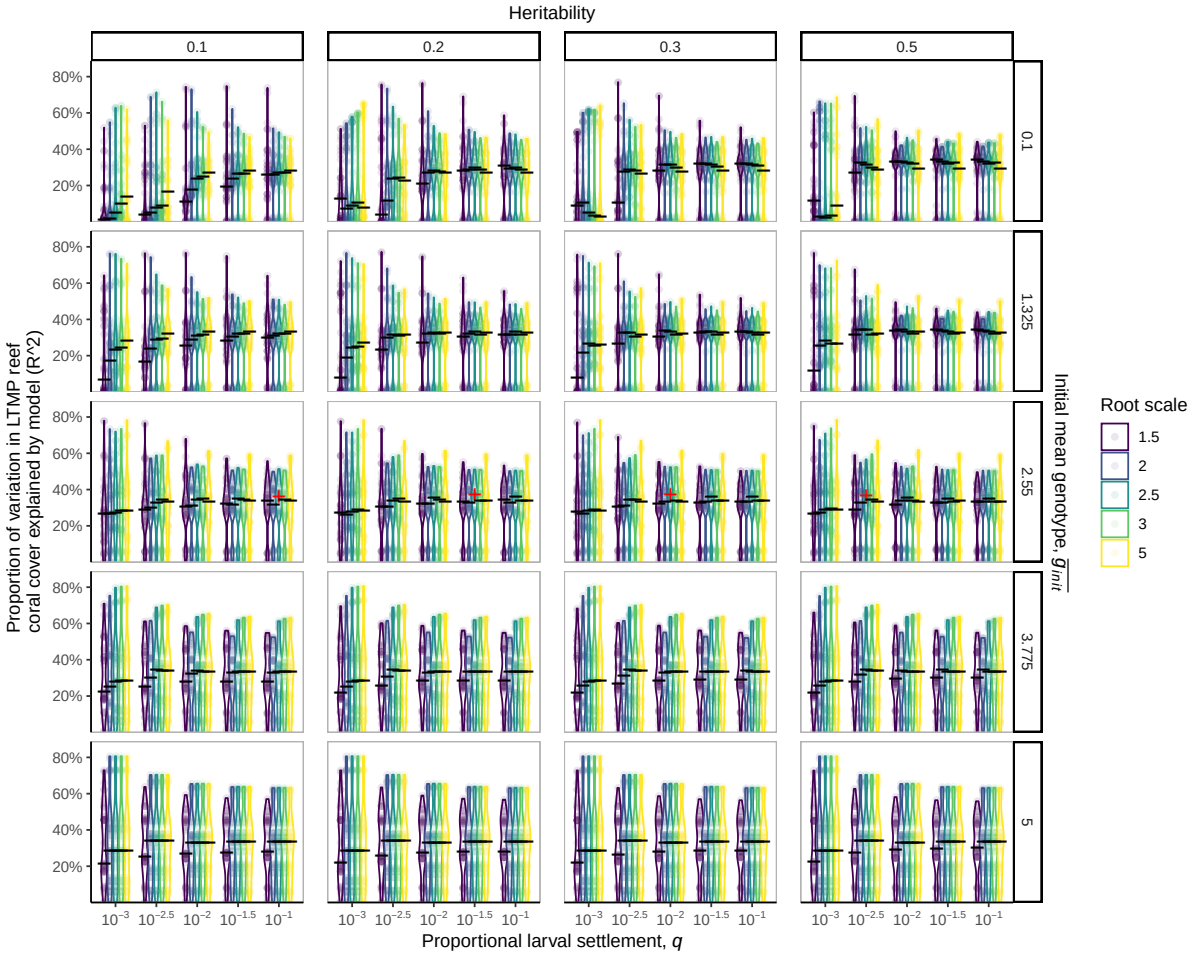

Fig. C2.8. Model accuracy across all 48 LTMP reefs and various parameter combinations, as assessed through model r^2 using the regression of observed ~ predicted coral cover. Points represent a single reef, with violin plots denoting the distribution of r^2 values and 'X's representing the median value of r^2. Red '+'s denote the highest median r^2 for simulations either with or without DHW-limited fecundity. All simulations have DHW-limited fecundity and constant genetic variance.

Table C2.1. Optimal parameter settings across varying narrow-sense heritability (h^2), validated using the AIMS LTMP dataset. The row in boldface indicates the highest median value for model r^2 between observed and predicted coral cover.

Optimal parameter settings for varying h^2 values							r^2 between observed vs. predicted coral cover		
Narrow-sense heritability, h^2	**Proportional larval settlement, q**	**Evolution type**	**Scale of evolution**	**Root-scale value, a**	**Initial genotype, $\overline{g}$**	**DHW-limited fecundity**	**Median**	**97.5% Lower CL**	**2.5% Upper CL**
0.1	0.1	Constant genetic variance	Root scale	2.5	2.55	Yes	0.353	0.0004	0.435
0.2	0.0316	Constant genetic variance	Root scale	2.5	2.55	Yes	0.363	0.0030	0.505
0.3	**0.01**	**Constant genetic variance**	**Root scale**	**2.5**	**2.55**	**Yes**	**0.363**	**0.0013**	**0.495**
0.4	0.00316	Constant genetic variance	Root scale	2.5	2.55	Yes	0.360	0.0010	0.544
0.5	0.00316	Constant genetic variance	Root scale	2.5	2.55	Yes	0.357	0.0008	0.593

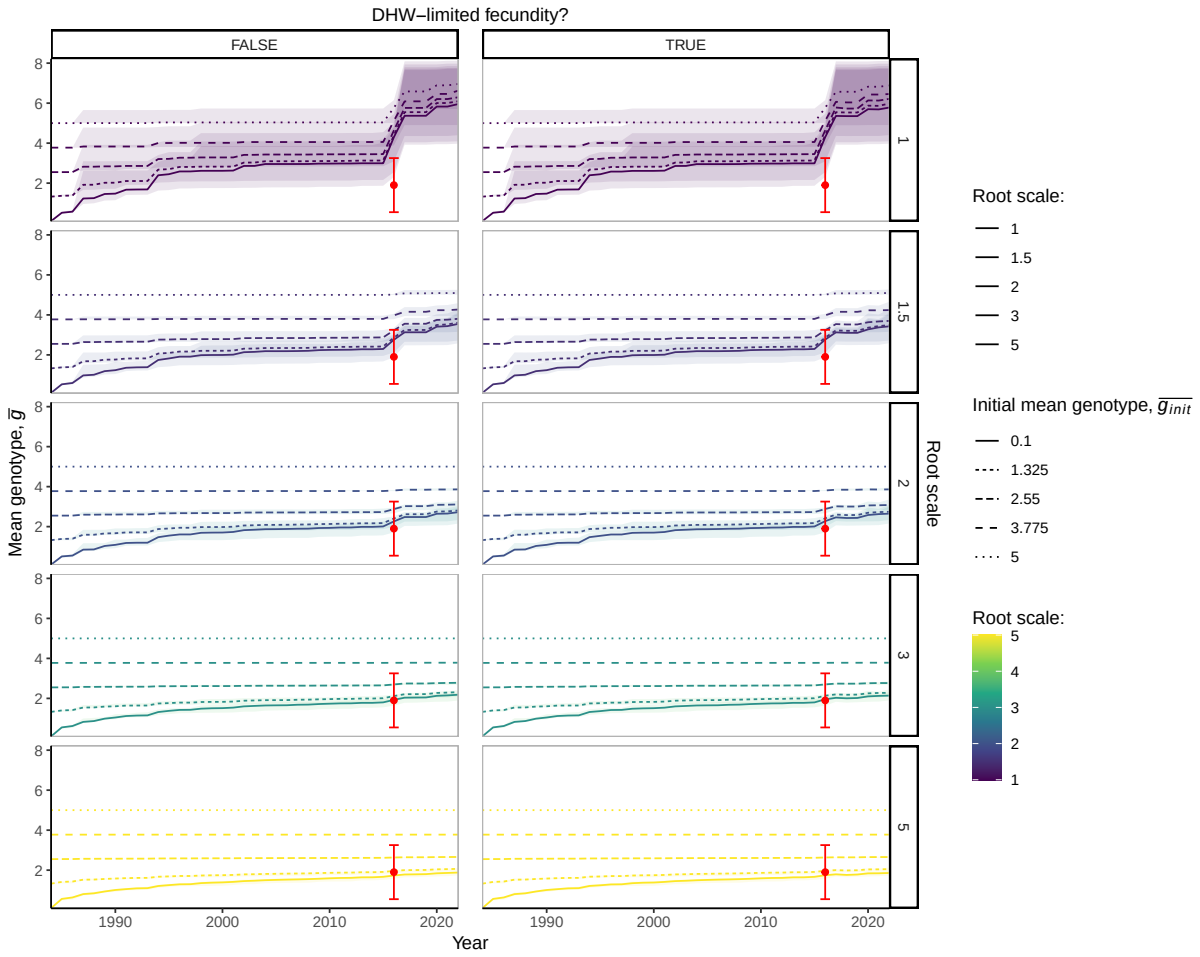

Fig. C2.9. Predicted evolution of genotypes using five different root-scale values ranging from 1–5 and five different magnitudes of starting mean genotypes (1 = mean genotype of 0.1, 5 = mean genotype equal to the red dot in each plot [scale-dependent], with even spacing on the given scale). Red points and error bars represent the 2.5th, 50th, and 97.5th quantiles from the exponential distribution of Hughes et al. (2018). All models were run using a settlement parameter, q = 0.01 and h^2 = 0.3.

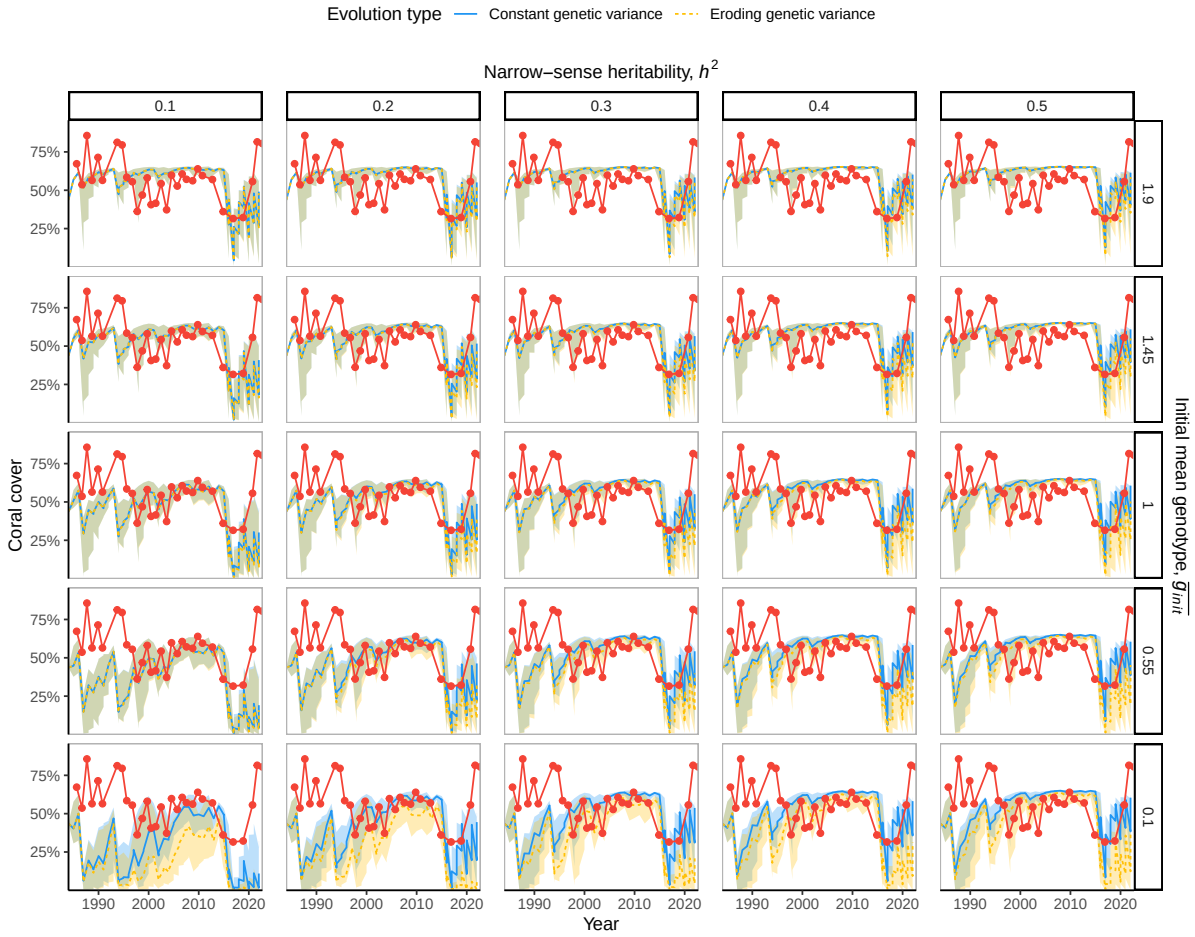

Fig. C2.10. Predicted coral cover for 156 historical model runs (blue and yellow lines) compared to Lizard Island coral cover patterns (red connected dots). Blue and yellow lines/uncertainties represent simulations with constant (maintained) vs. eroding genetic variance, respectively. Different heritabilities and initial genotypes are plotted as panels left-to-right and top-to-bottom, respectively. The coral covers depicted for Lizard Island are 4 times the original proportion coral cover reported to better match model coral covers. All models were run using a settlement parameter, $q = 0.01$.

C3: Simulating future heat stress

Using downscaled DHW predictions from McWhorter et al. (2022) (Fig. C3.1), a generalised additive mixed-effect model (GAMM) was fit to downscaled GBR grid data across 5 different climate models for each of the 4 future scenarios (Fig. C3.2). This GAMM predicted DHWs based on a scaled Student's t-distribution with inverse link, with SSP as a fixed effect, year as a smoother specific to each SSP (i.e. by = SSP, k = 4), a bivariate smooth of longitude and latitude to account for spatial autocorrelation, and used the specific climate model as a random effect. This produced the marginal mean DHW value (±SE) expected for each SSP scenario across time (Fig. C3.2), and allowed simulation of random DHW profiles using the R package *gratia*'s simulate() function. A single thermal stress profile is shown in Fig. C3.3 to highlight the highly variable nature of heat stress in future scenarios.

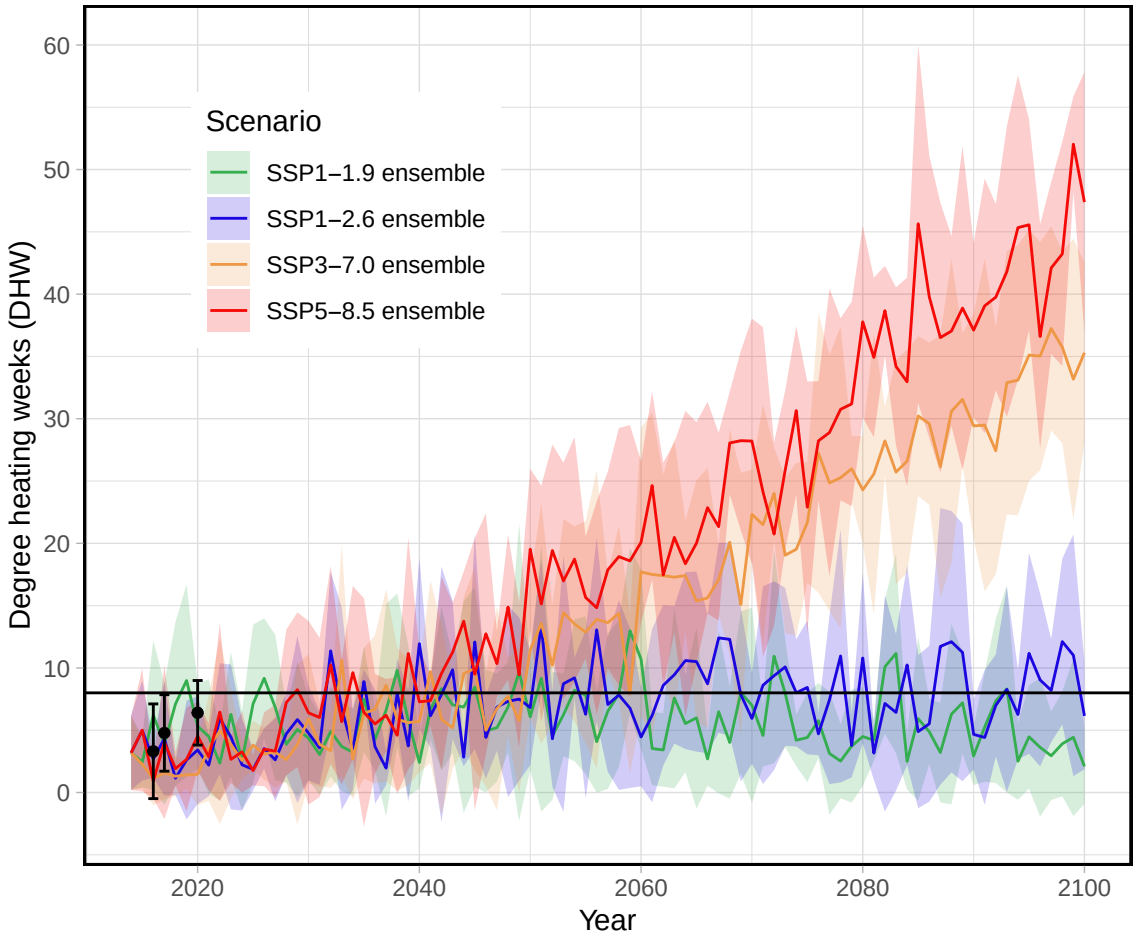

Fig. C3.1. Median heat stress observed across reef grid cells and 5 climate model predictions for 4 different climate scenarios ('shared socio-economic pathways' or SSPs) from McWhorter et al. (2022).

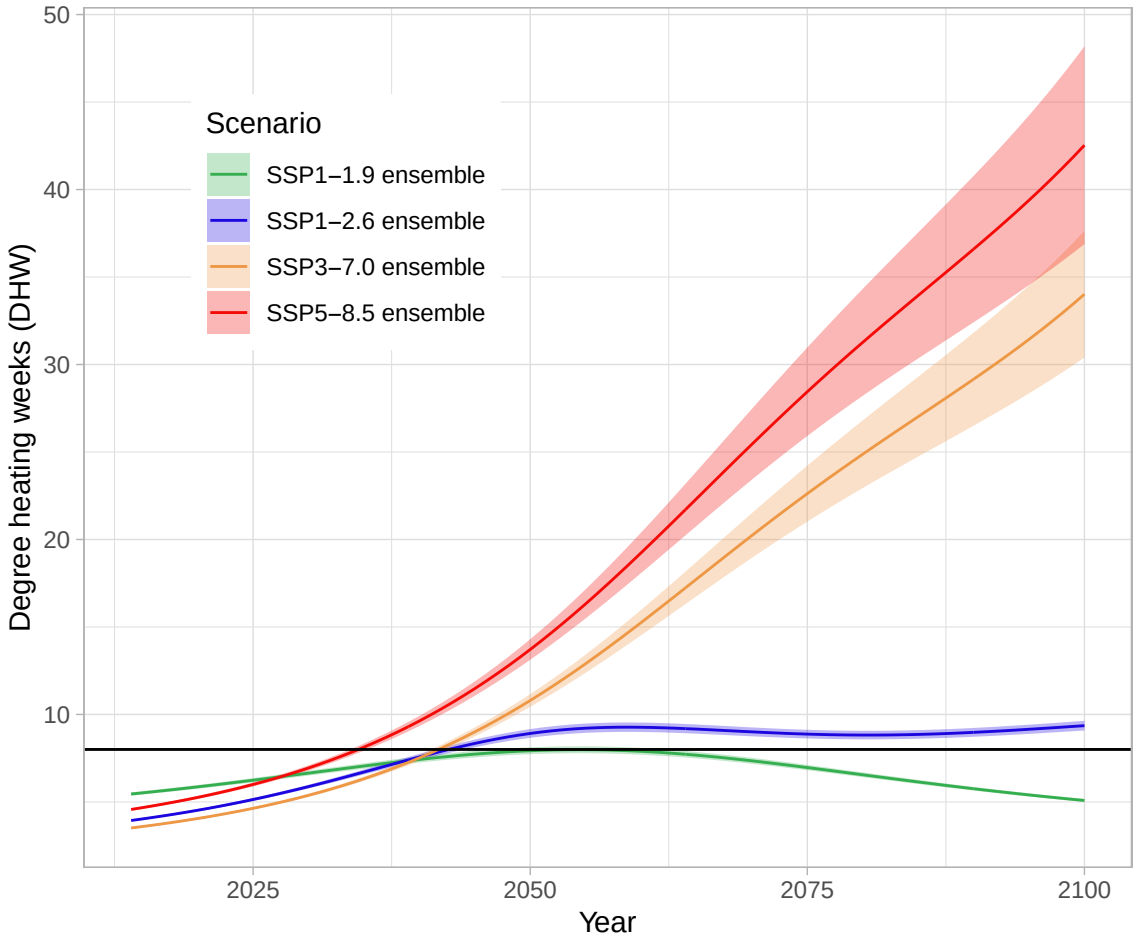

Fig. C3.2. Marginal mean DHWs across time and scenario, predicted by a generalised additive mixed model (GAMM) of future projected DHW values across the Great Barrier Reef and 5 different climate models, originally fit in McWhorter et al. (2022).

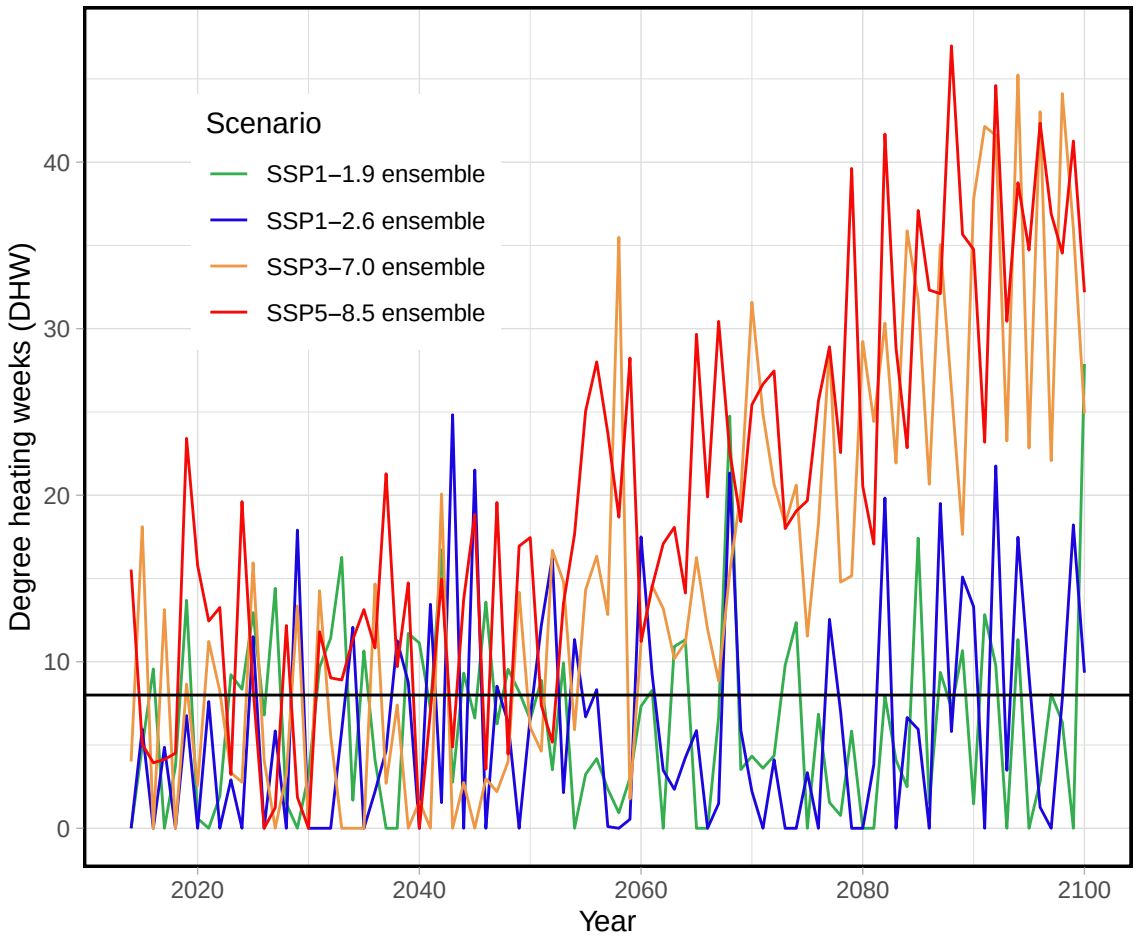

Fig. C3.3. A single thermal stress (DHW) profile sampled from the GAMM above using *gratia*'s `predicted_samples()` function while excluding the effect of longitude, latitude, and climate model.

C4: Model summary plots

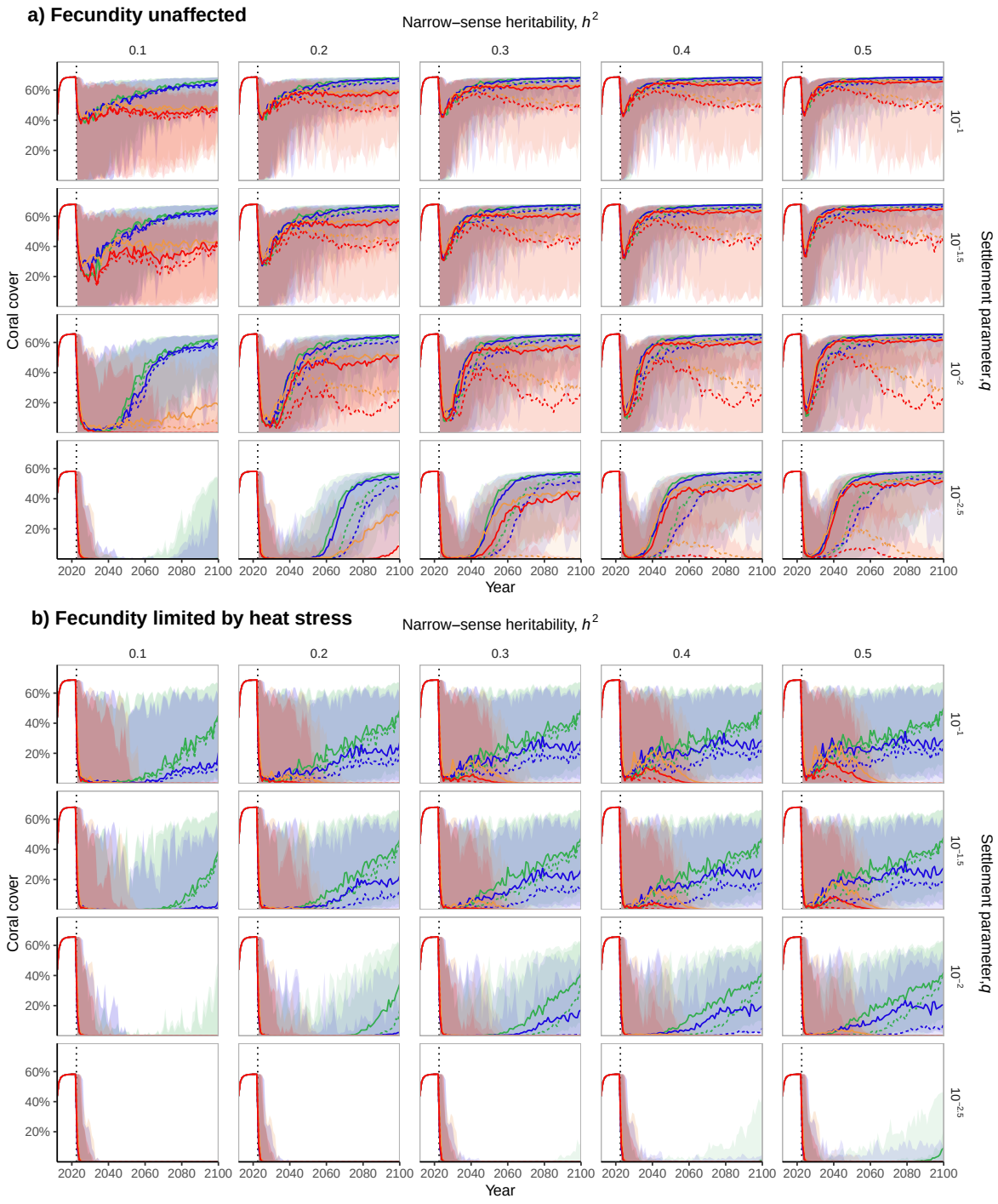

Fig. C4.1. Median proportion coral cover across future scenarios of heat stress (100 unique accumulated heat stress profiles given in degree heating weeks or DHW), with fecundity either (a) unaffected by heat stress or (b) limited by heat stress. Plots from left to right represent increasingly heritable thermal tolerance, while proportional larval settlement decreases from top to bottom. Colour represent four possible shared socio-economic pathways (SSP) of future heat stress. In order of

increasing future carbon emissions: SSP1-1.9 (+1.5°C) in green, SSP1-2.6 (+2.0°C) in blue, SSP3-7.0 in orange, and SSP5-8.5 in red. Solid lines represent model runs where genetic variance is maintained and constant while dashed lines represent runs with genetic variance being allowed to erode with selection. Shaded uncertainty regions represent 95% confidence intervals for each parameter combination, calculated using the percentile method. The onset of predicted future heat stress occurs in the year 2023 for all simulations (vertical black dotted line).

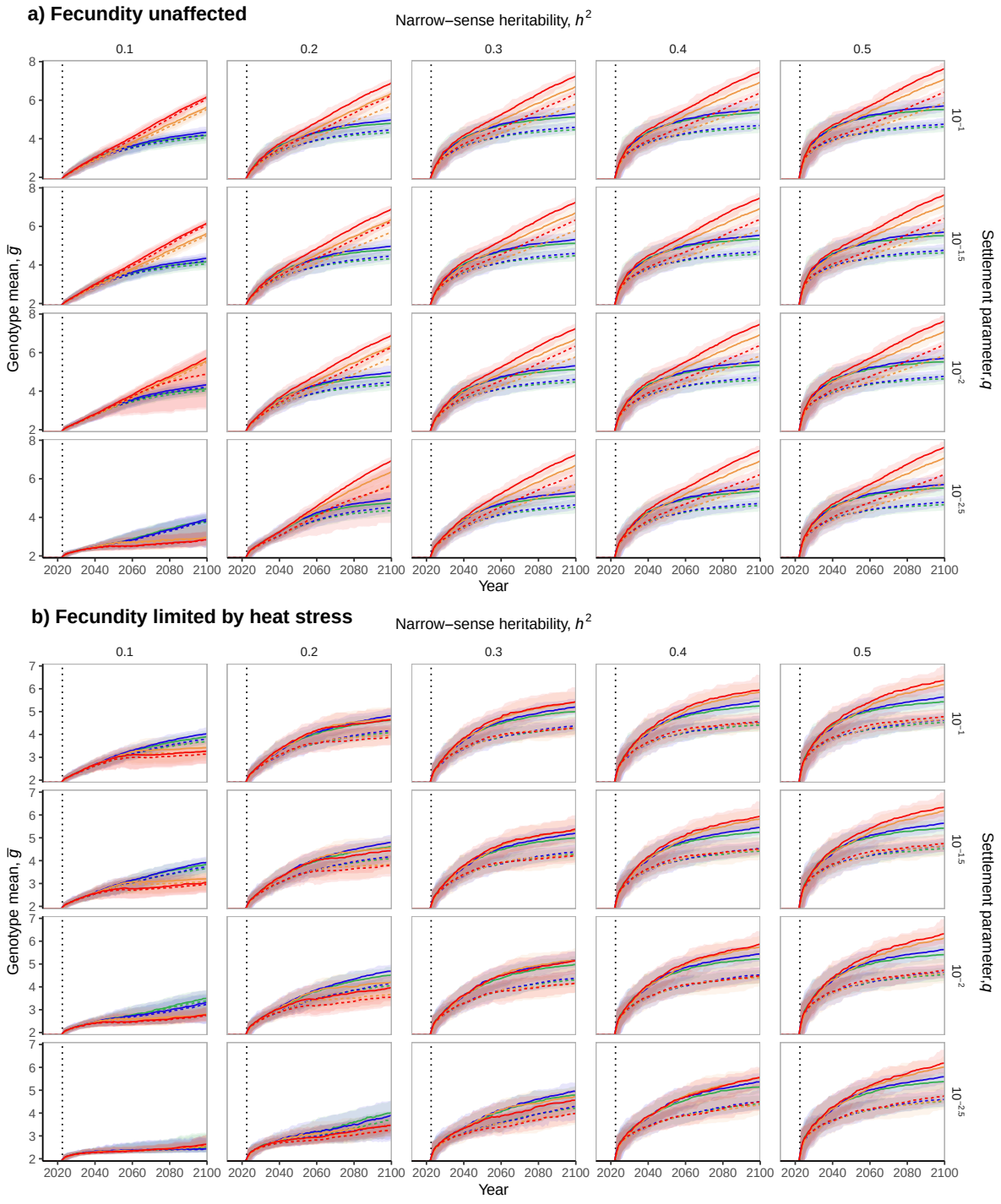

Fig. C4.2. Median mean genotype ($\bar{g}$) across future scenarios of heat stress (100 unique accumulated heat stress profiles given in degree heating weeks or DHW), with fecundity either (a) unaffected by heat stress or (b) limited by heat stress. Plots from left to right represent increasingly heritable thermal tolerance, while proportional larval settlement decreases from top to bottom. Colour represent four possible shared socio-economic pathways (SSP) of future heat stress. In order of increasing future carbon emissions: SSP1-1.9 (+1.5°C) in green, SSP1-2.6 (+2.0°C) in blue, SSP3-7.0 in orange, and SSP5-8.5 in red. Solid lines represent model runs where genetic variance is maintained and constant while dashed lines represent runs with genetic variance being allowed to erode with selection. Shaded uncertainty regions represent 95% confidence intervals for each parameter combination, calculated using the percentile method. The onset of predicted future heat stress occurs in the year 2023 for all simulations (vertical black dotted line).

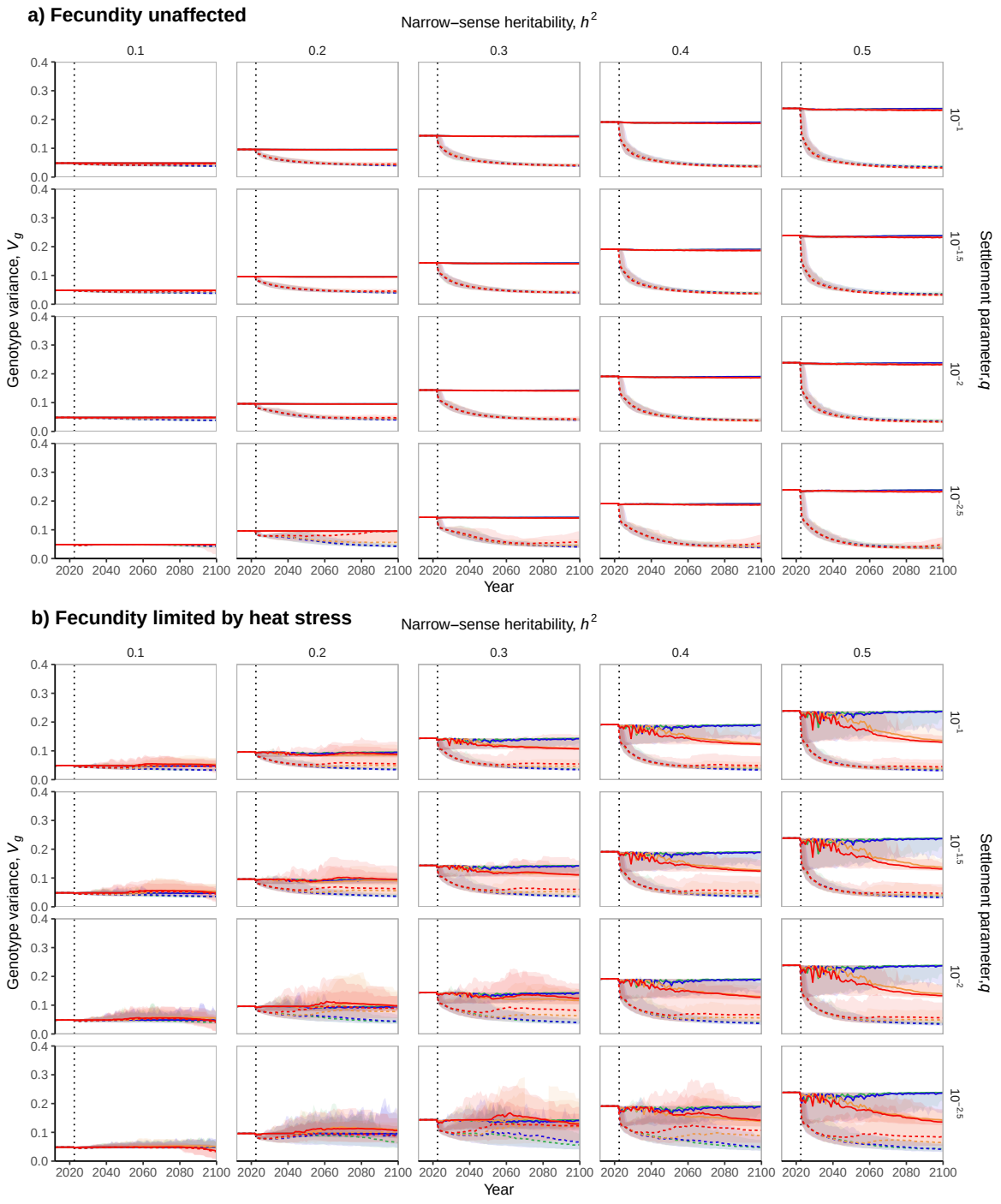

Fig. C4.3. Median genotypic variance (V_g) across future scenarios of heat stress (100 unique accumulated heat stress profiles given in degree heating weeks or DHW), with fecundity either (a) unaffected by heat stress or (b) limited by heat stress. Plots from left to right represent increasingly heritable thermal tolerance, while proportional larval settlement decreases from top to bottom. Colour represent four possible shared socio-economic pathways (SSP) of future heat stress. In order of

increasing future carbon emissions: SSP1-1.9 (+1.5°C) in green, SSP1-2.6 (+2.0°C) in blue, SSP3-7.0 in orange, and SSP5-8.5 in red. Solid lines represent model runs where genetic variance is maintained and constant while dashed lines represent runs with genetic variance being allowed to erode with selection. Shaded uncertainty regions represent 95% confidence intervals for each parameter combination, calculated using the percentile method. The onset of predicted future heat stress occurs in the year 2023 for all simulations (vertical black dotted line). Note that for high-emissions scenarios with DHW-limited fecundity (red and orange lines in bottom panels), no offspring tend to be produced past a certain point, leading to genetic variance being entirely determined by adults and thus deviating from the constant values expected.

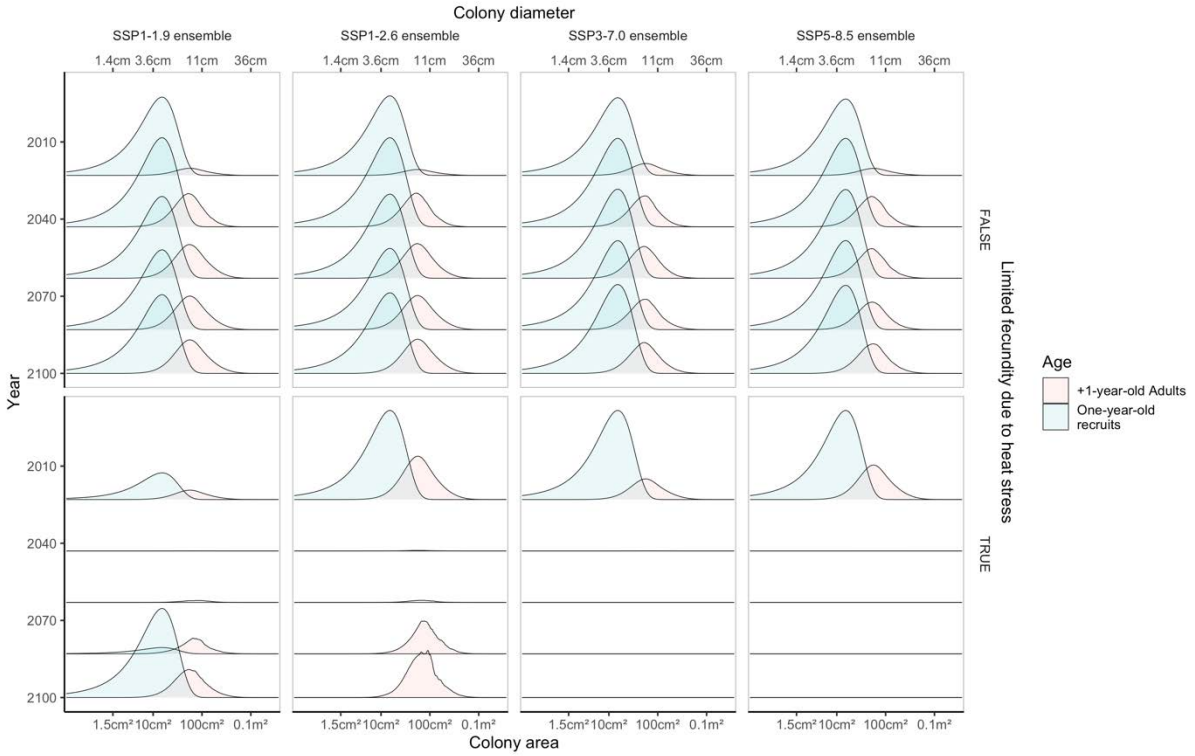

Fig. C4.4. Median size distribution across time for each SSP scenario (n=100 unique heat stress profiles), with fecundity either (a) unaffected by heat stress or (b) limited by heat stress. All models depicted use constant genetic variance, heritability of $h^2 = 0.3$ and proportional larval settlement of $q = 0.01$.

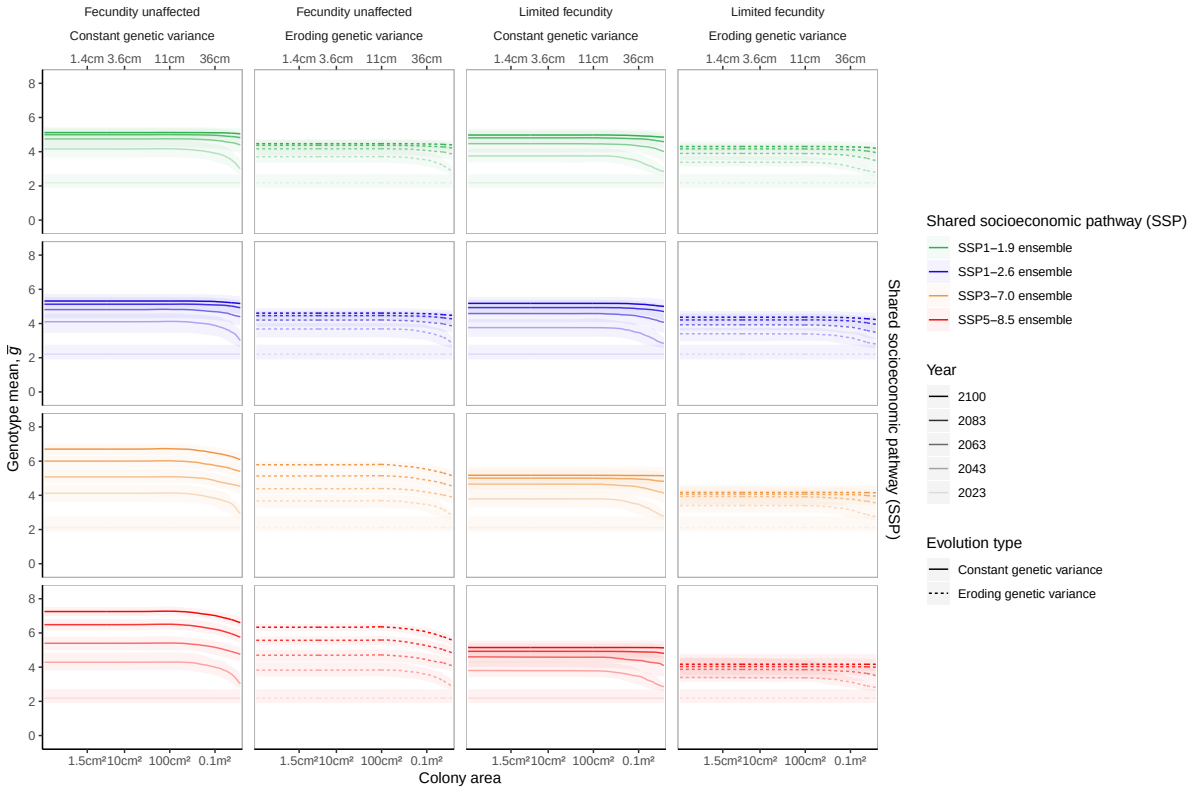

Fig. C4.5. Median mean genotype ($\bar{g}$) across coral sizes at the end of each SSP scenario (n=100 unique heat stress profiles), with fecundity either (a) unaffected by heat stress or (b) limited by heat stress. All models depicted use constant genetic variance, heritability of $h^2 = 0.3$ and proportional larval settlement of $q = 0.01$. Straight lines indicate all sizes share similar genotypes, while curved lines indicate different genotypes across sizes and dampened evolution due to size demography.

References List

Abram NJ, McGregor H V., Tierney JE, Evans MN, McKay NP, Kaufman DS, Thirumalai K, Martrat B, Goosse H, Phipps SJ, Steig EJ, Kilbourne KH, Saenger CP, Zinke J, Leduc G, Addison JA, Mortyn PG, Seidenkrantz MS, Sicre MA, Selvaraj K, Filipsson HL, Neukom R, Gergis J, Curran MAJ, Von Gunten L (2016) Early onset of industrial-era warming across the oceans and continents. Nature 536:411–418

Abrego D, Van Oppen MJH, Willis BL (2009) Onset of algal endosymbiont specificity varies among closely related species of *Acropora* corals during early ontogeny. Mol Ecol 18:3532–3543

van Aert RCM, Jackson D (2019) A new justification of the Hartung-Knapp method for random-effects meta-analysis based on weighted least squares regression. Res Synth Methods 10:515–527

Ahrens CW, Andrew ME, Mazanec RA, Ruthrof KX, Challis A, Hardy G, Byrne M, Tissue DT, Rymer PD (2020) Plant functional traits differ in adaptability and are predicted to be differentially affected by climate change. Ecol Evol 10:232–248

AIMS (2023) Long-Term Monitoring Program Annual Summary Reports of Coral Reef Condition 2006-2023. https://www.aims.gov.au/research-topics/monitoring-and-discovery/monitoring-great-barrier-reef/reef-reports-hub [accessed 2023-09-28]

AIMS (2022) Continued coral recovery leads to 36-year highs across two-thirds of the Great Barrier Reef; Annual Summary Report Of Coral Reef Condition. https://www.aims.gov.au/monitoring-great-barrier-reef/gbr-condition-summary-2021-22 [accessed 2023-09-28]

Allee WC (1931) Animal aggregations, a study in general sociology. University of Chicago Press, Chicago

Álvarez-Noriega M, Baird AH, Dornelas M, Madin JS, Cumbo VR, Connolly SR (2016) Fecundity and the demographic strategies of coral morphologies. Ecology 97:3485–3493

Angilletta Jr. MJ (2009) Thermal Adaptation: A Theoretical and Empirical Synthesis. Oxford University Press, Oxford. doi:10.1093/acprof:oso/9780198570875.001.1

Archambault JM, Cope WG, Kwak TJ (2018) Chasing a changing climate: Reproductive and dispersal traits predict how sessile species respond to global warming. Divers Distrib 24:880–891

van Asch M, Salis L, Holleman LJM, Van Lith B, Visser ME (2013) Evolutionary response of the egg hatching date of a herbivorous insect under climate change. Nat Clim Chang 3:244–248

Bachman SD, Kleypas JA, Erdmann M, Setyawan E (2022) A global atlas of potential thermal refugia for coral reefs generated by internal gravity waves. Front Mar Sci 9:1–13

Baird AH, Guest JR, Willis BL (2009) Systematic and biogeographical patterns in the reproductive biology of scleractinian corals. Annu Rev Ecol Evol Syst 40:551–571

Baird AH, Marshall PA (2002) Mortality, growth and reproduction in scleractinian corals following bleaching on the Great Barrier Reef. Mar Ecol Prog Ser 237:133–141

Bairos-Novak KR, Hoogenboom MO, van Oppen MJH, Connolly SR (2021) Coral adaptation to climate change: Meta-analysis reveals high heritability across multiple traits. Glob Chang Biol 27:5694–5710

Baker KG, Radford DT, Evenhuis C, Kuzhiumparam U, Ralph PJ, Doblin MA (2018) Thermal niche evolution of functional traits in a tropical marine phototroph. J Phycol 54:799–810

Ban SS, Graham NAJ, Connolly SR (2014) Evidence for multiple stressor interactions and effects on coral reefs. Glob Chang Biol 20:681–697

Barfield SJ, Aglyamova G V., Bay LK, Matz M V. (2018) Contrasting effects of *Symbiodinium* identity on coral host transcriptional profiles across latitudes. Mol Ecol 27:3103–3115

Baria MVB, Dela Cruz DW, Villanueva RD, Guest JR (2012) Spawning of three-year-old *Acropora millepora* corals reared from larvae in northwestern philippines. Bull Mar Sci 88:61–62

Barshis DJ, Ladner JT, Oliver TA, Seneca FO, Traylor-Knowles N, Palumbi SR (2013) Genomic basis for coral resilience to climate change. Proc Natl Acad Sci 110:1387–1392

Barton NH, Etheridge AM, Véber A (2017) The infinitesimal model: Definition, derivation, and implications. Theor Popul Biol 118:50–73

Baskett ML, Fabina NS, Gross K (2014) Response diversity can increase ecological resilience to disturbance in coral reefs. Am Nat 184:E16–E31

Baskett ML, Gaines SD, Nisbet RM (2009) Symbiont diversity may help coral reefs survive moderate climate change. Ecol Appl 19:3–17

Baskett ML, Salomon AK (2010) Recruitment facilitation can drive alternative states on temperate

reefs. Ecology 91:1763–1773

Bassar RD, Letcher BH, Nislow KH, Whiteley AR (2016) Changes in seasonal climate outpace compensatory density-dependence in eastern brook trout. Glob Chang Biol 22:577–593

Baums IB, Devlin-Durante MK, Polato NR, Xu D, Giri S, Altman NS, Ruiz D, Parkinson JE, Boulay JN (2013) Genotypic variation influences reproductive success and thermal stress tolerance in the reef building coral, *Acropora palmata*. Coral Reefs 32:703–717

Bay RA, Palumbi SR (2014) Multilocus adaptation associated with heat resistance in reef-building corals. Curr Biol 24:2952–2956

Bay RA, Palumbi SR (2015) Rapid acclimation ability mediated by transcriptome changes in reef-building corals. Genome Biol Evol 7:1602–1612

Bay RA, Palumbi SR (2017) Transcriptome predictors of coral survival and growth in a highly variable environment. Ecol Evol 7:4794–4803

Bay RA, Rose N, Barrett R, Bernatchez L, Ghalambor CK, Lasky JR, Brem RB, Palumbi SR, Ralph P (2017a) Predicting responses to contemporary environmental change using evolutionary response architectures. Am Nat 189:463–473

Bay RA, Rose NH, Logan CA, Palumbi SR (2017b) Genomic models predict successful coral adaptation if future ocean warming rates are reduced. Sci Adv 3:e1701413

Bayliss SLJ, Scott ZR, Coffroth MA, TerHorst CP (2019) Genetic variation in *Breviolum antillogorgium*, a coral reef symbiont, in response to temperature and nutrients. Ecol Evol 1–11

BBC (2020) Great Barrier Reef suffers third mass bleaching in five years. https://www.bbc.com/news/world-australia-52043554 [accessed 2023-09-28]

Bellantuono AJ (2013) Acclimatization of the tropical reef coral *Acropora millepora* to hyperthermal stress. PhD Thesis, Florida International University. doi:10.25148/etd.FI13120905

Bellwood DR (1996) Production and reworking of sediment by parrotfishes (family Scaridae) on the Great Barrier Reef, Australia. Mar Biol 125:795–800

Bena C, van Woesik R (2004) The impact of two bleaching events on the survival of small coral colonies (Okinawa, Japan). Bull Mar Sci 75:115–125

Berkelmans R, Van Oppen MJH (2006) The role of zooxanthellae in the thermal tolerance of corals: A

3475 “nugget of hope” for coral reefs in an era of climate change. Proc R Soc B Biol Sci 273:2305–
3476 2312
3477 Beverton RJH, Holt SJ (1957) On the dynamics of exploited fish populations, Fishery Investigations
3478 Series II Volume XIX.
3479 Bodensteiner BL, Agudelo-Cantero GA, Arietta AZA, Gunderson AR, Muñoz MM, Refsnider JM,
3480 Gangloff EJ (2020) Thermal adaptation revisited: How conserved are thermal traits of reptiles
3481 and amphibians? J Exp Zool Part A Ecol Integr Physiol 335:173–194
3482 Bogdziewicz M, Kelly D, Thomas PA, Lageard JGA, Hacket-Pain A (2020) Climate warming disrupts
3483 mast seeding and its fitness benefits in European beech. Nat Plants 6:88–94
3484 Bonin MC (2012) Specializing on vulnerable habitat: *Acropora* selectivity among damselfish recruits
3485 and the risk of bleaching-induced habitat loss. Coral Reefs 31:287–297
3486 Bonin MC, Munday PL, McCormick MI, Srinivasan M, Jones GP (2009) Coral-dwelling fishes
3487 resistant to bleaching but not to mortality of host corals. Mar Ecol Prog Ser 394:215–222
3488 Bouchard Jr. T (2013) The Wilson effect: The increase in heritability of IQ with age. Twin Res Hum
3489 Genet 16:923–930
3490 Bramanti L, Iannelli M, Fan TY, Edmunds PJ (2015) Using demographic models to project the effects
3491 of climate change on scleractinian corals: *Pocillopora damicornis* as a case study. Coral Reefs
3492 34:505–515
3493 Brander LM, Van Beukering P, Cesar HSJ (2007) The recreational value of coral reefs: A meta-
3494 analysis. Ecol Econ 63:209–218
3495 Bridge TCL, Hughes TP, Guinotte JM, Bongaerts P (2013) Call to protect all coral reefs. Nat Clim
3496 Chang 3:528–530
3497 Bruno JF, Ellner SP, Vu I, Kim K, Harvell CD (2011) Impacts of *Aspergillosis* on sea fan coral
3498 demography: Modeling a moving target. Ecol Monogr 81:123–139
3499 Bubliy OA, Loeschcke V (2002) Effect of low stressful temperature on genetic variation of five
3500 quantitative traits in *Drosophila melanogaster*. Heredity 89:70–75
3501 Buerger P, Alvarez-Roa C, Coppin CWC, Pearce SLS, Chakravarti LJ, Oakeshott JGJ, Edwards OR,
3502 van Oppen MJH (2020) Heat-evolved microalgal symbionts increase coral bleaching tolerance.

Sci Adv 6:eaba2498

Burger R (1995) Evolution and extinction in a changing environment: A quantitative-genetic analysis. Evolution 49:151

Burke L, Reytar K, Spalding M, Perry A (2011) Reefs at Risk Revisited. World Resour Inst https://www.wri.org/research/reefs-risk-revisited [accessed 2023-09-28]

Burke S, Pottier P, Lagisz M, Macartney E, Ainsworth T, Drobniak S, Nakagawa S (2023) The impact of rising temperatures on the prevalence of coral diseases and its predictability: A global meta-analysis. Ecol Lett 26:1466–1481

Burnham KP, Anderson DR (2004) Multimodel inference: Understanding AIC and BIC in model selection. Sociol Methods Res 33:261–304

Cameron KA, Harrison PL (2020) Density of coral larvae can influence settlement, post-settlement colony abundance and coral cover in larval restoration. Sci Rep 10:1–11

Cant J, Cook KM, Reimer JD, Mezaki T, Nakamura M, Flaherty CO (2022a) Transient amplification enhances the persistence of tropicalising coral assemblages in marginal high-latitude environments. Ecography 2022:e06156

Cant J, Reimer JD, Sommer B, Cook K, Kim SW, Sims CA, Mezaki T, O'Flaherty C, Brooks M, Malcolm HA, Pandolfi JM, Salguero-Gómez R, Beger M (2023) Coral assemblages at higher latitudes favour short-term potential over long-term performance. Ecology 104:e4138

Cant J, Salguero-Gómez R, Beger M (2022b) Transient demographic approaches can drastically expand the toolbox of coral reef science. Coral Reefs 885–896

Cant J, Salguero-Gómez R, Kim SW, Sims CA, Sommer B, Brooks M, Malcolm HA, Pandolfi JM, Beger M (2021) The projected degradation of subtropical coral assemblages by recurrent thermal stress. J Anim Ecol 90:233–247

Cantin NE, Van Oppen MJH, Willis BL, Mieog JC, Negri AP (2009) Juvenile corals can acquire more carbon from high-performance algal symbionts. Coral Reefs 28:405–414

Capon SJ, Stewart-Koster B, Bunn SE (2021) Future of freshwater ecosystems in a 1.5°C warmer world. Front Environ Sci 9:1–7

Carlon DB, Budd AF, Lippé C, Andrew RL (2011) The quantitative genetics of incipient speciation:

Heritability and genetic correlations of skeletal traits in populations of diverging *Favia fragum* ecomorphs. Evolution 65:3428–3447

Carlot J, Kayal M, Lenihan HS, Brandl SJ, Casey JM, Adjeroud M, Cardini U, Merciere A, Espiau B, Barneche DR, Rovere A, Hédouin L, Parravicini V (2021) Juvenile corals underpin coral reef carbonate production after disturbance. Glob Chang Biol 27:2623–2632

Castañeda LE, Romero-Soriano V, Mesas A, Roff DA, Santos M (2019) Evolutionary potential of thermal preference and heat tolerance in *Drosophila subobscura*. J Evol Biol 32:818–824

Caswell H (2001) Matrix Population Models: Construction, Analysis and Interpretation. Sinauer Associates Inc., Sunderland, MA

Caswell H (2010) Reproductive value, the stable stage distribution, and the sensitivity of the population growth rate to changes in vital rates. Demogr Res 23:531–548

Chakravarti LJ, Beltran VH, van Oppen MJH (2017) Rapid thermal adaptation in photosymbionts of reef-building corals. Glob Chang Biol 23:4675–4688

Chakravarti LJ, van Oppen MJH (2018) Experimental evolution in coral photosymbionts as a tool to increase thermal tolerance. Front Mar Sci 5:227

Charmantier A, Garant D (2005) Environmental quality and evolutionary potential: Lessons from wild populations. Proc Biol Sci 275:1415–1425

Charmantier A, Perrins C, McCleery RH, Sheldon BC (2006a) Age-dependent genetic variance in a life-history trait in the mute swan. Proc R Soc B Biol Sci 273:225–232

Charmantier A, Perrins C, McCleery RH, Sheldon BC (2006b) Quantitative genetics of age at reproduction in wild swans: Support for antagonistic pleiotropy models of senescence. Proc Natl Acad Sci 103:6587–6592

Cheung MWM, Hock K, Skirving W, Mumby PJ (2021) Cumulative bleaching undermines systemic resilience of the Great Barrier Reef. Curr Biol 31:5835–5392

Chevin LM, Lande R, Mace GM (2010) Adaptation, plasticity, and extinction in a changing environment: Towards a predictive theory. PLoS Biol 8:e1000357

Childs DZ, Sheldon BC, Rees M (2016) The evolution of labile traits in sex- and age-structured populations. J Anim Ecol 85:329–342

3559 Chown SL, Jumbam KR, Sørensen JG, Terblanche JS (2009) Phenotypic variance, plasticity and
3560 heritability estimates of critical thermal limits depend on methodological context. Funct Ecol
3561 23:133–140
3562 Coffroth MA, Santos SR, Goulet TL (2001) Early ontogenetic expression of specificity in a cnidarian-
3563 algal symbiosis. Mar Ecol Prog Ser 222:85–96
3564 Coles SL, Bahr KD, Rodgers KS, May SL, McGowan AE, Tsang A, Bumgarner J, Han JH (2018)
3565 Evidence of acclimatization or adaptation in Hawaiian corals to higher ocean temperatures. PeerJ
3566 6:e5347
3567 Comte L, Olden JD (2017) Evolutionary and environmental determinants of freshwater fish thermal
3568 tolerance and plasticity. Glob Chang Biol 23:728–736
3569 Connell JH, Hughes TP, Wallace CC (1997) A 30-year study of coral abundance, recruitment, and
3570 disturbance at several scales in space and time. Ecol Monogr 67:461–488
3571 Conti-Jerpe IE, Thompson PD, Wai C, Wong M, Lina N, Duprey NN, Moynihan MA, Baker DM
3572 (2020) Trophic strategy and bleaching resistance in reef-building corals. Science 6:eaaz5443
3573 Cook RD, Weisberg S (1982) Residuals and influence in regression. Chapman and Hall, London
3574 Cornwall CE, Comeau S, Kornder NA, Perry CT, van Hooidonk R, DeCarlo TM, Pratchett MS,
3575 Anderson KD, Browne N, Carpenter R, Diaz-Pulido G, D'Olivo JP, Doo SS, Figueiredo J,
3576 Fortunato SAV, Kennedy E, Lantz CA, McCulloch MT, González-Rivero M, Schoepf V,
3577 Smithers SG, Lowe RJ (2021) Global declines in coral reef calcium carbonate production under
3578 ocean acidification and warming. Proc Natl Acad Sci 118:e2015265118
3579 Cornwell B, Armstrong K, Walker N, Lippert M, Nestor V, Golbuu Y, Palumbi SR (2021)
3580 Widespread variation in heat tolerance and symbiont load are associated with growth tradeoffs in
3581 the coral *Acropora hyacinthus* in Palau. eLife 10:1–15
3582 Coulson T, Kendall BE, Barthold J, Plard F, Schindler S, Ozgul A, Gaillard JM (2017) Modeling
3583 adaptive and nonadaptive responses of populations to environmental change. Am Nat 190:313–
3584 336
3585 Coulson T, Macnulty DR, Stahler DR, VonHoldt B, Wayne RK, Smith DW (2011) Modeling effects
3586 of environmental change on wolf population dynamics, trait evolution, and life history. Science

334:1275–1278

Coulson T, Potter T, Felmy A (2021) Predicting evolution over multiple generations in deteriorating environments using evolutionarily explicit Integral Projection Models. Evol Appl 14:2490–2501

Cropp R, Norbury J (2020) The potential for coral reefs to adapt to a changing climate - an eco-evolutionary modelling perspective. Ecol Modell 426:109038

dela Cruz DW, Harrison PL (2017) Enhanced larval supply and recruitment can replenish reef corals on degraded reefs. Sci Rep 7:1–13

Császár NBM, Ralph PJ, Frankham R, Berkelmans R, van Oppen MJH (2010) Estimating the potential for adaptation of corals to climate warming. PLoS One 5:e9751

Cunning R, Gillette P, Capo T, Galvez K, Baker AC (2015a) Growth tradeoffs associated with thermotolerant symbionts in the coral *Pocillopora damicornis* are lost in warmer oceans. Coral Reefs 34:155–160

Cunning R, Gillette P, Capo T, Galvez K, Baker AC (2015b) Growth tradeoffs associated with thermotolerant symbionts in the coral *Pocillopora damicornis* are lost in warmer oceans. Coral Reefs 34:155–160

Curnock MI, Marshall NA, Thiault L, Heron SF, Hoey J, Williams G, Taylor B, Pert PL, Goldberg J (2019) Shifts in tourists' sentiments and climate risk perceptions following mass coral bleaching of the Great Barrier Reef. Nat Clim Chang 9:535–541

D'Angelo C, Hume BCC, Burt J, Smith EG, Achterberg EP, Wiedenmann J (2015) Local adaptation constrains the distribution potential of heat-tolerant *Symbiodinium* from the Persian/Arabian Gulf. ISME J 9:2551–2560

Dajka JC, Wilson SK, Robinson JPW, Chong-Seng KM, Harris A, Graham NAJ (2019) Uncovering drivers of juvenile coral density following mass bleaching. Coral Reefs 38:637–649

van Dang K, Pierangelini M, Roberty S, Cardol P (2019) Alternative photosynthetic electron transfers and bleaching phenotypes upon acute heat stress in *Symbiodinium* and *Breviolum* spp. (Symbiodiniaceae) in culture. Front Mar Sci 6:1–10

Dansgaard AW, Clausen HB, Gundestrup N, Hammer CU, Johnsen SF, Reeh N (1982) A new Greenland deep ice core. Science 218:1273–1277

Davies SW, Scarpino S V., Pongwarin T, Scott J, Matz M V. (2015) Estimating trait heritability in highly fecund species. G3 Genes|Genomes|Genetics 5:2639–2645

Davis MB, Shaw RG, Etterson JR (2005) Evolutionary responses to changing climate. Ecology 86:1704–1714

De'Ath G, Fabricius KE, Sweatman H, Puotinen M (2012) The 27-year decline of coral cover on the Great Barrier Reef and its causes. Proc Natl Acad Sci 109:17995–17999

DeFilippo LB, McManus LC, Schindler DE, Pinsky ML, Colton MA, Fox HE, Tekwa EW, Palumbi SR, Essington TE, Webster MM (2022) Assessing the potential for demographic restoration and assisted evolution to build climate resilience in coral reefs. Ecol Appl 32:1–15

Depczynski M, Gilmour JP, Ridgway T, Barnes H, Heyward AJ, Holmes TH, Moore JAY, Radford BT, Thomson DP, Tinkler P, Wilson SK (2013) Bleaching, coral mortality and subsequent survivorship on a West Australian fringing reef. Coral Reefs 32:233–238

Diamond SE (2017) Evolutionary potential of upper thermal tolerance: Biogeographic patterns and expectations under climate change. Ann N Y Acad Sci 1389:5–19

Díaz-Almeyda EM, Prada C, Ohdera AH, Moran H, Civitello DJ, Iglesias-Prieto R, Carlo TA, Lajeunesse TC, Medina M (2017) Intraspecific and interspecific variation in thermotolerance and photoacclimation in *Symbiodinium* dinoflagellates. Proc R Soc B Biol Sci 284:20171767

Dietzel A, Bode M, Connolly SR, Hughes TP (2020) Long-term shifts in the colony size structure of coral populations along the Great Barrier Reef: Demographic change in Australia's corals. Proc R Soc B Biol Sci 287:20201432

Dietzel A, Bode M, Connolly SR, Hughes TP (2021a) The population sizes and global extinction risk of reef-building coral species at biogeographic scales. Nat Ecol Evol 5:663–669

Dietzel A, Connolly SR, Hughes TP, Bode M (2021b) The spatial footprint and patchiness of large-scale disturbances on coral reefs. Glob Chang Biol 27:4825–4838

Dilworth J, Caruso C, Kahkejian VA, Baker AC, Drury C (2021) Host genotype and stable differences in algal symbiont communities explain patterns of thermal stress response of *Montipora capitata* following thermal pre-exposure and across multiple bleaching events. Coral Reefs 40:151–163

Dixon AM, Forster PM, Heron SF, Stoner AMK, Beger M (2022) Future loss of local-scale thermal

refugia in coral reef ecosystems. PLOS Clim 1:e0000004

Dixon G, Davies S, Aglyamova G, Meyer E, Bay L, Matz M (2015) Genomic determinants of coral heat tolerance across latitudes. Science 348:2014–2016

Doak DF, Waddle E, Langendorf RE, Louthan AM, Isabelle Chardon N, Dibner RR, Keinath DA, Lombardi E, Steenbock C, Shriver RK, Linares C, Begoña Garcia M, Funk WC, Fitzpatrick SW, Morris WF, Peterson ML (2021) A critical comparison of integral projection and matrix projection models for demographic analysis. Ecol Monogr 91:e01447

Done T, Turak E, Wakeford M, DeVantier L, McDonald A, Fisk D (2007) Decadal changes in turbid-water coral communities at Pandora Reef: Loss of resilience or too soon to tell? Coral Reefs 26:789–805

Doney SC, Ruckelshaus M, Emmett Duffy J, Barry JP, Chan F, English CA, Galindo HM, Grebmeier JM, Hollowed AB, Knowlton N, Polovina J, Rabalais NN, Sydeman WJ, Talley LD (2012) Climate change impacts on marine ecosystems. Ann Rev Mar Sci 4:11–37

Donner SD, Skirving WJ, Little CM, Oppenheimer M, Hoegh-Gulberg O (2005) Global assessment of coral bleaching and required rates of adaptation under climate change. Glob Chang Biol 11:2251–2265

Dornelas M, Madin JS, Baird AH, Connolly SR (2017) Allometric growth in reef-building corals.

Doropoulos C, Evensen NR, Gómez-Lemos LA, Babcock RC (2017) Density-dependent coral recruitment displays divergent responses during distinct early life-history stages. R Soc Open Sci 4:170082

Doropoulos C, Gómez-Lemos LA, Babcock RC (2018) Exploring variable patterns of density-dependent larval settlement among corals with distinct and shared functional traits. Coral Reefs 37:25–29

Doropoulos C, Gómez-Lemos LA, Salee K, McLaughlin MJ, Tebben J, Van Koningsveld M, Feng M, Babcock RC (2022) Limitations to coral recovery along an environmental stress gradient. Ecol Appl 32:1–16

Doropoulos C, Roff G, Bozec YM, Zupan M, Werminghausen J, Mumby PJ (2016a) Characterizing the ecological trade-offs throughout the early ontogeny of coral recruitment. Ecol Monogr

86:20–44

Doropoulos C, Roff G, Visser MS, Mumby PJ (2016b) Sensitivity of coral recruitment to subtle shifts in early community succession. Ecology 98:304–314

Doropoulos C, Ward S, Marshell A, Diaz-Pulido G, Mumby PJ (2012) Interactions among chronic and acute impacts on coral recruits: the importance of size-escape thresholds. Ecology 93:2131–2138

Doropoulos C, Ward S, Roff G, González-Rivero M, Mumby PJ (2015) Linking demographic processes of juvenile corals to benthic recovery trajectories in two common reef habitats. PLoS One 10:1–23

Doyle CM, Leberg PL, Klerks PL (2011) Heritability of heat tolerance in a small livebearing fish, *Heterandria formosa*. Ecotoxicology 20:535–542

Drury C (2020) Resilience in reef-building corals: the ecological and evolutionary importance of the host response to thermal stress. Mol Ecol 29:448–465

Drury C, Lirman D (2021) Genotype by environment interactions in coral bleaching. Proc R Soc B Biol Sci 288:20210177

Drury C, Manzello D, Lirman D (2017) Genotype and local environment dynamically influence growth, disturbance response and survivorship in the threatened coral, *Acropora cervicornis*. PLoS One 12:1–22

Dunstan PK, Johnson CR (1998) Spatio-temporal variation in coral recruitment at different scales on Heron, Sth GBR. Coral Reefs 17:71–81

Dziedzic KE, Elder H, Tavalire H, Meyer E (2019) Heritable variation in bleaching responses and its functional genomic basis in reef-building corals (*Orbicella faveolata*). Mol Ecol 28:2238–2253

Eakin CM, Morgan JA, Heron SF, Smith TB, Liu G, Alvarez-Filip L, Baca B, Bartels E, Bastidas C, Bouchon C, Brandt M, Bruckner AW, Bunkley-Williams L, Cameron A, Causey BD, Chiappone M, Christensen TRL, Crabbe MJC, Day O, de la Guardia E, Díaz-Pulido G, DiResta D, Gil-Agudelo DL, Gilliam DS, Ginsburg RN, Gore S, Guzmán HM, Hendee JC, Hernández-Delgado EA, Husain E, Jeffrey CFG, Jones RJ, Jordán-Dahlgren E, Kaufman LS, Kline DI, Kramer PA, Lang JC, Lirman D, Mallela J, Manfrino C, Maréchal JP, Marks K, Mihaly J, Miller WJ, Mueller EM, Muller EM, Toro CAO, Oxenford HA, Ponce-Taylor D, Quinn N, Ritchie KB, Rodríguez S,

Ramírez AR, Romano S, Samhouri JF, Sánchez JA, Schmahl GP, Shank B V., Skirving WJ, Steiner SCC, Villamizar E, Walsh SM, Walter C, Weil E, Williams EH, Roberson KW, Yusuf Y (2010) Caribbean corals in crisis: Record thermal stress, bleaching, and mortality in 2005. PLoS One 5:e13969

Easterling MR, Ellner SP, Dixon PM (2000) Size-specific sensitivity: Applying a new structured population model. Ecology 81:694–708

EAtlas.org.au (2022) Juvenile corals on the Great Barrier Reef - the sex life of corals and the importance of recruitment to coral reef recovery. https://eatlas.org.au/gbr/coral-recruitment-recovery [accessed 2023-09-28]

Eddy TD, Lam VWY, Reygondeau G, Cisneros-Montemayor AM, Greer K, Palomares MLD, Bruno JF, Ota Y, Cheung WWL (2021) Global decline in capacity of coral reefs to provide ecosystem services. One Earth 4:1278–1285

Edmunds PJ (2017) Unusually high coral recruitment during the 2016 El Niño in Mo'orea, French Polynesia. PLoS One 12:1–19

Edmunds PJ (2018) Implications of high rates of sexual recruitment in driving rapid reef recovery in Mo'orea, French Polynesia. Sci Rep 8:1–11

Edmunds PJ, Burgess SC, Putnam HM, Baskett ML, Bramanti L, Fabina NS, Han X, Lesser MP, Madin JS, Wall CB, Yost DM, Gates RD (2014) Evaluating the causal basis of ecological success within the scleractinia: an integral projection model approach. Mar Biol 161:2719–2734

Edmunds PJ, Riegl B (2020) Urgent need for coral demography in a world where corals are disappearing. Mar Ecol Prog Ser 635:233–242

Edwards AJ, Guest JR, Heyward AJ, Villanueva RD, Baria MV, Bollozos ISF, Golbuu Y (2015) Direct seeding of mass-cultured coral larvae is not an effective option for reef rehabilitation. Mar Ecol Prog Ser 525:105–116

Elahi R, Sebens KP, De Leo GA (2016) Ocean warming and the demography of declines in coral body size. Mar Ecol Prog Ser 560:147–158

Ellner SP, Adler PB, Childs DZ, Hooker G, Miller TEX, Rees M (2021) A critical comparison of integral projection and matrix projection models for demographic analysis: Comment. Ecology

103:e3605

Evensen NR, Vanwonterghem I, Doropoulos C, Gouezo M, Botté ES, Webster NS, Mumby PJ (2021) Benthic micro- and macro-community succession and coral recruitment under overfishing and nutrient enrichment. Ecology 102:1–16

Falconer DS, Mackay TF (1996) Introduction to Quantitative Genetics. Longman, Essex, UK

Fisher R (1930) The Genetical Theory of Natural Selection. Clarendon, Oxford, UK

Fisher R, Bessell-Browne P, Jones R (2019) Synergistic and antagonistic impacts of suspended sediments and thermal stress on corals. Nat Commun 10:2346

Fisher R, O'Leary RA, Low-Choy S, Mengersen K, Knowlton N, Brainard RE, Caley MJ (2015) Species richness on coral reefs and the pursuit of convergent global estimates. Curr Biol 25:500–505

Fisher RA (1919) The correlation between relatives on the supposition of Mendelian inheritance. Trans R Soc Edinburgh 52:399–433

Fisk DA, Harriott VJ (1990) Spatial and temporal variation in coral recruitment on the Great Barrier Reef: Implications for dispersal hypotheses. Mar Biol 107:485–490

Flood PJ, Kruijer W, Schnabel SK, Schoor R, Jalink H, Snel JFH, Harbinson J, Aarts MGM (2016) Phenomics for photosynthesis, growth and reflectance in *Arabidopsis thaliana* reveals circadian and long-term fluctuations in heritability. Plant Methods 12:1–14

Foster T, Gilmour J (2020) Egg size and fecundity of biannually spawning corals at Scott Reef. Sci Rep 10:1–9

Frieler K, Meinshausen M, Golly A, Mengel M, Lebek K, Donner SD, Hoegh-Guldberg O (2013) Limiting global warming to 2°C is unlikely to save most coral reefs. Nat Clim Chang 3:165–170

Fuller ZL, Mocellin VJL, Morris L, Cantin N, Shepherd J, Sarre L, Peng J, Liao Y, Pickrell J, Andolfatto P, Matz M, Bay LK, Przeworski M (2019) Population genetics of the coral *Acropora millepora*: Towards a genomic predictor of bleaching. Science 369:eaba4674

GBRMPA (2017) Final report: 2016 coral bleaching event on the Great Barrier Reef. https://elibrary.gbrmpa.gov.au/jspui/bitstream/11017/3206/1/Final-report-2016-coral-bleaching-GBR.pdf [accessed 2023-09-28]

GCRMN (2021) Status of Coral Reefs of the World: 2020. Glob Coral Reef Monit Netw Int Coral Reef Initiat https://www.unep.org/resources/status-coral-reefs-world-2020 [accessed 2023-09-28]

Geber MA, Dawson TE (1997) Genetic variation in stomatal and biochemical limitations to photosynthesis in the annual plant, *Polygonum arenastrum*. Oecologia 109:535–546

Ghalambor CK, McKay JK, Carroll SP, Reznick DN (2007) Adaptive versus non-adaptive phenotypic plasticity and the potential for contemporary adaptation in new environments. Funct Ecol 21:394–407

Gienapp P, Teplitsky C, Alho J, Mills J, Merilä J (2008) Climate change and evolution: Disentangling environmental and genetic responses. Mol Ecol 17:167–178

Godoy L, Mies M, Zilberberg C, Pastrana Y, Amaral A, Cruz N, Pereira CM, Garrido AG, Paris A, Santos LFA, Pires DO (2021) Southwestern Atlantic reef-building corals *Mussismilia* spp. are able to spawn while fully bleached. Mar Biol 168:1–8

Gouezo M, Olsudong D, Fabricius K, Harrison P, Golbuu Y, Doropoulos C (2020) Relative roles of biological and physical processes influencing coral recruitment during the lag phase of reef community recovery. Sci Rep 10:1–12

Gouezo M, Wolanski E, Critchell K, Fabricius K, Harrison P, Golbuu Y, Doropoulos C (2021) Modelled larval supply predicts coral population recovery potential following disturbance. Mar Ecol Prog Ser 661:127–145

Goulet TL, Coffroth MA (2003) Stability of an octocoral-algal symbiosis over time and space. Mar Ecol Prog Ser 250:117–124

Grant PR, Grant BR (2006) Evolution of character displacement in Darwin's finches. Science 313:224–226

Gray K, Hampton B, Silveti-Falls T, McConnell A, Bausell C (2015) Comparison of bayesian credible intervals to frequentist confidence intervals. J Mod Appl Stat Methods 14:43–52

Guest JR, Baird AH, Maynard JA, Muttaqin E, Edwards AJ, Campbell SJ, Yewdall K, Affendi YA, Chou LM (2012) Contrasting patterns of coral bleaching susceptibility in 2010 suggest an adaptive response to thermal stress. PLoS One 7:1–8

Gunay F, Alten B, Ozsoy ED (2011) Narrow-sense heritability of body size and its response to

different developmental temperatures in *Culex quinquefasciatus* (Say 1923). J Vector Ecol 36:348–354

Hadfield JD (2008) Estimating evolutionary parameters when viability selection is operating. Proc R Soc B Biol Sci 275:723–734

Hagedorn M, Carter VL, Lager C, Camperio Ciani JF, Dygert AN, Schleiger RD, Henley EM (2016) Potential bleaching effects on coral reproduction. Reprod Fertil Dev 28:1061–1071

Hajduk GK, Walling CA, Cockburn A, Kruuk LEB (2020) The algebra of evolution: The Robertson-Price identity and viability selection for body mass in a wild bird population. Philos Trans R Soc B Biol Sci 375:20190359

Hall VR, Hughes TP (1996) Reproductive strategies of modular organisms: Comparative studies of reef-building corals. Ecology 77:950–963

Hamilton RJ, Almany GR, Brown CJ, Pita J, Peterson NA, Howard Choat J (2017) Logging degrades nursery habitat for an iconic coral reef fish. Biol Conserv 210:273–280

Hansen TF, Pe C, Houle D (2011) Heritability is not evolvability. Evol Biol 38:258–277

Hartmann AC, Marhaver KL, Vermeij MJA (2018) Corals in healthy populations produce more larvae per unit cover. Conserv Lett 11:1–12

Hazraty-Kari S, Morita M, Tavakoli-Kolour P, Nakamura T, Harii S (2023) Reactions of juvenile coral to three years of consecutive thermal stress. Sci Total Environ 863:161227

Hazraty-Kari S, Tavakoli-Kolour P, Kitanobo S, Nakamura T, Morita M (2022) Adaptations by the coral *Acropora tenuis* confer resilience to future thermal stress. Commun Biol 5:1371

van Heerwaarden B, Kellermann V, Sgr CM (2016) Limited scope for plasticity to increase upper thermal limits. Funct Ecol 30:1947–1956

Hendry AP, Kinnison MT (1999) Perspective: the pace of modern life: measuring rates of contemporary microevolution. Int J Org Evol 53:1637–1653

Herben T, Klimešová J, Chytrý M (2018) Effects of disturbance frequency and severity on plant traits: An assessment across a temperate flora. Funct Ecol 32:799–808

Heron SF, Johnston L, Liu G, Geiger EF, Maynard JA, De La Cour JL, Johnson S, Okano R, Benavente D, Burgess TFFR, Iguel J, Perez DI, Skirving WJ, Strong AE, Tirak K, Eakin CM

(2016) Validation of reef-scale thermal stress satellite products for coral bleaching monitoring. Remote Sens 8:1–16

Higgins JPT, Thompson SG (2002) Quantifying heterogeneity in a meta-analysis. Stat Med 21:1539–1558

Hill WG, Goddard ME, Visscher PM (2008) Data and theory point to mainly additive genetic variance for complex traits. PLoS Genet 4:e1000008

Hoadley KD, Pettay DT, Lewis A, Wham D, Grasso C, Smith R, Kemp DW, LaJeunesse T, Warner ME (2021) Different functional traits among closely related algal symbionts dictate stress endurance for vital Indo-Pacific reef-building corals. Glob Chang Biol 27:5295–5309

Hoegh-Guldberg O, Poloczanska ES, Skirving W, Dove S (2017) Coral reef ecosystems under climate change and ocean acidification. Front Mar Sci 4:158

Hoegh O, Jacob D, Taylor M, Bindi M, Brown S, Camilloni I, Diedhiou A, Djalante R, Ebi K, Engelbrecht F, Guiot J, Hijioka Y, Mehrotra S, Payne A, Seneviratne S, Thomas A, Warren R, Zhou G (2018) Special report on global warming of 1.5 °C - Chapter 3: Impacts of 1.5º C global warming on natural and human systems. World Meteorol Organ Tech Doc 175–311

Holstein DM, Smith TBTB, van Hooidonk R, Paris CB (2022) Predicting coral metapopulation decline in a changing thermal environment. Coral Reefs 41:961–972

van Hooidonk R, Maynard J, Grimsditch G, Williams G, Tamelander J, Gove J, Koldewey H, Ahmadia G, Tracey D, Hum K, Conklin E, Berumen M (2020) Projections of future coral bleaching conditions using IPCC CMIP6 models: climate policy implications, management applications, and Regional Seas summaries. United Nations Environ Program

van Hooidonk R, Maynard J, Tamelander J, Gove J, Ahmadia G, Raymundo L, Williams G, Heron SF, Planes S (2016) Local-scale projections of coral reef futures and implications of the Paris Agreement. Sci Rep 6:1–8

Howe-Kerr LI, Bachelot B, Wright RM, Kenkel CD, Bay LK, Correa AMS (2020) Symbiont community diversity is more variable in corals that respond poorly to stress. Glob Chang Biol 26:2220–2234

Howells EJ, Abrego D, Meyer E, Kirk NL, Burt JA (2016) Host adaptation and unexpected symbiont

partners enable reef-building corals to tolerate extreme temperatures. Glob Chang Biol 22:2702–2714

Howells EJ, Beltran VH, Larsen NW, Bay LK, Willis BL, Van Oppen MJH (2012) Coral thermal tolerance shaped by local adaptation of photosymbionts. Nat Clim Chang 2:116–120

Howells EJ, Berkelmans R, Van Oppen MJH, Willis BL, Bay LK (2013) Historical thermal regimes define limits to coral acclimatization. Ecology 94:1078–1088

Hughes T, Baird A, Bellwood D, Card M, Connolly S, Folke C, Grosberg R, Hoegh-Guldberg O, Jackson JBC, Kleypas J, Lough JM, Marshall P, Palumbi SR, Pandolfi JM, Rosen B, Roughgarden J (2003) Climate change, human impacts, and the resilience of coral reefs. Science 301:877–1000

Hughes TP, Anderson KD, Connolly SR, Heron SF, Kerry JT, Lough JM, Baird AH, Baum JK, Berumen ML, Bridge TC, Claar DC, Eakin CM, Gilmour JP, Graham NAJJ, Harrison H, Hobbs JAPA, Hoey AS, Hoogenboom M, Lowe RJ, Mcculloch MT, Pandolfi JM, Pratchett M, Schoepf V, Torda G, Wilson SK, James T, Lough JM, Baird AH, Baum JK, Berumen ML, Tom C, Claar DC, Eakin CM, Gilmour JP, Graham NAJJ, Harrison H, Hobbs JAPA, Hoey AS, Hoogenboom M, Lowe RJ, Mcculloch MT, Pandolfi JM, Pratchett M, Schoepf V, Wilson SK, Cook J, Watch CR, Oceanic USN (2018a) Spatial and temporal patterns of mass bleaching of corals in the Anthropocene. Science 83:80–83

Hughes TP, Connell JH (1987) Population dynamics based on size or age? A reef-coral analysis. Am Nat 129:818–829

Hughes TP, Kerry JT, Álvarez-Noriega M, Álvarez-Romero JG, Anderson KD, Baird AH, Babcock RC, Beger M, Bellwood DR, Berkelmans R, Bridge TC, Butler IR, Byrne M, Cantin NE, Comeau S, Connolly SR, Cumming GS, Dalton SJ, Diaz-Pulido G, Eakin CM, Figueira WF, Gilmour JP, Harrison HB, Heron SF, Hoey AS, Hobbs JPA, Hoogenboom MO, Kennedy E V., Kuo CY, Lough JM, Lowe RJ, Liu G, McCulloch MT, Malcolm HA, McWilliam MJ, Pandolfi JM, Pears RJ, Pratchett MS, Schoepf V, Simpson T, Skirving WJ, Sommer B, Torda G, Wachenfeld DR, Willis BL, Wilson SK (2017) Global warming and recurrent mass bleaching of corals. Nature 543:373–377

Hughes TP, Kerry JT, Baird AH, Connolly SR, Chase TJ, Dietzel A, Hill T, Hoey AS, Hoogenboom MO, Jacobson M, Kerswell A, Madin JS, Mieog A, Paley AS, Pratchett MS, Torda G, Woods RM (2019) Global warming impairs stock–recruitment dynamics of corals. Nature 568:387-390

Hughes TP, Kerry JT, Baird AH, Connolly SR, Dietzel A, Eakin CM, Heron SF, Hoey AS, Hoogenboom MO, Liu G, McWilliam MJ, Pears RJ, Pratchett MS, Skirving WJ, Stella JS, Torda G (2018b) Global warming transforms coral reef assemblages. Nature 556:492–496

Hughes TP, Kerry JT, Simpson T (2018c) Large-scale bleaching of corals on the Great Barrier Reef. Ecology 99:501

Humanes A, Lachs L, Beauchamp EA, Bythell C, Edwards AJ, Golbuu Y, Martinez HM, Palmowski P, Treumann A, Steeg E Van Der, Hooidonk R Van, Guest JR (2022) Within-population variability in coral heat tolerance indicates climate adaptation potential. Proc R Soc B 289:20220872

IPCC (2019) Special Report on the Ocean and Cryosphere in a Changing Climate.

IPCC (2021) Climate Change 2021: The Physical Science Basis. Contribution of Working Group I to the Sixth Assessment Report of the Intergovernmental Panel on Climate Change.

Jaatinen K, Westerbom M, Norkko A, Mustonen O, Koons DN (2021) Detrimental impacts of climate change may be exacerbated by density-dependent population regulation in blue mussels. J Anim Ecol 90:562–573

Jackson D, White IR (2018) When should meta-analysis avoid making hidden normality assumptions? Biom J 60:1040–1058

Janeiro MJ, Coltman DW, Festa-Bianchet M, Pelletier F, Morrissey MB (2017) Towards robust evolutionary inference with integral projection models. J Evol Biol 30:270–288

Janhunen M, Koskela J, Ninh NH, Vehviläinen H, Koskinen H, Nousiainen A, Thoa NP (2016) Thermal sensitivity of growth indicates heritable variation in 1-year-old rainbow trout (*Oncorhynchus mykiss*). Genet Sel Evol 48:1–11

Jenouvrier S, Visser ME (2011) Climate change, phenological shifts, eco-evolutionary responses and population viability: Toward a unifying predictive approach. Int J Biometeorol 55:905–919

Jones A, Berkelmans R (2010) Potential costs of acclimatization to a warmer climate: Growth of a reef

coral with heat tolerant vs. sensitive symbiont types. PLoS One 5:e10437

Jonker M (2022) Juvenile corals on the Great Barrier Reef - the sex life of corals and the importance of recruitment to coral reef recovery. https://eatlas.org.au/gbr/coral-recruitment-recovery [accessed 2023-09-28]

Jouval F, Latreille AC, Bureau S, Adjeroud M, Penin L (2019) Multiscale variability in coral recruitment in the Mascarene Islands: From centimetric to geographical scale. PLoS One 14:1–17

Jump AS, Peñuelas J (2005) Running to stand still: Adaptation and the response of plants to rapid climate change. Ecol Lett 8:1010–1020

Jury CP, Toonen RJ (2019) Adaptive responses and local stressor mitigation drive coral resilience in warmer, more acidic oceans. Proc R Soc B 286:20190614

Kalmus P, Ekanayaka A, Kang E, Baird M, Gierach M (2022) Past the precipice? Projected coral habitability under global heating. Earth's Futur 10:e2021EF002608

Kawecki TJ, Ebert D (2004) Conceptual issues in local adaptation. Ecol Lett 7:1225–1241

Kayal M, Lenihan HS, Brooks AJ, Holbrook SJ, Schmitt RJ, Kendall BE (2018) Predicting coral community recovery using multi-species population dynamics models. Ecol Lett 21:1790–1799

Kelly LW, Williams GJ, Barott KL, Carlson CA, Dinsdale EA, Edwards RA, Haas AF, Haynes M, Lim YW, McDole T, Nelson CE, Sala E, Sandin SA, Smith JE, Vermeij MJA, Youle M, Rohwer F (2014) Local genomic adaptation of coral reef-associated microbiomes to gradients of natural variability and anthropogenic stressors. Proc Natl Acad Sci 111:10227–10232

Kenkel CD, Almanza AT, Matz M V. (2015a) Fine-scale environmental specialization of reef-building corals might be limiting reef recovery in the Florida Keys. Ecology 96:3197–3212

Kenkel CD, Setta SP, Matz M V. (2015b) Heritable differences in fitness-related traits among populations of the mustard hill coral, *Porites astreoides*. Heredity 115:509–516

Kinnison MT, Hendry AP (2001) The pace of modern life. II. From rates to pattern and process. Genetica 112–113:145–164

Kirk NL, Howells EJ, Abrego D, Burt JA, Meyer E (2018) Genomic and transcriptomic signals of thermal tolerance in heat-tolerant corals (*Platygyra daedalea*) of the Arabian/Persian Gulf. Mol

Ecol 27:5180–5194

Klausmeier CA, Osmond MM, Kremer CT, Litchman E (2020) Ecological limits to evolutionary rescue: Ecological limits to evolutionary rescue. Philos Trans R Soc B Biol Sci 375:20190453

Knapp G, Hartung J (2003) Improved tests for a random effects meta-regression with a single covariate. Stat Med 22:2693–2710

Knowlton N, Brainard RE, Fisher R, Moews M, Plaisance L, Caley MJ (2010) Coral reef biodiversity. Life in the world's oceans: Diversity distribution and Abundance. Blackwell Publishing Ltd., Hoboken, NJ, USA, pp 65–74

Koenker R (2020) quantreg: Quantile regression. R package version 5.67.

Koenker R, Hallock KF (2001) Quantile regression. J Econ Perspect 15:143–156

Koester A, Ford AK, Ferse SCA, Migani V, Bunbury N, Sanchez C, Wild C (2021) First insights into coral recruit and juvenile abundances at remote Aldabra Atoll, Seychelles. PLoS One 16:1–19

Komyakova V, Munday PL, Jones GP (2019) Comparative analysis of habitat use and ontogenetic habitat-shifts among coral reef damselfishes. Environ Biol Fishes 102:1201–1218

Kopp M, Matuszewski S (2014) Rapid evolution of quantitative traits: Theoretical perspectives. Evol Appl 7:169–191

Kremer A, Ronce O, Robledo-Arnuncio JJ, Guillaume F, Bohrer G, Nathan R, Bridle JR, Gomulkiewicz R, Klein EK, Ritland K, Kuparinen A, Gerber S, Schueler S (2012) Long-distance gene flow and adaptation of forest trees to rapid climate change. Ecol Lett 15:378–392

Kruuk LEB (2004) Estimating genetic parameters in natural populations using the "animal model." Philos Trans R Soc London B 359:873–890

Lande R (1979) Quantitative genetic analysis of multivariate evolution, applied to brain:body size allometry. Evolution 33:402–416

Lande R (1981) The minimum number of genes contributing to quantitative variation between and within populations. Genetics 99:541–553

Laporte M, Pavey SA, Rougeux C, Pierron F, Lauzent M, Budzinski H, Labadie P, Geneste E, Couture P, Baudrimont M, Bernatchez L (2016) RAD sequencing reveals within-generation polygenic selection in response to anthropogenic organic and metal contamination in North Atlantic eels.

3951 Mol Ecol 25:219–237
3952 Lasky JR, Hooten MB, Adler PB (2020) What processes must we understand to forecast regional-scale
3953 population dynamics?. Proc R Soc B Biol Sci 287:20202219
3954 Laughlin DC, Gremer JR, Adler PB, Mitchell RM, Moore MM (2020) The net effect of functional
3955 traits on fitness. Trends Ecol Evol 35:1037–1047
3956 Laurance WF (2010) Habitat destruction: Death by a thousand cuts. Conservation Biology For All. pp
3957 73–88
3958 Laverick JH, Piango S, Andradi-Brown DA, Exton DA, Bongaerts P, Bridge TCL, Lesser MP, Pyle
3959 RL, Slattery M, Wagner D, Rogers AD (2018) To what extent do mesophotic coral ecosystems
3960 and shallow reefs share species of conservation interest? A systematic review. Environ Evid 7:1–
3961 13
3962 Leinbach SE, Speare KE, Rossin AM, Holstein DM, Strader ME (2021) Energetic and reproductive
3963 costs of coral recovery in divergent bleaching responses. Sci Rep 11:1–10
3964 Levitan DR, Boudreau W, Jara J, Knowlton N (2014) Long-term reduced spawning in *Orbicella* coral
3965 species due to temperature stress. Mar Ecol Prog Ser 515:1–10
3966 Liew YJ, Howells EJ, Wang X, Michell CT, Burt JA, Idaghdour Y, Aranda M (2020)
3967 Intergenerational epigenetic inheritance in reef-building corals. Nat Clim Chang 10:254–259
3968 Limborg MT, Helyar SJ, De Bruyn M, Taylor MI, Nielsen EE, Ogden R, Carvalho GR, Bekkevold D
3969 (2012) Environmental selection on transcriptome-derived SNPs in a high gene flow marine fish,
3970 the Atlantic herring (*Clupea harengus*). Mol Ecol 21:3686–3703
3971 Lin L, Xu C (2020) Arcsine-based transformations for meta-analysis of proportions: Pros, cons, and
3972 alternatives. Heal Sci Reports 3:1–6
3973 Little AF, Oppen MJH Van, Willis BL (2004) Flexibility in algal endosymbioses shapes growth in
3974 reef corals. Science 304:1492–1494
3975 Logan CA, Dunne JP, Eakin CM, Donner SD (2014a) Incorporating adaptive responses into future
3976 projections of coral bleaching. Glob Chang Biol 20:125–139
3977 Logan CA, Dunne JP, Ryan JS, Baskett ML, Donner SD (2021) Quantifying global potential for coral
3978 evolutionary response to climate change. Nat Clim Chang 11:537–542

Logan ML, Cox RM, Calsbeek R (2014b) Natural selection on thermal performance in a novel thermal environment. Proc Natl Acad Sci 111:14165–14169

Logan ML, Curlis JD, Gilbert AL, Miles DB, Chung AK, McGlothlin JW, Cox RM (2018) Thermal physiology and thermoregulatory behaviour exhibit low heritability despite genetic divergence between lizard populations. Proc R Soc B Biol Sci 285:20180697

Lohr KE, Patterson JT (2017) Intraspecific variation in phenotype among nursery-reared staghorn coral *Acropora cervicornis* (Lamarck, 1816). J Exp Mar Bio Ecol 486:87–92

Lough JM, Anderson KD, Hughes TP (2018) Increasing thermal stress for tropical coral reefs: 1871-2017. Sci Rep 8:1–8

Loya Y, Sakai K, Yamazato K, Nakano Y, Sambali H, Van Woesik R (2001) Coral bleaching: The winners and the losers. Ecol Lett 4:122–131

Lundgren P, Vera JC, Peplow L, Manel S, van Oppen MJH (2013) Genotype - environment correlations in corals from the Great Barrier Reef. BMC Genet 14:9

Lush JL (1937) Animal breeding plans. Iowa State College Press, Ames, Iowa

Lynch M, Gabriel W, Wood AM (1991) Adaptive and demographic responses of plankton populations to environmental change. Limnol Oceanogr 36:1301–1312

Lynch M, Lande R (1993) Evolution and extinction in response to environmental change. In: Kareiva P., Kingsolver J., Huey R. (eds) Biotic Interactions and Global Change. Sinauer Associates, Sunderland, MA, pp 234–250

Ma FZ, Lü ZC, Wang R, Wan FH (2014) Heritability and evolutionary potential in thermal tolerance traits in the invasive Mediterranean cryptic species of *Bemisia tabaci* (Hemiptera: Aleyrodidae). PLoS One 9:1–7

Mackenzie J, Ridd P (2019) John Mackenzie Show with Peter Ridd discuss “Corals Roll with the Punches” news headline. 4CA AM Radio

Madin JS, Baird AH, Baskett ML, Connolly SR, Dornelas MA, Madin JS (2020) Partitioning colony size variation into growth and partial mortality. Biol Lett 16:20190727

Madin JS, Baird AH, Connolly SR, Dornelas MA, Álvarez-Noriega M, McWilliam MJ, Barbosa M, Blowes SA, Cetina-Heredia P, Christie AP, Cumbo VR, Diaz M, Emms MA, Graham E, Hansen

4007 D, Hisano M, Howells E, Kuo C, Palmer C, Hong JTC, Zhi En Teo T, Woods R (2023) Six years
4008 of demography data for 11 reef coral species. Ecology 104:e4017
4009 Madin JS, Baird AH, Dornelas M, Connolly SR (2014) Mechanical vulnerability explains size-
4010 dependent mortality of reef corals. Ecol Lett 17:1008–1015
4011 Madin JS, Hughes TP, Connolly SR (2012) Calcification, storm damage and population resilience of
4012 tabular corals under climate change. PLoS One 7:1–10
4013 Malhi Y, Franklin J, Seddon N, Solan M, Turner MG, Field CB, Knowlton N (2020) Climate change
4014 and ecosystems: Threats, opportunities and solutions. Philos Trans R Soc B Biol Sci
4015 375:20190104
4016 Manzello DP, Matz M V., Enochs IC, Valentino L, Carlton RD, Kolodziej G, Serrano X, Towle EK,
4017 Jankulak M (2019) Role of host genetics and heat-tolerant algal symbionts in sustaining
4018 populations of the endangered coral *Orbicella faveolata* in the Florida Keys with ocean warming.
4019 Glob Chang Biol 25:1016-1031
4020 Marangon E, Laffy PW, Bourne DG, Webster NS (2021) Microbiome-mediated mechanisms
4021 contributing to the environmental tolerance of reef invertebrate species. Mar Biol 168:1–18
4022 Marshall N, Adger WN, Benham C, Brown K, I Curnock M, Gurney GG, Marshall P, L Pert P,
4023 Thiault L (2019) Reef grief: Investigating the relationship between place meanings and place
4024 change on the Great Barrier Reef, Australia. Sustain Sci 14:579–587
4025 Martins F, Kruuk L, Llewelyn J, Moritz C, Phillips B (2019) Heritability of climate-relevant traits in a
4026 rainforest skink. Heredity 122:41–52
4027 Matz M V., Treml EA, Aglyamova G V., Bay LK (2018) Potential and limits for rapid genetic
4028 adaptation to warming in a Great Barrier Reef coral. PLoS Genet 14:1–20
4029 Matz M V., Treml EA, Haller BC (2020) Estimating the potential for coral adaptation to global
4030 warming across the Indo-West Pacific. Glob Chang Biol 26:3473–3481
4031 Maynard J, Van Hooidonk R, Eakin CM, Puotinen M, Garren M, Williams G, Heron SF, Lamb J,
4032 Weil E, Willis B, Harvell CD (2015) Projections of climate conditions that increase coral disease
4033 susceptibility and pathogen abundance and virulence. Nat Clim Chang 5:688–694
4034 Maynard JA, Anthony KRNN, Marshall PA, Masiri I (2008) Major bleaching events can lead to

4035 increased thermal tolerance in corals. Mar Biol 155:173–182
4036 McCleery RH, Pettifor RA, Armbruster P, Meyer K, Sheldon BC, Perrins CM (2004) Components of
4037 variance underlying fitness in a natural population of the great tit *Parus major*. Am Nat
4038 164:E62–72
4039 McCormick MI, Chivers DP, Ferrari MCO, Oona ML (2014) Habitat degradation is threatening reef
4040 replenishment by making fish fearless. J Anim Ecol 83:1178–1185
4041 McIlroy SE, Gillette P, Cunning R, Klueter A, Capo T, Baker AC, Coffroth MA (2016) The effects of
4042 *Symbiodinium* (Pyrrhophyta) identity on growth, survivorship, and thermal tolerance of newly
4043 settled coral recruits. J Phycol 52:1114–1124
4044 McManus LC, Forrest DL, Tekwa EW, Schindler DE, Colton MA, Webster MM, Essington TE,
4045 Palumbi SR, Mumby PJ, Pinsky ML, (2021a) Evolution and connectivity influence the
4046 persistence and recovery of coral reefs under climate change in the Caribbean, Southwest Pacific,
4047 and Coral Triangle. Glob Chang Biol 27:4307-4321
4048 McManus LC, Tekwa EW, Schindler DE, Walsworth TE, Colton MA, Webster MM, Essington TE,
4049 Forrest DL, Palumbi SR, Mumby PJ, Pinsky ML (2021b) Evolution reverses the effect of
4050 network structure on metapopulation persistence. Ecology 102:e03381
4051 McManus LC, Vasconcelos V V., Levin SA, Thompson DM, Kleypas JA, Castruccio FS, Curchitser
4052 EN, Watson JR (2020) Extreme temperature events will drive coral decline in the Coral Triangle.
4053 Glob Chang Biol 26:2120–2133
4054 McWhorter JK, Halloran PR, Roff G, Skirving WJ, Mumby PJ (2022a) Climate refugia on the Great
4055 Barrier Reef fail when global warming exceeds 3°C. Glob Chang Biol 28:5768–5780
4056 McWhorter JK, Halloran PR, Roff G, Skirving WJ, Perry CT, Mumby PJ (2022b) The importance of
4057 1.5°C warming for the Great Barrier Reef. Glob Chang Biol 28:1332–1341
4058 McWilliam M, Dornelas M, Álvarez-Noriega M, Baird AH, Connolly SR, Madin JS (2023) Net
4059 effects of life-history traits explain persistent differences in abundance among similar species.
4060 Ecology 104:e3863
4061 MEA (2005) A Report of the Millennium Ecosystem Assessment. Ecosystems and Human Well-
4062 Being. Millenium Ecosystem Assessment

4063 Meher PK, Rustgi S, Kumar A (2022) Performance of bayesian and BLUP alphabets for genomic
4064 prediction: analysis, comparison and results. Heredity 128:519–530
4065 Merow C, Dahlgren JP, Metcalf CJE, Childs DZ, Evans MEK, Jongejans E, Record S, Rees M,
4066 Salguero-Gómez R, Mcmahon SM (2014) Advancing population ecology with integral
4067 projection models: A practical guide. Methods Ecol Evol 5:99–110
4068 Meyer E, Davies S, Wang S, Willis BL, Abrego D, Juenger TE, Matz M V. (2009) Genetic variation
4069 in responses to a settlement cue and elevated temperature in the reef-building coral *Acropora*
4070 *millepora*. Mar Ecol Prog Ser 392:81–92
4071 Mieog JC, Olsen JL, Berkelmans R, Bleuler-Martinez SA, Willis BL, van Oppen MJH (2009a) The
4072 roles and interactions of symbiont, host and environment in defining coral fitness. PLoS One
4073 4:e6364
4074 Mieog JC, Van Oppen MJH, Berkelmans R, Stam WT, Olsen JL (2009b) Quantification of algal
4075 endosymbionts (*Symbiodinium*) in coral tissue using real-time PCR. Mol Ecol Resour 9:74–82
4076 Mills L, Bragina E V., Kumar A V., Zimova M, Lafferty DJR, Feltner J, Davis BM, Hackländer K,
4077 Alves PC, Good JM, Melo-Ferreira J, Dietz A, Abramov A V., Lopatina N, Fay K (2018) Winter
4078 color polymorphisms identify global hot spots for evolutionary rescue from climate change.
4079 Science 359:1033–1036
4080 Møller AP, Jennions MD (2001) Testing and adjusting for publication bias. Trends Ecol Evol 16:580–
4081 586
4082 Montero-Serra I, Garrabou J, Doak DF, Figuerola L, Hereu B, Ledoux JB, Linares C (2018)
4083 Accounting for life-history strategies and timescales in marine restoration. Conserv Lett 11:1–9
4084 Morais J, Morais RA, Tebbett SB, Pratchett MS, Bellwood DR (2021) Dangerous demographics in
4085 post-bleach corals reveal boom-bust versus protracted declines. Sci Rep 11:1–7
4086 Morikawa MK, Palumbi SR (2019) Using naturally occurring climate resilient corals to construct
4087 bleaching-resistant nurseries. Proc Natl Acad Sci 116:10586–10591
4088 Morrissey MB, Kruuk LEB, Wilson AJ (2010) The danger of applying the breeder's equation in
4089 observational studies of natural populations. J Evol Biol 23:2277–2288
4090 Morrissey MB, Parker DJ, Korsten P, Pemberton JM, Kruuk LEB, Wilson AJ, Morrissey MB, Parker

DJ, Korsten P, Pemberton JM, Kruuk LEB (2012) The prediction of adaptive evolution: Empirical application of the secondary theorem of selection and comparison to the Breeder's equation. Evolution 66:2399–2410

Moss R, Babiker M, Brinkman S, Calvo E, Carter T, Edmonds J, Elgizouli I, Emori S, Erda L, Hibbard K, Jones R, Kainuma M, Kelleher J, Lamarque JF, Manning M, Matthews B, Meehl J, Meyer L, Mitchell J, Nebojsa N, O'Neill B, Pichs R, Riahi K, Rose S, Runci P, Stouffer R, van Vuuren D, Weyant J, Wilbanks T, van Ypersele JP, Zurek M (2008) Towards new scenarios for analysis of emissions, climate change, impacts, and response strategies: IPCC Expert Meeting Report, 19-21 September, 2007, Noordwijkerhout, the Netherlands.

Mousseau TA, Roff DA (1987) Natural selection and the heritability of fitness components. Heredity 59:181–197

Muscatine L, Porter JW (1977) Reef corals: Mutualistic symbioses adapted to nutrient-poor environments. Bioscience 27:454–460

Mwachireya SA, McClanahan TR, Hartwick BE, Côte IM, Lesack L (2015) Effects of river sediments on coral recruitment, algal abundance benthic community structure on Kenyan coral reefs. African J Environ Sci Technol 9:615–631

Nakamura M, Murakami T, Kohno H, Mizutani A, Shimokawa S (2022) Rapid recovery of coral communities from a mass bleaching event in the summer of 2016, observed in Amitori Bay, Iriomote Island, Japan. Mar Biol 169:1–9

NOAA Coral Reef Watch (2022) NOAA Coral Reef Watch Version 3.1 Daily 5km satellite regional virtual station time series data for the Great Barrier Reef, Australia, 1985-2022. https://coralreefwatch.noaa.gov/product/vs/data.php [accessed 2023-09-28]

Noble DWA, Mcfarlane SE, Keogh JS, Whiting MJ (2014) Maternal and additive genetic effects contribute to variation in offspring traits in a lizard. Behav Ecol 25:633–640

Nolan C, Overpeck JT, Allen JRM, Anderson PM, Betancourt JL, Binney HA, Brewer S, Bush MB, Chase B, Cheddadi R, Djamali M, Dodson J, Edwards M, Gosling W, Haberle S, Hotchkiss S, Huntley B, Ivory S, Kershaw A, Kim S-H, Latorre C (2018) Past and future global transformation of terrestrial ecosystems under climate change. Science 361:920–923

O'Mahoney J, Simes R, Redhill D, Heaton K, Atkinson C, Hayward E, Nguyen M (2017) At what price? The economic, social and icon value of the Great Barrier Reef. Deloitte Access Econ, Brisbane, Australia

O'Neill BC, Tebaldi C, Van Vuuren DP, Eyring V, Friedlingstein P, Hurtt G, Knutti R, Kriegler E, Lamarque JF, Lowe J, Meehl GA, Moss R, Riahi K, Sanderson BM (2016) The Scenario Model Intercomparison Project (ScenarioMIP) for CMIP6. Geosci Model Dev 9:3461–3482

Oliver TA, Palumbi SR (2011) Do fluctuating temperature environments elevate coral thermal tolerance? Coral Reefs 30:429–440

Olsson L, et al. (2019) Climate change and land: An IPCC special report on climate change, desertification, land degradation, sustainable land management, food security, and greenhouse gas fluxes in terrestrial ecosystems. IPCC Spec Rep Clim Chang

Omori M, Iwao K, Tamura M (2008) Growth of transplanted *Acropora tenuis* 2 years after egg culture. Coral Reefs 27:165

Osman EO, Smith DJ, Ziegler M, Kürten B, Conrad C, El-Haddad KM, Voolstra CR, Suggett DJ (2018) Thermal refugia against coral bleaching throughout the northern Red Sea. Glob Chang Biol 24:e474–e484

Pandolfi JM, Bradbury RH, Sala E, Hughes TP, Bjorndal KA, Cooke RG, Mcardle D, McClenachan L, Newman MJH, Paredes G, Warner RR, Jackson JBC (2003) Global trajectories of the long-term decline of coral reef ecosystems. Science 301:955–959

Pandolfi JM, Connolly SR, Marshall DJ, Cohen AL (2011) Projecting coral reef futures under global warming and ocean acidification. Science 333:418–422

Pespeni MH, Barney BT, Palumbi SR (2013) Differences in the regulation of growth and biomineralization genes revealed through long-term common-garden acclimation and experimental genomics in the purple sea urchin. Evolution 67:1901–1914

Polderman TJC, Benyamin B, Leeuw CA De, Sullivan PF, van Bochoven A, Visscher PM, Posthuma D (2015) Meta-analysis of the heritability of human traits based on fifty years of twin studies. Nat Genet 47:702–709

Pratchett MS, Anderson KD, Hoogenboom MO, Widman E, Baird AH, Pandolfi JM, Edmunds PJ,

Lough JM (2015) Spatial, temporal and taxonomic variation in coral growth-implications for the structure and function of coral reef ecosystems. Oceanogr Mar Biol An Annu Rev 53:215–295

Pratchett MS, Hoey AS, Wilson SK, Messmer V, Graham NAJ (2011) Changes in biodiversity and functioning of reef fish assemblages following coral bleaching and coral loss. Diversity 3:424–452

Pratchett MS, McWilliam MJ, Riegl B (2020) Contrasting shifts in coral assemblages with increasing disturbances. Coral Reefs 39:783–793

Precoda K, Baird AH, Madsen A, Mizerek T, Sommer B, Su SN, Madin JS (2018) How does a widespread reef coral maintain a population in an isolated environment? Mar Ecol Prog Ser 594:85–94

Price GR (1970) Selection and Covariance. Nature 227:520–521

Price NN, Muko S, Legendre L, Steneck R, Van Oppen MJH, Albright R, Ang P, Carpenter RC, Chui APY, Fan TY, Gates RD, Harii S, Kitano H, Kurihara H, Mitarai S, Padilla-Gamiño JL, Sakai K, Suzuki G, Edmunds PJ (2019) Global biogeography of coral recruitment: Tropical decline and subtropical increase. Mar Ecol Prog Ser 621:1–17

Price T, Schluter D (1991) On the low heritability of life-history traits. Evolution 45:853

Price TD, Qvarnstro A, Irwin DE (2003) The role of phenotypic plasticity in driving genetic evolution. Proc R Soc B 270:1433–1440

Putnam HM, Gates RD (2015) Preconditioning in the reef-building coral *Pocillopora damicornis* and the potential for trans-generational acclimatization in coral larvae under future climate change conditions. J Exp Biol 218:2365–2372

Qu M, Zheng G, Hamdani S, Essemine J, Song Q, Wang H, Chu C, Sirault X, Zhu XG (2017) Leaf photosynthetic parameters related to biomass accumulation in a global rice diversity survey. Plant Physiol 175:248–258

Quigley KM, Bay LK, van Oppen MJH (2020a) Genome-wide SNP analysis reveals an increase in adaptive genetic variation through selective breeding of coral. Mol Ecol 29:2176–2188

Quigley KM, Randall CJ, van Oppen MJ, Bay LK (2020b) Assessing the role of historical temperature regime and algal symbionts on the heat tolerance of coral juveniles. J Exp Biol

4175 Quigley KM, Warner PA, Bay LK, Willis BL (2018) Unexpected mixed-mode transmission and
4176 moderate genetic regulation of *Symbiodinium* communities in a brooding coral. Heredity
4177 121:524–536
4178 Quigley KM, Willis BL, Bay LK (2017) Heritability of the *Symbiodinium* community in vertically-and
4179 horizontally-transmitting broadcast spawning corals. Sci Rep 7:1–14
4180 Radchuk V, Reed T, Teplitsky C, van de Pol M, Charmantier A, Hassall C, et al. (2019) Adaptive
4181 responses of animals to climate change are most likely insufficient. Nat Commun 10:3109
4182 Ramula S, Rees M, Buckley YM (2009) Integral projection models perform better for small
4183 demographic data sets than matrix population models: A case study of two perennial herbs. J
4184 Appl Ecol 46:1048–1053
4185 Randall CJ, Giuliano C, Heyward AJ, Negri AP (2021) Enhancing coral survival on deployment
4186 devices with microrefugia. Front Mar Sci 8:662263
4187 Raudenbush SW (2009) Analyzing effect sizes: Random effects models. In: Cooper H., Hedges L. V.,
4188 Valentine J.C. (eds) The handbook of research synthesis and meta-analysis. Russell Sage
4189 Foundation, New York, pp 295–315
4190 Rees M, Childs DZ, Ellner SP (2014) Building integral projection models: A user's guide. J Anim
4191 Ecol 83:528–545
4192 Rees M, Ellner SP (2019) Why so variable: Can genetic variance in flowering thresholds be
4193 maintained by fluctuating selection? Am Nat 194:E13–E29
4194 Rezende EL, Castañeda LE, Santos M (2014) Tolerance landscapes in thermal ecology. Funct Ecol
4195 28:799–809
4196 Riahi K, van Vuuren DP, Kriegler E, Edmonds J, O'Neill BC, Fujimori S, Bauer N, Calvin K, Dellink
4197 R, Fricko O, Lutz W, Popp A, Cuaresma JC, KC S, Leimbach M, Jiang L, Kram T, Rao S,
4198 Emmerling J, Ebi K, Hasegawa T, Havlik P, Humpenöder F, Da Silva LA, Smith S, Stehfest E,
4199 Bosetti V, Eom J, Gernaat D, Masui T, Rogelj J, Strefler J, Drouet L, Krey V, Luderer G,
4200 Harmsen M, Takahashi K, Baumstark L, Doelman JC, Kainuma M, Klimont Z, Marangoni G,
4201 Lotze-Campen H, Obersteiner M, Tabeau A, Tavoni M (2017) The Shared Socioeconomic
4202 Pathways and their energy, land use, and greenhouse gas emissions implications: An overview.

4203 Glob Environ Chang 42:153–168
4204 Richards TJ, McGuigan K, Aguirre JD, Humanes A, Bozec Y-M, Mumby PJ, Riginos C (2023)
4205 Moving beyond heritability in the search for coral adaptive potential. Glob Chang Biol 29:3869–
4206 3882.
4207 Ricker WE (1954) Stock and recruitment. J Fish Res Board Canada 11:559–623
4208 Ritland K (1996) A marker-based method for inferences about quantitative inheritance in natural
4209 populations. Evolution 50:1062–1073
4210 Ritson-Williams R, Arnold S, Fogarty N, Steneck RS, Vermeij M, Paul VJ (2009) New perspectives
4211 on ecological mechanisms affecting coral recruitment on reefs. Smithson Contrib Mar Sci 437–
4212 457
4213 Robertson A (1966) A mathematical model of the culling process in dairy cattle. Anim Sci 8:95–108
4214 Rosenberg MS (2005) The file-drawer problem revisited: A general weighted method for calculating
4215 fail-safe numbers in meta-analysis. Evolution 59:464–468
4216 Rosenthal R (1991) Meta-analytic procedures for social research. Sage Publications, Inc., Newbury
4217 Park, CA
4218 Roth L, Koksal S, Woesik R Van (2010) Effects of thermal stress on key processes driving coral
4219 population dynamics. Mar Ecol Prog Ser 411:73–87
4220 Rothschild D, Weissbrod O, Barkan E, Kurilshikov A, Korem T, Zeevi D, Costea PI, Godneva A,
4221 Kalka IN, Bar N, Shilo S, Lador D, Vila AV, Zmora N, Pevsner-fischer M, Israeli D, Kosower
4222 N, Malka G, Wolf BC, Avnit-sagi T, Lotan-pompan M, Weinberger A, Halpern Z, Carmi S, Fu J,
4223 Wijmenga C (2018) Environment dominates over host genetics in shaping human gut microbiota.
4224 Nature 555:210–215
4225 Rowínski PK, Rogell B (2017) Environmental stress correlates with increases in both genetic and
4226 residual variances: A meta-analysis of animal studies. Evolution 17:1339–1351
4227 Ruesink JL (1997) Coral injury and recovery: Matrix models link process to pattern. J Exp Mar Bio
4228 Ecol 210:187–208
4229 Sae-Lim P, Mulder H, Gjerde B, Koskinen H, Lillehammer M, Kause A (2015) Genetics of growth
4230 reaction norms in farmed rainbow trout. PLoS One 10:1–17

4231 Salguero-Gómez R, Jones OR, Archer CR, Bein C, de Buhr H, Farack C, Gottschalk F, Hartmann A,
4232 Henning A, Hoppe G, Römer G, Ruoff T, Sommer V, Wille J, Voigt J, Zeh S, Vieregg D,
4233 Buckley YM, Che-Castaldo J, Hodgson D, Scheuerlein A, Caswell H, Vaupel JW (2016)
4234 COMADRE: A global data base of animal demography. J Anim Ecol 85:371–384
4235 Salguero-Gómez R, Jones OR, Archer CR, Buckley YM, Che-Castaldo J, Caswell H, Hodgson D,
4236 Scheuerlein A, Conde DA, Brinks E, de Buhr H, Farack C, Gottschalk F, Hartmann A, Henning
4237 A, Hoppe G, Römer G, Runge J, Ruoff T, Wille J, Zeh S, Davison R, Vieregg D, Baudisch A,
4238 Altwegg R, Colchero F, Dong M, de Kroon H, Lebreton JD, Metcalf CJE, Neel MM, Parker IM,
4239 Takada T, Valverde T, Vélez-Espino LA, Wardle GM, Franco M, Vaupel JW (2015) The
4240 COMPADRE Plant Matrix Database: An open online repository for plant demography. J Ecol
4241 103:202–218
4242 Sasaki MC, Dam HG (2019) Integrating patterns of thermal tolerance and phenotypic plasticity with
4243 population genetics to improve understanding of vulnerability to warming in a widespread
4244 copepod. Glob Change Biol 25:4147–4164
4245 Scavo Lord K, Lesneski KC, Bengtsson ZA, Kuhn KM, Madin J, Cheung B, Ewa R, Taylor JF,
4246 Burmester EM, Morey J, Kaufman L, Finnerty JR (2020) Multi-year viability of a reef coral
4247 population living on mangrove roots suggests an important role for mangroves in the broader
4248 habitat mosaic of corals. Front Mar Sci 7:1–16
4249 Schaub M, Kéry M (2021) Integrated Projection Models: Theory and Ecological Applications with R
4250 and JAGS. Academic Press, London, UK
4251 Schaum CE, Buckling A, Smirnoff N, Studholme DJ, Yvon-Durocher G (2018) Environmental
4252 fluctuations accelerate molecular evolution of thermal tolerance in a marine diatom. Nat
4253 Commun 9:1719
4254 Scheufen T, Krämer WE, Iglesias-Prieto R, Enríquez S (2017) Seasonal variation modulates coral
4255 sensibility to heat-stress and explains annual changes in coral productivity. Sci Rep 7:1–16
4256 Schloss CA, Nuñez TA, Lawler JJ (2012) Dispersal will limit ability of mammals to track climate
4257 change in the Western Hemisphere. Proc Natl Acad Sci 109:8606–8611
4258 Schou MF, Engelbrecht A, Brand Z, Svensson EI, Cloete S, Cornwallis CK (2022) Evolutionary trade-

offs between heat and cold tolerance limit responses to fluctuating climates. Sci Adv 8:2–10

Schwarzer G, Chemaitelly H, Abu-Raddad LJ, Rücker G (2019) Seriously misleading results using inverse of Freeman-Tukey double arcsine transformation in meta-analysis of single proportions. Res Synth Methods 10:476–483

Setter RO, Franklin EC, Mora C (2022) Co-occurring anthropogenic stressors reduce the timeframe of environmental viability for the world's coral reefs. PLoS Biol 20:1–12

Sgrò CM, Hoffmann AA (2004) Genetic correlations, tradeoffs and environmental variation. Heredity 93:241–248

Shenkar N, Fine M, Loya Y (2005) Size matters: Bleaching dynamics of the coral *Oculina patagonica*. Mar Ecol Prog Ser 294:181–188

Shlesinger T, van Woesik R (2021) Different population trajectories of two reef-building corals with similar life-history traits. J Anim Ecol 90:1379–1389

Simmonds EG, Cole EF, Sheldon BC, Coulson T (2020) Testing the effect of quantitative genetic inheritance in structured models on projections of population dynamics. Oikos 129:559–571

Sims CA, Sampayo EM, Mayfield MM, Staples TL, Dalton SJ, Gutierrez-Isaza N, Pandolfi JM (2021) Janzen–Connell effects partially supported in reef-building corals: Adult presence interacts with settler density to limit establishment. Oikos 130:1310–1325

Smith EG, Hazzouri KM, Choi JY, Delaney P, Al-kharafi M, Howells EJ, Aranda M, Burt JA (2022) Signatures of selection underpinning rapid coral adaptation to the world's warmest reefs. Sci Adv 8:7287

Spalding M, Brown B (2015) Warm-water coral reefs and climate change. Science 350:769–771

Spalding M, Burke L, Wood SA, Ashpole J, Hutchison J, zu Ermgassen P (2017) Mapping the global value and distribution of coral reef tourism. Mar Policy 82:104–113

Speare KE, Adam TC, Winslow EM, Lenihan HS, Burkepile DE (2022) Size-dependent mortality of corals during marine heatwave erodes recovery capacity of a coral reef. Glob Chang Biol 28:1342–1358

Stinchcombe JR, Simonsen AK, Blows MW (2014) Estimating uncertainty in multivariate responses to selection. Evolution 68:1188–1196

4287 Strader ME, Quigley KM (2022) The role of gene expression and symbiosis in reef-building coral
4288 acquired heat tolerance. Nat Commun 13:4513
4289 Suggett DJ, Warner ME, Leggat W (2017) Symbiotic dinoflagellate functional diversity mediates
4290 coral survival under ecological crisis. Trends Ecol Evol 32:735–745
4291 Sully S, Burkepile DE, Donovan MK, Hodgson G, van Woesik R (2019) A global analysis of coral
4292 bleaching over the past two decades. Nat Commun 10:1–5
4293 Sully S, Hodgson G, van Woesik R (2022) Present and future bright and dark spots for coral reefs
4294 through climate change. Glob Chang Biol 28:4509–4522
4295 Suzuki G, Arakaki S, Suzuki K, Iehisa Y, Hayashibara T (2012) What is the optimal density of larval
4296 seeding in *Acropora* corals? Fish Sci 78:801–808
4297 Sweet M, Burian A, Bulling M (2021) Corals as canaries in the coalmine: Towards the incorporation
4298 of marine ecosystems into the 'one health' concept. J Invertebr Pathol 186:107538
4299 Teh LSL, Teh LCL, Sumaila UR (2013) A global estimate of the number of coral reef fishers. PLoS
4300 One 8:e65397
4301 Teplitsky C, Mills JA, Yarrall JW, Merilä J (2009) Heritability of fitness components in a wild bird
4302 population. Evolution 63:716–726
4303 Thomas L, Rose NH, Bay RA, López EH, Morikawa MK, Ruiz-Jones L, Palumbi SR (2018)
4304 Mechanisms of thermal tolerance in reef-building corals across a fine-grained environmental
4305 mosaic: Lessons from Ofu, American Samoa. Front Mar Sci 4:1–14
4306 Thompson DM, Kleypas J, Castruccio F, Curchitser EN, Pinsky ML, Jönsson B, Watson JR (2018)
4307 Variability in oceanographic barriers to coral larval dispersal: Do currents shape biodiversity?
4308 Prog Oceanogr 165:110–122
4309 Thomson DP, Babcock RC, Evans RD, Feng M, Moustaka M, Orr M, Slawinski D, Wilson SK, Hoey
4310 AS (2021) Coral larval recruitment in north-western Australia predicted by regional and local
4311 conditions. Mar Environ Res 168:105318
4312 Torda G, Donelson JM, Aranda M, Barshis DJ, Bay L, Berumen ML, Bourne DG, Cantin N, Foret S,
4313 Matz M, Miller DJ, Moya, AureliePutnam HM, Ravasi T, van Oppen MJH, Vega Thurber R,
4314 Vidal-Dupiol J, Voolstra CR, Watson S-A, Whitelaw E, Willis BL, Munday PL (2017) Rapid

4315 adaptive responses to climate change in corals. Nat Clim Chang 7:627–636
4316 Tschakert P, Ellis NR, Anderson C, Kelly A, Obeng J (2019) One thousand ways to experience loss: A
4317 systematic analysis of climate-related intangible harm from around the world. Glob Environ
4318 Chang 55:58–72
4319 Tuhina-Khatun M, Hanafi MM, Rafii Yusop M, Wong MY, Salleh FM, Ferdous J (2015) Genetic
4320 variation, heritability, and diversity analysis of upland rice (*Oryza sativa* L.) genotypes based on
4321 quantitative traits. Biomed Res Int 2015:1–8
4322 UN Office of Human Rights (2022) Climate change the greatest threat the world has ever faced.
4323 https://www.ohchr.org/en/press-releases/2022/10/climate-change-greatest-threat-world-has-ever-
4324 faced-un-expert-warns [accessed 2023-09-28]
4325 Uyarra MC, Watkinson AR, Côté IM (2009) Managing dive tourism for the sustainable use of coral
4326 reefs: Validating diver perceptions of attractive site features. Environ Manage 43:1–16
4327 Varona L, Legarra A, Toro MA, Vitezica ZG (2018) Non-additive effects in genomic selection. Front
4328 Genet 9:1–12
4329 Vermeij MJA, Sandin SA (2008) Density-dependent settlement and mortality structure the earliest life
4330 phases of a coral population. Ecology 89:1994–2004
4331 Victor BC (2015) How many coral reef fish species are there? Cryptic diversity and the new molecular
4332 taxonomy. Ecology of Fishes on Coral Reefs. Cambridge University Press, pp 76–87
4333 Viechtbauer W (2010) Conducting meta-analyses in R with the metafor package. J Stat Softw 36:1–48
4334 Viechtbauer W, López-López JA, Sánchez-Meca J, Marín-Martínez F (2015) A comparison of
4335 procedures to test for moderators in mixed-effects meta-regression models. Psychol Methods
4336 20:360–374
4337 Visscher PM, Hill WG, Wray NR (2008) Heritability in the genomics area – concepts and
4338 misconceptions. Nat Rev Genet 9:255–267
4339 Visser ME (2008) Keeping up with a warming world; assessing the rate of adaptation to climate
4340 change. Proc R Soc B Biol Sci 275:649–659
4341 Walker NS, Nestor V, Golbuu Y, Palumbi SR (2022) Coral bleaching resistance variation is linked to
4342 differential mortality and skeletal growth during recovery. Evol Appl 16:504–517

Walsh B, Blows MW (2009) Abundant genetic variation + strong selection = multivariate genetic constraints: A geometric view of adaptation. Annu Rev Ecol Evol Syst 40:41–59

Walsworth TE, Schindler DE, Colton MA, Webster MS, Palumbi SR, Mumby PJ, Essington TE, Pinsky ML (2019) Management for network diversity speeds evolutionary adaptation to climate change. Nat Clim Chang 9:632–636

Walters RJ, Berger D (2019) Implications of existing local (mal)adaptations for ecological forecasting under environmental change. Evol Appl 12:1487–1502

Wang N (2018) Conducting Meta-Analyses of proportions in R: A comprehensive tutorial. John Jay College of Criminal Justice, NY pp. 1–62 https://www.researchgate.net/publication/325486099_How_to_Conduct_a_Meta-Analysis_of_Proportions_in_R_A_Comprehensive_Tutorial [accessed 2023-09-28]

Ward S, Harrison P, Hoegh-guldberg O (2000) Coral bleaching reduces reproduction of scleractinian corals and increases susceptibility to future stress. Proc 9th Int Coral Reef Symp 1123–1128

Warton DI, Hui FKC (2011) The arcsine is asinine: The analysis of proportions in ecology. Ecology 92:3–10

Webster NS, Reusch TBH (2017) Microbial contributions to the persistence of coral reefs. ISME J 11:2167–2174

Weis VM, Reynolds WS, DeBoer MD, Krupp DA (2001) Host-symbiont specificity during onset of symbiosis between the dinoflagellates *Symbiodinium* spp. and planula larvae of the scleractinian coral Fungia scutaria. Coral Reefs 20:301–308

West-Eberhard MJ (2005) Developmental plasticity and the origin of species differences. Proc Natl Acad Sci 102:6543–6549

Wheelwright NT, Keller LF, Postma E (2014) The effect of trait type and strength of selection on heritability and evolvability in an island bird population. Evolution 68:3325–3336

WHO (2021) Climate change and health. https://www.who.int/news-room/fact-sheets/detail/climate-change-and-health [accessed 2023-09-28]

Williams JL, Miller TEX, Ellner SP, Doak DF (2012) Avoiding unintentional eviction from integral projection models. Ecology 93:2008–2014

4371 Williamson OM, Allen CE, Williams DE, Johnson MW, Miller MW, Baker AC (2021) Neighboring
4372 colonies influence uptake of thermotolerant endosymbionts in threatened Caribbean coral
4373 recruits. Coral Reefs 40:867–879
4374 Wilson AJ (2008) Why h^2 does not always equal V_A/V_P? J Evol Biol 21:647–650
4375 Wilson AJ, Charmantier A, Hadfield JD (2008) Evolutionary genetics of ageing in the wild: Empirical
4376 patterns and future perspectives. Funct Ecol 22:431–442
4377 Wilson AJ, Pemberton JM, Pilkington JG, Coltman DW, Mifsud D V., Clutton-Brock TH, Kruuk LEB
4378 (2006) Environmental coupling of selection and heritability limits evolution. PLoS Biol 4:1270–
4379 1275
4380 Wilson AJ, Réale D, Clements MN, Morrissey MM, Postma E, Walling CA, Kruuk LEB, Nussey DH
4381 (2010) An ecologist's guide to the animal model. J Anim Ecol 79:13–26
4382 van Woesik R, Köksal S, Ünal A, Cacciapaglia CW, Randall CJ (2018) Predicting coral dynamics
4383 through climate change. Sci Rep 8:1–10
4384 van Woesik R, Shlesinger T, Grottoli AG, Toonen RJ, Vega Thurber R, Warner ME, Marie Hulver A,
4385 Chapron L, McLachlan RH, Albright R, Crandall E, DeCarlo TM, Donovan MK, Eirin-Lopez J,
4386 Harrison HB, Heron SF, Huang D, Humanes A, Krueger T, Madin JS, Manzello D, McManus
4387 LC, Matz M, Muller EM, Rodriguez-Lanetty M, Vega-Rodriguez M, Voolstra CR, Zaneveld J
4388 (2022) Coral-bleaching responses to climate change across biological scales. Glob Chang Biol
4389 28:4229–4250
4390 Woodhead AJ, Hicks CC, Norström A V., Williams GJ, Graham NAJ (2019) Coral reef ecosystem
4391 services in the Anthropocene. Funct Ecol 33:1023–1034
4392 Wright A, Charlesworth B, Rudan I, Carothers A, Campbell H (2003) A polygenic basis for late-onset
4393 disease. Trends Genet 19:97–106
4394 Wright RM, Mera H, Kenkel CD, Nayfa M, Bay LK, Matz M V. (2019) Positive genetic associations
4395 among fitness traits support evolvability of a reef-building coral under multiple stressors. Glob
4396 Chang Biol 25:3294–3304
4397 Wulff JL (2006) Rapid diversity and abundance decline in a Caribbean coral reef sponge community.
4398 Biol Conserv 127:167–176

WWF (2020) Bending the curve of biodiversity loss. WWF, Gland, Switzerland

Yang S, Liu Y, Jiang N, Chen J, Leach L, Luo Z, Wang M (2014) Genome-wide eQTLs and heritability for gene expression traits in unrelated individuals. BMC Genomics 15:13

Yarlett RT, Perry CT, Wilson RW (2021) Quantifying production rates and size fractions of parrotfish-derived sediment: A key functional role on Maldivian coral reefs. Ecol Evol 11:16250–16265

Yetsko K, Ross M, Bellantuono A, Merselis D, Lanetty MR, Gilg MR (2020) Genetic differences in thermal tolerance among colonies of threatened coral *Acropora cervicornis*: Potential for adaptation to increasing temperature. Mar Ecol Prog Ser 646:45–68

Yuyama I, Higuchi T (2014) Comparing the effects of symbiotic algae (*Symbiodinium*) clades C1 and D on early growth stages of *Acropora tenuis*. PLoS One 9:1–8

Yuyama I, Nakamura T, Higuchi T, Hidaka M (2016) Different stress tolerances of juveniles of the coral *Acropora tenuis* associated with clades C1 and D *Symbiodinium*. Zool Stud 55:1–9

Zhang Y, Million WC, Ruggeri M, Kenkel CD (2019) Family matters: Variation in the physiology of brooded *Porites astreoides* larvae is driven by parent colony effects. Comp Biochem Physiol Part A Mol Integr Physiol 238:110562

Zuk O, Hechter E, Sunyaev SR, Lander ES (2012) The mystery of missing heritability: Genetic interactions create phantom heritability. Proc Natl Acad Sci 109:1193–1198

Zuur AF, Ieno EN, Smith GM (2007) Analysing Ecological Data. Springer Science + Business Media, LCC, New York

Zuur AF, Ieno EN, Walker NJ, Saveliev AA, Smith GM (2009) Mixed Effects Models and Extensions in Ecology with R. Springer Science+Business Media, LLC, New York

Figure D1. The last supper of the JCU Ecological Modelling Group, headed by Sean R. Connolly.